

# Journal of Electrochemical Science and Engineering

J. Electrochem. Sci. Eng. 14(1) 2024, 1-118

Special Issue:

Nanomaterials as the powerful catalysts in electroanalysis





Open Access : : ISSN 1847-9286

www.jESE-online.org

**Editorial** 

### Nanomaterials as the powerful catalysts in electroanalysis

Ceren Karaman¹,<sup>™</sup>, Fatemeh Karimi² and Onur Karaman³

<sup>1</sup>Akdeniz University, Department of Electricity and Energy, 07058, Antalya, Turkey

<sup>2</sup>Department of Chemical Engineering, Laboratory of Nanotechnology, Quchan University of Technology, Quchan, Iran

<sup>3</sup>Akdeniz University, Department of Medical Imaging Techniques, 07058, Antalya, Turkey

Corresponding author: <sup>™</sup><u>cerenkaraman@akdeniz.edu.tr</u>; Tel.: + +90 242 310 670

Received: January 30, 2024; Accepted: January 31, 2024; Published: February 6, 2024

In the rapidly evolving landscape of electroanalysis, the role of nanomaterials has emerged as a transformative force, propelling the field to the upper stages. This special issue delves into the groundbreaking contributions of nanomaterials, exploring their potential as catalysts and their impact on shaping the future of electroanalytical techniques.

Nanomaterials, with their unique physicochemical properties, have proven to be game-changers in electroanalysis. From enhanced conductivity to increased surface area, with their superior physicochemical properties, these materials provide an ideal platform for boosting electrochemical reactions. The special properties of materials at nanoscale level attract the huge attention of industry and academia which is reflected in ever-increasing number of publications published in the prestigious international journals. This special issue compiles cutting-edge research that showcases how various nanomaterials, such as metal nanoparticles, nanotubes, and hybrid nanocomposites, serve as potent catalysts, unlocking new possibilities in the design and optimization of electroanalytical methods.

Engineering of nanomaterials helps in overcoming many challenges faced in many applications. The electronic structure of nanomaterials and its wide surface area open a great potential in improving the catalytic performance of traditional catalysts toward many chemical and electrochemical processes in monitoring different substances in biological or ecological environments. Also, many electrochemical energy storage and conversion systems take advantage of nanomaterials to speed up the reaction rates, decrease overvoltage, and enable fast and easy penetration of the intercalating ions in the layered structures of electrode materials.

The articles featured in this special issue span a wide range of applications, highlighting the versatility of nanomaterials in electroanalysis. Researchers have explored the use of nanocatalysts in sensing and detection of biomolecules, environmental monitoring, energy storage, and beyond. The special issue includes eight papers addressing new production methods and applications of nanomaterials, mostly in the electroanalysis of various substrates. A review paper by Dodevska *et al.* 

gives view of advances of nanomaterials in areas of electrode modification, successful strategies for signal amplification, and miniaturization techniques used in electroanalytical devices for cosmetics control and safety. The analysis of food products has also gained a special attention in two papers. Dehdashtian *et al.* used single wall CNTs modified carbon paste electrodes for analyizing tert-butylhydroquinone in food products. Arab *et al.* prepared the composite of ZnO/SWCNT for the determination of caffeic acid in wine samples. Pharmaceutical applications of nanomaterials for the determinations of lorazepam, methionine, hydrazine and N-acetylcysteine were also addressed in this special issue. Finally, in the paper by Elagib *et al.* the application of heteroatom-doped carbon nanotubes to create a porous structure for facilitating oxygen reduction and increase the supercapacitive properties of electrodes.

©2023 by the authors; licensee IAPC, Zagreb, Croatia. This article is an open-access article distributed under the terms and conditions of the Creative Commons Attribution license (<a href="https://creativecommons.org/licenses/by/4.0/">https://creativecommons.org/licenses/by/4.0/</a>)





Open Access :: ISSN 1847-9286 www.jESE-online.org

Review paper

## Electrochemical sensors for the safety and quality control of cosmetics: An overview of achievements and challenges

Totka Dodevska<sup>™</sup>, Dobrin Hadzhiev and Ivan Shterev

Department of Organic Chemistry and Inorganic Chemistry, University of Food Technologies, Plovdiv, Bulgaria

Corresponding author: <sup>™</sup>dodevska@mail.ba; Tel.: +359-32-603-679; Fax: +359-32-644-102 Received: September 5, 2022; Accepted: November 19, 2022; Published: November 22, 2022

#### **Abstract**

Due to the rapid growth of the cosmetic industry in recent years, the development of new, reliable, cost-effective, ease of use and rapid methods to assay cosmetics' quality is of particular importance. Modern electrochemistry provides powerful analytical techniques with excellent sensitivity, instrumental simplicity and portability, providing reliable alternatives to conventional analytical methods. This review aims to give readers a clear view of advances in areas of electrode modification, successful strategies for signal amplification, and miniaturization techniques used in electroanalytical devices for cosmetics control and safety. We have summarized recent trends in the nonenzymatic electrochemical sensor systems applied in the analysis of cosmetic products revealing that there are a variety of efficient sensors for whitening agents, preservatives, UV filters, heavy metals, etc. In conclusion, current challenges related to the sensors design and future perspectives are outlined.

#### **Keywords**

Personal care products; ingredients; analytical methods; electroanalysis

#### **Abbreviations**

AdsASV adsorptive anodic stripping voltammetry
AR arbutin (4-hydroxyphenyl-β-D-glucopyranoside)

BP butylparaben BZ3 benzophenone-3

CC catechol (1,2-dihydroxybenzene)

CPE carbon paste electrode

DPAdSV differential pulse adsorptive stripping voltammetry

DPV differential pulse voltammetry

EP ethylparaben

ErGO electrochemically reduced graphene oxide

Fc ferrocene

FIA flow injection analysis GCE glassy carbon electrode

HQ hydroquinone (1,4-dihydroxybenzene)

8-HQ 8-hydroxyquinoline

IL-GO ionic liquid functionalized graphene oxide

LOD limit of detection
LOQ limit of quantification
LSV linear sweep voltammetry

MB methylene blue

4-MBC 4-methylbenzylidene camphor MIPs molecularly imprinted polymers

MP methylparaben

MWCNTs multi-wall carbon nanotubes

NPs nanoparticles OCR octocrylene

OMC octyl-methoxycinammate PHBA p-hydroxybenzoic acid

PP propylparaben
PPD p-phenylenediamine

RS resorcinol (1,3-dihydroxybenzene)

SPE screen-printed electrode

SWAdSV square wave adsorptive stripping voltammetry

SWV square wave voltammetry

TCS triclosan (5-chloro-2-(2,4-dichlorophenoxy) phenol

TGA thioglycolic acid

ZPT zinc pyrithione (bis[(2-pyridyl-1-oxo)-thio]zinc)

#### Introduction

In general, cosmetics (body and personal care products) are mixtures of substances intended to be applied to the external parts of the human body for the purposes of cleaning, moisturizing, beautifying, keeping them in good condition or correcting body odors. As cosmetic preparations are repeatedly applied directly to the human body (epidermis, hair, nails, lips, external genital organs, teeth), they should be efficient and safe for health. To ensure the safety and quality of cosmetics, all the ingredients used in cosmetic products meet certain regulatory requirements.

Variety substances are allowed within certain limits as they may produce pharmacological or toxic effects at higher concentrations. In terms of safety, some other important aspects should be considered, which include the possibility of long-term effects. Recently, it was recognized that some topically applied substances penetrate through the skin and produce human systemic exposure. Unfortunately, using cosmetic products in some cases is related to the occurrence of unfavorable effects resulting from the intentional or accidental presence of toxic chemical ingredients [1]. Such substances may be a major component of the raw materials used in cosmetic manufacture or are deliberately added in cosmetics. It is considered that a small part of substandard cosmetics is falsified. The rest result from poor manufacturing practices, incorrect storage or inappropriate packaging.

Comprehensive coverage of the specific analytical procedure for various analytes and cosmetics samples, as well as the most recent developments in global legalization governing the cosmetics industry, were provided by Salvador and Chisvert [2]. A wide range of analytical techniques is used to accurately characterize and quantify ingredients in cosmetics. Conventional methods such as high-performance liquid chromatography (HPLC), gas chromatography, spectrophotometry, chemiluminescence, and fluorescence have been established for the analysis of cosmetic products. However, most of these methods have some disadvantages, such as specific expensive equipment, the need for complex pretreatment resulting in large time consumption and use of organic solvents in excess volumes, complicated operation, or a narrow linear range. Therefore, the development of a precise and easy-to-handle alternative for quick and efficient quantitative detection of various ingredients in cosmetic products is necessary for consumer safety [3]. New analytical methodologies

are expected to use modern and efficient techniques with highly selective detectors, as well as rapid and simple sample preparation procedures with a high level of automation [4].

Electrochemical techniques have attracted significant interest due to their high sensitivity, low detection limit, simple operation, extremely low sample consumption, and rapid analysis. Electrochemical detection is also advantageous in terms of sensor fabrication cost, power consumption and miniaturization capability [5]. The following part will provide an overview of how advances in electroanalytical technology have contributed to developing sensor devices to screen for safety and quality markers associated with cosmetics and personal care products.

#### Current stage of electrochemical sensors for the analysis of cosmetics ingredients

Whitening agents

Hydroquinone, catechol, and resorcinol

The popularity of skin-lightening (whitening/bleaching) products has grown markedly in recent years. The motivation for skin whitening may be to treat a pigmentary disorder, but it is often simply for cosmetic enhancement, as skin complexion is considered one of the most important beauty features. Nowadays, skin lightening is a global phenomenon, with the highest rates in Africa, Asia, and the Middle East.

One of the most frequent targets for the development of hypopigmenting agents is tyrosinase - a copper-containing enzyme that catalyzes the rate-limiting step of melanin biosynthesis. The skinlightening agents act by inhibiting of tyrosinase activity, thereby reducing the conversion of dihydroxybenzoic acid to melanin. The isomers of dihydroxybenzene hydroquinone (1,4-dihydroxybenzene, HQ), catechol (1,2-dihydroxybenzene, CC), and resorcinol (1,3-dihydroxybenzene, RS) specifically inhibit the melanogenesis in cells and are used in hair dyes and medical whitening creams [6]. The most commonly used treatment of hyperpigmentation for over 50 years is topical HQ. Although very effective, its long-term application causes a number of adverse reactions, including skin irritation, burning sensations, leukoderma, ochronosis, and degenerative changes followed by the skin's loss of elasticity and may have a cytotoxic effect on melanocytes. RS is an endocrine disruptor that can affect thyroid function by inhibiting thyroxin peroxidase. After prolonged exposure to RS, suppression of thyroid hormone synthesis in humans, hematological abnormalities, carcinogenesis, and fatal cases of human fetus poisoning have been observed [7]. HQ, CC, and RS are included among the substances prohibited for use as skin whitening agents in cosmetic products (Annex II and Annex III) to Regulation (EC) No 1223/2009 [8]. In the USA, the Food and Drug Administration has proposed concentrations of HQ between 1.5 and 2 % in skin lighteners [9]. According to China's hygienic standard for cosmetics, HQ is limited to oxidation colorants for hair dyeing, with a maximum allowable concentration of 2 wt.% [6]. However, in developing countries, whitening cosmetics containing HQ are circulating illegally, not to mention that the concentration level is relatively high [10].

HQ, CC and RS are electroactive substances that can be detected using various electrochemical methods. Conventional working electrodes, such as glassy carbon, graphite, carbon paste electrodes, and boron-doped diamond electrodes, have low reproducibility and stability for phenolic compounds detection because the redox reaction that occurs usually produces a polymer layer that adsorbs on the surface of the electrode, resulting in a fouling effect. This phenomenon severely affects the analytical performance in terms of sensitivity and linearity of the electrode signal. In order to reduce this effect and improve the electrode efficiency, modification of the working electrodes with nanomaterials (metal/metal oxide nanoparticles, CNTs), graphene or polymers has been extensively investigated.

Cotchim et al. [9] reported a simple electrochemical sensor for the determination of HQ at trace levels using a carboxylic acid-functionalized graphene-modified glassy carbon electrode (Gr-COOH/GCE) for adsorptive anodic stripping voltammetry (AdsASV). The electroanalytical procedure involves two steps: i) accumulation or preconcentration of the analyte at the electrode surface, and ii) stripping of the accumulated analyte from the electrode surface by using a potential sweep. Gr-COOH acts as an adsorbent, resulting in HQ being closely adsorbed on the electrode surface. As a result, the detection efficiency increases, leading to high sensitivity and a low limit of detection (LOD). The Gr-COOH/GCE exhibited good electrochemical oxidation behavior of HQ with sensitivity ten times higher than the bare GCE. The authors point out that after each experiment, the modified electrode was cleaned in the supporting electrolyte at a potential of +1.0 V (vs. Ag/AgCl) for 60 s to minimize electrode fouling and improve the electrochemical response. Under the optimized conditions, the analytical performance of the proposed method was validated and exhibited a wide linear range (0.1 to 40.0 μM), high sensitivity (19.86 μA μM<sup>-1</sup> cm<sup>-2</sup>), LOD of 0.04 μM, good selectivity, high accuracy and precision. The modified electrode provides rapid response and good repeatability, and it successfully detects trace HQ in cosmetic and skin-lightening products. Concentrations of HQ determined by the proposed sensor and by UV-derivative spectrophotometry showed no significant differences, indicating that the developed method can be successfully applied for the determination of HQ in various cosmetic products.

A simple electrochemical sensor based on nano-sepiolite clay-modified carbon paste electrode was developed for the analysis of HQ in cosmetic samples by using differential pulse adsorptive stripping voltammetry (DPAdSV) and square wave adsorptive stripping voltammetry (SWAdSV) [11]. The electrode has the advantages of high sensitivity, large linear range, low limit of detection, ease of preparation, practical surface renewal, and low cost. The authors reported that in order to prevent electrode fouling before all assays, surface cleaning of carbon paste sensors was carried out by washing with a water-ethanol mixture (1:1). The proposed sensor was applied to the analysis of HQ in the cosmetic sample (Expigment cream) with satisfying results. According to the presented results, the proposed methods have definite precision and accuracy.

Electrochemical techniques in combination with screen-printed electrodes (SPEs) have been proven as capable sensors to accelerate the change from conventional benchtop techniques/equipment to low-cost, robust and quick sensing devices [12]. With respect to the most used glassy carbon electrodes, SPEs show numerous advantages such as easy customization, cost-effectiveness, miniaturization, measurements that consume only a few microliters of sample, suitability for in-field analysis, and the absence of surface pre-treatment or polishing. It is therefore considered a potential tool for on-site applications [13]. A small and portable graphene-modified carbon paste sensor for HQ was developed using the screen-printing technique [14]. The electrochemical detection is based on a one-drop analysis (60  $\mu$ L of the sample). A linear calibration was achieved in the range of  $10^{-4}$  to  $5\times10^{-3}$  M HQ (LOD =  $7\times10^{-5}$  M). The authors stated that the sensor provided good precision and accuracy with an analysis time of less than a minute. This device was applied to determine the presence of HQ in whitening cosmetic products. The results obtained from the developed sensor satisfactorily agreed with HPLC, indicating the reliability of the electrochemical method.

An anodically pretreated screen-printed ring disk carbon electrode (SPRDCE\*) coupling with a flow injection analysis (FIA) system was developed as a simple, rapid, sensitive, and self-validated HQ sensor [15]. Using carbon-based electrode preanodized in phosphate buffer (a nontoxic solution), the sensitivity of electrochemical detection of HQ was significantly improved owing to the increase of the polar oxygen-containing functional group during the anodization. The developed anodized SPRDCE\*

presented high ability and feasibility for HQ detection. Under the optimized conditions, a linear range of 0.25 to 160 ppm and LOD = 0.024 ppm for HQ were defined. Using this method, HQ in cosmetic products was successfully quantified without any pre-treatment. SPRDCE\* combined with the FIA system offers important practical features for routine analysis of HQ in cosmetic products (Figure 1).

A carbon paste electrode spiked with ferrocene (Fc/CPE) was constructed by incorporation of ferrocene in a graphite powder–paraffin matrix [16]. Ferrocene (Fc) is a stable organometallic complex of iron. Fast and reversible redox reactions involving the Fc/Fc $^+$  couple make it a suitable mediator that accelerates electron transfer in the electrochemical systems. Linear sweep voltammetry (LSV) data confirm that Fc/CPE possesses good analytical performance - working range of 0.20 to 10  $\mu$ M, a sensitivity of 10.436  $\mu$ A  $\mu$ M $^{-1}$ , and a detection limit of 0.06  $\mu$ M HQ.

An efficient and economically viable electrochemical sensor for the quantitative determination of RS based on 77Maghemite/multi-wall carbon nanotubes (M/MWCNTs) modified carbon paste electrode was developed by Manasa *et al.* [17]. Quantitative analysis of RS was performed in PBS (pH 7.0) using differential pulse voltammetry (DPV) and two linear ranges (0.5 to 10 and 10 to 100  $\mu$ M) were obtained as a result of the kinetic limitation at the electrode/solution interface; LOD was found to be 0.02  $\mu$ M. Furthermore, to demonstrate the feasibility of the M/MWCNTs/MCPE, the amounts of RS in hair dye samples were tested by DPV, which showed good recovery and practical applicability.

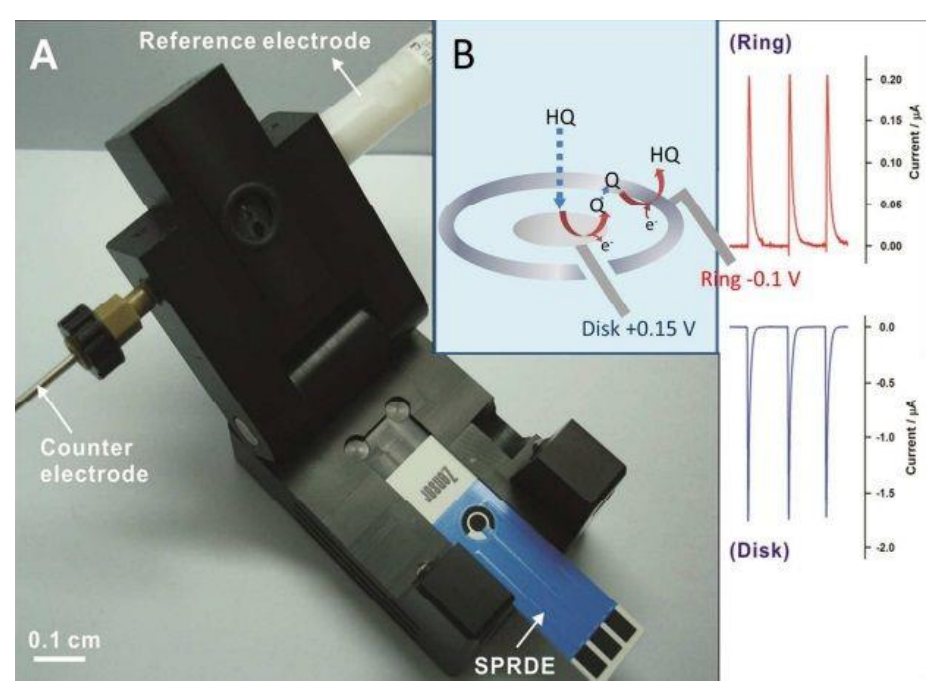


**Figure 1.** Schematic representation for monitoring of HQ at the SPRDCE\* using FIA. Reproduced from Ref. [15] with permission from the Royal Society of Chemistry

Nowadays, the effective simultaneous detection of phenolic compounds that have analogous chemical features is a subject of major study interest in the field of analytical chemistry [18]. Because of the similar electrochemical behaviour of HQ, RS, and CC, their redox peaks tend to overlap and cannot be effectively distinguished using conventional glassy carbon electrodes [19]. Therefore, to improve the detection sensitivity and selectivity of electrochemical sensors, it is necessary to search for new nanomaterials that are eco-friendly, economical, and show good catalytic performance. Electrodes modified with magnetic nanomaterials present stable conductivity and accelerate the redox process. Feng *et al.* studied the electrochemical behavior of dihydroxybenzene isomers on N-doped nickel carbide spheres (N-NiCSs/GCE) in 0.1 M PBS (pH 7.0) using cyclic voltammetry (CV) and

DPV. N-NiCSs/GCE has been applied to the simultaneous determination of HQ, CC and RS with a wide linear range, good stability, reproducibility and high sensitivity, which fully meet the requirements of cosmetics testing [6]. Under the experimental conditions, the three analytes are distinguishable by their peak potentials. The detection limits of HQ, CC, and RS were 0.00152, 0.015 and 0.24 mM, respectively. The N-NiCSs/GCE sensor has been successfully used to detect simultaneously HQ, CC, and RS in local tap water, hair dye, and whitening cream samples with satisfactory recoveries demonstrating its practicability and reliability. The authors have concluded that their future research will focus on appropriate reverse electrode passivation materials to reduce the effect of fouling.

Ascorbic acid (AA), known as vitamin C, is a naturally occurring water-soluble organic compound with antioxidant properties. Ascorbic acid plays a key role in maintaining skin health. It provides protection against UV-induced photodamage and participates in the formation of skin barrier lipids and collagen in the dermis. Although the antipigmentary and skin-protective mechanisms of AA still need to be clarified, AA has been used widely as a skin-lightening, anti-aging, anti-oxidant and anti-inflammatory agent in commercially available cosmetics such as creams and lotions, designed to protect and rejuvenate photoaged skin [20].

A new sensor based on copper oxide (CuO) nanostructures modified glassy carbon electrode (CuONPs/GCE) was designed for the simultaneous electrochemical determination of AA and HQ [21]. CuONPs with nanoflakes morphology were synthesized through an aqueous chemical growth method using copper acetate as precursor salt and sodium hydroxide as a reducing agent. CuONPs were deposited on the GCE surface by drop casting method. Under the optimal conditions, the prepared electrode CuONPs/GCE reveals excellent sensitivity, selectivity and stability with a wide linear dynamic range (0.0001 to 0.30 mM for AA, and 0.0003 to 0.355 mM for HQ) and limit of detection (0.01  $\mu$ M for AA, and 0.009  $\mu$ M for HQ). The proposed sensor has shown a potential for the simultaneous determination of AA and HQ and can be effectively used in real samples of skin-lightening creams.

Here it should be pointed out that the drop-casting approach could be characterized by some drawbacks, such as low homogeneity and stability of the resulting modified surface. A phenomenon known as the "coffee ring" effect was observed due to capillary forces present as a result of solvent evaporation which can push the modifier to the edges of the underlying electrode [13]. Agglomeration of particles upon electrode surface modification during the drop-casting process affects many physical and chemical properties, thus affecting sensing performance by decreasing the fraction of electroactive nanoparticles. Due to NPs agglomeration, these modified electrodes may lack reproducibility. Additionally, the modifier that has been physically adsorbed onto the electrode surface may be gradually stripped off in long-term operations.

A sensor based on electrochemically reduced graphene oxide (ErGO), carboxylated multi-wall carbon nanotubes (cMWCNT), and gold nanoparticles (AuNPs) was developed by Domínguez-Aragón *et al.* for the simultaneous detection of dihydroxybenzene isomers [22]. The authors emphasize that carbon-based nanocomposites of ErGO and MWCNT can be prepared within a single step, avoiding common drawbacks such as agglomeration and restacking of layers. Carboxylated MWCNT shows good mechanical properties, porous structure, high surface area, enhanced hydrophilicity, excellent chemical stability, ability to promote electron transfer reactions and higher attachment properties due to the functional groups on their surface. Therefore, cMWCNT can help to generate a more homogeneous surface with the better electrochemical activity of the material compared with MWCNT. The ErGO-cMWCNT nanocomposite can be used as an excellent scaffold for catalytic nanomaterials deposition. On the other hand, AuNPs are of great significance for electrode modification because they provide additional features such as excellent conductivity, high

surface area and catalytic properties that make them excellent materials for the electrochemical detection of a wide range of analytes [23]. Under optimized conditions, using differential pulse voltammetry, the GCE/ErGO-cMWCNT/AuNPs sensor exhibited a linear concentration range of 1.2 to 170  $\mu$ M for HQ and CC, and 2.4 to 400  $\mu$ M for RS with detection limits of 0.39, 0.54 and 0.61  $\mu$ M, respectively. The proposed sensor showed a great potential for the simultaneous, highly sensitive, precise, and easy-to-handle detection of HQ, CC and RS in complex samples such as tap water and commercial skin-lightening cream (Figure 2).

Edris and Sulaiman presented a novel highly sensitive composite of electrochemically reduced graphene oxide-poly(Procion Red MX-5B)/gold nanoparticles modified glassy carbon electrode (GCE/ErGO-poly(PR)/AuNPs) for voltammetric detection of HQ, CC, and RS [18]. The involvement of azo dye (PR) with multi-functional groups as a mediator makes the ErGO more soluble as well as stabilizes the AuNPs in the composite. The synergistic effect makes the composite have better electrochemical catalytic activity for dihydroxybenzene isomers. The composite material showed the feature of high specific surface area and high conductivity that enhanced the electrocatalysis of HQ, CC, and RC. The proposed sensor displays a linear range of 0.1 to 90  $\mu$ M for HQ, 0.4 to 90  $\mu$ M for CC, and 4 to 350  $\mu$ M for RS. The limits of detection are extremely low: 53, 53, and 79 nM for HQ, CC, and RC, respectively. The GCE/ErGOpoly(PR)/AuNPs was used for simultaneous voltammetric detection of HQ, CC, and RS in the cosmetic sample (Melashine cream 4 %) with satisfactory recoveries. The nanocomposite possesses adequate reproducibility, good stability and acceptable recoveries for wastewater and cosmetic samples analyses.

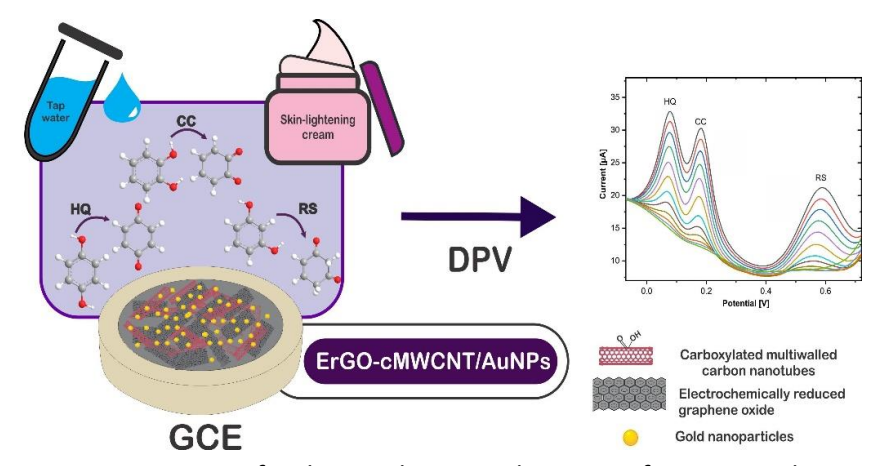


**Figure 2.** Schematic representation for the simultaneous detection of HQ, CC, and RS at the GCE/ErGO-cMWCNT/AuNPs sensor. Reproduced from Ref. [22]. Licensee MDPI, Basel, Switzerland (2021)

Butwong *et al.* [19] described a simple strategy for the fabrication of a new modified electrode exploiting the synergetic effect of CNTs and AgNPs capped by cysteamine (Cst) for simultaneous detection of HQ and CC [19]. Cysteamine stabilized AgNPs and binds strongly to CNTs to form a stable and sensing layer on a GCE surface. The resulting AgCst-CNTs/GCE possesses a large active surface area, high conductivity and excellent catalysis, with a detection limit of 10 and 40 nM for HQ and CC, respectively. The sensor was demonstrated for the analysis of river water and a topical cream, as manifested by high accuracy and reproducibility.

#### Arbutin

Arbutin (4-hydroxyphenyl- $\beta$ -D-glucopyranoside, AR), is a naturally occurring skin-lightening agent and has been found in the species of various plant families such as marjoram, cranberry,

blueberry, and several pear species. AR is often used in skin care products as it is an efficient agent for the treatment of hyperpigmentation disorders and shows less melanocyte cytotoxicity than HQ.

The practical applicability of hydroxyapatite-ZnO-PdNPs modified carbon paste electrode (HAP-ZnO-PdNPs/CPE) [24], and a sepiolite clay-modified carbon paste electrode (Clay/CPE) [25] to detect AR electively in cosmetics was tested and satisfactory results were obtained. HAP-ZnO-PdNPs/CPE for simultaneous quantitative detection of AR and AA (vitamin C) was developed by Shahamirifard et~al. [24] DPV data reveal that the modified electrode has exhibited excellent electrocatalytic activity towards the oxidations of AR and AA in buffer solution (pH 7.0). The corresponding electrochemical signals have appeared as two well-resolved oxidation peaks with a potential difference of 0.23 V (vs. Ag/AgCl, 3.0 M KCl) which is high enough for the simultaneous determination of the concentration of AR and AA. The linear response ranges were 0.12 to 56  $\mu$ M for AR and 0.12 to 55.36  $\mu$ M for vitamin C, with detection limits of 85.7 and 19.4 nM, respectively. The practical applicability of the fabricated sensor was confirmed in commercial lightening Seagull cream.

Online derivatization followed by a disposable electrochemical sensor was also used to determine AR in cosmetic products [26]. The AR was chemically oxidized by  $MnO_2$  and subsequently reduced at a screen-printed carbon electrode using a low detection potential which improved the selectivity of the method.

The so-called "green synthesis", using mild reaction conditions and natural resources such as plant extracts, has received more attention as a cost-effective and valuable alternative for environmentally safe and energy-efficient production of metal nanoparticles (MNPs) [20]. Unlike chemical and physical processes, bio-inspired synthetic methods restrict the use of toxic chemicals, energy and sophisticated instruments. Nowadays, there is convincing evidence that green synthesis of MNPs has the potential to provide a new direction in the fabrication of cheap and effective electrocatalysts applicable in pharmaceutical, environmental, and food analysis. Khatoon *et al.* [27] reported for the first time utilization of bell pepper (BP) extract as a capping, stabilizing, and reducing agent for the cost-effective and environmentally safe synthesis of AgNPs and applicability of the nanoparticles for the development of an electrochemical sensor for AR detection [27]. The fabricated electrochemical platform based on BP-AgNPs-GCE exhibits a linear current response in the concentration range from 10 to 350  $\mu$ M, LOD of 0.03  $\mu$ M, and LOQ of 0.09  $\mu$ M, respectively. The applicability of this sensor for sensitive detection of AR in real samples was confirmed in commercially available skin whitening creams.

Here we must note that the experimental data published so far show that the surfaces modified with biosynthesized MNPs remain challenging as they are often not as stable and reproducible as one would hope. It is important to ensure that metal nanoparticles produced by the plants or plant extracts remain stable during their storage without changes in their morphology and size before using them in practical applications. Further research needs to be done to address these issues and improve the electrode performance in terms of higher operational and storage stability of the electrocatalysts modified with nanoparticles synthesized in a green way.

#### Hydrogen peroxide

Hydrogen peroxide ( $H_2O_2$ ) is classified as an antimicrobial agent, cosmetic biocide, oral health care agent, and oxidizing agent. Hydrogen peroxide can often be found in many day-to-day life cosmetic products such as hair dyes, hair bleaches (diluted  $H_2O_2$  mixed with ammonium hydroxide solution is used as a constituent), tooth whitening products and sold as an antiseptic. The EC restricts

the amount of  $H_2O_2$  that may be present in cosmetic products. These restrictions included a maximum concentration of 4 % in products applied to the skin and 12 % in products applied to the hair; dyes intended to be used on eyelashes (professional use only) are safe when they contain up to 2 %  $H_2O_2$  [28]. Since  $H_2O_2$  is an aggressive oxidizer that damages human skin, a higher concentration of  $H_2O_2$  (> 20 %) is considered to be highly hazardous.

The determination of H<sub>2</sub>O<sub>2</sub> plays an important role in clinical research, medical diagnostics as well as in many industrial applications (food processing, paper, textile, pharmaceuticals, cosmetics, cleaning and disinfection products) [29]. The electrochemical nonenzymatic detection of  $H_2O_2$  can provide many attractive characteristics, such as simple fabrication, ultrahigh sensitivity, and excellent stability. Considering the rapid expansion of nonenzymatic H<sub>2</sub>O<sub>2</sub> detection using advanced nanomaterials, several review papers were devoted to the design strategies for electrocatalysts used in H<sub>2</sub>O<sub>2</sub> sensors by focusing on the sensing performance, electrocatalytic mechanism, and morphology of electrode materials [30-33]. Here we refine the search and present exclusively the electrochemical sensors applicable in the H<sub>2</sub>O<sub>2</sub> analysis of cosmetics, medical and cleaning products. Copper oxide/graphitic carbon nitride composite (CuO/g-C<sub>3</sub>N<sub>4</sub>) dropped onto GCE [34], nanosized bismuth particles modified electrode (SPAgE-Bi<sup>nano</sup>) [35], carbon paste electrode modified with nano-composite of reduced graphene oxide and CuFe<sub>2</sub>O<sub>4</sub> nanoparticles (RGO/CuFe<sub>2</sub>O<sub>4</sub>/CPE) [36], CuO/Cu wire [37], 3D printed graphene electrode with Prussian blue (3DGrE/PB) (Figure 3) [38], as well as carbon electrodes modified with perovskites-type oxides [39-42] were developed, characterized and successfully used as working electrodes for the electrochemical detection of H<sub>2</sub>O<sub>2</sub> in a wide range of cosmetics and antiseptic products (Table 1).

**Table 1.** Comparison of the analytical parameters of electrochemical nonenzymetic sensors for the determination of  $H_2O_2$  in cosmetics, medical and cleaning products

Electrode material	Method	Linear range	LOD	Real sample	Ref.
CuO/g-C <sub>3</sub> N <sub>4</sub> /GCE <sup>1</sup>	$DPV^4$	0.5 – 50 μM	0.31 μΜ	makeup remover	[34]
SPAgE-Bi <sup>nano 2</sup>	CV⁵	$100 \mu M - 5 mM$	56.59 μΜ	hair dyes	[35]
RGO/CuFe <sub>2</sub> O <sub>4</sub> /CPE	Amp. <sup>6</sup>	$2 - 200 \mu M$	0.52 μΜ	hair dye,	[36]
	$DPV^4$	$2-1000~\mu M$	0.064 μΜ	mouthwash solution	[30]
CuO/Cu wire	Amp. <sup>6</sup>	10 – 1800 μΜ	1.34 μΜ	Listerine mouthwash	[37]
3DGrE/PB <sup>3</sup>	Amp. <sup>6</sup>	1 – 700 μM	0.11 μΜ	mouthwash	[38]
LaNi <sub>0.5</sub> Ti <sub>0.5</sub> O <sub>3</sub> /CoFe <sub>2</sub> O <sub>4</sub> /GCE	Amp. <sup>6</sup>	$0.1  \mu M - 8.2  mM$	23 nM	toothpaste	[39]
La <sub>0.66</sub> Sr <sub>0.33</sub> MnO <sub>3</sub> /CPE	Amp. <sup>6</sup>	_	_	cleaning product	[40]
LaNi <sub>0.6</sub> Co <sub>0.4</sub> O <sub>3</sub> /CPE	Amp. <sup>6</sup>	10 nM – 100 μM	1 nM	toothpaste	[41]
$\underline{\text{La}_{0.7}\text{Sr}_{0.3}\text{Mn}_{0.75}\text{Co}_{0.25}\text{O}_{3}/\text{CPE}}$	Amp. <sup>6</sup>	0.5 – 1000 μM	0.17 μΜ	toothpaste, medical solution	[42]

 $^1$ CuO/g-C<sub>3</sub>N<sub>4</sub>/GCE: copper oxide/graphitic carbon nitride composite/glassy carbon electrode;  $^2$ SPAgE-Bi<sup>nano</sup>: three-in-one screen-printed electrode assembly containing nano bismuth species deposited silver as working, pre-oxidized silver as a reference and unmodified silver as counter electrodes;  $^3$ 3DGrE/PB: 3D printed graphene electrode with Prussian blue;  $^4$ DPV: differential pulse voltammetry;  $^5$ CV: cyclic voltammetry;  $^6$ Amp.: amperometry.

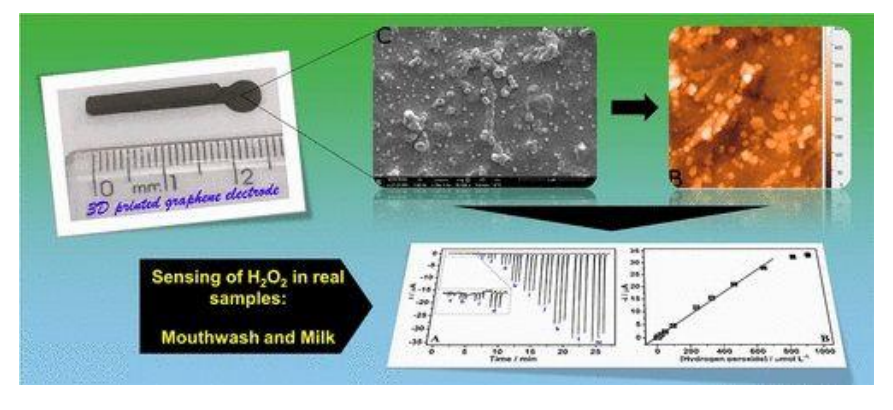


Figure 3. Schematic representation for the detection of  $H_2O_2$  using 3D printed graphene electrode with Prussian blue (3DGrE/PB). Reprinted with permission from Ref. [38]. Copyright (2019) American Chemical Society

#### **Preservatives**

Preservatives are added to cosmetics in order to prevent microbial spoilage, and therefore prolonging products' shelflife. Parabens, aldehydes, phenoxyethanol, glycol ether, isothiazolinones, quarternary ammonium compounds and organic acids (benzoic acid, hydroxybenzoic acid, dehydroacetic acid, sorbic acid, etc.) are commonly added as preservatives to a wide range of cosmetics. Michalkiewicz et al. [43] reviewed the research achievements on modified carbon materials in the electroanalysis of preservatives most frequently used in food, cosmetic, and pharmaceutical preparations [43].

#### p-hydroxybenzoic acid

*p*-hydroxybenzoic acid (4-hydroxybenzoic acid, PHBA) is a frequently used preservative substance in cosmetics. Moreover, PHBA is the hydrolysis product of parabens, a popular preservative in cosmetics and foodstuffs. A few published works have reported the detection of PHBA using an electrochemical technique.

Electrochemical determination of PHBA is required for efficient surface modification. Nickel titanate (NiTiO<sub>3</sub>) nanoceramics, synthesized by the sol-gel method, were used to fabricate a modified carbon paste electrode (NiTiO<sub>3</sub>/CPE) for quantitative detection of PHBA [44]. DPV results suggest that the modified electrode exhibits an electrocatalytic effect on the oxidation of PHBA, resulting in a marked enhancement of the peak current response at 1.0 V (vs. Ag/AgCl, 3 M KCl). Under the optimized conditions in Britton-Robinson buffer solution (pH 2.0), the oxidation peak current was linearly dependent on the concentration of PHBA in the ranges of 0.7 – 80  $\mu$ M and 80 – 1000  $\mu$ M. The detection limit was estimated to be 62 nM. Common interfering ions, such as Na<sup>+</sup>, K<sup>+</sup>, NH<sub>4</sub><sup>+</sup>, Cl<sup>-</sup>, CO<sub>3</sub><sup>2-</sup>, NO<sub>3</sub><sup>-</sup> and l<sup>-</sup>, do not influence the DPV response of PHBA with deviations below 5 %. However, the authors reported that methylparaben and propylparaben have the same oxidation potential and show interference effects. The ability of the nanostructured modified electrode was examined in the detection of PHBA in an oil-free liquid cream foundation. The satisfactory results from the analysis proved the practical applicability of NiTiO<sub>3</sub>/CPE towards the determination of PHBA in real samples.

The same electrode was tested for the simultaneous voltammetric determination of *o*-hydroxybenzoic acid (OHBA) and *p*-hydroxybenzoic acid (PHBA) [45]. Peak overlap in voltammetry is a challenge for the quantitative analysis of electroactive isomers. The experimental results show that the optimum pH 2.0 can be used for the determination of OHBA and PHBA individually. But, when OHBA and PHBA determine simultaneously at pH 2.0, only one peak in DPV was registered at about 1.05 V. In order to obtain improved voltammetric peak separation, the authors used a higher pH value. In electrolyte Britton-Robinson buffer solution (pH 5.0), DPV shows an oxidation peak of PHBA at about 0.8 V, whereas an oxidation peak of OHBA was observed at about 0.9 V. However, from the presented voltammogram, it is clear that the signals are not completely resolved. Therefore, it is doubtful that the peak current can be measured accurately. The results would be more convincing if the authors presented the DPV records for various concentrations of PHBA and OHBA, respectively, in the presence of a constant concentration of the counterpart.

Recently, Charoenkitamorn *et al.* proposed the anodized SPGE (SPGE\*) for PHBA detection [46]. The facile electrode preparation for PHBA detection and the utilization of phosphate buffer solution is environmentally friendly that could be counted as a green chemistry process. Under optimal conditions, the detection limit for PHBA was achieved at  $0.073~\mu M$ . The results from the interference tests revealed that the ionic substances have no effects on PHBA detection, whereas uric and

ascorbic acid can interfere after adding a concentration 50 times higher than PHBA. The oxidation potentials of both species were found to be 0.30 and 0.40 V (vs. Ag/AgCl), respectively, which is closed to the oxidation potential of PHBA and caused a lower tolerance limit than those obtained from other studied species. The established feature would limit the use of this sensor for PHBA analysis in cosmetics with high vitamin C content. Here it should also be noted that the interference of parabens has not been investigated. Five samples of skin lotions were determined to verify the practical performance of the proposed SPGE\*. The HPLC, a standard method for PHBA analysis, was performed in parallel with the same samples. The obtained results reveal that the proposed SPGE\* has a highly effective feasibility for the determination of PHBA in cosmetics. Not least, the SPGE\* can be applied using a portable potentiostat, which is accessible and eligible for the end-users to operate onsite.

#### **Parabens**

Parabens (alkyl esters of *p*-hydroxybenzoic acid) have been used for over 70 years in cosmetics, foods, and pharmaceuticals as preservatives due to their broad antimicrobial spectrum, effectiveness and low price. Methylparaben (MP), ethylparaben (EP), propylparaben (PP) and butylparaben (BP) are most frequently used in commercial applications. The antimicrobial activity of parabens increases with the increasing length of the ester group, but water solubility decreases. In practice, shorter esters (MP and EP) are commonly used because of their high solubility in water. Product ingredient labels typically list more than one paraben in a cosmetic product. Parabens are often used in combination since they have synergetic effects in a wide variety of products such as cosmetics, ointments and suspensions, which allows the use of lower levels while increasing preservative activity [47,48].

For the last few years, parabens have been the topic of controversies among scientists and consumers. Long-term studies indicated that the use of these compounds could result in potential health risks [49-54]. Oishi reported that PP adversely affects hormonal secretion and decreases male reproductive potential [51]. MP has a pronounced estrogenic effect and its constant use is associated with causes of breast cancer, ovarian cancer and endometriosis. According to the Cosmetic Directive in Europe, the maximum allowable concentration of such compounds in cosmetic formulations in the final product is 0.4 wt.% for a single ester and 0.8 wt.% for ester mixtures, expressed as PHBA [55].

A few electroanalytical methods have been reported for the determination of parabens in cosmetics [48,56-61]. Electrochemical quantification of MP was successfully performed using sensors based on: GCE modified with graphene oxide and ruthenium nanoparticles [56], MWCNTs coupled with Nafion-modified GCE [60], gold electrodes modified with Layer-by-Layer (LbL) films of magnetite nanoparticles and polypyrrole [57], pencil graphite electrode modified by molecularly imprinted polymer [61]. Electroanalytical detection of PP using gold nanoparticles-electrodeposited onto indium-tinoxide electrode (AuNP-ITO) functionalized with PEI (poly(ethylene imine)) and NiTsPc (nickel(II) phthalocyanine tetrasulfonate) in the film (ITO-AuNPs-(PEI/NiTsPc)<sub>3</sub> was described by de Lima *et al.* [58].

A new approach to the study and simultaneous determination of MP and PP based on electrochemical and chemometric methods has been reported by Behpour *et al.* [48]. The selective and reliable electrochemical method based on molecularly imprinted polymers (MIPs) with dual templates was developed by Wang *et al.* in order to determine the total content of parabens in cosmetics [59]. Rapid response of the MIPs sensor was obtained within 1 min. MIPs sensor was used to determine the total content of parabens in cosmetic samples with recoveries between 98.7 and 101.8 %.

#### 8-hydroxyquinoline

8-hydroxyquinoline (8-HQ), also known as oxine or 8-quinolinol, is an excellent antiseptic, preservative, bactericide and disinfector. 8-HQ is widely used in the production and preservation of cosmetic products due to its strong antimicrobial properties.

Guo *et al.*, 2011 fabricated a modified electrode by dropping a supernatant of MWCNTs/Nafion on a GCE and, for the first time, reported the determination of trace 8-HQ in cosmetics by electroanalytical method [62]. As a voltammetric sensor, MWCNTs/Nafion/GCE shows excellent electrocatalytic activity towards the oxidation of 8-HQ because of the synergistic effect of MWCNTs and Nafion – extremely low detection limit (9.0 nM) and high electrode sensitivity in the concentration range from 2×10<sup>-8</sup> to 10<sup>-5</sup> M. The results from the interference experiments showed that general concomitant substance in cosmetic products, such as 300-fold coconut oil propylbetaine, sodium lauryl sulfacid, glycerol, citric acid, vitamin C, and vitamin E, did not interfere with the determination of 8-HQ. These data demonstrated that the MWNT/Nafion/GCE voltammetric sensor possessed high selectivity for 8-HQ in cosmetic formulations. The analytical results obtained in the shampoo sample proved the practical applicability of the proposed method.

A modified electrode, obtained by the electrodeposition of 1-amino-2-naphthol-4-sulfonic acid (ANSA) on the surface of GCE, for the rapid and inexpensive determination of 8-HQ in cosmetic samples, was reported by Calam *et al.* [63]. ANSA/GCE is a reliable sensor for the SWV detection of 8-HQ in a wide linear range of  $5\times10^{-7}$  to  $1.4\times10^{-5}$  M with a detection limit of  $1.6\times10^{-7}$  M. The voltammetric analysis using the ANSA/GCE provided excellent reproducibility (RSD = 4.45 %, n = 10), repeatability (RSD = 2.26 %, n = 10) and selectivity: the results showed that 100-fold excess concentrations of NaCl, NaOH, KOH, and ascorbic acid; 30-fold excess concentrations of phosphoric acid, citric acid, alanine, and lysine; and 10-fold concentration of Al(OH)<sub>3</sub>, glycerin, and benzyl alcohol did not significantly influence the peak current height, with variations of less than 5 %. The long-term storage stability of the electrode was also reasonable – a reduction of 9.56 % in the peak current was observed after 15 days. The real sample analysis reveals the applicability of the sensor for 8-HQ detection in blush cosmetic products.

Recently, Gao and co-authors [64] have established an electrochemical senor for the determination of 8-HQ developed by electropolymerization of tannic acid (TA) on GCE [64]. The modified electrode (PTA/GCE) showed a strong electrocatalytic activity toward the oxidation of 8-HQ due to the enhanced surface area and abundant functional groups that exhibit affinity to 8-HQ. Using DPV, PTA/GCE shows two linear plots with 8-HQ concentrations from 0.5 to 5  $\mu$ M and 5 to 50  $\mu$ M (LOD = 36 nM). The electrochemical senor was applied in the quantitative determination of 8-HQ in hair conditioner samples with a satisfactory result.

#### Triclosan

Triclosan (5-chloro-2-(2,4-dichlorophenoxy) phenol, TCS) as an antibacterial and an antifungal agent has been used in various cosmetic, healthcare, and personal care products, such as mouthwashes, toothpaste, soaps, dish-washing liquids, and antibacterial creams [65]. The European Community Cosmetic Directive approved TCS usage as a preservative in cosmetics and toiletries up to 0.3 wt.% [66]. Literature and related studies have shown inflammatory skin conditions and endocrine disruption after exposure to TCS. It was also reported that TCS is toxic to aquatic living organisms. Once in the aquatic environment, TCS can undergo a series of transformation reactions to produce chlorophenols, chloroform and dioxin-type derivatives classified as human carcinogens [65,67]. Therefore, the safety of TCS has been questioned in regard to environmental and human

health. A review article presented by Sri *et al.* describes the progress made in the use of nanostructured particles as active electrode materials for the electrochemical sensing of TCS in environmental samples [68].

To the best of our knowledge, there are only a few reports on electrochemical sensors for TCS successfully applied in cosmetic samples [65,67,69-73]. Table 2 presents a comparison of the analytical parameters of these sensors used for the determination of TCS in cosmetics and cleaning products.

**Table 2.** Comparison of analytical parameters of electrochemical sensors for determination of triclosan (TCS) in cosmetics and cleaning products

Electrode material	Method	Linear range	LOD	Real sample	Ref.		
GCE <sup>1</sup>	DPV <sup>7</sup>	$10 - 600  \mu g  L^{-1}$	5 μg L <sup>-1</sup>	toothpaste, hand gel,	[65]		
	DPV	$1 - 8 \text{ mg L}^{-1}$	э μg L	liquid soap	[63]		
Fe <sub>3</sub> O <sub>4</sub> @Au-	DPV <sup>7</sup>	10 nM – 1 μM 2.5 nM		to	toothpaste, shampoo,	toothpaste, shampoo, liquid	[67]
PPy/GO/GCE <sup>2</sup>	DFV	10 ΠΙΝΙ – 1 μΙΝΙ	2.3 11101	soap	[07]		
SPCE <sup>3</sup>	$DPV^7$	$1.2 \mu M - 1 mM$	_	toothpaste, mouthwash	[69]		
MWCNTs/GCE	$DPV^7$	$50  \mu g  L^{-1} - 1.75  mg  L^{-1}$	16.5 $\mu g L^{-1}$	toothpaste	[70]		
CNDs-CS/GCE <sup>4</sup>	LSV <sup>8</sup>	10 nM – 1 mM	9.2 nM	toothpaste, mouthwash,	[71]		
				hand sanitizer	[/1]		
LS11-ODA-AuNPs/GCE <sup>5</sup>	$DPV^7$	0.01 – 0.5 μM	0.005 μΜ	toothpaste, liquid soap	[72]		
ZIF-11/HRAC/GCE <sup>6</sup>	DPV <sup>7</sup>	0.1 – 8 μM	0.076 μΜ	lipstick, skin cream, cleansers	[73]		

<sup>1</sup>GCE: glassy carbon electrode; <sup>2</sup>PPy: polypyrrole, GO: graphene oxide; <sup>3</sup>SPCE: screen-printed carbon electrode;

The extremely low detection limit of 2.5 nM was reported recently by Saljooqi  $et\ al.\ [67]$ . The electroanalysis of TCS was demonstrated by the use of Fe<sub>3</sub>O<sub>4</sub>@AuPPy/GO-nanocomposite modified GCE. Nanocomposites consisting of conducting polymers and nanomaterials have received great attention. The appropriate combination of different nanoscaled materials with the conductive polymer may open a new vista for utilizing novel enhanced electrochemical sensing platforms with high performance. The combination of carbon nanomaterials with metal nanoparticles and/or polymers to form composites could increase surface active sites to readily accumulate TCS into the hybrid films. Iron oxide magnetic nanoparticles (Fe<sub>3</sub>O<sub>4</sub>NPs) were frequently applied in electrochemical sensors because of their great surface-to-volume ratio, fast electron transfer, and strong adsorption ability. In particular, if Fe<sub>3</sub>O<sub>4</sub> surface is loaded or coated with noble metal nanoparticles like Au, the transfer of electrons and conductivity increase significantly. To evaluate the applicability of the present methodology on real samples, the authors performed experiments in toothpaste, shampoo, liquid soap, and urine. The results showed that the Fe<sub>3</sub>O<sub>4</sub>@Au-PPy/GO nanocomposite displays an acceptable recovery and can be utilized for TCS sensing with the purpose of pharmacokinetics investigations and quality control.

#### Zinc pyrithione

Zinc pyrithione (bis[(2-pyridyl-1-oxo)-thio]zinc) is a broad-spectrum antimicrobial agent that has been used for more than 60 years to treat dandruff and seborrheic dermatitis. Its effective bactericide, fungicide and algaecide functions are utilized in most daily hair care products. Zinc pyrithione (ZPT) has been established as one of the most effective antidandruff ingredients for use in shampoo, conditioner, rinse and hairdressing formulations. Being subject to several safety evaluations, ZPT was previously found safe as an antidandruff agent in rinse-off hair care products at a maximum concentration of 2.0 %. On the 4<sup>th</sup> March 2020, the Scientific Committee on

<sup>&</sup>lt;sup>4</sup>CNDs-CS: composite film based on chitosan and carbon nanodots; <sup>5</sup>LS11-ODA-AuNPs: core-shell structure of bacteriochlorin-supported AuNPs; <sup>6</sup>ZIF-11/HRAC/GCE: composite of zeolite imidazolate framework-11 and activated carbon derived from rice husks; <sup>7</sup>DPV: differential pulse voltammetry; <sup>8</sup>LSV: linear sweep voltammetry.

Consumer Safety concluded that ZPT is safe when used in a concentration of maximum 1 % [74]. ZPT is currently regulated as a preservative in rinse-off products (with the exception of oral hygiene products) in a concentration of up to 0.5 % in general products and up to 1.0 % in hair products [75].

ZPT is substantially insoluble in water and is present in aqueous-based products as a dispersion of fine solid particles. The electrochemical oxidation of ZPT using a metal oxide-modified carbon paste electrode ( $M_xO_y$ /CPE) has been investigated in various alkaline solutions and the optimum experimental conditions for the determination of ZPT containing cosmetic samples were described [76]. The higher catalytic activities among ten metal oxides dispersed on CPE are shown at SnO<sub>2</sub>, ZrO<sub>2</sub> and Bi<sub>2</sub>O<sub>3</sub>. The authors also have presented the results of a comparative study of various pH and supporting electrolytes. The height of the ZPT wave in solutions of 0.1 M tetrabutylammonium hydroxide (Bu<sub>4</sub>NOH) was found to be higher. The calibration plot of SnO<sub>2</sub>/CPE obtained by plotting the peak current at 0.620 V (vs. SCE) against the concentration of ZPT shows linearity over the range of 1.6 to 32 mg L<sup>-1</sup>. The direct determination of the concentration of ZPT in commercial products (shampoo, conditioner, rinse and hairdressing products) was successfully accomplished by means of DPV using the same modified electrode.

A disposable type of cobalt phthalocyanine-modified screen-printed carbon electrode (CoPc/SPE) in a couple with FIA was developed for the analysis of ZPT in commercial hair care products [77]. The presented method shows several advantages for ZPT detection over the  $SnO_2/CPE$ -based DPV assay, such as lower over-potential, the limit of detection and working volume. Under the optimized hydrodynamic flow injection parameters, the CoPc/SPE yielded a linear calibration plot in the window of 6 to 576  $\mu$ M with a detection limit of 0.9  $\mu$ M in 0.1 M KOH solution at an applied potential of 0.3 V (vs. Ag/AgCl). The authors demonstrated that the CoPc/SPE is effective and selective for the ZPT analysis in commercial shampoos.

Both commented studies offer rapid, easy, selective and inexpensive approaches for direct routine ZPT analysis in hair care products. The electrochemical procedures described above do not have the drawbacks of classical methods, namely trans-chelation at HPLC analysis (the need for preceding formation of the Cu(II) complex), photodegradation of ZPT at thin-layer chromatography, a lack of selectivity of titrimetric methods, *etc*.

#### UV filters in sunscreen products

Sunscreens have been recommended by dermatologists for a long time as a protective measure against excessive amounts of sunlight to prevent UV-induced erythema. Moreover, numerous studies show that the regular use of sunscreens contributes to the prevention of skin cancer and photoaging [78,79]. UV filters can be classified into two groups according to their nature: i) the inorganic UV filters (physical UV filters) principally work by reflecting and scattering the UV radiation; ii) the organic UV filters (chemical UV filters) absorb ultraviolet radiation. Chemical UV filters are organic compounds with high molar absorptivity in the UV range and usually possess single or multiple aromatic structures, sometimes conjugated with C=C double bonds and/or carbonyl moieties [80].

Cosmetics containing organic UV filters are most commonly used, despite causing different side effects. The adverse reactions to sunscreens include subjective irritation (stinging, burning), contact dermatitis and comedogenicity. The potential adverse effects induced by UV filters in experimental animals include reproductive/developmental toxicity and disturbance of hypothalamic–pituitary–thyroid axis (HPT) [81,82].

Organic chemicals that absorb UV radiation are added to sunscreen products in concentrations of up to 10 % for skin protection. Some of these compounds are also included in other cosmetics, such as skin lotions, beauty creams, lipsticks, hair sprays, etc. The level and quality of UV protection provided by sunscreen products has improved significantly during the last three decades. Nowadays, the trend toward cosmetic products with higher protective effects and screening efficiency against both UVB (290 – 320 nm) and UVA (320 – 400 nm) wavelengths has led to the extensive development of formulations containing combinations of various organic UV filters at different concentrations. Modern sunscreens should provide broad-spectrum UV protection because this ensures that the natural spectrum of sunlight is attenuated without compromising its quality. For example, octyl-methoxycinammate (OMC), benzophenone-3 (BZ3) and 4-methylbenzylidene camphor (4-MBC) are UV filters usually combined in sunscreen formulations because their UV spectra have overlapping bands and the mixture allows a good sun protection factor (SPF) in the whole range of UVB and UVA radiation [83].

There are positive lists for sunscreen agents in the three main legislations regarding cosmetic products, that is, those in force in EU, USA and Japan (in the USA they are considered as OTC drugs) where the maximum authorized contents are stipulated [80]. However, until today there are no official analytical methods. Methods based on HPLC are the most widely employed for the separation and determination of sunscreen agents [84].

To the best of our knowledge, there is a limited number of published articles dealing with the determination of sunscreen agents in cosmetics by means of electrochemical techniques. Differential pulse voltammetry using a carbon-epoxy composite electrode in non-aqueous solvents [85] or mercury film electrode in strongly alkaline media [86] have been successfully applied to determine different UV filters in sunscreen products. Square wave voltammetry using GCE is fast and sufficiently sensitive to ensure octocrylene (OCR) quantification at low concentrations [87]. OCR was reduced at a potential of -0.97 V (vs. Ag/AgCl) on a GCE using a mixture of 0.04 M Britton-Robinson buffer and ethanol (7:3, v/v) as a supporting electrolyte. The results reveal satisfactory precision and accuracy, demonstrating that the proposed method is an acceptable alternative for the analytical determination of OCR in cosmetic preparations.

Cardoso *et al.*, 2007 studied the voltammetric behavior of 4-MBC by square wave voltammetry (SWV) using mercury electrode in Britton-Robinson buffer and cationic surfactant, cetyltrimethylammoniun bromide (CTAB) [83]. A single peak of 4-MBC reduction was observed at -1.21 V (*vs.* Ag/AgCl), the calculated LOD was 2.99 nM and the LOQ was 9.98 nM. Authors applied the developed methodology to determine 4-MBC in commercial sunscreen SPF 15, 20 and 30 and for the simultaneous determination when other protection agents were associated, such as BZ3 or OMC. Subsequently, the research group published the first study dealing with the simultaneous determination of the three UV filters using surfactant and polarography [88]. A method based on electrochemical reduction for the simultaneous determination of three sunscreen agents (4-MBC, BZ3 and OMC) by differential-pulse polarography (DPP) was proposed. The authors validated the methodology using four commercial sunscreen preparations and the results showed high recovery rates.

Lopes Neves *et al.* [89] developed a new analytical methodology for the determination of BZ3, 4-MBC and OMC in cosmetics samples by SWV using a mercury film modified gold electrode as an alternative to dropping mercury electrode, contributing to the generation of less toxic residues, a safer process for the analyst, and a low cost in terms of analysis.

#### Hair-waiving agents

#### Thioglycolic acid

Thioglycolic acid (TGA) is an organic compound containing both a thiol and a carboxylic acid functional groups. TGA and its salts are frequently used in hair-waving and depilatory products. The chemistry of hair-waving is based on the cleavage of hair disulfide bonds by the thiol groups of the TGA. Here, it should be noted that skin contact with low-molecular-weight organic acids can lead to severe pain and burns, which can heal slowly with the formation of scar tissue. TGA, even in dilute solutions, may cause conjunctival hyperemia and corneal injury. In this regard, the EU Cosmetics Directive has limited the maximum permissible concentration of TGA and its salts, calculated as TGA, to 11.0 % at pH 7.0 to 9.5 [90].

The voltammetric behavior of TGA at a carbon paste electrode modified with cobalt phthalocyanine (CoPc) was studied by Shahrokhian *et al.* [91]. The CoPc/CPE shows high electrocatalytic activity toward oxidation of TGA, substantially lowering the overpotential of an anodic reaction. The results of these studies were used to develop a potentiometric method for determining TGA and its salts in hair-treatment products. However, the authors note that other compounds with reducing properties and redox potentials close to TGA, such as hydrogen sulfide, sulfite and mercaptoethanol, may interfere if they are present in the sample. This issue has been resolved by Zen and co-authors, who developed a sensitive and selective method combining HPLC with electrochemical detection for the quantitative determination of TGA [92]. In this study, HPLC was used to eliminate interference from the matrix of real samples, and preanodized screen-printed carbon electrodes (SPCEs\*) were used to determine TGA. SPCEs\* have the advantages of being inexpensive, easy to handle, disposable, flexible and stable. Under optimized conditions, the linear range for TGA is up to 20 ppm with a detection limit of 0.042 ppm. The practical application of the proposed method was demonstrated by the determination of TGA in commercial hair-waving products. The authors stated that the new method offers a viable alternative to previous approaches used in the routine determination of TGA.

#### **Sulfites**

Sulfites are commonly used as preservatives/antioxidants in the food and cosmetic industry. Sodium sulfite is a reducing agent that alters the structure of hair; including sulfite in hair setting products, hair curvature or straightening can be regulated. In addition, to use as a hair-waiving/straightening agent, it can also function as a preservative in various cosmetic formulations [93]. Exposure to sulfites has been reported to induce a range of adverse clinical effects in sensitive individuals, ranging from allergic contact dermatitis, urticaria, flushing, and life-threatening anaphylactic and asthmatic reactions [94]. Scientific Committee on Cosmetic Products and Non-Food Products (SCCNFP) has suggested that the sulfite concentration added to cosmetic products has to be lower than 6.7 % to maintain the safety of hair settings and skin care products [95].

Conventional methods applied in industry for sulfite analysis are Monier–Williams and iodometric methods. At present, only one publication is available on the development of an electrochemical method for the analysis of sulfites in cosmetics. Chen *et al.* developed an oxygen-incorporated gold electrode by depositing gold particles on a screen-printed electrode in an aqueous solution [96]. The detection sensitivity of dissolved sulfite at the oxygen-rich gold electrode (AuOSPE) and that at oxygen-poor gold electrodes was studied by an FIA in a 0.1 M PBS (pH 6.0) at an applied potential of 0.3 V (vs. Ag/AgCl). Bisulfite is the active species in this system according to its various forms at different pH solutions. The results showed that oxygen-incorporated atoms play an important role in improving the sensitivity of the new gold electrode. The practical applicability of developed electrode

material coupled with FIA (AuOSPE/FIA) to detect selectively sulfite content in cosmetics was tested in two hair-waving products and satisfactory results were obtained.

#### Coloring agents in hair dyes

Commercial oxidative dye products form the permanent color in situ by a coupling reaction and oxidation. Permanent hair dyes are generally composed of three constituents: a precursor agent (pphenylenediamine, PPD), a coupling agent (electron-donating group substituted aromatic compounds, for example, resorcin) and an alkaline medium-based oxidizer (e.g., H<sub>2</sub>O<sub>2</sub> – ammonia mixture) [97]. Black henna, used to color the hair or skin, also contains PPD as a chromophoric constituent. At the same time, PPD is the most frequent contact sensitizer, and thus a primary patch test is recommended before using any hair dyes/henna containing PPD. The clinical findings of hair dye allergy vary and include contact dermatitis, lichen simplex chronicus, non-specific eczema and dermographism on the hair dye-exposed area or/and extended area [98]. Several experiments have shown a significant association between the use of products containing PPD and mutagenicity, according to the Scientific Committee on Consumer Products (SCCP) [99]. A safe limit for PPD in hair dye products that can provide desirable coloring with minimum body exposure to PPD needs to be carefully defined [100]. European Union Cosmetic Directive Regulation has banned PPD in topical products intended for superficial purposes while allowing PPD inclusion in cosmetic products marketed as oxidizing coloring agents with a maximum concentration of 4 % (free base). Specifically, the permitted concentration is 2 % (free base) when mixing PPD with H<sub>2</sub>O<sub>2</sub> following the preparation protocol of hair dyeing products [101,102]. The risk associated with using PPD has motivated researchers to develop new strategies and reliable analytical techniques to detect and quantify this chemical in cosmetic products to guarantee legislative requirements and ensure their safety.

Due to their similar structural and chemical characteristics for phenylenediamine isomers and dihydroxybenzenes isomers, there are few reports on detection using the electrochemical method alone. A review article that discusses the sources and toxic effects of PPD, and makes a critical comparison between conventional and electrochemical methods (reported from 1935 to 2021) to detect and quantify PPD in various samples, was presented by Singh *et al.* [97]. Table 3 summarizes the electrochemical sensors applicable in the analysis of PPD in hair dyes.

**Table 3.** Comparison of analytical parameters of electrochemical sensors for analysis of p-phenylenediamine (PPD) in hair dyes

Electrode material	Method	Linear range	LOD	Ref.
β-MnO <sub>2</sub> /CS/GCE <sup>1</sup>	Amp. <sup>5</sup>	0.2 – 150 μM	50 nM	[103]
PSC82/GCE <sup>2</sup>	Amp. <sup>5</sup>	0.5 – 2900 μM 2900 – 10400 μM	0.17 μΜ	[104]
PANI/ZnO-starch-rGO/GCE <sup>3</sup>	$DPV^6$	1 – 180 μΜ	0.1 μΜ	[105]
IL-GO@Cu-Ag/GCE⁴	$DPV^6$	0.018 – 22 μM	3.96 nM	[106]

 $^1$ B-MnO<sub>2</sub>/CS/GCE: glassy carbon electrode modified with  $\beta$ -MnO<sub>2</sub> nanowires/chitosan hydrogel;  $^2$ PSC82/GCE: Sr-doped perovskite oxide with the composition of  $Pr_{1-x}Sr_xCoO_{3-\delta}(x=0.2)$ ;  $^3$ PANI/ZnO-starch-rGO/GCE: glassy carbon electrode modified with nanocomposite "polyaniline/ZnO-anchored bio-reduced graphene oxide";  $^4$ IL-GO@Cu-Ag/GCE: glassy carbon electrode modified with bimetallic nanocomposite "ionic liquid functionalized graphene oxide wrapped Cu-Ag nanoalloy particles";  $^5$ Amp.: amperometry;  $^6$ DPV: differential pulse voltammetry.

Recently, Singh and co-authors [106] reported an efficient electrochemical sensor based on a novel bimetallic nanocomposite "ionic liquid functionalized graphene oxide wrapped Cu-Ag nanoalloy particles" modified glassy carbon electrode (IL-GO@Cu-Ag/GCE). The synergism between ionic liquid functionalized graphene oxide and Cu-Ag nanoalloy facilitated the electron transfer and

increased surface area, and therefore, excellent performance was explored with good storage stability, high sensitivity, the negligible influence of common interferents and the best limit of detection as compared to other reported works. The sensor demonstrated a high electrocatalytic effect on the oxidation of PPD at a potential of 0.21 V (vs. Ag/AgCl) in a linear concentration range of 0.018 to 22  $\mu$ M and LOD of 3.96 nM. The fabricated electrode showed good selectivity towards PPD in the presence of o-phenylenediamine, m-phenylenediamine, hydroquinone, resorcinol, ammonia and  $H_2O_2$ . Real sample analysis in spiked dye and water samples exhibited good recovery results, which established the prepared nanocomposite as an alternative for the development of an efficient electrochemical tool for PPD detection.

#### Aluminium

Aluminium compounds are often used in personal care products, including antiperspirants, lipsticks and toothpastes. In particular, the most extensively used aluminium compound in cosmetic products as an antiperspirant is aluminium chlorohydrate ( $Al_2(OH)_5Cl\times 2H_2O$ ) in various cosmetic application forms, such as aerosols, liquid/powder roll-ons, solid sticks, gels, and creams. Here, it should be noted that aluminium chlorohydrate is a cosmetic ingredient not regulated in Cosmetic Regulation 1223/2009. Other aluminium salts, such as aluminium zirconium chloride hydroxide glycine complexes, are covered by entry 50 in Annex III of the Cosmetic Regulation for use as antiperspirants with specific conditions of use.

There is convincing evidence that the use of aluminium salts-based antiperspirant products continues to increase worldwide. Recent reports indicated that continuous usage of the aluminium chlorohydrate-containing cosmetic products allows transdermal absorption of cutaneous generated hormones and pheromones and as a link to breast and prostate cancers [107]. Frequent application of aluminium salts to the underarm as an antiperspirant adds a high additional exposure directly to the local area of the human breast. Coincidentally the upper outer quadrant of the breast is where there is also a disproportionately high incidence of breast cysts and breast cancer. Aluminium has been measured in human breast tissues/fluids at higher levels than in blood, and experimental evidence suggests that at physiologically relevant concentrations, aluminium can adversely impact human breast epithelial cell biology [108].

The examination revealed that the number of published electrochemical sensors for the analysis of aluminium in cosmetics is limited. A new flow injection analysis (FIA) based electrochemical measurement using built-in three-in-one screen-printed silver electrode (SPAgE) suitable for rapid, low cost and low working volume detection of aluminium chlorohydrate has been introduced by Chiu et al. [109]. SPAgE configuration of Ag-working, Ag-counter and Ag/Ag<sub>x</sub>O (silver oxides) pseudo-reference electrodes was developed for sensitive and selective electroanalysis of aluminum chlorohydrate present in antiperspirants, through the free Cl<sup>-</sup> ion liberated from aluminum chlorohydrate in aqueous medium, as a redox signal at Ag-working electrode. The calibration graph was linear in the concentration range of 1 to 200 ppm and the limit of detection was 295 ppb aluminum chlorohydrate. The detection limit obtained is about ten times lower than that of previous work on aluminum chlorohydrate detection by linear sweep voltammetry approach (3.03 ppm) [110]. Finally, four real antiperspirant samples (in the form of roll-on liquid and lotion) assays were successfully demonstrated, with recovery values lying in the potential window of 98 to 106 %.

#### Heavy metals

Bocca *et al.* [111] reviewed the concentration of metals in different types of cosmetics manufactured and sold worldwide and the data on metals' dermal penetration and systemic

toxicology. Next year, a review article focused on the problems related to the presence of heavy metals in cosmetics, including their sources, concentrations and law regulations, as well as the danger to the health of these products users was presented by Borowska *et al.* [1]. Studies have shown that low-dose but long-term exposure to heavy metals in the human body can cause chronic poisoning, causing irreversible adverse effects on human organs and seriously threatening human health. Consequently, developing effective methods that are sensitive, highly selective and affordable for heavy metal ions detection is indispensable in the quality control of cosmetics.

Mercury (Hg) has a long history of use as a whitening agent in cosmetic products. Mercury suppresses melanin production and eliminates dead skin cells, resulting in a stereotyped slate-grey skin color [112]. Inorganic mercury can be absorbed via the sweat glands, sebaceous glands, and hair follicles, and after absorption, it is distributed to all tissues. Repeated topical applications can result in systemic toxicity, neurological disorders and kidney dysfunction. Recently, a case of mercury intoxication caused by daily-use whitening cosmetics was reported by Wang *et al.* [113].

Japan strictly prohibits the use of mercury in cosmetics. In Europe and China, the maximum concentration of mercury in cosmetic products for eyes and lips is 0.07 ppm. The Food and Drug Administration (FDA) limits the amount of mercury in cosmetics to trace amounts under 1 ppm. Nevertheless, many cosmetics contain mercury above 1000 ppm to increase the whitening effect [114]. Many studies were carried out to identify and quantify mercury in cosmetic products and detected too high mercury levels [115]. Additionally, mercury is not always listed as an ingredient in mercury-containing products; in many cosmetics, the concentration of mercury is specifically hidden in their product labels [116,117]. Monitoring the mercury ion levels in cosmetic products is therefore of fundamental importance.

Suherman *et al.* [118] presented a review article focused on recent advances in voltammetric techniques to detect ultra-trace levels of inorganic  $Hg^{2+}$  in an aqueous solution, providing an overview and a critical evaluation. It is well known that the preconcentration time required to detect trace or ultra-trace levels of  $Hg^{2+}$ , can affect analysis sensitivity and sampling frequency. Thus, an important improvement in the voltammetric analysis is decreasing the accumulation time without compromising the sensitivity, selectivity and linear range of the response.

Zen et al. [116] reported the determination of mercury in cosmetics using an in-built screen-printed three electrodes containing partially crosslinked poly(4-vinlylpyridine) (pcPVP) modified carbon working, carbon-counter, and Ag<sup>+</sup>-quasi reference electrodes (SPE/pcPVP) by means of square wave anodic stripping voltammetric (SWASV) technique. The preconcentration was performed at a fixed applied potential of -0.5 V (vs. Ag/AgCl) for 60 s. The calibration graph was linear in the window of 100 to 1000 ppb with a detection limit of 69.5 ppb. Two unbranded skin-lightening lotions were tested in parallel with inductively coupled plasma-optical emission spectroscopic (ICP-OES) measurements. Calculated recovery values were 94.29 and 98.07 %, respectively. The authors concluded that the analytical methodology is suitable for rapid and easy single-use mercury detection in cosmetic products.

A new method for selective determination of trace mercury by linear scan voltammetry using silver ink screen-printed electrode (AgSPE) in the presence of KI dissolved 0.05 M  $H_2SO_4$  solution has been demonstrated [117]. Electrooxidation of iodide at AgSPE showed a systematic increase in inhibitory current against the mercury concentration at 0 V (vs. Ag/AgCl). The linear dynamic range of 500 to 4500 ppb was established; LOD and LOQ were found to be 98 and 318 ppb, respectively. The method was considered appropriate for constructing a new detection technique without any preconcentration. Such an approach is suitable for constructing a new detection technique without any interference from arsenic, cadmium, and lead ions.

Chemically modified MWCNTs paste electrode with chloroplatinum(II) complex for the determination of mercury using square wave stripping voltammetry was presented [119]. Under optimal conditions, the linear range was from  $5.0\,\mu\text{M}$  to  $0.1\,\text{mM}$  with a LOD of  $3.7\,\mu\text{M}$ . The recovery values were between 98.9 and 101.1 %, indicating that the modified electrode was capable of the quantification of Hg²+ in the skin-lightening cosmetics.

PANI/MWCNTs/AuNP-modified ITO electrode was developed *via* direct electrodeposition of PANI, MWCNTs and AuNPs on a film-coated ITO electrode and applied to analyze mercury in cosmetic products [112]. The optimum conditions for mercury detection using the modified ITO electrode were of Tris-HCl buffer (pH 7.0) in the presence of 1 mM methylene blue (MB) as a redox indicator. The sensor response was linear from 0.01 to 10.0 ppm (LOD = 0.03 ppm), which gave a platform for the sensitive detection of mercury in real samples. However, the interference studies are inconclusive. The concentrations of mercury and the tested common substances in cosmetics are not specified. The presented graph clearly shows that some electrochemically active substances have significant interference. So the selectivity of this sensing platform remains questionable.

Lead (Pb) and cadmium (Cd) are two potentially harmful heavy metals that cause considerable concern. Lead can impair almost all the organs of the human body and causes physical and mental impairments. Lead affects the neurological, reproductive, and renal systems. Symptoms may include headaches, memory problems, reduced fertility, etc. [120]. Lead and its compounds are banned in the European Union according to Regulation (EC) No 1123/2009 of the European Parliament and of the Council of 30 November 2009 on cosmetics products under Annex II: List of Substances Prohibited in Cosmetic Products [121]. A compound of lead, lead acetate, is allowed as a colorant only in hair dyeing at concentrations lower than 0.6 % in ASEAN countries under ASEAN Cosmetics Directory (ACD) Annex III [122]. Cadmium is classified as a group I carcinogen; it can accumulate in various organs and tissues, but mostly in the kidney cortex [123]. Cadmium and its compounds are listed as substances that must not form part of the composition of cosmetic products [124].

Among cosmetic products, lipstick and eye cosmetics are most commonly used. They are produced by adding pigments that may contain heavy metals as impurities in the pigment formulation. An important non-dietary Pb exposure pathway for women is the mouthing or ingesting lip products such as lipsticks and lip glosses. Zhao and co-authors identified PbCrO<sub>4</sub> as the dominant Pb species in lip products with extremely high Pb concentrations [125]. Feizi *et al.* [123] analyzed by ICP-OES 60 samples of lipstick and eye pencil of different brands (produced by China, France, Turkey, Germany, and Korea). Mean concentrations of Pb and Cd in all the brands studied were 41.86 and 53.42  $\mu$ g g<sup>-1</sup>, respectively. The overall results showed that in all brands and colors of lipsticks, only 33 % had Pb content less than the FDA limit (20  $\mu$ g g<sup>-1</sup>) [126], and 44 % of all samples among lipsticks had Cd content less than the FDA limit of 3  $\mu$ g g<sup>-1</sup>. In eye pencils, 100 % of samples had Cd content above the recommended value of 3  $\mu$ g g<sup>-1</sup>.

In particular, kohl (also known as surma or kajal) is extensively used as traditional eye cosmetics in different countries of Africa and South Asia [127]. Kohl is applied to the conjunctival surfaces rather than to the outside of the eyelids and can cause eye damage or long-term health problems because it contains lead (galena stone, PbS) and antimony (stibnite,  $Sb_2S_3$ ). Lead is mainly responsible for kohl's toxic effects, being associated with high concentrations of this element in blood samples from regular cosmetic users. Several studies have demonstrated that Pb levels are extremely high in this product and its use has been associated with the development of plumbism. Although Pb is the main component of kohl, Sb also promotes pathological dysfunctions, and dermal and DNA strand lesions [128].

Swetha *et al.* [129] reported a novel electrochemical sensor approach based on a high-index facets (HIF)-silver nanoflower modified GCE (AgNF@GCE) for anodic stripping voltammetric detection of Pb<sup>2+</sup> in cosmetics and human blood serum. Unlike the conventional AgNPs, this platform displayed remarkable activity for sensitive and selective electrochemical analysis of Pb<sup>2+</sup> because it provides a highly crystalline and large surface area with HIFs {422} and {111}. The newly developed AgNF@ GCE system can effectively determine Pb<sup>2+</sup> in the presence of other common interfering metal ions, such as Cu<sup>2+</sup>, Fe<sup>2+</sup>, Mg<sup>2+</sup>, Ni<sup>2+</sup>, K<sup>+</sup>, and Na<sup>+</sup>. The method is defined as a promising approach for the rapid, sensitive detection of Pb<sup>2+</sup> without any complicated offline preparation of real samples.

Coated wire ion selective electrode (CW-ISE) [130], composite cork–graphite sensor (Figure 4) [131], disposable screen-printed non-single crystal silver electrode (AgSPE) [132], gold nanoparticle (AuNP)/hexaammineruthenium(III) ([Ru(NH $_3$ ) $_6$ ] $^{3+}$ )/Nafion modified GCE [133], and carbon black-modified carbon paste (CB-CP) electrode [134], were fabricated and used as working electrodes in the determination of Pb $^{2+}$  in various commercial cosmetics.

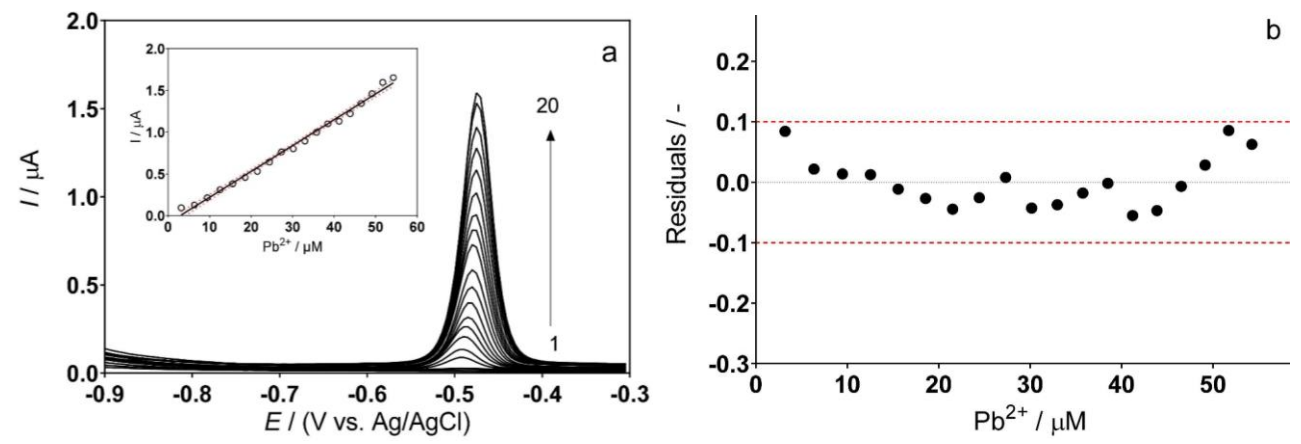


Figure 4. DPSV responses for the determination of Pb(II) using the cork—graphite sensor. (a) DPSV curves recorded for different concentrations of Pb(II) in 0.1M acetate buffer (pH 4.5): (1) 0, supporting electrolyte; (2) 3.19; (3) 6.35; (4) 9.46; (5) 12.53; (6) 15.57; (7) 18.56; (8) 21.51; (9) 24.43; (10) 27.31; (11) 30.16; (12) 32.92; (13) 35.75; (14) 38.49; (15) 41.19; (16) 43.87; (17) 46.51; (18) 49.13; (19) 51.70 and (20) 54.26 μM. Inset: plot of the electrochemical response, in terms of current, as a function of lead concentration. (b) Graphical representation of the residuals behavior, which confirms the linearity of the calibration curve. Reproduced from Ref. [131]. Licensee MDPI, Basel, Switzerland (2022)

A comprehensive elucidation of the recent developments in the electrochemical detection of Cd<sup>2+</sup> was presented by Yi *et al.* [135]. The determination of Cd<sup>2+</sup> at trace and ultra-trace levels in environmental water samples by means of electrochemical methods was discussed in details. However, there hasn't yet been a published electroanalytical method for Cd<sup>2+</sup> alone in cosmetics.

It is a challenging task to simultaneously, reliably and conveniently measure heavy metal ions in complex samples, such as cosmetics. New strategies were presented by de Furtado  $et\ al.$  [136] for the simultaneous voltammetric quantification of Pb<sup>2+</sup> and Zn<sup>2+</sup> in hair cosmetics (color wash lotion and anti-dandruff shampoo) employing chemically modified composite electrodes. Two methods for simultaneous determination of Pb<sup>2+</sup>, Zn<sup>2+</sup> and Cd<sup>2+</sup>, with a cheap and easy to fabricate graphite-epoxy composite electrode, were developed. One method uses an *in situ* bismuth film modification and the other uses an *ex situ* organic film modification via diazonium salt reduction. Determinations were carried out in acetate buffer (pH 6.0) with a deposition potential of -1.4 V (applied during 120 s), followed by SWV measurements and subsequent cleaning with an application of 0.3 V potential. Detection limits of 0.07, 0.05 and 0.06  $\mu$ M were achieved for Pb<sup>2+</sup>, Cd<sup>2+</sup> and Zn<sup>2+</sup>, respectively. The data were compared to those found by applying flame atomic absorption spectrometry (FAAS), being

considered statistically equivalent. The results are remarkable, considering that the cosmetic samples tested are quite complex, especially due to the greasy content and high concentration of surfactants. In summary, a comparison of various sensors applied to the electroanalysis of heavy metals in cosmetics is shown in Table 4.

**Table 4.** Comparison of analytical parameters of the electrochemical sensors for determination of  $Hg^{2+}$  and  $Pb^{2+}$  in cosmetics

Analyte	Electrode material	Method	Linear range	LOD	Real sample	Ref.
Hg <sup>2+</sup>	SPE/pcPVP <sup>1</sup>	SWASV <sup>7</sup>	100 – 1000 ppb	69.5 ppb	skin-	[116]
	AgSPE <sup>2</sup>	LSV <sup>8</sup>	500 – 4500 ppb	98 ppb	lightening	[117]
	CPC/MWCNTs/PE <sup>3</sup>	SWASV <sup>7</sup>	$5.0  \mu M - 0.1  mM$	3.7 μΜ	cosmetics	[119]
Pb <sup>2+</sup>	AgNF@GCE⁴	ASV <sup>9</sup>	10 – 700 ppb	0.74 ppb	eyeliner,	[129]
					lipstick	
	CW-ISE <sup>5</sup>	Pot. <sup>10</sup>	10 – 100 μM	8.0 μΜ	lipstick	[130]
	Cork-graphite	DPSV <sup>11</sup>	3.19 – 54.26 μM	1.06 μΜ	_	[131]
	AgSPE	SWV <sup>12</sup>	0.06 – 0.79 μM	0.31 nM	- hair dyes	[132]
	AuNPs([Ru(NH <sub>3</sub> ) <sub>6</sub> ] <sup>3+</sup> )Nafion/GCE	ASV <sup>9</sup>	0.3 – 0.75 ppm	0.045 ppm	liali uyes	[133]
	CB-CP <sup>6</sup>	DPV <sup>13</sup>	0.04 – 3.2 μg	4 ng		[134]

<sup>1</sup>SPE/pcPVP: an in-built screen-printed three electrodes containing partially crosslinked poly(4-vinlylpyridine) modified carbon working, carbon-counter, and Ag<sup>+</sup>-quasireference electrodes; <sup>2</sup>AgSPE: silver ink screen-printed electrode; <sup>3</sup>CPC/MWCNTs/PE: chloroplatinum (II) complex-modified MWCNTs paste electrode; <sup>4</sup>AgNF@GCE: silver nanoflower modified glassy carbon electrode; <sup>5</sup>CW-ISE: coated wire ion selective electrode; <sup>6</sup>CB-CP: carbon black-modified carbon paste; <sup>7</sup>SWASV: square wave anodic stripping voltammetry; <sup>8</sup>LSV: linear scan voltammetry; <sup>9</sup>ASV: anodic stripping voltammetry; <sup>10</sup>Pot.: potentiometry; <sup>11</sup>DPSV: differential pulse stripping voltammetry; <sup>12</sup>SWV: square wave voltammetry; <sup>13</sup>DPV: differential pulse voltammetry.

Wang *et al.* [137] reported the first simultaneous analysis of mercury, lead, and arsenic (As) in cosmetics based on the electrochemical method. A disposable cost-effective gold-sputtered plastic electrode was used for the simultaneous detection of  $Pb^{2+}$ ,  $As^{3+}$ , and  $Hg^{2+}$  in cosmetics based on differential pulse stripping voltammetry (DPSV). Under the optimized conditions, the DPSV peaks of these three metal ions could be well and reproducibly separated with satisfactory linear range and low detection limits of 2, 5 and 0.5  $\mu$ g L<sup>-1</sup> for  $Pb^{2+}$ ,  $As^{3+}$ , and  $Hg^{2+}$ , respectively. The method was successfully applied for the simultaneous determination of three target ions in real cosmetic samples (eye shadow, skin lotion and talcum powder) with satisfactory results. Noting the low cost and convenient fabrication of the plastic-based sensors, the authors concluded that this approach might serve as an attractive alternative to conventional methods in routine analysis of those trace heavy metal ions in cosmetics.

#### **Conclusion remarks**

Considering that the use of cosmetic and personal care products in daily life has increased globally, it is important for researchers to keep on improving the performance of existing analytical methodologies, as well as developing innovative solutions. As the demand for cost-effective, rapid, highly selective and ultrasensitive quantification of various cosmetics ingredients rapidly increases, the electroanalytical methods provide a feasible path toward the next generation of reliable sensing devices (Figure 5).



Figure 5. Cosmetic ingredients considered for electrochemical analysis

The miniaturization potential of electrochemical systems attracts increasing research attention because electronic measurements can be integrated in hand-held devices and smartphones, which would allow fast, accurate, and on-site detection.

#### Perspectives

The large number of applications discussed in the present article clearly demonstrates the feasibility and utility of electrochemical sensors for analyzing ingredients in real cosmetics samples. After a thorough critical review of previous research studies, the following challenges were identified as priorities for the development of new advanced electroanalytical devices for the quality control of cosmetics.

- Considering the high matrix complexity of cosmetic samples, effective approaches should be developed to suppress the non-specific adsorption of interfering species.
- Currently, nanotechnology in the field of electrochemical sensors has been a crucial strategy
  for constructing reliable monitoring systems for cosmetic products safety. Future
  developments in electrochemical design will inevitably focus on the technology of new
  nanomaterials to improve the selectivity, reproducibility and operational stability of the
  sensor systems.
- Using easy and low-cost fabrication methods for mass production while maintaining the accuracy and precision achieved within a laboratory environment.
- The review showed that mainly single analyte methods had been proposed. Regarding the
  variety of ingredients considered for analytical control, the multianalyte arrays will be much
  more useful in real cosmetic analysis. Such sensor systems provide a simple, simultaneous
  multianalyte assay with a short analytical time.
- Producing portable and commercially available electroanalytical devices in order to extend their applications in extra-laboratory areas.

**Conflicts of interest:** The authors declare no conflict of interest.

#### References

- [1] S. Borowska, M.M. Brzóska, Metals in cosmetics: implications for human health, *Journal of Applied Toxicology* **35** (2015) 551-572. <a href="https://doi.org/10.1002/jat.3129">https://doi.org/10.1002/jat.3129</a>
- [2] A. Salvador, A. Chisvert, *Analysis of Cosmetic Products*, Elsevier, Amsterdam, The Netherlands, 2017. <a href="https://doi.org/10.1016/B978-0-444-63508-2.00016-3">https://doi.org/10.1016/B978-0-444-63508-2.00016-3</a>

- [3] H. Karimi-Maleh, R. Darabi, M. Shabani-Nooshabadi, M. Baghayeri, F. Karimi, J. Rouhi, M. Alizadeh, O. Karaman, Y. Vasseghian, C. Karaman, Determination of D&C Red 33 and Patent Blue V Azo dyes using an impressive electrochemical sensor based on carbon paste electrode modified with ZIF-8/g-C<sub>3</sub>N<sub>4</sub>/Co and ionic liquid in mouthwash and toothpaste as real samples, *Food and Chemical Toxicology* **162** (2022) 112907. <a href="https://doi.org/10.1016/j.fct.2022.112907">https://doi.org/10.1016/j.fct.2022.112907</a>
- [4] M. Lores, M. Llompart, G. Alvarez-Rivera, E. Guerra, M. Vila, M. Celeiro, J.P. Lamas, C. Garcia-Jares, Positive lists of cosmetic ingredients: Analytical methodology for regulatory and safety controls—A review, *Analytica Chimica Acta* 915 (2016) 1-26. <a href="https://doi.org/10.1016/j.aca.2016.02.033">https://doi.org/10.1016/j.aca.2016.02.033</a>
- [5] H. Karimi-Maleh, H. Beitollahi, P. Senthil Kumar, S. Tajik, P. M. Jahani, F. Karimi, C. Karaman, Y. Vasseghian, M. Baghayeri, J. Rouhi, P. L. Show, S. Rajendran, L. Fu, N. Zare, Recent advances in carbon nanomaterials-based electrochemical sensors for food azo dyes detection, *Food and Chemical Toxicology* 164 (2022) 112961. https://doi.org/10.1016/j.fct.2022.112961
- [6] Y. Feng, Y. Li, Y. Tong, C. Cui, X. Li, B.-C. Ye, Simultaneous determination of dihydroxybenzene isomers in cosmetics by synthesis of nitrogen-doped nickel carbide spheres and construction of ultrasensitive electrochemical sensor, *Analytica Chimica Acta* **1176** (2021) 338768. https://doi.org/10.1016/j.aca.2021.338768
- [7] B. S. Lynch, E. S. Delzell, D. H. Bechtel, Toxicology review and risk assessment of resorcinol: Thyroid effects, Regulatory Toxicology and Pharmacology 36 (2002) 198-210. <a href="https://doi.org/10.1006/rtph.2002.1585">https://doi.org/10.1006/rtph.2002.1585</a>
- [8] Regulation (EC) No 1223/2009 of the European Parliament and of the Council, of 30 November 2009, on Cosmetic Products. *Off. J. Eur. Union* 2009. <a href="https://eur-lex.europa.eu/legal-content/EN/ALL/?uri=celex%3A32009R1223">https://eur-lex.europa.eu/legal-content/EN/ALL/?uri=celex%3A32009R1223</a> (Accessed on August 30, 2022).
- [9] S. Cotchim, K. Promsuwan, M. Dueramae, S. Duerama, A. Dueraning, P. Thavarungkul, P. Kanatharana, W. Limbut, Development and Application of an Electrochemical Sensor for Hydroquinone in Pharmaceutical Products, *Journal of The Electrochemical Society*, 167 (2020) 155528. <a href="https://doi.org/10.1149/1945-7111/abd0cd">https://doi.org/10.1149/1945-7111/abd0cd</a>
- [10] Y. Olumide, A. Akinkugbe, D. Altraide, T. Tahir, N. Ahamefule, S. Ayanlowo, C. Onyekonwu, N. Essen, Complications of chronic use of skin lightening cosmetics, *International Journal of Dermatology* 47 (2008) 344-53. <a href="https://doi.org/10.1111/j.1365-4632.2008.02719.x">https://doi.org/10.1111/j.1365-4632.2008.02719.x</a>
- [11] S. Aydar, D. E. Bayraktepe, H. Filik, Z. Yazan, A Nano-Sepiolite Clay Electrochemical Sensor for the Rapid Electro–Catalytic Detection of Hydroquinone in Cosmetic Products, *Acta Chimica Slovenica* **65** (2018) 946-954. <a href="http://dx.doi.org/10.17344/acsi.2018.4615">http://dx.doi.org/10.17344/acsi.2018.4615</a>
- [12] A. Ferrari, S. Rowley-Neale, C. Banks, Screen-printed electrodes: Transitioning the laboratory in-to-the field, *Talanta Open* **3** (2021) 100032. https://doi.org/10.1016/j.talo.2021.100032
- [13] S. Cinti, F. Arduini, Graphene-based screen-printed electrochemical (bio)sensors and their applications: Efforts and criticisms, *Biosensors and Bioelectronics* **89** (2017) 107-122. <a href="https://doi.org/10.1016/j.bios.2016.07.005">https://doi.org/10.1016/j.bios.2016.07.005</a>
- [14] W. Duekhuntod, C. Karuwan, A. Tuantranont, D. Nacapricha, S. Teerasong, A Screen Printed Graphene Based Electrochemical Sensor for Single Drop Analysis of Hydroquinone in Cosmetic Products, *International Journal of Electrochemical Science* **14** (2019) 7631-7642. <a href="https://doi.org/10.20964/2019.08.94">https://doi.org/10.20964/2019.08.94</a>
- [15] H.-H. Yang, H.-H.Ting, Y. Shih, Self-validated detection of hydroquinone in medicated cosmetic products using a preanodized screen-printed ring disk carbon electrode, *Analytical Methods* **8** (2016) 5495-5502. <a href="https://doi.org/10.1039/C6AY01000H">https://doi.org/10.1039/C6AY01000H</a>



- [16] M. Harsini, U. Untari, E. Fitriany, A. N. Farida, M. Z. Fahmi, S.C.W. Sakti, G. Pari, Voltammetric analysis of hydroquinone in skin whitening cosmetic using ferrocene modified carbon paste electrode, *Rasāyan Journal of Chemistry* **12** (2019) 2296-2305. <a href="http://dx.doi.org/10.31788/RJC.2019.1245479">http://dx.doi.org/10.31788/RJC.2019.1245479</a>
- [17] G. Manasa, A. K. Bhakta, Z. Mekhalif, R. J. Mascarenhas, Voltammetric Study and Rapid Quantification of Resorcinol in Hair Dye and Biological Samples Using Ultrasensitive Maghemite/MWCNT Modified Carbon Paste Electrode, *Electroanalysis* **31** (2019) 1363. <a href="https://doi.org/10.1002/elan.201900143">https://doi.org/10.1002/elan.201900143</a>
- [18] N. M. A. Edris, Y. Sulaiman, Ultrasensitive voltammetric detection of benzenediol isomers using reduced graphene oxide-azo dye decorated with gold nanoparticles, Ecotoxicology and Environmental Safety 203 (2020) 111026. <a href="https://doi.org/10.1016/j.ecoenv.2020.111026">https://doi.org/10.1016/j.ecoenv.2020.111026</a>
- [19] N. Butwong, S. Srijaranai, J. D. Glennon, J. H. T. Luong, Cysteamine Capped Silver Nanoparticles and Single-walled Carbon Nanotubes Composite Coated on Glassy Carbon Electrode for Simultaneous Analysis of Hydroquinone and Catechol, *Electroanalysis* 30 (2018) 962-968. <a href="https://doi.org/10.1002/elan.201700704">https://doi.org/10.1002/elan.201700704</a>
- [20] T. Dodevska, D. Hadzhiev, I. Shterev, Y. Lazarova, Application of biosynthesized metal nanoparticles in electrochemical sensors: Review, *Journal of the Serbian Chemical Society* **87** (2022) 401-435. https://doi.org/10.2298/JSC200521077D
- [21] J. A. Buledi, S. Ameen, N. H. Khand, A. R. Solangi, I. H. Taqvi, M. H. Agheem, Z. Wajdan, CuO Nanostructures Based Electrochemical Sensor for Simultaneous Determination of Hydroquinone and Ascorbic Acid, *Electroanalysis* 32 (2020) 1600. <a href="https://doi.org/10.1002/elan.202000083">https://doi.org/10.1002/elan.202000083</a>
- [22] A. Domínguez-Aragón, R. B. Dominguez, E. A. Zaragoza-Contreras, Simultaneous Detection of Dihydroxybenzene Isomers Using Electrochemically Reduced Graphene Oxide-Carboxylated Carbon Nanotubes/Gold Nanoparticles Nanocomposite, *Biosensors* **11** (2021) 321. <a href="https://doi.org/10.3390/bios11090321">https://doi.org/10.3390/bios11090321</a>
- [23] K. Saha, S. S. Agasti, C. Kim, X. Li, V. M. Rotello, Gold Nanoparticles in Chemical and Biological Sensing, *Chemical Reviews* **112** (2012) 2739-2779. https://doi.org/10.1021/cr2001178
- [24] S. A. Shahamirifard, M. Ghaedi, A new electrochemical sensor for simultaneous determination of arbutin and vitamin C based on hydroxyapatite-ZnO-Pd nanoparticles modified carbon paste electrode, *Biosensors and Bioelectronics* **141** (2019) 111474. https://doi.org/10.1016/j.bios.2019.111474
- [25] S.A. Barutçu, D.E. Bayraktepe, Z. Yazan, K. Polat, F. Hayati, Investigation of electrochemical oxidation mechanism, rapid and low-level determination for whitening cosmetic: arbutin in aqueous solution by nano sepiolite clay, *Chemical Papers* **75** (2021) 3483-3491. https://doi.org/10.1007/s11696-021-01581-3
- [26] J.-M. Zen, H.-H. Yang, M.-H. Chiu, C.-H. Yang, Y. Shih, Selective Determination of Arbutin in Cosmetic Products Through Online Derivatization Followed by Disposable Electrochemical Sensor, *Journal of AOAC International* 94 (2011) 985-990. <a href="https://doi.org/10.1093/jaoac/94.3.985">https://doi.org/10.1093/jaoac/94.3.985</a>
- [27] A. Khatoon, J.A. Syed, J.A. Buledi, S. Shakeel, A. Mallah, A.R. Solangi, Sirajuddin, S.T.H. Sherazi, M.R. Shah, Bio-green fabrication of bell pepper mediated silver nanoparticles: an efficient material for electrochemical sensing of arbutin in cosmetics, *Journal of the Iranian Chemical Society* **19** (2022) 3659-3672. <a href="https://doi.org/10.1007/s13738-022-02558-z">https://doi.org/10.1007/s13738-022-02558-z</a>
- [28] Scientific Committee on Safety (SCCS). Opinion on oxidative hair dye substances and hydrogen peroxide used in products to colour eyelashes. Brussels, Belgium, European Commission. 2012. Report No. SCCS/1475/12. pp. 1-21. <a href="http://ec.europa.eu/health/scientific committees/consumer safety/docs/sccs">http://ec.europa.eu/health/scientific committees/consumer safety/docs/sccs o 111.pdf</a>

- [29] A. Müller, S. Sachse, M. Decker, F.-M. Matysik, W. Vonau, Comparison of H<sub>2</sub>O<sub>2</sub> screen-printed sensors with different Prussian blue nanoparticles as electrode material, *Journal of Electrochemical Science and Engineering* **10** (2020) 199-207. https://doi.org/10.5599/jese.719
- [30] S. Chen, R. Yuan, Y. Chai, F. Hu, Electrochemical sensing of hydrogen peroxide using metal nanoparticles, *Microchimica Acta* **180** (2013) 15-32. <a href="https://doi.org/10.1007/s00604-012-0904-4">https://doi.org/10.1007/s00604-012-0904-4</a>
- [31] K. Dhara, D. R. Mahapatra, Recent advances in electrochemical nonenzymatic hydrogen peroxide sensors based on nanomaterials: a review, *Journal of Materials Science* **54** (2019) 12319-12357. <a href="https://doi.org/10.1007/s10853-019-03750-y">https://doi.org/10.1007/s10853-019-03750-y</a>
- [32] H. Shamkhalichenar, J.-W. Choi. Review—Non-Enzymatic Hydrogen Peroxide Electrochemical Sensors Based on Reduced Graphene Oxide, *Journal of The Electrochemical Society* **167** (2020) 037531. https://doi.org/10.1149/1945-7111/ab644a
- [33] M. A. Riaz, Y. Chen, Electrodes and electrocatalysts for electrochemical hydrogen peroxide sensors: a review of design strategies, *Nanoscale Horizons* **7** (2022) 463-479. https://doi.org/10.1039/D2NH00006G
- [34] K. Atacan, M. Özacar. Construction of a non-enzymatic electrochemical sensor based on CuO/g-C<sub>3</sub>N<sub>4</sub> composite for selective detection of hydrogen peroxide, *Materials Chemistry and Physics* **266** (2021) 124527. https://doi.org/10.1016/j.matchemphys.2021.124527
- [35] M.-H. Chiu, A. S. Kumar, S. Sornambikai, P.-Y. Chen, Y. Shih, J.-M. Zen, Cosmetic Hydrogen Peroxide Detection Using Nano Bismuth Species Deposited Built-in Three-in-One Screen-Printed Silver Electrode, *International Journal of Electrochemical Science* **6** (2011) 2352-2365. http://www.electrochemsci.org/papers/vol6/6072352.pdf
- [36] A. Benvidi, M. T. Nafar, S. Jahanbani, M. D. Tezerjani, M. Rezaeinasab, S. Dalirnasab, Developing an electrochemical sensor based on a carbon paste electrode modified with nano-composite of reduced graphene oxide and CuFe<sub>2</sub>O<sub>4</sub> nanoparticles for determination of hydrogen peroxide, *Materials Science and Engineering C* **75** (2017) 1435-1447. <a href="https://doi.org/10.1016/j.msec.2017.03.062">https://doi.org/10.1016/j.msec.2017.03.062</a>
- [37] I. Mihailova, V. Gerbreders, M. Krasovska, E. Sledevskis, V. Mizers, A. Bulanovs, A. Ogurcovs, A non-enzymatic electrochemical hydrogen peroxide sensor based on copper oxide nanostructures, *Beilstein Journal of Nanotechnology* **13** (2022) 424-436. <a href="https://doi.org/10.3762/bjnano.13.35">https://doi.org/10.3762/bjnano.13.35</a>
- [38] V. Katic, P. L. dos Santos, M. F. dos Santos, B. M. Pires, H. C. Loureiro, A. P. Lima, J. C. M. Queiroz, R. Landers, R. A. A. Muñoz, J. A. Bonacin, 3D Printed Graphene Electrodes Modified with Prussian Blue: Emerging Electrochemical Sensing Platform for Peroxide Detection, ACS Applied Materials and Interfaces 11 (2019) 35068-35078. https://doi.org/10.1021/acsami.9b09305
- [39] D. Ye, Y. Xu, L. Luo, Y. Ding, Y. Wang, X. Liu, L. Xing, J. Peng, A novel non-enzymatic hydrogen peroxide sensor based on LaNi<sub>0.5</sub>Ti<sub>0.5</sub>O<sub>3</sub>/CoFe<sub>2</sub>O<sub>4</sub> modified electrode, *Colloids and Surfaces B* **89** (2012) 10-14. <a href="https://doi.org/10.1016/j.colsurfb.2011.08.014">https://doi.org/10.1016/j.colsurfb.2011.08.014</a>
- [40] G. L. Luque, N. F. Ferreyra, A. G. Leyva, G. A. Rivas, Characterization of carbon paste electrodes modified with manganese based perovskites-type oxides from the amperometric determination of hydrogen peroxide, *Sensors and Actuators B* **142** (2009) 331-336. <a href="https://doi.org/10.1016/j.snb.2009.07.038">https://doi.org/10.1016/j.snb.2009.07.038</a>
- [41] Z. Zhang, S. Gu, Y. Ding, J. Jin, A novel nonenzymatic sensor based on LaNi<sub>0.6</sub>Co<sub>0.4</sub>O<sub>3</sub> modified electrode for hydrogen peroxide and glucose, *Analytica Chimica Acta* **745** (2012) 112-117. https://doi.org/10.1016/j.aca.2012.07.039



- [42] D. Xu, L. Li, Y. Ding, S. Cui, Electrochemical hydrogen peroxide sensors based on electrospun La<sub>0.7</sub>Sr<sub>0.3</sub>Mn<sub>0.75</sub>Co<sub>0.25</sub>O<sub>3</sub> nanofiber modified electrodes, *Analytical Methods* **7** (2015) 6083-6088. https://doi.org/10.1039/c5ay01131k
- [43] S. Michalkiewicz, A. Skorupa, M. Jakubczyk, Carbon Materials in Electroanalysis of Preservatives, *Materials* **14** (2021) 7630-7653. <a href="https://doi.org/10.3390/ma14247630">https://doi.org/10.3390/ma14247630</a>
- [44] F. Z. Kashani, S. M. Ghoreishi, A. Khoobi, Experimental and statistical analysis on a nanostructured sensor for determination of p-hydroxybenzoic acid in cosmetics, *Materials Science and Engineering: C* **94** (2019) 45-55. <a href="https://doi.org/10.1016/j.msec.2018.08.068">https://doi.org/10.1016/j.msec.2018.08.068</a>
- [45] F. Z. Kashani, S. M. Ghoreishi, A. Khoobi, M. Enhessari, A carbon paste electrode modified with a nickel titanate nanoceramic for simultaneous voltammetric determination of *ortho*-and *para*-hydroxybenzoic acids, *Microchimica Acta* **186** (2019) 12. https://doi.org/10.1007/s00604-018-3113-y
- [46] K. Charoenkitamorn, W. Siangproh, O. Chailapakul, M. Oyama, S. Chaneam, Simple Portable Voltammetric Sensor Using Anodized Screen-Printed Graphene Electrode for the Quantitative Analysis of *p*-Hydroxybenzoic Acid in Cosmetics, *ACS Omega* **7** (2022) 16116-16126. https://doi.org/10.1021/acsomega.2c01434
- [47] K. M. Naik, S.T. Nandibewoor, Electroanalytical method for the determination of methylparaben, Sensors and Actuators A 212 (2014) 127-132. https://doi.org/10.1016/j.sna.2014.03.033
- [48] M. Behpour, S. Masoum, A. Lalifar, A. Khoobi, A novel method based on electrochemical approaches andmultivariate calibrations for study and determination of methylparaben in the presence of unexpected interferencein cosmetics, *Sensors and Actuators B* **214** (2015) 10-19. http://dx.doi.org/10.1016/j.snb.2015.03.003
- [49] P. D. Darbre, Underarm cosmetics and breast cancer, *Journal of Applied Toxicology* **23** (2003) 89-95. <a href="https://doi.org/10.1002/jat.899">https://doi.org/10.1002/jat.899</a>
- [50] P. Harvey, Parabens, oestrogenicity, underarm cosmetics and breast cancer: a perspective on a hypothesis, *Journal of Applied Toxicology* **23** (2003) 285-288. https://doi.org/10.1002/jat.946
- [51] S. Oishi, Effects of propyl paraben on the male reproductive system, *Food and Chemical Toxicology* **40** (2002) 1807-1813. <a href="https://doi.org/10.1016/s0278-6915(02)00204-1">https://doi.org/10.1016/s0278-6915(02)00204-1</a>
- [52] J. J. Prusakiewicz, H. M. Harville, Y. H. Zhang, C. Ackermann, R. L. Voorman, Parabens inhibit human skin estrogen sulfotransferase activity: possible link to paraben estrogenic effects, *Toxicology* **232** (2007) 248-256. <a href="https://doi.org/10.1016/j.tox.2007.01.010">https://doi.org/10.1016/j.tox.2007.01.010</a>
- [53] R. S. Tavares, F. C. Martins, P. J. Oliveira, J. Santosa, F. P. Peixoto, Parabens in male infertility-is there a mitochondrial connection, *Reproductive Toxicology* 27 (2009) 1-7. https://doi.org/10.1016/j.reprotox.2008.10.002
- [54] Y. Okamoto, T. Hayashi, S. Matsunami, K. Ueda, N. Kojima N. Combined activation of methyl paraben by light irradiation and esterase metabolism toward oxidative DNA damage, *Chemical Research in Toxicology* 21 (2008) 1594-1603. <a href="https://doi.org/10.1021/tx800066u">https://doi.org/10.1021/tx800066u</a>
- [55] Regulation (EC). No 1223/2009 of the European Parliament and of the Council, of 30 November 2009, on Cosmetic Products. Off. J. Eur. Union 2009. ANNEX V, p. 136. <a href="https://eur-lex.europa.eu/legal-content/EN/ALL/?uri=celex%3A32009R1223">https://eur-lex.europa.eu/legal-content/EN/ALL/?uri=celex%3A32009R1223</a> (Acessed on August 30, 2022).
- [56] C. D. Mendonça, T. M. Prado, F. H. Cincotto, R. T. Verbinnen, S. A. S. Machadop, Methylparaben Quantification Via Electrochemical Sensor Based On Reduced Graphene Oxide Decorated With Ruthenium Nanoparticles, *Sensors and Actuators B* 251 (2017) 739-745. <a href="http://dx.doi.org/10.1016/j.snb.2017.05.083">http://dx.doi.org/10.1016/j.snb.2017.05.083</a>

- [57] L. F. de Lima, M. D. Cristiane, M. M. Celina, A. P. Elisabete, F. Marystela, Layer-by-Layer nanostructured films of magnetite nanoparticles and polypyrrole towards synergistic effect on methylparaben electrochemical detection, *Applied Surface Science* **505** (2020) 144278. <a href="https://doi.org/10.1016/j.apsusc.2019.144278">https://doi.org/10.1016/j.apsusc.2019.144278</a>
- [58] L. F. de Lima, E. A. Pereira, M. Ferreira, Electrochemical sensor for propylparaben using hybrid Layer-by-Layer films composed of gold nanoparticles, poly(ethylene imine) and nickel(II) phthalocyanine tetrasulfonate, *Sensors and Actuators B* **310** (2020) 127893. <a href="https://doi.org/10.1016/j.snb.2020.127893">https://doi.org/10.1016/j.snb.2020.127893</a>
- [59] Y. Wang, Y. Cao, C. Fang, Q. Gong, Electrochemical sensor for parabens based on molecular imprinting polymers with dual-templates, *Analytica Chimica Acta* 673 (2010) 145-150 <a href="https://doi.org/10.1016/j.aca.2010.05.039">https://doi.org/10.1016/j.aca.2010.05.039</a>
- [60] P. Luo, J. Liu, Y. Li, Y. Miao, B. Ye, Voltammetric Determination of Methylparaban in Cosmetics Using a Multi-Wall Carbon Nanotubes/Nafion Composite Modified Glassy Carbon Electrode, *Analytical Letters* 45 (2012) 2445-2454. https://doi.org/10.1080/00032719.2012.691589
- [61] M. Soysal, An Electrochemical Sensor Based on Molecularly Imprinted Polymer for Methyl Paraben Recognition and Detection, *Journal of Analytical Chemistry* **76** (2021) 381-389. https://doi.org/10.1134/S1061934821030114
- [62] S. Guo, X. Wu, J. Zhou, J. Wang, B. Yang, B. Ye, MWNT/Nafion Composite Modified Glassy Carbon Electrode as the Voltammetric Sensor for Sensitive Determination of 8-Hydroxyquinoline in Cosmetic, *Journal of Electroanalytical Chemistry* **656** (2011) 45-49. https://doi.org/10.1016/j.jelechem.2011.02.010
- [63] T. T. Calam, E. B. Yılmaz, Electrochemical determination of 8-hydroxyquinoline in a cosmetic product on a glassy carbon electrode modified with 1-amino-2-naphthol-4-sulphonic acid, *Instrumentation Science and Technology* 49 (2021) 1-20. <a href="https://doi.org/10.1080/10739149.2020.1765175">https://doi.org/10.1080/10739149.2020.1765175</a>
- [64] Z. Gao, Q. Zeng, M. Wang, L. Wang, Sensitive Detection of 8-Hydroxyquinoline in Cosmetics by Using a Poly(tannic acid)-Modified Glassy Carbon Electrode, *ChemistrySelect* 7 (2022) e202200257. <a href="https://doi.org/10.1002/slct.202200257">https://doi.org/10.1002/slct.202200257</a>
- [65] L. Fotouhi, H. R. Shahbaazi, A. Fatehi, M. M. Heravi, Voltammetric Determination of Triclosan in Waste Water and Personal Care Products, *International Journal of Electrochemical Science* 5 (2010) 1390-1398. <a href="http://www.electrochemsci.org/papers/vol5/5091390.pdf">http://www.electrochemsci.org/papers/vol5/5091390.pdf</a>
- [66] Regulation (EC). No 1223/2009 of the European Parliament and of the Council, of 30 November 2009, on Cosmetic Products. Off. J. Eur. Union 2009. ANNEX V, p. 138. <a href="https://eur-lex.europa.eu/legal-content/EN/ALL/?uri=celex%3A32009R1223">https://eur-lex.europa.eu/legal-content/EN/ALL/?uri=celex%3A32009R1223</a> (Accessed on August 30, 2022).
- [67] A. Saljooqi, T. Shamspur, A. Mostafavi, A Sensitive Electrochemical Sensor Based on Graphene Oxide Nanosheets Decorated by Fe<sub>3</sub>O<sub>4</sub>@AuNanostructure Stabilized on Polypyrrole for Efficient Triclosan Sensing, *Electroanalysis* **32** (2020) 1297-1303. https://doi.org/10.1002/elan.201900634
- [68] V. R. Sri, R. Shwetharani, J. Mohammed, A. Mabkhoot, R. G. Balakrishna, F. A. Harraz, Review on Electrochemical Sensing of Triclosan using Nanostructured Semiconductor Materials, ChemElectroChem 9 (2022) e202101664. <a href="https://doi.org/10.1002/celc.202101664">https://doi.org/10.1002/celc.202101664</a>
- [69] R. M. Pemberton, J. P. Hart, Electrochemical behaviour of triclosan at a screen-printed carbon electrode and its voltammetric determination in toothpaste and mouthrinse products, *Analytica Chimica* Acta **390** (1999) 107-115. <a href="https://doi.org/10.1016/s0003-2670(99)00194-4">https://doi.org/10.1016/s0003-2670(99)00194-4</a>



- [70] J. Yang, P. Wang, X. Zhang, K. Wu, Electrochemical sensor for rapid detection of triclosan using a multiwall carbon nanotube film, *Journal of Agricultural and Food Chemistry* **57** (2009) 9403-9407. https://doi.org/10.1021/jf902721r
- [71] H. Dai, G. Xu, L. Gong, C. Yang, Y. Lin, Y. Tong, J. Chen, G. Chen, Electrochemical detection of triclosan at a glassy carbon electrode modifies with carbon nanodots and chitosan, *Electrochimica Acta* **80** (2012) 362-367. https://doi.org/10.1016/j.electacta.2012.07.032
- [72] Y. L. Su, H. C. You, S. H. Cheng, C. Y. Lin, Fabrication of bacteriochlorin shell/gold core nanoparticles for the sensitive determination of trichlosan using differential pulse voltammetry, *Analytica Chimica Acta* **1123** (2020) 44-55. <a href="https://doi.org/10.1016/j.aca.2020.04.070">https://doi.org/10.1016/j.aca.2020.04.070</a>
- [73] N. D. Luyen, T. T. T. Toan, H. T. Trang, V. T. Nguyen, L. V. T. Son, T. S. Thanh, N. M. Thanh, P. T. Quy, D. Q. Khieu, D. T. Nguyen, Electrochemical Determination of Triclosan Using ZIF-11/Activated Carbon Derived from the Rice Husk Modified Electrode, *Journal of Nanomaterials* 2021 (2021) 8486962. https://doi.org/10.1155/2021/8486962
- [74] Scientific Committee on Consumer Safety SCCS OPINION ON Zinc Pyrithione (ZPT) (CAS No 13463-41-7) Submission III, p. 25. <a href="https://ec.europa.eu/health/document/download/aa535110-c020-4924-8507-5f867adc9972">https://ec.europa.eu/health/document/download/aa535110-c020-4924-8507-5f867adc9972</a> en
- [75] Regulation (EC). No 1223/2009 of the European Parliament and of the Council, of 30 November 2009, on Cosmetic Products. Off. J. Eur. Union 2009. ANNEX V, p. 135. <a href="https://eur-lex.europa.eu/legal-content/EN/ALL/?uri=celex%3A32009R1223">https://eur-lex.europa.eu/legal-content/EN/ALL/?uri=celex%3A32009R1223</a> (Accessed on August 30, 2022).
- [76] L. H. Wang, Determination of Zinc Pyrithione in Hair Care Products on Metal Oxides Modified Carbon Electrodes, *Electroanalysis* 12 (2000) 227-232. <a href="https://doi.org/10.1002/(sici)1521-4109(200002)12:3<227::aid-elan227>3.0.co;2-i</a>
- [77] Y. Shih, Flow injection analysis of zinc pyrithione in hair care products on a cobalt phthalocyanine modified screen-printed carbon electrode, *Talanta* **6** (2004) 912-917. https://doi.org/10.1016/j.talanta.2003.10.039
- [78] L. R. Gaspar, P. M. B. G. Maia Campos, Evaluation of the photostability of different UV filters associations in a sunscreen, *International Journal of Pharmaceutics* **307** (2006) 123-128. https://doi.org/10.1016/j.ijpharm.2005.08.029
- [79] S. Seité, A. Fourtanier, D. Moyal, A. R. Young, Photodamage to human skin by suberythemal exposure to solar ultraviolet radiation can be attenuated by sunscreens, *British Journal of Dermatology* **163** (2010) 903-914. <a href="https://doi.org/10.1111/j.1365-2133.2010.10018.x">https://doi.org/10.1111/j.1365-2133.2010.10018.x</a>
- [80] A. Chisvert, A. Salvador, UV Filters in Sunscreens and other Cosmetics. Regulatory Aspects and Analytical Methods, *Analysis of Cosmetic Products* (2007) 83-120. https://doi.org/10.1016/b978-044452260-3/50028-0
- [81] M. Krause, A. Klit, M. Blomberg Jensen, T. Søeborg, H. Frederiksen, M. Schlumpf, W. Lichtensteiger, N.E. Skakkebaek, K.T. Drzewiecki, Sunscreens: are they beneficial for health? An overview of endocrine disrupting properties of UV-filters, *International Journal of Andrology* **35** (2012) 424-436. <a href="https://doi.org/10.1111/j.1365-2605.2012.01280.x">https://doi.org/10.1111/j.1365-2605.2012.01280.x</a>
- [82] M. Ghazipura, R. McGowan, A. Arslan, T. Hossain, Exposure to benzophenone-3 and reproductive toxicity: A systematic review of human and animal studies, *Reproductive Toxicology* **73** (2017) 175-183. https://doi.org/10.1016/j.reprotox.2017.08.015
- [83] J. C. Cardoso, B. M. L. Armondes, T. A. de Araújo, J. L. Raposo, N. R. Poppi, V. S. Ferreira, Determination of 4-methylbenzilidene camphor in sunscreen by square wave voltammetry in media of cationic surfactant, *Microchemical Journal* 85 (2007) 301-307. <a href="https://doi.org/10.1016/j.microc.2006.07.006">https://doi.org/10.1016/j.microc.2006.07.006</a>

- [84] I. Narloch G. Wejnerowska, An Overview of the Analytical Methods for the Determination of Organic Ultraviolet Filters in Cosmetic Products and Human Samples, *Molecules* 26 (2021) 4780-4807. <a href="https://doi.org/10.3390/molecules26164780">https://doi.org/10.3390/molecules26164780</a>
- [85] M.-L. Chang, C.-M. Chang, Voltammetric determination of sunscreen by convenient epoxycarbon composite electrodes, *Journal of Food and Drug Analysis* 9 (2001) 199-206 <a href="https://doi.org/10.38212/2224-6614.2783">https://doi.org/10.38212/2224-6614.2783</a>
- [86] L. H. Wang, Voltammetric Behavior of Sunscreen Agents at Mercury Film Electrode, Electroanalysis 14 (2002) 773-781. <a href="https://doi.org/10.1002/1521-4109(200206)14:11</a> 773::AID-ELAN773>3.0.CO;2-A
- [87] J. B. G. Júnior, T. A. Araujo, M. A. G. Trindade, V. S. Ferreira, Electroanalytical determination of the sunscreen agent octocrylene in cosmetic products, *International Journal of Cosmetic Science* **34** (2011) 91-96. https://doi.org/10.1111/j.1468-2494.2011.00686.x
- [88] J. C. Cardoso, B. M. L. Armondes, J.B.G.eV. Ferreira, Simultaneous electrochemical determination of three sunscreens using cetyltrimethylammonium bromide, *Colloids and Surfaces B* **63** (2008) 34-40. <a href="https://doi.org/10.1016/j.colsurfb.2007.11.001">https://doi.org/10.1016/j.colsurfb.2007.11.001</a>
- [89] R. A. Lopes Neves, F. Moreira Araujo, F. Siqueira Pacheco, G. Chevitarese Azevedo, M. A. Costa Matos, R. Camargo Matos, Electrochemical Determination of Sunscreens Agents in Cosmetic Using Square Wave Voltammetry, *Electroanalysis* 313 (2018) 496-503. https://doi.org/10.1002/elan.201800747
- [90] Regulation (EC). No 1223/2009 of the European Parliament and of the Council, of 30 November 2009, on Cosmetic Products. Off. J. Eur. Union 2009. ANNEX III, p. 71. <a href="https://eur-lex.europa.eu/legal-content/EN/ALL/?uri=celex%3A32009R1223">https://eur-lex.europa.eu/legal-content/EN/ALL/?uri=celex%3A32009R1223</a> (Accessed on August 30, 2022).
- [91] S. Shahrokhian, Y. Javad, Electrocatalytic oxidation of thioglycolic acid at carbon paste electrode modified with cobalt phthalocyanine: application as a potentiometric sensor, *Electrochimica Acta* **48** (2003) 4143-4148. <a href="https://doi.org/10.1016/S0013-4686(03)00582-6">https://doi.org/10.1016/S0013-4686(03)00582-6</a>
- [92] J. M. Zen, H. H. Yang, M. H. Chiu, Y. J. Chen, Y. Shih, Determination of Thioglycolic Acid in Hair-Waving Products by Disposable Electrochemical Sensor Coupled with High-Performance Liquid Chromatography, *Journal of AOAC International* **92** (2009) 574-579. https://doi.org/10.1093/jaoac/92.2.574
- [93] B. Nair, A. R. Elmore, Cosmetic Ingredients Review Expert Panel. Final report on the safety assessment of sodium sulfite, potassium sulfite, ammonium sulfite, sodium bisulfite, ammonium bisulfite, sodium metabisulfite and potassium metabisulfite, *International Journal of Toxicology* **22** (2003) 63-88. <a href="https://doi.org/10.1080/10915810305077x">https://doi.org/10.1080/10915810305077x</a>
- [94] H. Vally, N. L. Misso, Adverse reactions to the sulphite additives, *Gastroenterol Hepatol Bed Bench* **5** (2012) 16-23 <a href="http://www.ncbi.nlm.nih.gov/pmc/articles/pmc4017440/">http://www.ncbi.nlm.nih.gov/pmc/articles/pmc4017440/</a>
- [95] The Scientific Committee on Cosmetic Products and Non Food Products intended for consumers, Evaluation and Opinion on: Inorganic Sulfites and Bisulfites, 23<sup>rd</sup> Plenary Meeting of the SCCNFP, 18 March, 2003 <a href="https://ec.europa.eu/health/ph\_risk/committees/sccp/documents/out\_200.pdf">https://ec.europa.eu/health/ph\_risk/committees/sccp/documents/out\_200.pdf</a>
- [96] P. Y. Chen, C. C. Huang, M. C. Chen, J. C. Hsu, Y. Shih, Determination of Sulfite in Hair Waving Products Using Oxygen-Incorporated Gold-Modified Screen-Printed Electrodes. *Electroanalysis* **24** (2012) 2267-2272. <a href="https://doi.org/10.1002/elan.201200126">https://doi.org/10.1002/elan.201200126</a>
- [97] M. Singh, S. R. Bhardiya, A. Rai, V. K. Rai, Electrochemical approach for recognition and quantification of p-phenylenediamine: a review, *Sensors and Diagnostics* **1** (2022) 376-386. <a href="https://doi.org/10.1039/d1sd00070e">https://doi.org/10.1039/d1sd00070e</a>
- [98] H. J. Han, H. J. Lee, C. H. Bang, J. H. Lee, Y. M. Park, J. Y. Lee, P-Phenylenediamine Hair Dye Allergy and Its Clinical Characteristics, *Annals of Dermatology* **30** (2018) 316-321. https://doi.org/10.5021/ad.2018.30.3.316



- [99] Scientific Committee on Consumer Products (SCCP). Opinion on Exposure to Reactants and Reaction Products of Oxidative Hair Dye Formulations; European Commission, Health & Consumer Protection Directorate-General: Luxembourg, 2005. https://ec.europa.eu/health/ph/risk/committees/04/sccp/docs/sccp/o/032.pdf
- [100] M. H. Al-Enezi, F. S. Aldawsari, Study of P-Phenylenediamine (PPD) Concentrations after Hair Dye Mixing: A Call for Safety Reassessment, *Cosmetics* **9** (2022) 41-57. https://doi.org/10.3390/cosmetics9020041
- [101] A. Chisvert, P. Miralles, A. Salvador. Chapter 8 Hair Dyes in Cosmetics: Regulatory Aspects and Analytical Methods. In Analysis of Cosmetic Products, 2nd ed.; A. Salvador, A. Chisvert, Eds.; Elsevier: Boston, MA, USA, 2018; pp. 159-173 <a href="https://doi.org/10.1016/B978-0-444-63508-2.00008-4">https://doi.org/10.1016/B978-0-444-63508-2.00008-4</a>
- [102] O. J. X. Morel, R. M. Christie, Current Trends in the Chemistry of Permanent Hair Dyeing, *Chemical Reviews* **111** (2011) 2537-2561. <a href="https://doi.org/10.1021/cr1000145">https://doi.org/10.1021/cr1000145</a>
- [103] Y. H. Bai, J. Y. Li, Y. Zhu, J. J. Xu, H. J. Chen, Selective Detection of *p*-Phenylenediamine in Hair Dyes Based on a Special CE Mechanism Using MnO<sub>2</sub> Nanowires, *Electroanalysis* **22** (2010) 1239-1247. https://doi.org/10.1002/elan.200900576
- [104] J. He, J. Sunarso, J. Miao, H. Sun, J. Dai, C. Zhang, W. Zhou, Z. Shao, A highly sensitive perovskite oxide sensor for detection of p-phenylenediamine in hair dyes, *Journal of Hazardous Materials* **369** (2019) 699-706 <a href="https://doi.org/10.1016/j.jhazmat.2019.02.070">https://doi.org/10.1016/j.jhazmat.2019.02.070</a>
- [105] M. Singh, A. Sahu, S. Mahata, P. Shukla, A. Rai, V. K. Rai, Efficient electrocatalytic oxidation of p-phenylenediamine using a novel PANI/ZnO anchored bio-reduced graphene oxide nanocomposite, *New Journal of Chemistry* **43** (2019) 6500-6506. https://doi.org/10.1039/c9nj00837c
- [106] M. Singh, S. R. Bhardiya, A. Asati, H. Sheshma, V.K. Rai, A. Rai, Sensitive electrocatalytic determination of p-phenylenediamine using bimetallic nanocomposite of Cu-Ag nanoalloy and ionic liquid-graphene oxide, *Journal of Electroanalytical Chemistry* **894** (2021) 115360. <a href="https://doi.org/10.1016/j.jelechem.2021.115360">https://doi.org/10.1016/j.jelechem.2021.115360</a>
- [107] K. G. McGrath, Apocrine sweat gland obstruction by antiperspirants allowing transdermal absorption of cutaneous generated hormones and pheromones as a link to the observed incidence rates of breast and prostate cancer in the 20th century, *Medical Hypotheses* **72** (2009) 665-674. https://doi.org/10.1016/j.mehy.2009.01.025
- [108] P. D. Darbre, Aluminium and the human breast, *Morphologie* **100** (2016) 65-74. https://doi.org/10.1016/j.morpho.2016.02.001
- [109] M. H. Chiu, A. S. Kumar, S. Sornambikai, J. M. Zen, Y. Shih, Flow Injection Analysis of Aluminum Chlorohydrate in Antiperspirant Deodorants Using a Built-in Three-in-one Screen-Printed Silver Electrode, *Electroanalysis* 22 (2010) 2421-2427. https://doi.org/10.1002/elan.200900635
- [110] J. M. Zen, T. H. Yang, A. Kumar, Y. J. Chen, J. C. Hsu, Y. Shih, Detection of Aluminum Chlorohydrate Content in Antiperspirant Deodorants Using Screen-Printed Silver Electrodes by One Drop Analysis, *Electroanalysis* **21** (2009) 2272-2276. https://doi.org/10.1002/elan.200904670
- [111] B. Bocca, A. Pino, A. Alimonti, G. Forte, Toxic metals contained in cosmetics: a status report, *Regulatory Toxicology and Pharmacology* **68** (2014) 447-467. https://doi.org/10.1016/j.yrtph.2014.02.003
- [112] N. A. Bohari, S. Siddiquee, S. Saallah, M. Misson, S. E. Arshad, Optimization and Analytical Behavior of Electrochemical Sensors Based on the Modification of Indium Tin Oxide (ITO) Using PANI/MWCNTs/AuNPs for Mercury Detection, *Sensors* **20** (2020) 6502. https://doi.org/10.3390/s20226502

- [113] Z. Wang X. Fang, Chronic Mercury Poisoning from Daily Cosmetics: Case Report and Brief Literature Review, *Cureus* **13** (2021) e19916. <a href="https://doi.org/10.7759/cureus.19916">https://doi.org/10.7759/cureus.19916</a>
- [114] G. F. Sun, W. T. Hu, Z. H. Yuan, B. A. Zhang, H. Lu, Characteristics of mercury intoxication induced by skin-lightening products, *Chinese Medical Journal* **130** (2017) 3003-3004. https://doi.org/10.4103/0366-6999.220312
- [115] N. M. Hepp, W. R. Mindak, J. W. Gasper, C. B. Thompson, J. N. Barrows, Survey of cosmetics for arsenic, cadmium, chromium, cobalt, lead, mercury, and nickel content, *Journal of Cosmetic Science* **65** (2014) 125-145 <a href="https://pubmed.ncbi.nlm.nih.gov/25043485/">https://pubmed.ncbi.nlm.nih.gov/25043485/</a>
- [116] J. M. Zen, A. S. Kumar, S. C. Lee, Y. Shih, Microliter Volume Determination of Cosmetic Mercury with a Partially Crosslinked Poly(4-vinylpyridine) Modified Screen-Printed Three-Electrode Portable Assembly, *Electroanalysis* 19 (2007) 2369-2374. <a href="https://doi.org/10.1002/elan.200703990">https://doi.org/10.1002/elan.200703990</a>
- [117] M. H. Chiu, J. M. Zen, A. S. Kumar, D. Vasu, Y. Shih, Selective Cosmetic Mercury Analysis Using a Silver Ink Screen-Printed Electrode with Potassium Iodide Solution, *Electroanalysis* **20** (2008). 2265-2270. https://doi.org/10.1002/elan.200804307
- [118] A. L. Suherman, E. E. L. Tanner, R.G. Compton, Recent developments in inorganic Hg<sup>2+</sup> detection by voltammetry, *TrAC Trends in Analytical Chemistry* **94** (2017) 161-172. <a href="https://doi.org/10.1016/j.trac.2017.07.020">https://doi.org/10.1016/j.trac.2017.07.020</a>
- [119] I. M. Isaa, M. I. Saidin, M. Ahmad, N. Hashim, S. A. Bakar, N. M. Ali, S. M. Si, Chloroplatinum(II) complex-modified MWCNTs paste electrode for electrochemical determination of mercury in skin lightening cosmetics, *Electrochimica Acta* 253 (2017) 463-471. <a href="http://dx.doi.org/10.1016/j.electacta.2017.09.092">http://dx.doi.org/10.1016/j.electacta.2017.09.092</a>
- [120] A. L. Wani, A. Ara, J. A. Usmani, Lead toxicity: a review, *Interdisciplinary Toxicology* **8** (2015) 55-64. <a href="http://dx.doi.org/10.1515/intox-2015-0009">http://dx.doi.org/10.1515/intox-2015-0009</a>
- [121] Regulation (EC). No 1223/2009 of the European Parliament and of the Council, of 30 November 2009, on Cosmetic Products. Off. J. Eur. Union 2009. ANNEX II, p. 32. <a href="https://eur-lex.europa.eu/legal-content/EN/ALL/?uri=celex%3A32009R1223">https://eur-lex.europa.eu/legal-content/EN/ALL/?uri=celex%3A32009R1223</a> (Accessed on August 30, 2022)
- [122] ASEAN definition of cosmetics and illustrative list by category of cosmetic products. https://www.aseancosmetics.org/docdocs/technical.pdf (Accessed on August 30, 2022)
- [123] R. Feizi, N. Jaafarzadeh, H. Akbari, S. Jorfi, Evaluation of lead and cadmium concentrations in lipstick and eye pencil cosmetics, *Environmental Health Engineering and Management Journal* **6** (2019) 277-282. http://dx.doi.org/10.15171/EHEM.2019.31
- [124] Regulation (EC). No 1223/2009 of the European Parliament and of the Council, of 30. 11. 2009, on Cosmetic Products. Off. J. Eur. Union 2009. ANNEX II, p. 26. <a href="https://eur-lex.europa.eu/legal-content/EN/ALL/?uri=celex%3A32009R1223">https://eur-lex.europa.eu/legal-content/EN/ALL/?uri=celex%3A32009R1223</a> (Accessed on August 30, 2022).
- [125] D. Zhao, J. Li, C. Li, A.L. Juhasz, K.G. Scheckel, J. Luo, H.B. Li, L.Q. Ma, Lead relative bioavailability in lip products and their potential health risk to women, *Environmental Science and Technology* **50** (2016) 6036-6043. http://dx.doi.org/10.1021/acs.est.6b01425
- [126] FDA. Lipstick and Lead: Questions and Answers. U.S. Food and Drug Administration (FDA) (2011) http://www.fda.gov/cosmetics/productsingredients/products/ucm137224.htm
- [127] K. Goswami, Eye cosmetic 'surma': hidden threats of lead poisoning, *Indian Journal of Clinical Biochemistry* **28** (2013) 71-73. <a href="http://dx.doi.org/10.1007/s12291-012-0235-6">http://dx.doi.org/10.1007/s12291-012-0235-6</a>
- [128] E. Navarro-Tapia, M. Serra-Delgado, L. Fernández-López, M. Meseguer-Gilabert, M. Falcón, G. Sebastiani, S. Sailer, O. Garcia-Algar, V. Andreu-Fernández, Toxic Elements in Traditional Kohl-Based Eye Cosmetics in Spanish and German Markets, *International Journal of Environmental Research and Public Health* 18 (2021) 6109-6125. <a href="https://doi.org/10.3390/ijerph18116109">https://doi.org/10.3390/ijerph18116109</a>
- [129] P. Swetha, J. Chen, A. S. Kumar, S. P. Feng, High index facets-Ag nanoflower enabled efficient electrochemical detection of lead in blood serum and cosmetics, *Journal of*



- Electroanalytical Chemistry **878** (2020) 114657. http://dx.doi.org/10.1016/j.jelechem.2020.114657
- [130] Q. Fardiyah, B. Rumhayati, I. Rosemiyani, Determination of lead in cosmetic sampels using coated wire lead(II) ion selective electrode based on phyropillite, *UNEJ e-Proceeding* (2017) 270-272. https://jurnal.unej.ac.id/index.php/prosiding/article/view/4239
- [131] T. M. Barros, D. M. de Araújo, A. T. L. de Melo, C. A. Martínez-Huitle, M. Vocciante, S. Ferro, E.V. dos Santos, An Electroanalytical Solution for the Determination of Pb<sup>2+</sup> in Progressive Hair Dyes Using the Cork–Graphite Sensor, *Sensors* **22** (2022) 1466. https://doi.org/10.3390/s22041466
- [132] Y. Shih, J. M. Zen, A. S. Kumar, Y. C. Lee, H. R. Huang, Determination of the toxic lead level in cosmetic-hair dye formulations using a screen-printed silver electrode, *Bulletin of the Chemical Society of Japan* **77** (2004) 311-312 https://doi.org/10.1246/bcsj.77.311
- [133] S. Palisoc, A. M. Causing, M. Natividad, Gold nanoparticle/hexaammineruthenium/Nafion® modified glassy carbon electrodes for trace heavy metal detection in commercial hair dyes, *Analytical Methods* **9** (2017) 4240-4246 <a href="https://doi.org/10.1039/c7ay01114h">https://doi.org/10.1039/c7ay01114h</a>
- [134] J. V. Maciel, G. D. da Silveira, A. M. M. Durigon, O. Fatibello-Filho, D. Dias, Use of carbon black based electrode as sensor for solid-state electrochemical studies and voltammetric determination of solid residues of lead, *Talanta* **236** (2022) 122881. <a href="https://doi.org/10.1016/j.talanta.2021.122881">https://doi.org/10.1016/j.talanta.2021.122881</a>
- [135] Y. Yi, Y. Zhao, Z. Zhang, Y. Wu, G. Zhu, Recent developments in electrochemical detection of cadmium, *Trends in Environmental Analytical Chemistry* **33** (2022) e00152. https://doi.org/10.1016/j.teac.2021.e00152
- [136] L. A. De Furtado, I. O. de Lucena, J. O. de Fernandes, F. G. Lepri, D. L. de Martins, F. S. Semaan, New strategies for the simultaneous voltammetric quantification of Pb and Zn in hair cosmetics samples employing chemically modified composite electrodes, *Journal of the International Measurement Confederation* **125** (2018) 651-658. https://doi.org/10.1016/j.measurement.2018.05.042
- [137] W. Wang, N. Bao, W. Yuan, N. Si, H. Bai, Haiyu Li, Q. Zhang, Simultaneous determination of lead, arsenic, and mercury in cosmetics using a plastic based disposable electrochemical sensor, *Microchemical Journal* 148 (2019) 240-247. <a href="https://doi.org/10.1016/j.microc.2019.05.011">https://doi.org/10.1016/j.microc.2019.05.011</a>



Open Access :: ISSN 1847-9286 www.jESE-online.org

Original scientific paper

# Electroanalysis of tert-butylhydroquinone in food products using a paste electrode enlarged with single wall carbon nanotubes as catalyst

Niloofar Dehdashtian<sup>1</sup>, Seyed-Ahmad Shahidi<sup>1</sup>, Azade Ghorbani-HasanSaraei<sup>1,⊠</sup>, Shabnam Hosseini<sup>2</sup> and Mohammad Ahmadi<sup>3</sup>

<sup>1</sup>Department of Food Science and Technology, Ayatollah Amoli Branch, Islamic Azad University, Amol, Iran

<sup>2</sup>Department of Materials Science and Engineering, Ayatollah Amoli Branch, Islamic Azad University, Amol, Iran

<sup>3</sup>Department of Food Hygiene, Ayatollah Amoli Branch, Islamic Azad University, Amol, Iran Corresponding authors: <sup>™</sup>Az.GhorbaniHasanSaraei@iau.ac.ir; Tel.: +98-11-43217089 Received: August 5, 2023; Accepted: September 26, 2023; Published: October 11, 2023

#### **Abstract**

In this study, an electrochemical sensor was introduced as a simple and fast electroanalytical tool to monitor and sensing of tert-butylhydroquinone (TBHQ) in food products. The suggested electrochemical sensor is fabricated by modification of paste electrode (PE) by single wall carbon nanotubes (SWCNTs) as nanocatalyst. The oxidation current of TBHQ was improved by about 2.62 times and its oxidation potential was reduced by about 50 mV after using SWCNTs as conductive catalyst on a carbon paste matrix. The oxidation current of TBHQ showed a linear dynamic range of 0.05 to 390 µM in the sensing process using SWCNTs/PE as the electroanalytical sensor. On the other hand, SWCNTs/PE successfully monitored TBHQ with a detection limit of 10 nM at optimum conditions. The real sample analysis data clearly showed a recovery range of 97.2 to 104.3 %, which is very interesting for a new analytical tool in the food-sensing process.

# **Keywords**

Food analysis; electroanalysis; modified electrode; carbon paste; voltammetry

# Introduction

Monitoring food additives is one of the best methods for investigating quality food products and checking the presence of prohibited substances [1-7]. For this purpose, different measurement methods have been reported in food samples [8-13]. In the meantime, attention to electrochemical methods has grown significantly due to many advantages and low cost [14-18]. By presenting various solutions for modification in electrochemical sensors, various reports have been presented

for the use of these sensors in the construction of measuring instruments [19-24]. High overpotentials and low redox signals of electroactive materials and, especially, food additives are the main problems to trace level monitoring of them in real samples [25-29]. Therefore, conductive catalysts were suggested for the fabrication of highly conductive and sensitive electrochemical sensors [30-33].

It is important to check the concentration of food additives and especially antioxidants widely used in the food industry to determine the food quality [34]. The tert-butylhydroquinone (TBHQ) is one of the phenolic-type antioxidants with a wide range of applications in many edible animal fats and vegetable oils [35]. High concentrations of TBHQ can be harmful to the human body and create some problems, such as vision disturbances and neurotoxic effects [35]. Therefore, many research works focused on monitoring them in food products [36,37]. However, efforts are still being made to provide simpler and more sensitive solutions.

Carbon nanotubes (CNT) are one of the main and useful carbon nanocatalysts widely used in different branches of science, especially in sensors and energy majors [38-40]. Easy modification and high surface area with good electrical conductivity have introduced them as a unique catalyst [41,42]. On the other hand, according to the literature, single wall carbon nanotubes (SWCNTs) showed more advantages than other carbon-based nanomaterials as catalysts for the fabrication of electrochemical sensors due to high electrical conductivity and good surface area and were selected for this work [43].

In this research work, a carbon paste electrode (PE) was modified with single-walled CNTs (SWCNTs) as conductive catalysts and a fabricated sensor was used to determine TBHQ in food products. The results clearly showed the powerful ability of SWCNTs/PE in trace analysis of TBHQ with acceptable recovery data in real sample analysis.

# **Experimental**

# Instrument and materials

A potentiostat/galvanostat (Metrohm Company) was used to record redox signals of TBHQ in an aqueous solution. All potentials were recorded using Ag/AgCl/KCl<sub>sat</sub> as a reference electrode. Pt wire was used as a counter electrode and SWCNTs/PE as the working electrode. The TBHQ (99 %) was purchased from ACROS Company and a stock solution of TBHQ was prepared by dissolving 0.0166 g TBHQ in PBS (pH 7.0) + ethanol (1:1 v/v) (10 mL) under ultrasonication to 10 min. SWCNTs were purchased from Sigma-Aldrich Company and used to fabricate SWCNTs/PE electrodes. The orthophosphoric acid (85 %) was purchased from Merck Company and used to prepare phosphate buffer solution (PBS, 0.1 M).

# Fabrication of SWCNTs/PE

The ratio of SWCNTs was prepared by mixing 0.15 g SWCNTs + 0.85 g graphite powder in the presence of paraffin oil as a binder. The powder dissolved in 10 mL diethyl ether solution and then stirred at 25 °C to evaporate the solvent. Then paraffin oil was added dropwise and the sample was hand-mixed for 45 min. The SWCNTs/PE was added to the end of the glass tube and an electrical connection was established by a copper wire.

#### Real sample preparation

Orange and apple juices and soybean oil were selected as real samples to study the capability of SWCNTs/PE in monitoring TBHQ. The orange and apple juices were centrifuged for 20 min at 4000 rpm



and then the solution was filtered to preparation of pure sample and diluted by PBS (pH 7.0). The soybean oil was extracted with 50 mL ethanol for 1 h and then was filtered to prepare a pure sample and diluted by PBS (pH 7.0). The standard addition was used as an analytical method.

#### **Results and discussion**

# **Optimization of SWCNTs**

The ratio of SWCNTs catalyst to graphite powder is one of the important factors in the fabrication of SWCNTs/PE as a new sensor. Therefore, the oxidation signal of 200  $\mu$ M TBHQ was recorded at the surface of the carbon paste electrode (CPE) modified with 0, 5, 10, 15 and 20 wt.% SWCNTs. The results showed maximum sensitivity in the presence of 15 wt.% of SWCNTs in SWCNTs/PE matrix (Figure 1).

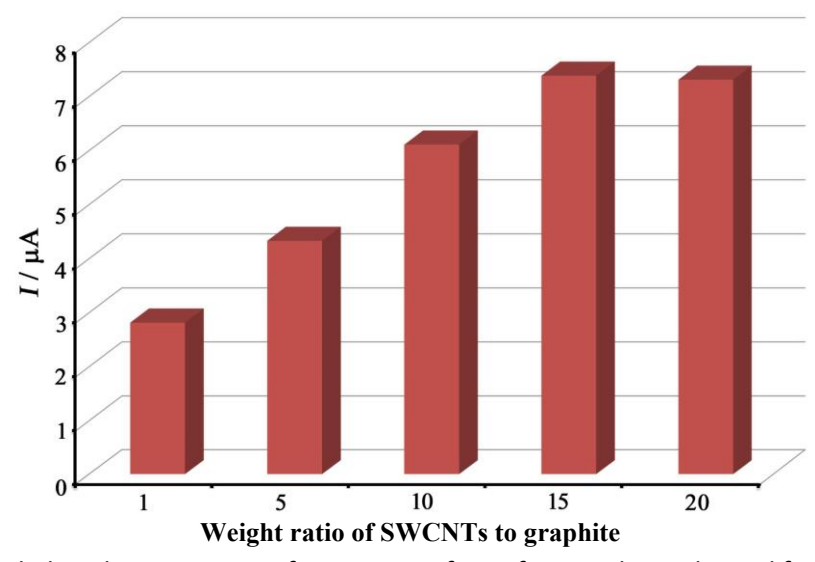


**Figure 1.** Recorded oxidation current of TBHQ at surface of paste electrode modified with different percentage of catalyst

# Electrochemical investigation

The oxidation signal of TBHQ was recorded at a pH range of 5.0 to 9.0 and results showed in Figure 2 inset. The plot of the oxidation current of TBHQ vs. pH is shown in Figure 2 and clearly confirms maximum sensitivity at neutral conditions. On the other hand, the plot of the oxidation peak potential vs. pH follows the linear equation E = -0.057 pH + 0.784 ( $R^2 = 0.9942$ ) (not shown). Therefore, the reaction mechanism shown in Scheme 1 was suggested for the redox reaction of TBHQ at the surface of SWCNTs/PE [44].

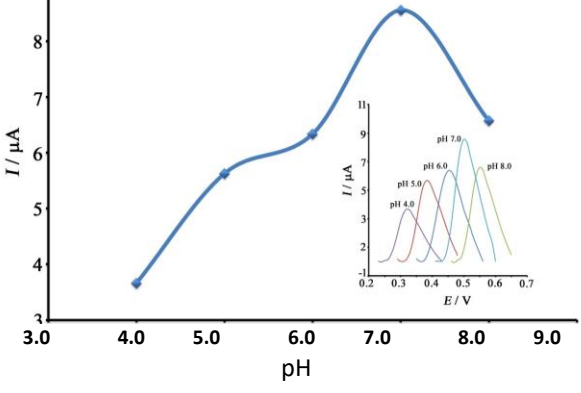
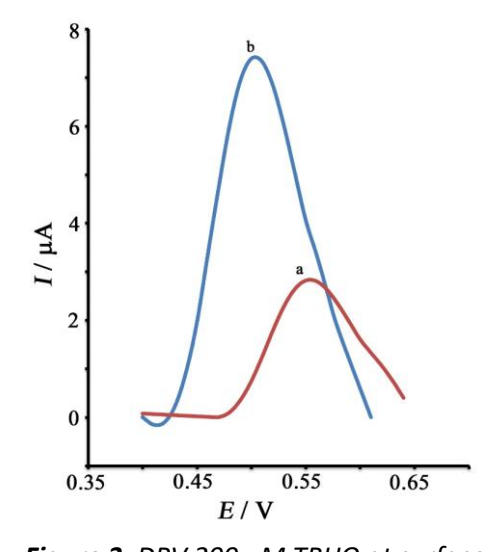


**Figure 2.** I-pH curve for electrooxidation of 220  $\mu$ M TBHQ at surface of SWCNTs/PE. Inset: DPV of 220  $\mu$ M TBHQ at surface of SWCNTs/PE in pH range 4.0 to 9.0

Scheme 1. TBHQ electrooxidation mechanism

The oxidation signal of 200  $\mu$ M TBHQ was recorded at the surface of PE (Figure 3 curve a) and SWCNTs/PE (Figure 3 curve b), respectively. The increase in current from 2.816 to 7.386  $\mu$ A and the decrease in potential from 550 mV to 500 mV are the main advantages of SWCNTs as catalysts at the surface of the paste electrode. On the other hand, the active surface area of PE and SWCNTs/PE were calculated at about 0.13 and 0.19 cm², respectively. This issue clearly confirms the high electrical conductivity of SWCNTs as a catalyst for the electrooxidation of TBHQ.

A positive shift was observed in the oxidation potential of TBHQ with the increase in the scan rate (see Figure 4 inset), revealing kinetic limitations and quasi-reversible behavior in the redox reaction of TBHQ at the surface of SWCNTs/PE. In addition, a linear dependence of the current peak height and the square root of the scan rate was observed,  $I = 1.5580 v^{1/2} + 2.6282$ , confirming a diffusion-controlled electrooxidation process (Figure 4) [45].



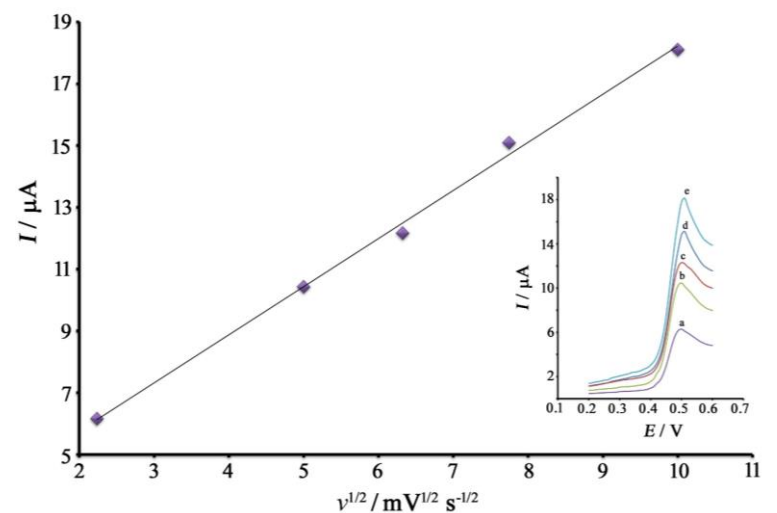


**Figure 3.** DPV 200 μM TBHQ at surface of PE (a) and SWCNTs/PE (b)

**Figure 4.** I-  $v^{1/2}$  curve to redox reaction of TBHQ at the surface of SWCNTs/PE. Inset: linear sweep voltammograms TBHQ at scan rates a) 5; b) 25; c) 40; d) 60 and e) 100 mV  $s^{-1}$ 

The stability of SWCNTs/PE in monitoring 200  $\mu$ M TBHQ was investigated over 70 days. Results are shown in Figure 5 and data showed good stability of SWCNTs/PE in monitoring TBHQ in an aqueous solution after 60 days.

The differential pulse voltammograms (DPV) of TBHQ in the concentration range 0.05 to 390  $\mu$ M were recorded at the surface of SWCNTs/PE and results are shown in Figure 6 inset. Results displayed a linear equation I = 0.0325C + 0.8047 ( $R^2 = 0.9974$ ) where C is concentration. The limit of

detection 10 nM ( $Y_{LOD} = 3S_b/m$  where  $S_b$  is the standard deviation of blank solution and m is sensitivity or slope of LDR plot) was calculated for SWCNTs/PE as a new sensor.

In the final step, the standard addition results relative to monitoring of TBHQ using SWCNTs/PE are shown in Table 1. The experiments were repeated three times and mean values were displayed in the table. Results clearly confirm the powerful ability of SWCNTs/PE in sensing TBHQ in orange juice and soybean oil samples.

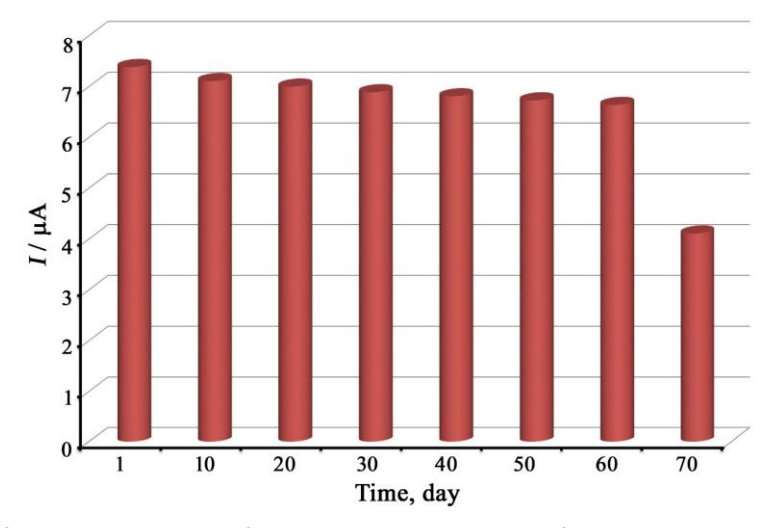


**Figure 5.** Diagram of oxidation current of 200  $\mu$ M TBHQ in period of 70 days at the surface of SWCNTs/PE

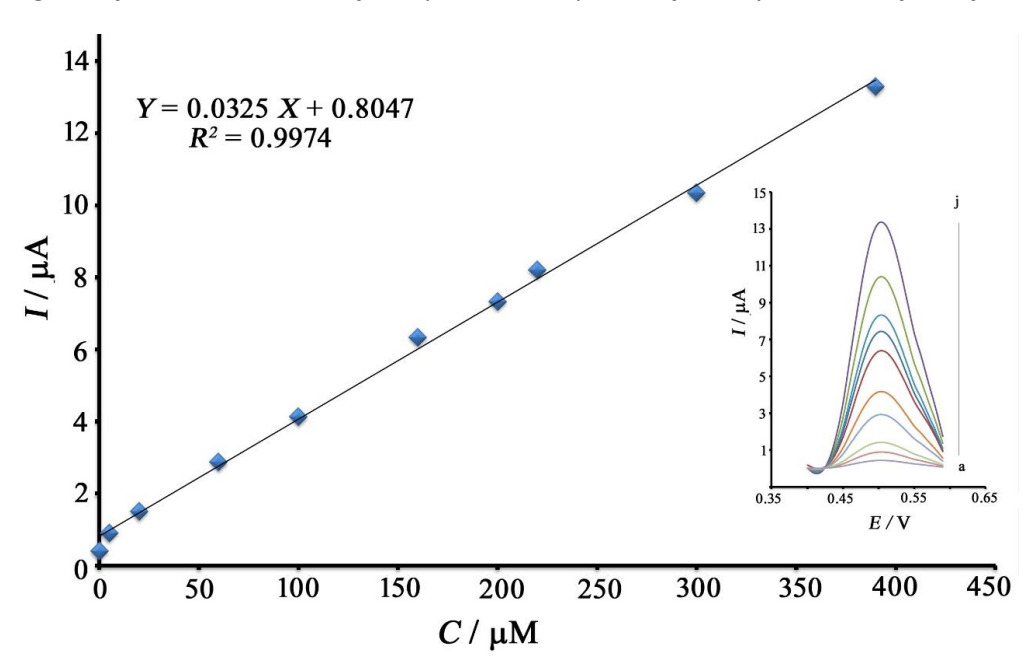


**Figure 6.** LDR plot to sensing of TBHQ using SWCNTs/PE as sensor. Inset: DP voltammograms TBHQ in the concentration range 0.05 to 390  $\mu$ M (from a to j)

Camanda		Amount of TBHQ, μM		
Sample	Added	Expected	Found by proposed method	Recovery, %
Caubaan ail			1.86 ± 0.22	
Soybean oil –	5.00	6.86	6.98±0.44	101.74
Oranga iuiga			<lod< td=""><td></td></lod<>	
Orange juice -	10.00	10.00	9.72±0.73	97.2
Apple juice -			<lod< td=""><td></td></lod<>	
	20.00	20.00	20.86±0.99	104.3

**Table 1.** Monitoring of TBHQ in food samples

#### **Conclusions**

The presence study suggested a very attractive and capable electroanalytical sensor to monitor TBHQ in food products. The new sensor was fabricated using the modification of a paste electrode with SWCNTs as a conductive and powerful catalyst. The SWCNTs/PE showed catalytic activity to sensing of TBHQ by reducing 50 mV oxidation potential and increasing the 2.62-time oxidation potential of antioxidants compared to the unmodified electrode. The SWCNTs/PE showed a good limit of detection (10 nM) for monitoring TBHQ in an aqueous solution that is sufficient for sensing this antioxidant in real samples. The SWCNTs/PE showed a recovery range of 97.2 to 104.3 % to sensing of TBHQ in food products.

**Acknowledgment:** This is thesis of Niloofar Dehdashtian, who was inducted in Ayatollah Amoli Branch, Islamic Azad University, Amol, Iran.

#### References

- [1] M. Ghalkhani, N. Zare, F. Karimi, C. Karaman, M. Alizadeh, Y. Vasseghian, Recent advances in Ponceau dyes monitoring as food colorant substances by electrochemical sensors and developed procedures for their removal from real samples, *Food and Chemical Toxicology*, (2022) 112830. <a href="https://doi.org/10.1016/j.fct.2022.112830">https://doi.org/10.1016/j.fct.2022.112830</a>
- [2] S. Cheraghi, F. Shalali, M.A. Taher, Kojic acid exploring as an essential food additive in real sample by a nanostructure sensor amplified with ionic liquid, *Journal of Food Measurement and Characterization* **17** (2023) 1728-1734. <a href="https://doi.org/10.1007/s11694-022-01738-y">https://doi.org/10.1007/s11694-022-01738-y</a>
- [3] J.A. Buledi, A.R. Solangi, A. Mallah, Z.-u.-H. Shah, S.T. Sherazi, M.R. Shah, A. Hyder, S. Ali, Electrochemical monitoring of isoproturon herbicide using NiO/V<sub>2</sub>O<sub>5</sub>/rGO/GCE, *Journal of Food Measurement and Characterization* **17** (2023) 1628-1639. <a href="https://doi.org/10.1007/s11694-022-01733-3">https://doi.org/10.1007/s11694-022-01733-3</a>
- [4] H. Karimi-Maleh, M. Ghalkhani, Z.S. Dehkordi, M. M. Tehran, J. Singh, Y. Wen, M. Baghayeri, J. Rouhi, L. Fu, S. Rajendran, MOF-enabled pesticides as developing approach for sustainable agriculture and reducing environmental hazards, *Journal of Industrial and Engineering Chemistry* **129** (2023) 105-123. https://doi.org/10.1016/j.jiec.2023.08.044
- [5] F. Khademi, S.N. Raeisi, M. Younesi, A. Motamedzadegan, K. Rabiei, M. Shojaei, H. Rokni, M. Falsafi, Effect of probiotic bacteria on physicochemical, microbiological, textural, sensory properties and fatty acid profile of sour cream, *Food and Chemical Toxicology* **166** (2022) 113244. <a href="https://doi.org/10.1016/j.fct.2022.113244">https://doi.org/10.1016/j.fct.2022.113244</a>
- [6] S.N. Raeisi, H.B. Ghoddusi, E.J. Boll, N. Farahmand, B. Stuer-Lauridsen, E. Johansen, J.P. Sutherland, L.I.I. Ouoba, Antimicrobial susceptibility of bifidobacteria from probiotic milk products and determination of the genetic basis of tetracycline resistance in *Enterococcus* species after *in vitro* conjugation with *Bifidobacterium animalis* subsp. *lactis*, *Food Control* **94** (2018) 205-211. https://doi.org/10.1016/j.foodcont.2018.07.016
- [7] F. Fazeli, S.M.S. Ardabili, Z. Piravivanak, M. Honarvar, N. Mooraki, Optimization of extraction conditions for polycyclic aromatic hydrocarbons determination in smoked rice using the high performance liquid chromatography-fluorescence detection, *Journal of Food Measurement and Characterization* **14** (2020) 1236-1248. <a href="https://doi.org/10.1007/s11694-020-00372-w">https://doi.org/10.1007/s11694-020-00372-w</a>
- [8] K.N. Waliszewski, V.T. Pardio, S.L. Ovando, A simple and rapid HPLC technique for vanillin determination in alcohol extract, *Food Chemistry* 101 (2007) 1059-1062. https://doi.org/10.1016/j.foodchem.2006.03.004
- [9] R. Rebane, I. Leito, S. Yurchenko, K. Herodes, A review of analytical techniques for determination of Sudan I–IV dyes in food matrixes, *Journal of Chromatography A* **1217** (2010) 2747-2757. <a href="https://doi.org/10.1016/j.chroma.2010.02.038">https://doi.org/10.1016/j.chroma.2010.02.038</a>



- [10] Q. Xiang, Y. Gao, Y. Xu, E. Wang, Capillary electrophoresis-amperometric determination of antioxidant propyl gallate and butylated hydroxyanisole in foods, *Analytical Sciences* **23** (2007) 713-717. <a href="https://doi.org/10.2116/analsci.23.713">https://doi.org/10.2116/analsci.23.713</a>
- [11] N. Ermis, N. Zare, R. Darabi, M. Alizadeh, F. Karimi, J. Singh, S.-A. Shahidi, E.N. Dragoi, M.B. Camarada, M. Baghayeri, Recent advantage in electrochemical monitoring of gallic acid and kojic acid: a new perspective in food science, *Journal of Food Measurement and Characterization* 17 (2023) 3644-3653. https://doi.org/10.1007/s11694-023-01881-0
- [12] S.-A. Shahidi, Effect of solvent type on ultrasound-assisted extraction of antioxidant compounds from *Ficaria kochii*: Optimization by response surface methodology, *Food and Chemical Toxicology* **163** (2022) 112981. <a href="https://doi.org/10.1016/j.fct.2022.112981">https://doi.org/10.1016/j.fct.2022.112981</a>
- [13] S.M. Razi, A. Motamedzadegan, L. Matia-Merino, S.-A. Shahidi, A. Rashidinejad, The effect of pH and high-pressure processing (HPP) on the rheological properties of egg white albumin and basil seed gum mixtures, *Food Hydrocolloids* **94** (2019) 399-410. <a href="https://doi.org/10.1016/j.foodhyd.2019.03.029">https://doi.org/10.1016/j.foodhyd.2019.03.029</a>
- [14] M. Vardini, N. Abbasi, A. Kaviani, M. Ahmadi, E. Karimi, Graphite electrode potentiometric sensor modified by surface imprinted silica gel to measure valproic acid, *Chemical Methodologies* **6** (2022) 398-408. <a href="https://doi.org/10.22034/chemm.2022.328620.1437">https://doi.org/10.22034/chemm.2022.328620.1437</a>
- [15] S. Saghiri, M. Ebrahimi, M.R. Bozorgmehr, Electrochemical amplified sensor with MgO nanoparticle and ionic liquid: A powerful strategy for methyldopa analysis, *Chemical Methodologies* 5 (2021) 234-239. <a href="https://doi.org/10.22034/chemm.2021.128530">https://doi.org/10.22034/chemm.2021.128530</a>
- [16] W.H. Danial, N.A. Norhisham, A.F. Ahmad Noorden, Z. Abdul Majid, K. Matsumura, A. Iqbal, A short review on electrochemical exfoliation of graphene and graphene quantum dots, *Carbon Letters* **31** (2021) 371-388. <a href="https://doi.org/10.1007/s42823-020-00212-3">https://doi.org/10.1007/s42823-020-00212-3</a>
- [17] Y.F. Mustafa, G. Chehardoli, S. Habibzadeh, Z. Arzehgar, Electrochemical detection of sulfite in food samples, *Journal of Electrochemical Science and Engineering* **12** (2022) 1061-1079. <a href="https://doi.org/10.5599/jese.1555">https://doi.org/10.5599/jese.1555</a>
- [18] M. Akbari, M.S. Mohammadnia, M. Ghalkhani, M. Aghaei, E. Sohouli, M. Rahimi-Nasrabadi, M. Arbabi, H.R. Banafshe, A. Sobhani-Nasab, Development of an electrochemical fentanyl nanosensor based on MWCNT-HA/Cu-H<sub>3</sub>BTC nanocomposite, *Journal of Industrial and Engineering Chemistry* **114** (2022) 418-426. https://doi.org/10.1016/j.jiec.2022.07.032
- [19] R.M. Mohabis, F. Fazeli, I. Amini, V. Azizkhani, An overview of recent advances in the detection of ascorbic acid by electrochemical techniques, *Journal of Electrochemical Science and Engineering* **12** (2022) 1081-1098. https://doi.org/10.5599/jese.1561
- [20] H. Medetalibeyoğlu, An investigation on development of a molecular imprinted sensor with graphitic carbon nitride (g-C<sub>3</sub>N<sub>4</sub>) quantum dots for detection of acetaminophen, *Carbon Letters* **31** (2021) 1237-1248. https://doi.org/10.1007/s42823-021-00247-0
- [21] G. Li, J. Li, Z. Yang, An electrochemical sensor based on graphene-chitosan-cyclodextrin modification for the detection of Staphylococcus aureus, *Carbon Letters* (2023) <a href="https://doi.org/10.1007/s42823-023-00518-y">https://doi.org/10.1007/s42823-023-00518-y</a>
- [22] S. Ariavand, M. Ebrahimi, E. Foladi, Design and construction of a novel and an efficient potentiometric sensor for determination of sodium ion in urban water samples, *Chemical Methodologies* **6** (2022) 886-904. <a href="https://doi.org/10.22034/chemm.2022.348712.1567">https://doi.org/10.22034/chemm.2022.348712.1567</a>
- [23] A.R. Umar, K. Hussain, Z. Aslam, M.A.U. Haq, H. Muhammad, M.R. Shah, Ultra-trace level voltammetric sensor for MB in human plasma based on a carboxylic derivative of Calix [4] resorcinarene capped silver nanoparticles, *Journal of Industrial and Engineering Chemistry* **107** (2022) 81-92. <a href="https://doi.org/10.1016/j.jiec.2021.11.024">https://doi.org/10.1016/j.jiec.2021.11.024</a>
- [24] B. Muthukutty, J. Ganesamurthi, T.-W. Chen, S.-M. Chen, J. Yu, X. Liu, A novel high-performance electrocatalytic determination platform for voltammetric sensing of eugenol in acidic media using pyrochlore structured lanthanum stannate nanoparticles, *Journal of*

- *Industrial and Engineering Chemistry* **106** (2022) 103-112. https://doi.org/10.1016/j.jiec.2021.10.015
- [25] B.B. Mulik, A.V. Munde, R.P. Dighole, B.R. Sathe, Electrochemical determination of semicarbazide on cobalt oxide nanoparticles: Implication towards environmental monitoring, Journal of Industrial and Engineering Chemistry 93 (2021) 259-266. <a href="https://doi.org/10.1016/j.jiec.2020.10.002">https://doi.org/10.1016/j.jiec.2020.10.002</a>
- [26] A.R. Cherian, L. Benny, A. George, A. Varghese, G. Hegde, Recent advances in functionalization of carbon nanosurface structures for electrochemical sensing applications: tuning and turning, *Journal of Nanostructure in Chemistry* 12 (2021) 441-466. <a href="https://doi.org/10.1007/s40097-021-00426-5">https://doi.org/10.1007/s40097-021-00426-5</a>
- [27] A. John, L. Benny, A.R. Cherian, S.Y. Narahari, A. Varghese, G. Hegde, Electrochemical sensors using conducting polymer/noble metal nanoparticle nanocomposites for the detection of various analytes: a review, *Journal of Nanostructure in Chemistry* **11** (2021) 1-31. https://doi.org/10.1007/s40097-020-00372-8
- [28] B. Davarnia, S.-A. Shahidi, H. Karimi-Maleh, A. Ghorbani-HasanSaraei, F. Karimi, Biosynthesis of Ag nanoparticle by peganum harmala extract; antimicrobial activity and ability for fabrication of quercetin food electrochemical sensor, *International Journal of Electrochemical Science* 15 (2020) 2549-2560. <a href="https://doi.org/10.20964/2020.03.70">https://doi.org/10.20964/2020.03.70</a>
- [29] H. Karimi-Maleh, R. Darabi, M. Baghayeri, F. Karimi, L. Fu, J. Rouhi, D.E. Niculina, E.S. Gündüz, E. Dragoi, Recent developments in carbon nanomaterials-based electrochemical sensors for methyl parathion detection, *Journal of Food Measurement and Characterization* 17 (2023) 5371-5389. <a href="https://doi.org/10.1007/s11694-023-02050-z">https://doi.org/10.1007/s11694-023-02050-z</a>
- [30] P. Ebrahimi, S.-A. Shahidi, M. Bijad, A rapid voltammetric strategy for determination of ferulic acid using electrochemical nanostructure tool in food samples, *Journal of Food Measurement and Characterization* **14** (2020) 3389-3396. https://doi.org/10.1007/s11694-020-00585-z
- [31] H. Sadeghi, S.-A. Shahidi, S.N. Raeisi, A. Ghorbani-HasanSaraei, F. Karimi, Electrochemical determination of vitamin B6 in water and juice samples using an electrochemical sensor amplified with NiO/CNTs and Ionic liquid, *International Journal of Electrochemical Science* **15** (2020) 10488-10498. <a href="https://doi.org/10.20964/2020.10.51">https://doi.org/10.20964/2020.10.51</a>
- [32] F. Karimi, E. Demir, N. Aydogdu, M. Shojaei, M.A. Taher, P.N. Asrami, M. Alizadeh, Y. Ghasemi, S. Cheraghi, Advancement in electrochemical strategies for quantification of Brown HT and Carmoisine (Acid Red 14) From Azo Dyestuff class, *Food and Chemical Toxicology* **165** (2022) 113075. https://doi.org/10.1016/j.fct.2022.113075
- [33] M. Alizadeh, E. Demir, N. Aydogdu, N. Zare, F. Karimi, S.M. Kandomal, H. Rokni, Y. Ghasemi, Recent advantages in electrochemical monitoring for the analysis of amaranth and carminic acid food colors, *Food and Chemical Toxicology* **163** (2022) 112929. https://doi.org/10.1016/j.fct.2022.112929
- [34] A. L. Branen, P. M. Davidson, S. Salminen, J. Thorngate, *Food Additives*, CRC Press, 2001. https://doi.org/10.1201/9780367800505
- [35] G. Van Esch, Toxicology of tert-butylhydroquinone (TBHQ), *Food and Chemical Toxicology* **24** (1986) 1063-1065. <a href="https://doi.org/10.1016/0278-6915(86)90289-9">https://doi.org/10.1016/0278-6915(86)90289-9</a>
- [36] W. Cao, Y. Wang, Q. Zhuang, L. Wang, Y. Ni, Developing an electrochemical sensor for the detection of tert-butylhydroquinone, *Sensors and Actuators B* **293** (2019) 321-328. https://doi.org/10.1016/j.snb.2019.05.012
- [37] Y. Pan, K. Lai, Y. Fan, C. Li, L. Pei, B.A. Rasco, Y. Huang, Determination of tert-butylhydroquinone in vegetable oils using surface-enhanced Raman spectroscopy, *Journal of Food Science* **79** (2014) T1225-T1230. https://doi.org/10.1111/1750-3841.12482



- [38] S.S. Siwal, A.K. Saini, S. Rarotra, Q. Zhang, V.K. Thakur, Recent advancements in transparent carbon nanotube films: chemistry and imminent challenges, *Journal of Nanostructure in Chemistry* **11** (2021) 93-130. <a href="https://doi.org/10.1007/s40097-020-00378-2">https://doi.org/10.1007/s40097-020-00378-2</a>
- [39] A. Mohammadnavaz, F. Garkani-Nejad, Voltammetric determination of hydrochlorothiazide at a modified carbon paste electrode with polypyrrole nanotubes, *ADMET and DMPK* **11** (2023) 293-302. <a href="https://doi.org/10.5599/admet.1706">https://doi.org/10.5599/admet.1706</a>
- [40] A. Hosseinian-Roudsari, S.-A. Shahidi, A. Ghorbani-HasanSaraei, S. Hosseini, F. Fazeli, A new electroanalytical approach for sunset yellow monitoring in fruit juices based on a modified sensor amplified with nanocatalyst and ionic liquid, *Food and Chemical Toxicology* **168** (2022) 113362. <a href="https://doi.org/10.1016/j.fct.2022.113362">https://doi.org/10.1016/j.fct.2022.113362</a>
- [41] S. Salmanpour, A. Sadrnia, F. Karimi, N. Majani, M.L. Yola, V.K. Gupta, NiO nanoparticle decorated on single-wall carbon nanotubes and 1-butyl-4-methylpyridinium tetrafluoroborate for sensitive raloxifene sensor, *Journal of Molecular Liquids* **254** (2018) 255-259. https://doi.org/10.1016/j.molliq.2018.01.105
- [42] Q. Zhao, Z. Gan, Q. Zhuang, Electrochemical sensors based on carbon nanotubes, *Electroanalysis* **14** (2002) 1609-1613. https://doi.org/10.1002/elan.200290000
- [43] A. Ambika, N. Navya, S. Kiran Kumar, B. Suresha, Electrochemical determination of paracetamol by SWCNT-modified carbon paste electrode: a cyclic voltammetric study, *Carbon Letters* **32** (2022) 1287-1295. <a href="https://doi.org/10.1007/s42823-022-00354-6">https://doi.org/10.1007/s42823-022-00354-6</a>
- [44] S. Zheng, J. Fan, F. Yin, J. Chen, Z. Hui, J. Tang, X. Wang, J. Guo, Electrochemical determination of tert-butylhydroquinone by ZIF-67@ TiO<sub>2</sub> derived hierarchical TiO<sub>2</sub>/Co/NCNTs, *New Journal of Chemistry* **47(33)** (2023) 15569-15578. https://doi.org/10.1039/D3NJ02149A
- [45] M.-H. Karimi-Harandi, M. Shabani-Nooshabadi, R. Darabi, Cu-BTC metal-organic frameworks as catalytic modifier for ultrasensitive electrochemical determination of methocarbamol in the presence of methadone, *Journal of The Electrochemical Society* 168 (2021) 097507. <a href="https://doi.org/10.1149/1945-7111/ac2468">https://doi.org/10.1149/1945-7111/ac2468</a>



Open Access :: ISSN 1847-9286 www.jESE-online.org

Original scientific paper

# The performance of heteroatom-doped carbon nanotubes synthesized *via* a hydrothermal method on the oxygen reduction reaction and specific capacitance

Tienah H. H. Elagib<sup>1,2,⊠</sup>, Nassereldeen A. Kabbashi<sup>1</sup>, Md Zahangir Alam<sup>1</sup>, Ma'an F. Al-Khatib<sup>1</sup>, Mohamed E. S. Mirghani<sup>1</sup> and Elwathig A. M. Hassan<sup>2</sup>

<sup>1</sup>Kulliyyah of Engineering, Department of Chemical Engineering and Sustainability, International Islamic University Malaysia, Jalan Gombak 53100, Kuala Lumpur, Malaysia

<sup>2</sup>Department of Materials Engineering, Faculty of Industrial Engineering and Technology, University of Gezira, Wad Madani, Sudan

Corresponding author: <sup>™</sup>tienahhussain25024@gmail.com

Received: February 7, 2023; Accepted: April 16, 2023; Published: May 15, 2023

# **Abstract**

Due to the increasing demand for electrochemical energy storage, various novel electrode and catalysis materials for supercapacitors and rechargeable batteries have developed over the last decade. The structure and characteristics of these catalyst materials have a major effect on the device's performance. In order to lower the costs associated with electrochemical systems, metal-free catalysis materials can be employed. In this study, metal-free catalysts composed of nitrogen (N) and sulfur (S) dual-doped multi-walled carbon nanotubes were synthesized using a straightforward and cost-effective single-step hydrothermal method. Carbon nanotubes served as the carbon source, while I-cysteine amino acid and thiourea acted as doping elements. As a result of the physicochemical characterization, many defects and a porous structure were noted, along with the successful insertion of nitrogen and sulfur into the carbon nanotube was confirmed. According to the cyclic voltammetry tests for the dual-doped samples in alkaline conditions, the D-CNT2 catalyst exhibited onset potential of -0.30 V higher than -0.37 V observed for the D-CNT3 catalyst. This indicates enhanced oxygen-reduction reaction due to the synergistic effects of the heteroatoms in the structure and the presence of chemically active sites. Moreover, the outstanding specific capacitance of the D-CNT2 catalyst (214.12 F g<sup>-1</sup> at scanning rate of 1 mV s<sup>-1</sup>) reflects the effective porosity of the proposed catalyst. These findings highlight the potential of N/S dual-doped carbon nanotubes for electrocatalytic applications, contributing to efficient energy conversion.

#### **Keywords**

Metal-free catalyst; electrochemical energy storage; catalytic activity; porous structure

#### Introduction

In recent years, fostering a sustainable society has been a focus [1-3]. Developing renewable energy is important in achieving sustainable development and reducing pollution from fossil fuels [4-6]. The creation of clean energy storage and generation with low costs and great efficiency has garnered a lot of interest [7-9]. Traditional energy supplies, according to the Exxon Mobil paper titled 2018 Outlook for Energy: a view of 2040, will play an irreplaceable part in our future daily lives. Despite efficiency increases between 2016 and 2040, it expected worldwide energy consumption to increase by approximately 25 %, while they expected global electricity demand to climb by 60 %. Thus, building green electro-based energy systems is urgently needed to support economic progress and accomplish the Paris Agreement's climate targets, and it surely bears enormous market opportunities [10].

Presently, vital research is being focused on advanced technologies for electrochemical energy storage and conversion systems such as electrochemical capacitors, regenerative fuel cells, and rechargeable batteries (including Na-ion batteries, Li–sulfur batteries, Li-ion batteries, and K-ion batteries [11]), including electrocatalysis due to their flexible capacities [12], eco-friendly [13-15], remarkable energy conversion ability, and sustainability [16,17]. Electrochemical processes, like electrocatalysis, are crucial to electrochemical energy storage and conversion systems [18]. During discharging, such energy systems undergo an oxygen reduction reaction (ORR) on their negative electrode [19]. It is important to rationally design highly active [20], durable, and low-cost electrocatalyst for effective ORR as it represents a critical reaction in energy conversion systems [21]. Although a variety of factors influence the performance of energy-related devices, the structure and characteristics of the materials utilized heavily influence the overall performance [22].

In fact, ORR is slow in an acidic medium and requires noble catalysts such as Pt to occur; however, ORR has a lower over-potential in an alkaline medium than that in an acidic medium, allowing the use of noble-free catalysts [23]. To meet the needs of industry and advanced energy systems, the advancement of cost-effective metal-free electrocatalytic materials is of great interest [24]. In this direction, numerous non-precious ORR electrocatalysts, such as transition metal chalcogenides [25], transition metal nitrogen-containing complexes, and metal-free doped carbon materials [26], have been explored and developed [27]. It is broadly acknowledged that doping nanostructured carbons with heteroatoms such as boron, nitrogen (N), phosphorus, and sulfur (S) improves oxygen-reaction activities significantly [28]. For instance, J. H. Kim et al. [29] used chemical vapor deposition to create sulfur-doped carbon nanotubes (S-CNTs) using dimethyl disulfide as the sulfur source. At a high discharge current density of 100 mA cm<sup>-2</sup>, the proposed material exhibited excellent specific capacitance of 120.2 F g<sup>-1</sup>. The doping effect was responsible for the superior electrochemical performance of S-CNTs. As earlier reported in the literature, the doped heteroatoms can modify the spin-charge densities, causing charge redistribution in the carbon matrix [30]. The S element, in particular, increases the positive charge density and spin density of adjacent carbon atoms, promoting oxygen molecular adsorption on the carbon matrix and conferring carbon materials with effective ORR catalytic activity [31,32]. The creation of C-N structures, such as graphitic-N and pyridinic-N, can aid in electron transfer during the ORR process [31]. Previous research has shown that incorporating heteroatoms improves the distribution and preserves the electrical conductivity of nanostructured carbons and, thus, catalytic activity. The doped material also has long-term durability, good stability [33], and exceptional poison resistance during the ORR process [34,35]. Raji Atchudan and co-workers [36], for example, synthesized nitrogen-doped porous carbon, which showed a high specific capacity (160 F g<sup>-1</sup>) with a good cycling stability of 95 % and a high rate performance of 52 % retention from 0.5 to 5.0 A g<sup>-1</sup> in a three-electrode system in an aqueous 1 M H<sub>2</sub>SO<sub>4</sub> electrolyte. To the best of our knowledge, dual or even triple heteroatom doping treatments have been employed to improve the ORR catalytic performance of carbon-based nanostructures [37,38]. Y. Zheng and colleagues [39] used a simple and straightforward template-free technique to fabricate nitrogen/sulfur dual-doped hollow mesoporous carbon nanospheres for ORR electrocatalysis. The unique hollow spherical and mesoporous structure formed in situ from an intricately engineered covalent triazine framework *via* a thermally initiated hollowing pathway. The material that resulted exhibited high N and S contents, large specific surface areas, and excellent electrochemical performance [39].

Generally speaking, carbon materials have been designed for effective energy conversion and storage due to their unique physicochemical properties, such as high electronic conductivity, large surface area, and adjustable porous structure [22]. In this direction, CNTs have sparked considerable interest in the fields of electrocatalysis, biosensors, and energy storage due to their amazing features, which include exceptional electronic conductivity, great thermal stability, and good mechanical characteristics [40]. Herein, CNTs, I-cysteine (L-Cys), and thiourea (TU) were utilized for dual-doping with a hydrothermal treatment for electrocatalysis. Although N and S dual-doped CNTs have been extensively studied, little attention has been paid to the study of CNTs treated with amino acids-cothiourea for electrochemical catalysis. Therefore, we investigated the structural change caused by inserting dual heteroatoms into the surface of CNTs, as well as the electrochemical performance in terms of the ORR. For comparison, investigated heteroatom doping of oxidized CNTs to test the hypothesis that heteroatom-doped CNT catalysts functionalized with selective oxygenic groups (COOH or OH) can improve intrinsic reactivity. Neat CNTs, doped CNT prepared at 4 h, and doped (CNT and oxidized CNTs (OCNTs)) prepared at 16 h are denoted as CNTO, D-CNT1, D-CNT2, and D-CNT3, respectively.

# **Experimental**

#### Materials

Multiwall carbon nanotubes (MWCNTs,  $\geq$ 98 % purity) were provided by Sigma Aldrich. L-Cys ( $\geq$ 99 % purity) was purchased from Beijing Solarbio Science & Technology. Thiourea (>98 % purity), N, N-Dimethyleformamide DMF, NaNO<sub>3</sub> (>98 % purity), and H<sub>2</sub>SO<sub>4</sub> (98 %) were supplied by R&M Chemicals. KMNO<sub>4</sub> (>99 % purity) and hydrogen peroxide were provided by Chemiz Sdn. Bhd., and Bendosen Laboratory Chemicals, respectively.

#### Oxidation of CNTs

Typically, 0.1 g of CNTs with 0.1 g of NaNO<sub>3</sub> were dispersed in 60 ml  $H_2SO_4$  (78 %) and placed in the sonicated for around 40 minutes at 11 °C in an ice bath, after which 0.2 g of KMNO<sub>4</sub> was added to the dispersion portion wise and sonicated for 2 h at (35 to 45 °C). Then 20 ml of 30 wt.%  $H_2O_2$  was progressively added, followed by 300 ml of deionized water. Finally, the CNTs were filtered, washed, and dried.

# Hydrothermal synthesis

Typically, 0.2 g of CNTs were dispersed in 100 ml deionized water before being placed in an ultrasonic bath for 2 h at room temperature (Solution A). Then after, 0.15 g of L-Sys and T-U (weight ratio 2:1) was added to 30 ml of solution A and then sonicated for 30 min (Solution B). Solution B was placed into a Teflon-autoclave reactor for hydrothermal reaction and in an oven for the

appropriate reaction time at 160 °C. The reactor was then allowed to cool naturally before the CNTs were filtered, washed, and freeze-dried. The same method was used to treat the oxidized CNTs.

#### Measurements

X-ray diffractometer (XRD) (D2 PHASER – Bruker, Germany)was used to measure phase patterns of D-CNTs. Cu K $\alpha$  radiation, Cu anode, and a scanning rate of 10° min<sup>-1</sup> were used for measurements. Raman spectroscopy (Renishaw inVia, Germany) was used to identify the final chemical structure of modified CNTs.

To further reveal the chemical structure, a Fourier transfer infrared (FTIR) spectrometer (Nicolet iS50 FT-IR, USA) was used to characterize the functional group attached to doped CNTs. Analyses were performed by using the ATR method over a spectral range of 4000 to 500 cm<sup>-1</sup>. Differential scanning calorimetry (DSC) analysis was performed by using a high-temperature DSC (METTLER TOLEDO, Switzerland) instrument. About 0.5 mg of each sample was heated in an aluminum crucible with a heating rate of 10 °C min<sup>-1</sup> from 30 to 450 °C.

The morphology and EDS elemental analysis of doped-CNTs were studied using scanning electron microscopy (SEM, JSM-5600LV, Japan). Thermo Scientific elemental analyzer (Flash smart CHNS, Italy) was employed to measure the element content inserted in the modified CNTs. About 3 mg of dried samples were used and the atomic percentage of nitrogen, carbon, hydrogen, and sulfur were determined. ORR of modified samples was carried out on a potentiostat (Auto-Lab PGSTAT302N, Netherlands).

#### Results and discussion

#### XRD phase evaluation

XRD patterns for nitrogen-co-sulfur-doped CNTs are shown in Figure 1. The XRD patterns show major peaks at around  $2\theta \approx 25$  and  $42^\circ$ . These peaks are assigned to the hexagonal graphite structures (0 0 2) and (1 0 0), respectively [41]. Obviously, when compared to untreated samples, the intensity of reflection of all doped CNTs decreased, which may be attributable to the insertion of doping elements such as N and S. The substitution of a heteroatom (N or S) in the CNTs generates defect sites and disrupts the carbon lattice; these findings demonstrated their less crystalline nature [42]. The Raman spectra support this result, as seen in Figure 2.

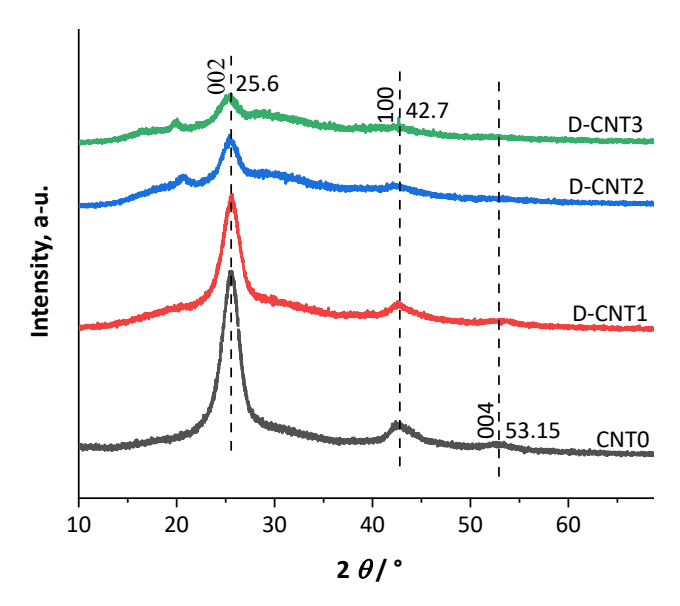


Figure 1. XRD pattern for the sample of (a) Neat CNTs, (b) D-CNT1, (c) D-CNT2, (d) D-CNT3

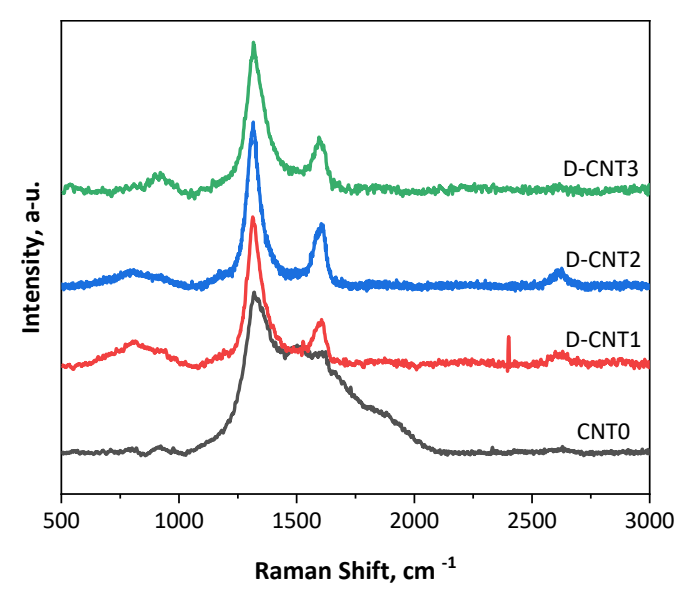


Figure 2. Raman spectra for the sample of (a) Neat CNTs, (b) D-CNT1, (c) D-CNT2, (d) D-CNT3

In particular, D-CNT2 and D-CNT3 exhibited lower intensity for both diffraction peaks than D-CNT1, which could be attributable to a longer doping time. Furthermore, the (100) graphitic plane diffraction peak appears to have vanished in sample D-CNT3, possibly because oxidizing CNTs provided more sites for chemical reactions. CNTs can, in fact, be functionalized in an oxidative environment, therefore CNTs with OH, =CO, O, COOH functionalization are more effective for subsequent reactions [43].

#### Raman spectroscopy analysis

Raman spectroscopy was used to explore further the sulfur-co-Nitrogen functionalization of CNTs (Figure 2). Two distinct peaks centered at 1350 and 1580 cm<sup>-1</sup> are identified, corresponding to the disordered carbon (D-band) and the ordered graphitic carbon (G-band). The presence of a D-band with a high intensity indicates the existence of several defects and non-graphitic carbon in the doped CNTs sample, which may have resulted from heteroatoms doping [44]. As can be seen, sample D-CNT2 seems to have the maximum intensity when compared to the other samples. Furthermore, as shown in Figure S-1, a corresponding endothermic peak on the DSC curve was identified, which is associated with the degradation/decomposition of the carbon framework. When compared to doped CNT, neat CNT has a lower decomposition temperature. The heat of the reaction rises when doping elements are introduced. These results can be a sign of interaction between CNT and heteroatoms.

Some time ago, it was pointed out that doping with heteroatoms can create chemically active regions, which can boost electrocatalytic activity [44]. The G-band of D-CNT1, DCNT2, and D-CNT3 is obviously shifted to a lower frequency by about  $10~\text{cm}^{-1}$ . In the literature, we observed a similar redshift behavior in sulfur-doped carbon nanotubes, indicating the electron delocalization effect caused by  $\pi$ - $\pi$  interactions between the electron-donor doping precursors and CNT [35]. Overall, the XRD and Raman spectroscopy results suggest the nanocomposite is doped with N and S successfully by our one-step hydrothermal method and that variable doping levels are realized by varying the doping time [45]. In addition, clear evidence and additional conformation of nitrogen and sulfur incorporated into carbon nanotubes are provided in Figure S-2.

Furthermore, the D/G peak intensity ratios ( $I_D/I_G$ ) of D-CNT1, D-CNT2, and D-CNT3 are 1.75, 1.43, and 1.30, respectively. Due to the fact that doping precursors wrapped around the surface of CNTs and covered the partial defect sites, the  $I_D/I_G$  ratio was slightly reduced [35].

# SEM morphological observation

Figures 3 show SEM images of doped-CNTs. As can be observed, D-CNT2 and D-CNT3 samples contain more clearly irregular nanoparticles, Figure 3b and 3c. This finding indicated their porous nature and high surface area [41]. Several corners and edges are visible on the surfaces of D-CNT2 and D-CNT3, which could become active sites of oxygen adsorption in the ORR process. D-CNT2 has a significant number of pores in its morphology and appears to have a considerably looser porous structure, which helps to improve its ORR activity [46]. To the best of our knowledge, the presence of porous carbons, which give an enhanced accessible surface area for electrolyte ions, is principally responsible for the improved performance of the working electrode [44]. Furthermore, in samples D-CNT2 and D-CNT3, the particles appear densely stacked and agglomerated, implying that agglomeration occurred when amino acids were employed [22,47]. The overlapping and agglomeration behavior leads to forming complex three-dimensional stacked structures [34].

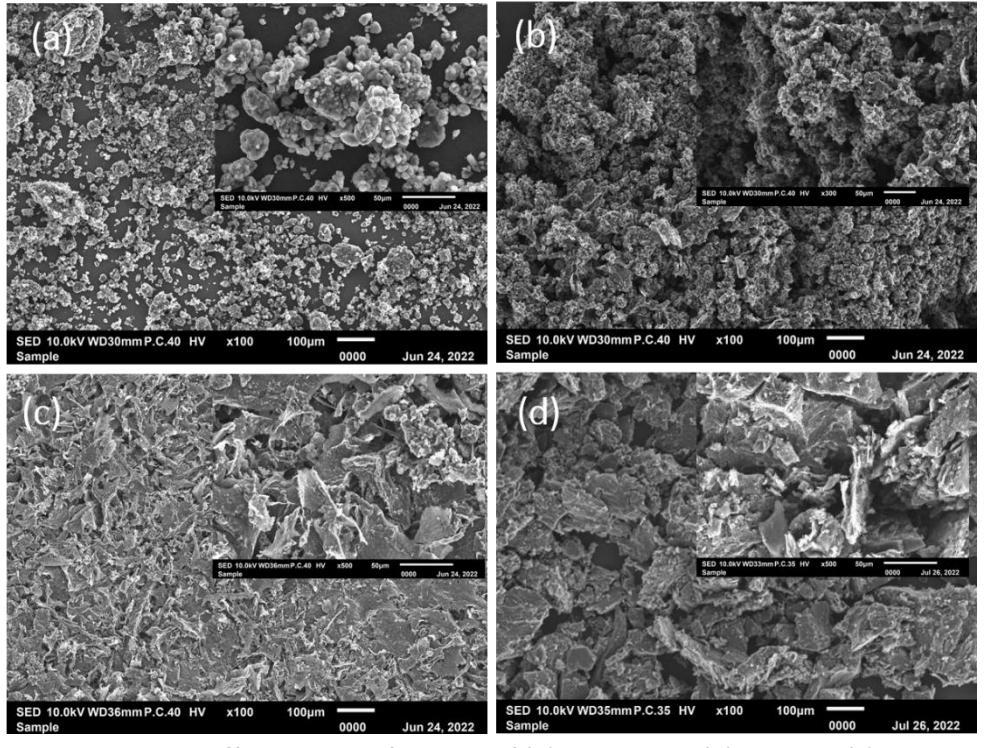


Figure 3 – SEM images with different magnifications of (a) Neat CNTs, (b) D-CNT1, (c) D-CNT2, (d) D-CNT3

# Elemental analysis

The data from the (CHNS) analysis are shown in Table 1 to confirm the incorporation of doping elements into CNTs' surface. As we can see, The D-CNT3 sample has a slightly lower C content than the other samples, but it has the highest N and S content of 9.38 and 15.20 %, respectively. This is most likely because of the significant doping amount of N and S atoms caused by oxidation of the CNT prior to the doping process, which is consistent with the XRD results. The result of EDS color mapping (Figure S3) further describes the heteroatoms doping of CNTs. As seen the D-CNT3 has a higher S content than D-CNT2. Nitrogen is not detected by SEM-EDX, presumably because nitrogen has a very faint response, making detection unreliable for most materials [48]. Furthermore, EDS may detect major elements with concentrations greater than 10 wt.% [49].

Sample	Content, wt.%			
	Nitrogen	Carbon	Hydrogen	Sulfur
CNT0	0	88.41	0.102	0.105
D-CNT1	0.572	77.11	0.893	2.744
D-CNT2	1.428	75.695	4.722	5.389
D-CNT3	9.378	41.167	1.872	15.203

**Table 1**. Elemental content for the doped sample

# Cyclic voltammetry – CV test

The catalytic activity for oxygen reduction reaction of the doped CNTs was measured using cyclic voltammetry (CV) with a three-electrode system (working electrode, counter electrode, and reference electrode) in 1.0 M KOH aqueous electrolyte with potential between – 0.6 and 0.1 V at a scanning rate of 1 and 10 mV s<sup>-1</sup>. The working electrode was prepared without the addition of any binding materials. The following procedure was used to prepare all working electrodes; 4 mg of D-CNTs were dispersed in 500  $\mu$ L Alcohol and sonicated for 30 minutes. 1 to 2  $\mu$ L of dispersion was loaded to the electrode's surface and dried.

Typical cyclic voltammogram curves of doped CNTs cathode/catalyst for the first two or three cycles are displayed in Figure 4. On the CV curves of the D-CNT2 and D-CNT3 samples, a significant ORR peak was observed. D-CNT2 and D-CNT3 have ORR onset potentials of -0.30 and -0.37 V, respectively, while the reduction (cathodic) peaks are at -0.26 and -0.35 V, respectively. The reduction peak of DCNT2 and DCNT3 marginally changed to -0.24 and -0.39 V, respectively, when the scanning rate was increased to 10 mV s<sup>-1</sup>. These findings demonstrated that D-CNT2 catalysts have stronger ORR catalytic performance than D-CNT3 catalysts. Furthermore, the higher onset potential of D-CNT2 than D-CNT3 implies that the ORR occurs more easily on its surface [34].

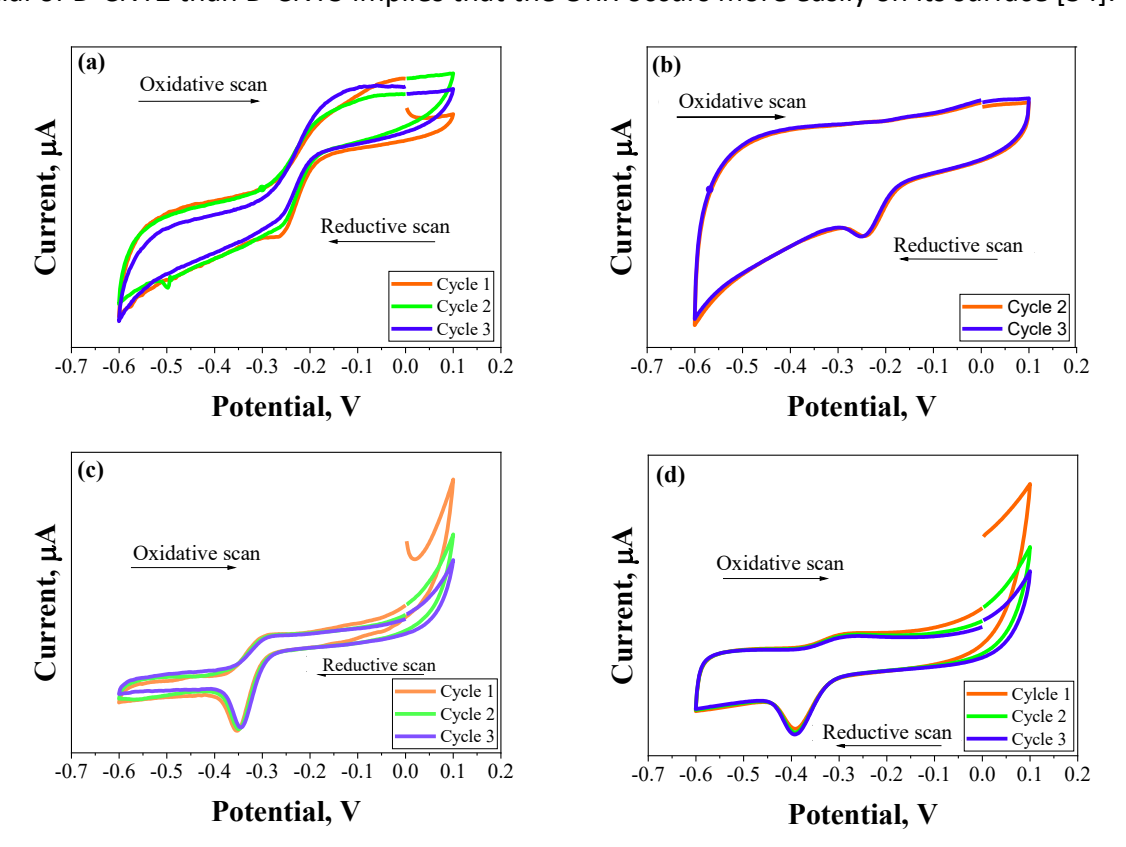


**Figure 4.** Cyclic voltammogram variations with altering scan rates of proposed catalysts (a) D-CNT2, scan rate 1 mV s<sup>-1</sup>; (b) D-CNT2, scan rate 10 mV s<sup>-1</sup>; (c) D-CNT3, scan rate 1 mV s<sup>-1</sup>; (d) D-CNT3, scan rate 10 mV s<sup>-1</sup>

Because of the large number of holes and edges, the DCNT2 electrode has increased activity and a positively shifted onset potential compared to the DCNT3 electrode [50]. To our knowledge, doping with heteroatom can improve the electron-transfer kinetics and consequently the catalytic activity [34]. Besides, Due to a unique electron distribution, the synergistic effect of dual-doping with two dopant elements of different electro-negativities can enhance catalytic activity [51].

Although D-CNT3 contains more N and S than D-CNT2, the latter demonstrated higher ORR catalytic activity, which could be attributed to oxygen-containing functional groups being primarily eliminated below 400 °C [34]. As a result, the reduced oxygen functional group of D-CNT3 during the hydrothermal reaction slightly inhibits ORR activity. According to the Raman analysis, another impact could be the wrapping of doping precursors on the surface of OCNTs and the coverage of partial defect sites.

Additionally, because heteroatom doping can alter surface activity via conjugation between a lone pair of electrons and the  $\pi$ -system of the carbon lattice, it has the potential to generate further pseudo-capacitance improved electrocatalytic activity [22]. Using the CV data, the following equation was used to calculate the variation of specific capacitance with changing scan rates [52]:

$$C_{p} = \frac{A}{2mk(E_{2} - E_{1})} \tag{1}$$

where; A is the CV loop's enclosed area and m is the mass of material at the working electrode, k is the scanning rate, and  $(E_2 - E_1)$  is the potential window (i.e., the entire voltage range through which the electrode system was tested for electrochemical behavior). Table 2 compares the specific capacitance of each doped sample. As shown,  $C_p$  is noticeably higher when the scanning rate is low (1 mV s<sup>-1</sup>) and higher in D-CNT2 samples than in D-CNT3 samples, reflecting their effective porosity. To the best of our knowledge, determining specific capacitance at differing scan rates is an essential step in understanding the inherent properties of any electrode material, particularly porosity influences ionic diffusion [52]. The analysis suggests that the dual-doped CNT can be used as an electrocatalyst, and D-CNT2 appears more capacitive than the other sample.

Dual-doped samples	Scan rate, mV s <sup>-1</sup>	Specific capacity, F g <sup>-1</sup>	
D-CNT2	1	214.12	
D-CN12	10	91.14	
D CNT3	1	197.70	
D-CNT3	10	124.18	

**Table 2**. Specific capacity  $C_p$  for two differing scanning rates

# **Conclusions**

The nitrogen and sulfur dual-doped carbon materials were successfully synthesized with various morphological aspects through a hydrothermal method using l-cysteine and thiourea as precursors. After freeze drying, the resulting D-CNT2 and D-CNT3 exhibited a porous structure. The examination of elemental content proved the existence of sulfur and nitrogen functional groups in CNTs after dual heteroatoms doping. The finding of the electrochemical characterization of the proposed catalysts demonstrates the great ORR activity, which can be attributed to the synergistic effect of dual-doping with dopant elements of different electro-negativities, in addition to the presence of numerous active sites and effective porosity. Besides, heteroatom doping generated the electro-chemical capacitance characteristics. The proposed D-CNT2 catalyst achieved stronger ORR catalytic performance and higher specific capacitance at a lower scanning rate than D-CNT3 catalysts.



**Acknowledgements:** The authors gratefully acknowledge the support and funding provided by the postdoctoral scholarship research program of the Islamic Development Bank (IsDB), KSA (Grant No. 600040856) and the project of Prof. Md Zahangir Alam, Kulliyyah of Engineering, (IIUM) (Grant No. RC-RIGS20-004-0004).

#### References

- [1] A. Hojjati-Najafabadi, M. Mansoorianfar, T. Liang, K. Shahin, H. Karimi-Maleh, A review on magnetic sensors for monitoring of hazardous pollutants in water resources, *Science of the Total Environment* **824** (2022) 153844. <a href="https://doi.org/10.1016/j.scitotenv.2022.153844">https://doi.org/10.1016/j.scitotenv.2022.153844</a>
- [2] C. Karaman, O. Karaman, P.-L. Show, Y. Orooji, H. Karimi-Maleh, Utilization of a double-cross-linked amino-functionalized three-dimensional graphene networks as a monolithic adsorbent for methyl orange removal: equilibrium, kinetics, thermodynamics and artificial neural network modeling, *Environmental Research* **207** (2022) 112156. https://doi.org/10.1016/j.envres.2021.112156
- [3] Y. Orooji, B. Tanhaei, A. Ayati, S. H. Tabrizi, M. Alizadeh, F. F. Bamoharram, F. Karimi, S. Salmanpour, J. Rouhi, S. Afshar, Heterogeneous UV-Switchable Au nanoparticles decorated tungstophosphoric acid/TiO2 for efficient photocatalytic degradation process, *Chemosphere* **281** (2021) 130795. <a href="https://doi.org/10.1016/j.chemosphere.2021.130795">https://doi.org/10.1016/j.chemosphere.2021.130795</a>
- [4] W. Fan, Y. Hao, An empirical research on the relationship amongst renewable energy consumption, economic growth and foreign direct investment in China, *Renewable Energy* **146** (2020) 598-609. https://doi.org/10.1016/j.renene.2019.06.170
- [5] W. S. Ebhota, T.-C. Jen, Fossil fuels environmental challenges and the role of solar photovoltaic technology advances in fast tracking hybrid renewable energy system, *International Journal of Precision Engineering and Manufacturing-Green Technology* **7** (2020) 97-117. https://doi.org/10.1007/s40684-019-00101-9
- [6] R. Kumar, A. Pérez del Pino, S. Sahoo, R. K. Singh, W. K. Tan, K. K. Kar, A. Matsuda, E. Joanni, Laser processing of graphene and related materials for energy storage: State of the art and future prospects, *Progress in Energy and Combustion Science* **91** (2022) 100981. https://doi.org/10.1016/j.pecs.2021.100981
- [7] A. Aygun, F. Gulbagca, E. E. Altuner, M. Bekmezci, T. Gur, H. Karimi-Maleh, F. Karimi, Y. Vasseghian, F. Sen, Highly active PdPt bimetallic nanoparticles synthesized by one-step bioreduction method: Characterizations, anticancer, antibacterial activities and evaluation of their catalytic effect for hydrogen generation, *International Journal of Hydrogen Energy* **48** (2023) 6666-6679. https://doi.org/10.1016/j.ijhydene.2021.12.144
- [8] W. Nimir, A. Al-Othman, M. Tawalbeh, A. Al Makky, A. Ali, H. Karimi-Maleh, F. Karimi, C. Karaman, Approaches towards the development of heteropolyacid-based high temperature membranes for PEM fuel cells, *International Journal of Hydrogen Energy* **48** (2023) 6638-6656. <a href="https://doi.org/10.1016/j.ijhydene.2021.11.174">https://doi.org/10.1016/j.ijhydene.2021.11.174</a>
- [9] H. Karimi-Maleh, C. Karaman, O. Karaman, F. Karimi, Y. Vasseghian, L. Fu, M. Baghayeri, J. Rouhi, P. Senthil Kumar, P.-L. Show, Nanochemistry approach for the fabrication of Fe and N co-decorated biomass-derived activated carbon frameworks: a promising oxygen reduction reaction electrocatalyst in neutral media, *Journal of Nanostructure in Chemistry* 12 (2022) 429-439. https://doi.org/10.1007/s40097-022-00492-3
- [10] X. Wu, J. Jiang, C. Wang, J. Liu, Y. Pu, A. Ragauskas, S. Li, B. Yang, Lignin-derived electrochemical energy materials and systems, Biofuels, *Bioproducts and Biorefining* **14** (2020) 650-672. <a href="https://doi.org/10.1002/bbb.2083">https://doi.org/10.1002/bbb.2083</a>
- [11] H. Kim, J. C. Kim, M. Bianchini, D.-H. Seo, J. Rodriguez-Garcia, G. Ceder, Recent Progress and Perspective in Electrode Materials for K-Ion Batteries, *Advanced Energy Materials* **8** (2018) 1702384. <a href="https://doi.org/10.1002/aenm.201702384">https://doi.org/10.1002/aenm.201702384</a>

- [12] A. G. Olabi, Q. Abbas, A. Al Makky, M. A. Abdelkareem, Supercapacitors as next generation energy storage devices: Properties and applications, *Energy* **248** (2022) 123617. https://doi.org/10.1016/j.energy.2022.123617
- [13] X. Li, J. Zhou, J. Zhang, M. Li, X. Bi, T. Liu, T. He, J. Cheng, F. Zhang, Y. Li, X. Mu, J. Lu, B. Wang, Bamboo-Like Nitrogen-Doped Carbon Nanotube Forests as Durable Metal-Free Catalysts for Self-Powered Flexible Li–CO2 Batteries, *Advanced Materials* **31** (2019) 1903852. <a href="https://doi.org/10.1002/adma.201903852">https://doi.org/10.1002/adma.201903852</a>
- [14] Z. Peng, Y. Zou, S. Xu, W. Zhong, W. Yang, High-Performance Biomass-Based Flexible Solid-State Supercapacitor Constructed of Pressure-Sensitive Lignin-Based and Cellulose Hydrogels, ACS Applied Materials & Interfaces 10 (2018) 22190-22200. https://doi.org/10.1021/acsami.8b05171
- [15] W. Cai, X. Tong, X. Yan, H. Li, Y. Li, X. Gao, Y. Guo, W. Wu, D. Fu, X. Huang, J. Liu, H. Wang, Direct carbon solid oxide fuel cells powered by rice husk biochar, *International Journal of Energy Research* **46** (2022) 4965-4974. https://doi.org/10.1002/er.7489
- [16] B. He, Q. Zhang, Z. Pan, L. Li, C. Li, Y. Ling, Z. Wang, M. Chen, Z. Wang, Y. Yao, Q. Li, L. Sun, J. Wang, L. Wei, Freestanding Metal—Organic Frameworks and Their Derivatives: An Emerging Platform for Electrochemical Energy Storage and Conversion, *Chemical Reviews* **122** (2022) 10087-10125. https://doi.org/10.1021/acs.chemrev.1c00978
- [17] N. Roy, S. Yasmin, A. Ejaz, H.S. Han, S. Jeon, Influence of pyrrolic and pyridinic-N in the size and distribution behaviour of Pd nanoparticles and ORR mechanism, *Applied Surface Science* **533** (2020) 147500. <a href="https://doi.org/10.1016/j.apsusc.2020.147500">https://doi.org/10.1016/j.apsusc.2020.147500</a>
- [18] I. Baskin, Y. Ein-Eli, Electrochemoinformatics as an Emerging Scientific Field for Designing Materials and Electrochemical Energy Storage and Conversion Devices—An Application in Battery Science and Technology, Advanced Energy Materials 12 (2022) 2202380. <a href="https://doi.org/10.1002/aenm.202202380">https://doi.org/10.1002/aenm.202202380</a>
- [19] J. Wang, C.-X. Zhao, J.-N. Liu, D. Ren, B.-Q. Li, J.-Q. Huang, Q. Zhang, Quantitative kinetic analysis on oxygen reduction reaction: A perspective, *Nano Materials Science* **3** (2021) 313-318. <a href="https://doi.org/10.1016/j.nanoms.2021.03.006">https://doi.org/10.1016/j.nanoms.2021.03.006</a>
- [20] X. Yu, Y. Ma, C. Li, X. Guan, Q. Fang, S. Qiu, A Nitrogen, Sulfur co-Doped Porphyrin-based Covalent Organic Framework as an Efficient Catalyst for Oxygen Reduction, *Chemical Research in Chinese Universities* **38** (2022) 167-172. <a href="https://doi.org/10.1007/s40242-021-1374-1">https://doi.org/10.1007/s40242-021-1374-1</a>
- [21] S. Shi, Y. Wang, B. Wang, F. Wu, Y. Suo, Z. Zhang, Y. Xu, Cobalt, sulfur, nitrogen co-doped carbon as highly active electrocatalysts towards oxygen reduction reaction, International *Journal of Hydrogen Energy* **47** (2022) 39058-39069. https://doi.org/10.1016/j.ijhydene.2022.09.073
- [22] D. Wu, T. Wang, L. Wang, D. Jia, Hydrothermal synthesis of nitrogen, sulfur co-doped graphene and its high performance in supercapacitor and oxygen reduction reaction, *Microporous and Mesoporous Materials* **290** (2019) 109556. https://doi.org/10.1016/j.micromeso.2019.06.018
- [23] G. Rambabu, Z. Turtayeva, F. Xu, G. Maranzana, M. Emo, S. Hupont, M. Mamlouk, A. Desforges, B. Vigolo, Insights into the electrocatalytic behavior of nitrogen and sulfur codoped carbon nanotubes toward oxygen reduction reaction in alkaline media, *Journal of Materials Science* **57** (2022) 16739-16754. <a href="https://doi.org/10.1007/s10853-022-07653-3">https://doi.org/10.1007/s10853-022-07653-3</a>
- [24] D. Yan, Y. Han, Z. Ma, Q. Wang, X. Wang, Y. Li, G. Sun, Magnesium lignosulfonate-derived N, S co-doped 3D flower-like hierarchically porous carbon as an advanced metal-free electrocatalyst towards oxygen reduction reaction, *International Journal of Biological Macromolecules* 209 (2022) 904-911. <a href="https://doi.org/10.1016/j.ijbiomac.2022.04.063">https://doi.org/10.1016/j.ijbiomac.2022.04.063</a>



- [25] Z. Chen, D. Higgins, A. Yu, L. Zhang, J. Zhang, A review on non-precious metal electrocatalysts for PEM fuel cells, *Energy & Environmental Science* **4** (2011) 3167-3192. https://doi.org/10.1039/C0EE00558D
- [26] M. Zhang, L. Dai, Carbon nanomaterials as metal-free catalysts in next generation fuel cells, *Nano Energy* **1** (2012) 514-517. <a href="https://doi.org/10.1016/j.nanoen.2012.02.008">https://doi.org/10.1016/j.nanoen.2012.02.008</a>
- [27] W. Wong, W. Daud, A. Mohamad, A. Kadhum, K. Loh, E. Majlan, Recent progress in nitrogen-doped carbon and its composites as electrocatalysts for fuel cell applications, *International Journal of Hydrogen Energy* 38 (2013) 9370-9386. https://doi.org/10.1016/j.ijhydene.2012.12.095
- [28] Y. Jiao, Y. Zheng, K. Davey, S.-Z. Qiao, Activity origin and catalyst design principles for electrocatalytic hydrogen evolution on heteroatom-doped graphene, *Nature Energy* **1** (2016) 16130. https://doi.org/10.1038/nenergy.2016.130
- [29] J.H. Kim, Y.-i. Ko, Y.A. Kim, K.S. Kim, C.-M. Yang, Sulfur-doped carbon nanotubes as a conducting agent in supercapacitor electrodes, *Journal of Alloys and Compounds* **855** (2021) 157282. https://doi.org/10.1016/j.jallcom.2020.157282
- [30] W.-L. Xin, L.-H. Xu, K.-K. Lu, D. Shan, Boosting oxygen reduction catalysis with Fe-N@ ZnO codoped highly graphitized carbon derived from N, N'-carbonyldiimidazole-Induced bimetallic coordinated polymer, *Applied Surface Science* **505** (2020) 144605. https://doi.org/10.1016/j.apsusc.2019.144605
- [31] X. Qiu, Y. Yu, Z. Peng, M. Asif, Z. Wang, L. Jiang, W. Wang, Z. Xu, H. Wang, H. Liu, Cobalt sulfides nanoparticles encapsulated in N, S co-doped carbon substrate for highly efficient oxygen reduction, *Journal of Alloys and Compounds* **815** (2020) 152457. https://doi.org/10.1016/j.jallcom.2019.152457
- [32] D.-W. Wang, D. Su, Heterogeneous nanocarbon materials for oxygen reduction reaction, Energy & Environmental Science 7 (2014) 576-591. https://doi.org/10.1039/C3EE43463J
- [33] R. Atchudan, T. N. J. I. Edison, S. Perumal, A. S. Parveen, Y. R. Lee, Electrocatalytic and energy storage performance of bio-derived sulphur-nitrogen-doped carbon, *Journal of Electroanalytical Chemistry* **833** (2019) 357-369. https://doi.org/10.1016/j.jelechem.2018.12.007
- [34] X. Xu, T. Yuan, Y. Zhou, Y. Li, J. Lu, X. Tian, D. Wang, J. Wang, Facile synthesis of boron and nitrogen-doped graphene as efficient electrocatalyst for the oxygen reduction reaction in alkaline media, *International Journal of Hydrogen Energy* **39** (2014) 16043-16052. https://doi.org/10.1016/j.ijhydene.2013.12.079
- [35] J.-J. Fan, Y.-J. Fan, R.-X. Wang, S. Xiang, H.-G. Tang, S.-G. Sun, A novel strategy for the synthesis of sulfur-doped carbon nanotubes as a highly efficient Pt catalyst support toward the methanol oxidation reaction, *Journal of Materials Chemistry* A **5** (2017) 19467-19475. https://doi.org/10.1039/C7TA05102F
- [36] R. Atchudan, T.N. Jebakumar Immanuel Edison, S. Perumal, R. Vinodh, R. S. Babu, A. K. Sundramoorthy, A. A. Renita, Y. R. Lee, Facile synthesis of nitrogen-doped porous carbon materials using waste biomass for energy storage applications, *Chemosphere* **289** (2022) 133225. https://doi.org/10.1016/j.chemosphere.2021.133225
- [37] Y. Shen, Y. Li, G. Yang, Q. Zhang, H. Liang, F. Peng, Lignin derived multi-doped (N, S, Cl) carbon materials as excellent electrocatalyst for oxygen reduction reaction in proton exchange membrane fuel cells, *Journal of Energy Chemistry* **44** (2020) 106-114. https://doi.org/10.1016/j.jechem.2019.09.019
- [38] Z. Lu, Z. Li, S. Huang, J. Wang, R. Qi, H. Zhao, Q. Wang, Y. Zhao, Construction of 3D carbon network with N, B, F-tridoping for efficient oxygen reduction reaction electrocatalysis and high performance zinc air battery, *Applied Surface Science* **507** (2020) 145154. <a href="https://doi.org/10.1016/j.apsusc.2019.145154">https://doi.org/10.1016/j.apsusc.2019.145154</a>

- [39] Y. Zheng, S. Chen, K. A. I. Zhang, J. Guan, X. Yu, W. Peng, H. Song, J. Zhu, J. Xu, X. Fan, C. Zhang, T. Liu, Template-free construction of hollow mesoporous carbon spheres from a covalent triazine framework for enhanced oxygen electroreduction, *Journal of Colloid and Interface Science* **608** (2021) 3168-3177. https://doi.org/10.1016/j.jcis.2021.11.048
- [40] J. Wang, X. Yan, Z. Zhang, H. Ying, R. Guo, W. Yang, W.Q. Han, Facile preparation of high-content N-doped CNT microspheres for high-performance lithium storage, *Advanced Functional Materials* **29** (2019) 1904819. https://doi.org/10.1002/adfm.201904819
- [41] A. Osikoya, D. Wankasi, R. Vala, C. Dikio, A. Afolabi, N. Ayawei, E. Dikio, Synthesis, characterization and sorption studies of nitrogen—doped carbon nanotubes, *Digest Journal of Nanomaterials and Biostructures* **10** (2015) 125-134.
- [42] A. Ariharan, B. Viswanathan, V. Nandhakumar, Nitrogen-incorporated carbon nanotube derived from polystyrene and polypyrrole as hydrogen storage material, *International Journal of Hydrogen Energy* **43** (2018) 5077-5088. https://doi.org/10.1016/j.ijhydene.2018.01.110
- [43] J. Wei, R. Lv, N. Guo, H. Wang, X. Bai, A. Mathkar, F. Kang, H. Zhu, K. Wang, D. Wu, Preparation of highly oxidized nitrogen-doped carbon nanotubes, *Nanotechnology* **23** (2012) 155601. <a href="https://doi.org/10.1088/0957-4484/23/15/155601">https://doi.org/10.1088/0957-4484/23/15/155601</a>
- [44] G. Sun, H. Xie, J. Ran, L. Ma, X. Shen, J. Hu, H. Tong, Rational design of uniformly embedded metal oxide nanoparticles into nitrogen-doped carbon aerogel for high-performance asymmetric supercapacitors with a high operating voltage window, *Journal of Materials Chemistry A* **4** (2016) 16576-16587. <a href="https://doi.org/10.1039/C6TA07240B">https://doi.org/10.1039/C6TA07240B</a>
- [45] J. Zhao, Y. Liu, X. Quan, S. Chen, H. Zhao, H. Yu, Nitrogen and sulfur co-doped graphene/carbon nanotube as metal-free electrocatalyst for oxygen evolution reaction: the enhanced performance by sulfur doping, *Electrochimica Acta* **204** (2016) 169-175. https://doi.org/10.1016/j.electacta.2016.04.034
- [46] J. Guo, S. Zhang, M. Zheng, J. Tang, L. Liu, J. Chen, X. Wang, Graphitic-N-rich N-doped graphene as a high performance catalyst for oxygen reduction reaction in alkaline solution, *International Journal of Hydrogen Energy* **45** (2020) 32402-32412. <a href="https://doi.org/10.1016/j.ijhydene.2020.08.210">https://doi.org/10.1016/j.ijhydene.2020.08.210</a>
- [47] T. Wang, L. Wang, D. Wu, W. Xia, H. Zhao, D. Jia, Hydrothermal synthesis of nitrogen-doped graphene hydrogels using amino acids with different acidities as doping agents, *Journal of Materials Chemistry A* **2** (2014) 8352-8361. https://doi.org/10.1039/C4TA00170B
- [48] W. J. Wolfgong, Chemical analysis techniques for failure analysis: Common instrumental methods, in Handbook of Materials Failure Analysis with Case Studies from the Aerospace and Automotive Industries ,A. S. H. Makhlouf, M. Aliofkhazraei, Eds., Butterworth-Heinemann, Boston, USA, 2016 pp. 279-307. <a href="https://doi.org/10.1016/B978-0-12-800950-5.00014-4">https://doi.org/10.1016/B978-0-12-800950-5.00014-4</a>
- [49] S. Nasrazadani, S. Hassani, Modern analytical techniques in failure analysis of aerospace, chemical, and oil and gas industries, in Handbook of Materials Failure Analysis with Case Studies from the Oil and Gas Industry, A. S. H. Makhlouf, M. Aliofkhazraei, Eds., Butterworth-Heinemann, Boston, USA, 2016 pp. 39-54. <a href="https://doi.org/10.1016/B978-0-08-100117-2.00010-8">https://doi.org/10.1016/B978-0-08-100117-2.00010-8</a>
- [50] K. Kakaei, G. Ghadimi, A green method for Nitrogen-doped graphene and its application for oxygen reduction reaction in alkaline media, *Materials Technology* 36 (2021) 46-53. https://doi.org/10.1080/10667857.2020.1724692
- [51] H. Liu, P. Sun, M. Feng, H. Liu, S. Yang, L. Wang, Z. Wang, Nitrogen and sulfur co-doped CNT-COOH as an efficient metal-free catalyst for the degradation of UV filter BP-4 based on sulfate radicals, *Applied Catalysis B: Environmental* **187** (2016) 1-10. <a href="https://doi.org/10.1016/j.apcatb.2016.01.036">https://doi.org/10.1016/j.apcatb.2016.01.036</a>



[52] H. Siraj, K. S. Ahmad, S. B. Jaffri, M. Sohail, Synthesis, characterization and electrochemical investigation of physical vapor deposited barium sulphide doped iron sulphide dithiocarbamate thin films, *Microelectronic Engineering* 233 (2020) 111400. https://doi.org/10.1016/j.mee.2020.111400

© 2023 by the authors; licensee IAPC, Zagreb, Croatia. This article is an open-access article distributed under the terms and conditions of the Creative Commons Attribution license (<a href="https://creativecommons.org/licenses/by/4.0/">https://creativecommons.org/licenses/by/4.0/</a>)



Open Access :: ISSN 1847-9286 www.jESE-online.org

Original scientific paper

# A simple, sensitive and cost-effective electrochemical sensor for the determination of N-acetylcysteine

Peyman Mohammadzadeh Jahani¹, Somayeh Tajik²,⊠, and Fariba Garkani Nejad²

<sup>1</sup>School of Medicine, Bam University of Medical Sciences, Bam, Iran

<sup>2</sup>Research Centre for Tropical and Infectious Diseases, Kerman University of Medical Sciences, Kerman, Iran

*Corresponding author:* <sup>™</sup>tajik s1365@yahoo.com

Received: August 23, 2023; Accepted: October 20, 2023; Published: November 29, 2023

#### **Abstract**

In the present work, we prepared a simple and novel electrochemical sensor based on zeolitic imidazolate framework-67 (ZIF-67) and ionic liquid 1-Butyl-3-methylimidazolium hexafluorophosphate (BMIM.PF6) modified carbon paste electrode (CPE), which was effectively used for the determination of N-acetylcysteine. The cyclic voltammetry studies demonstrated the lowest peak potential and the enhanced peak current response for N-acetylcysteine at the surface of ZIF-67/BMIM.PF6-modified CPE compared to the other CPEs due to the significant catalytic effect of ZIF-67 and BMIM.PF6, as well as the combination of them. Under the optimized conditions, the electrochemical response of ZIF-67/BMIM.PF6/CPE sensor provided a good linear relationship with N-acetylcysteine concentration from 0.04 to 435.0  $\mu$ M. The limit of detection is estimated to be 0.01  $\mu$ M for N-acetylcysteine. In further studies and measurements, the estimation of N-acetylcysteine in tablet samples confirms the usefulness of the ZIF-67/BMIM.PF6/CPE sensor.

#### **Keywords**

Zeolitic imidazolate framework-67; ionic liquid; carbon paste electrode; metal-organic framework; nanomaterials

#### Introduction

N-acetylcysteine (as one of the thiol-containing drugs) is an acetylated derivative of the non-essential amino acid L-cysteine. N-acetylcysteine has been primarily used as a mucolytic agent for treating chronic bronchitis and other chronic respiratory disorders characterized by the excessive production of thick mucus [1]. N-acetylcysteine has the ability to break disulfide bonds, transforming them into two sulfhydryl groups. This process reduces the length of the main chain, resulting in the thinning of mucus and makes it easier to eliminate [2]. Also, N-acetylcysteine is widely used as the antidote for hepatoxicity caused by acetaminophen (paracetamol) overdose [3]. Furthermore, due to

its antioxidant properties, N-acetylcysteine is also known as an antitumor, antiviral, and antiinflammatory agent [4]. It also has a potential therapeutic in the treatment of acquired immune deficiency syndrome (AIDS) [5], types of cancer [6], elimination of heavy metals [7], etc. The antioxidant action of N-acetylcysteine can be primarily attributed to two mechanisms [8,9]. Firstly, N-acetylcysteine acts as a precursor of reduced glutathione (GSH), which indirectly exerts antioxidant effects. GSH is a potent intracellular antioxidant crucial in neutralizing reactive oxygen species (ROS) and minimizing oxidative damage. Secondly, N-acetylcysteine exhibits direct antioxidant activity by directly scavenging reactive radicals. It can directly react with highly reactive species such as hydroxyl radicals (HO) and hydrogen peroxide ( $H_2O_2$ ), reducing their reactivity and forming less reactive species. This scavenging action helps mitigate ROS's harmful effects on cells and tissues. Therefore, due to N-acetylcysteine's medical and biological importance, a highly sensitive and selective method is required for its determination. To this day, various analytical techniques have been used for the determination of N-acetylcysteine, such as chromatography [10], chromatography-tandem mass spectrometry [11,12], fluorescence [13], spectrophotometry [14], chemiluminescence [15], capillary electrophoresis [16], and electrochemistry [17-19].

In recent years, electrochemical methods have gained more attention than other methods due to simple and low-cost instrumentation, short analysis time, and portability [20-28]. The application of chemically modified electrodes in the design and fabrication of electrochemical sensors has a special place in the field of electroanalysis and has brought significant growth. Progress in this field can significantly help improve the efficiency, sensitivity, and selectivity of electrochemical sensors, making them more practical [29-36]. Therefore, researchers are continuously discovering and investigating new materials as modifiers to improve the performance of chemically modified electrodes.

Nanotechnology has many applications in various fields, and research is being conducted in this field to improve the efficiency and performance of multiple fields [37-47]. Nanostructures are materials with at least one nanometer-range dimension (1-100 nm). Nanostructures have unique physical and chemical properties that make them suitable for enhancing the performance of electrochemical sensors. Many studies have been conducted on developing nanostructures in electrochemical sensors for applications in fields such as environmental monitoring, healthcare diagnostics, and industrial process control [48-55].

Metal-organic frameworks (MOFs) are crystalline materials of metal ions or clusters coordinated to organic ligands. The metal ions and organic ligands in MOFs provide flexibility in designing the structure and properties of these materials. MOFs exhibit a highly porous structure with a large surface area, making them useful in various applications, including energy storage [56], catalysis [57], sensing [58], drug delivery [59], environmental remediation [60], and so on. One of the promising applications of MOFs is in electrochemical sensing, which can be used as sensing elements to enhance the performance of electrochemical sensors [61-63]. Ionic liquids )ILs) are compounds that have revolutionized many research fields in recent years due to negligible volatility, high polarity, high thermal stability, high chemical stability, low melting point, non-flammability, high ionic conductivity, large electrochemical window, and structural designability. Focusing on the electrochemical aspects of ionic liquids shows that one of their interesting applications is their use as modifying materials of electrodes for the fabrication of sensors [64,65]. Also, the combination of nanomaterials with ILs can play a key role in the efficiency of electrochemical sensors. Several outstanding attributes are observed when incorporating ILs and nanomaterials into electrodes, including long-term stability, higher conductivity, higher sensitivity, improved linearity, superior catalytic ability, and better selectivity [66-68].

The main objective of this work is to develop a simple and fast platform for the electrochemical determination of N-acetylcysteine by using a CPE modified with zeolitic imidazolate framework-67 (ZIF-67) and 1-Butyl-3-methylimidazolium hexafluorophosphate (BMIM.PF<sub>6</sub>) ionic liquid. The electrochemical studies and measurements were performed by cyclic voltammetry (CV), differential pulse voltammetry (DPV), and chronoamperometry (CHA). The developed ZIF-67/BMIM.PF<sub>6</sub>/CPE sensor exhibited better electrochemical performance for sensitive determination of N-acetylcysteine than the other CPEs with low limit of detection (LOD) and wide linear range. Importantly, this sensor's great potential in quantifying N-acetylcysteine in N-acetylcysteine tablet samples is also confirmed.

#### **Experimental**

# Instruments and materials

All electrochemical studies and measurements were done using a potentiostat/galvanostat device (Metrohm Autolab – PGSTAT302N (Utrecht, The Netherlands)), controlled by the GPES 4.9004 software. The electrochemical tests were performed in a typical three-electrode setup by using a reference electrode (RE) (Ag/AgCl/KCl (3.0 M)), counter electrode (CE) (platinum), and working electrode (modified CPE). All solvents and chemicals were commercially available with analytical grade and used directly without further purification.

# Synthesis of ZIF-67

For the preparation of ZIF-67, 2 mmol of cobalt(II) nitrate hexahydrate (0.582 g) was dissolved in 10 mL of methanol by stirring for 15 min. Then, 15 mL methanolic solution of 8 mmol 2-methylimidazole (0.656 g) was added slowly into the cobalt solution for 15 min. This prepared solution was stirred at ambient temperature for 24 h. Finally, the prepared precipitate was collected by centrifugation, washed with deionized water and ethanol several times, and dried at 65 °C in a vacuum oven for 14 h.

The morphology of the as-prepared ZIF-67 was observed by the FE-SEM image (Figure 1). It shows the growth of ZIF-67 crystals with regular rhombic dodecahedral morphology and almost uniform size.

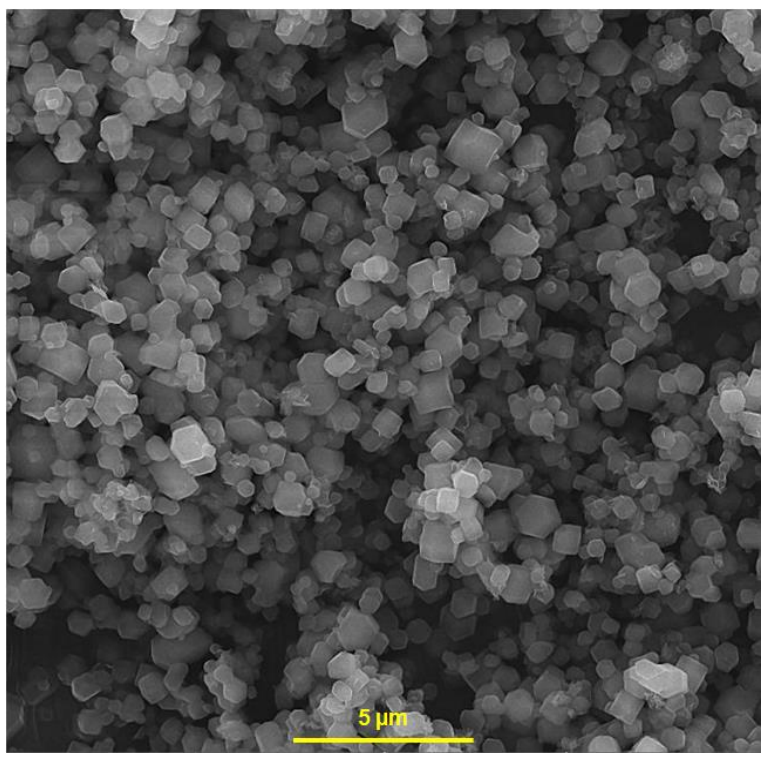


Figure 1. FE-SEM image of ZIF-67

# Preparation of ZIF-67/BMIM.PF<sub>6</sub>/CPE

The ZIF-67-BMIM.PF<sub>6</sub>-modified CPE with a mass of 0.5 g was achieved by hand-mixing 0.47 g of graphite powder and 0.03 g of ZIF-67 for 5 min until a homogeneous blend was formed. Then, paraffin oil and BMIM.PF<sub>6</sub> in the ratio 3:1 was added to the blend of graphite and ZIF-67, which was mixed again for at least 30 min to obtain the ZIF-67/BMIM.PF<sub>6</sub> modified carbon paste. Finally, the modified paste was packed into the glass tube cavity. The electrical contact was established through a conductive copper wire. Also, the surface of the prepared electrode (ZIF-67/BMIM.PF<sub>6</sub>/CPE) was polished on a smooth paper to obtain a shiny and smooth appearance.

To calculate the electrochemically active surface area (EASA) of the unmodified CPE and ZIF-67/BMIM.PF6/CPE, the CVs were recorded at different scan rates in 0.1 M KCl solution containing 1.0 mM  $K_3$ [Fe(CN)<sub>6</sub>] as a redox probe. By using the Randles–Ševčik equation, the value of the ESCA for ZIF-67/BMIM.PF6/CPE (0.396 cm²) was 4.4 times greater than unmodified CPE.

#### **Results and discussion**

Electrocatalytic response of ZIF-67/BMIM.PF<sub>6</sub>/CPE towards N-acetylcysteine

The effect of pH values (from 2.0 to 9.0) of the supporting electrolyte (0.1 M phosphate buffer solution (PBS)) on the electrochemical oxidation of N-acetylcysteine was studied by using the ZIF-67/BMIM.PF<sub>6</sub> modified CPE via the DPV technique. By changing the pH value of PBS, the prepared electrode showed different voltammograms for oxidation of N-acetylcysteine. The peak potential and peak current from the oxidation of N-acetylcysteine showed a strong dependence on pH. By increasing the pH from lower to higher values, the anodic peak potential of N-acetylcysteine was shifted towards the negative potentials. Also, the  $I_{pa}$  of N-acetylcysteine gradually increased with the increase of pH from 2.0 to 7.0 and then decreased. The maximum  $I_{pa}$  was obtained at pH 7.0 (Figure 2). Therefore, pH 7.0 was used for further electrochemical studies.

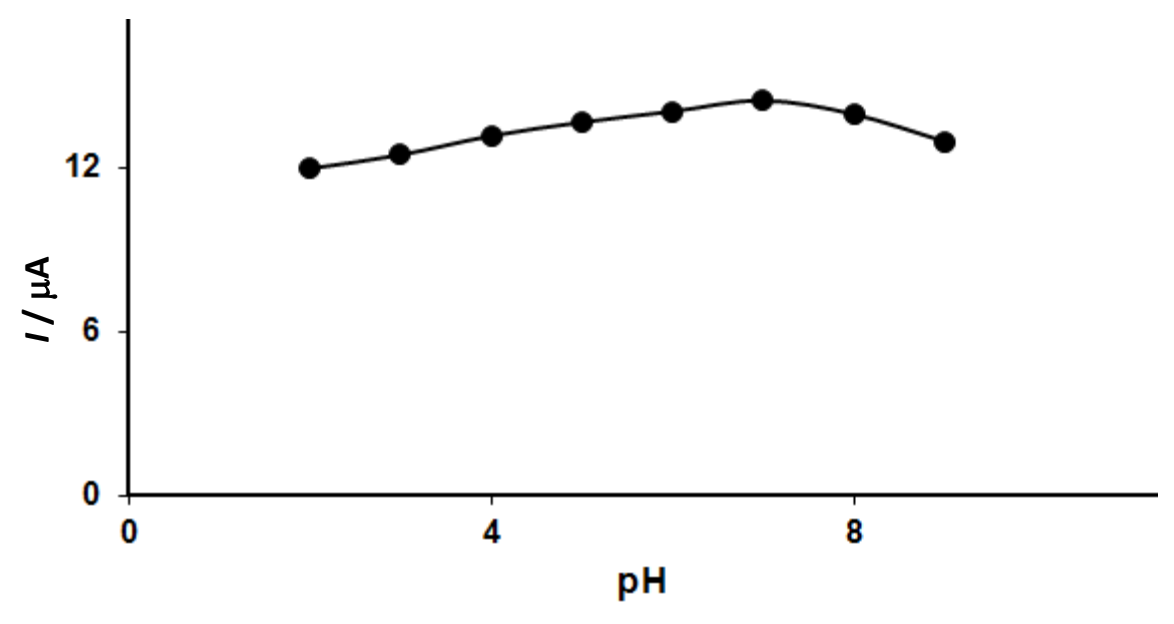


**Figure 2.** Plot of the oxidation peak current of 200.0  $\mu$ M N-acetylcysteine as a function of pH solution at ZIF-67/BMIM.PF<sub>6</sub>/CPE in 0.1 M PBS at different pH values (2.0 to 9.0)

To assess the electrocatalytic activity of the IL (BMIM.PF<sub>6</sub>) and as-prepared ZIF-67, the electrochemical responses of N-acetylcysteine on various electrodes were examined by cyclic voltammetry (CV). Figure 3 shows the cyclic voltammograms from the response of unmodified CPE

(voltammogram a) ZIF-67/CPE (voltammogram b), BMIM.PF<sub>6</sub>/CPE (voltammogram c), and ZIF-67/BMIM.PF<sub>6</sub>/CPE (voltammogram d) towards the 200.0  $\mu$ M N-acetylcysteine in 0.1 M PBS (pH 7.0). As can be seen, a broad oxidation peak with a low anodic peak current ( $I_{pa}$ ) was shown in unmodified CPE. On the other hand, the modification of CPE with ZIF-67 (voltammogram b), BMIM.PF<sub>6</sub> (voltammogram c), and ZIF-67 together with BMIM.PF<sub>6</sub> (voltammogram d) has led to an increase in  $I_p$  intensity and a decrease in overpotential. However, the best case of increasing the  $I_p$  and reducing the overpotential of the N-acetylcysteine oxidation is related to the voltammogram d, which uses both ZIF-67 and BMIM.PF<sub>6</sub> in the composition of the CPE. This result could be related to the electrocatalytic effect of the BMIM.PF<sub>6</sub> and ZIF-67, as well as their synergistic effects. In addition, the absence of any reduction peak on the reverse scan revealed the irreversible oxidation of N-acetylcysteine over unmodified and modified CPEs.

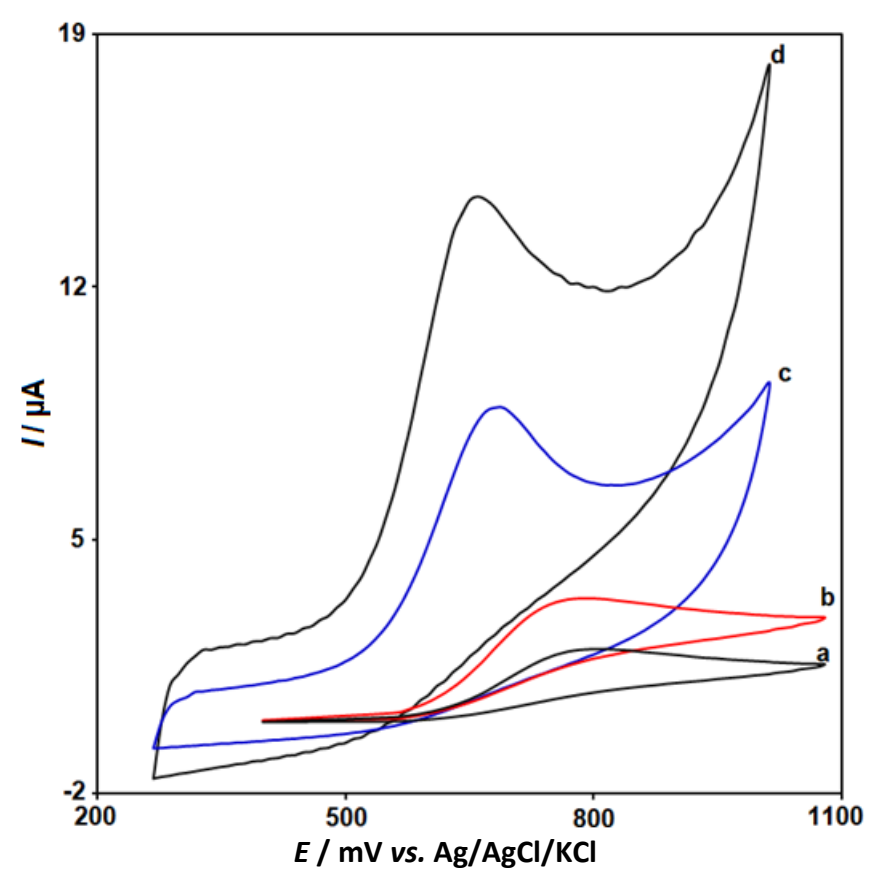


**Figure 3.** CVs of unmodified CPE (a), ZIF-67/CPE (b), BMIM.PF<sub>6</sub>/CPE (c), and ZIF-67/BMIM.PF<sub>6</sub>/CPE (d) in 0.1 M PBS (pH 7.0) containing 200.0  $\mu$ M N-acetylcysteine at a scan rate of 50 mV s<sup>-1</sup>

Effect of scan rate on the oxidation reaction of N-acetylcysteine

To investigate the effect of scan rate, CVs of the ZIF-67/BMIM.PF<sub>6</sub>/CPE were recorded at different scan rates (10 to 500 mV s<sup>-1</sup>) in 0.1 M PBS containing 100.0  $\mu$ M N-acetylcysteine (Figure 4). An increase in the anodic peak current ( $I_{pa}$ ) with an increase in scan rate can be observed. Also, from the obtained voltammograms, it was possible to observe a linear dependence between  $I_{pa}$  of N-acetylcysteine and the square root of scan rate ( $v^{1/2}$ ) (Figure 4 inset). This observation suggests that the oxidation reaction is controlled by the diffusion of N-acetylcysteine species from the bulk solution to the surface of ZIF-67/BMIM.PF<sub>6</sub>/CPE.

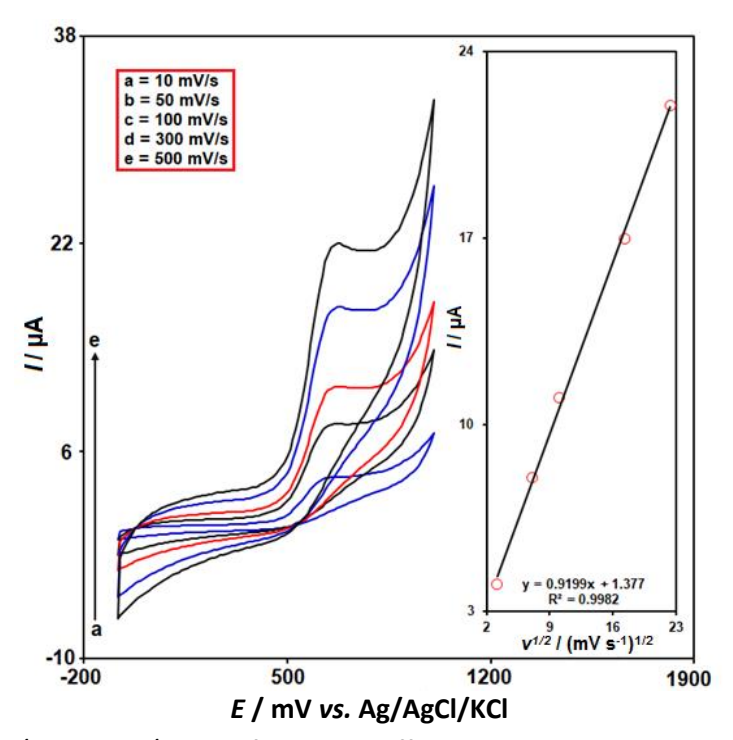


**Figure 4.** CVs of ZIF-67/BMIM.PF<sub>6</sub>/CPE performed at different scan rates in 0.1 M PBS (pH 7.0) containing 100.0  $\mu$ M N-acetylcysteine. Inset: the linear dependence between  $I_{pa}$  vs.  $v^{-1/2}$ 

Chronoamperometric measurements of N-acetylcysteine at ZIF-67/BMIM.PF6/CPE

To measure the diffusion coefficient (*D*) of N-acetylcysteine, the chronoamperometric responses of ZIF-67/BMIM.PF6/CPE was plotted for different concentrations of N-acetylcysteine from 0.1 to 1.6 mM at a fixed potential of 0.71 V (Figure 5).

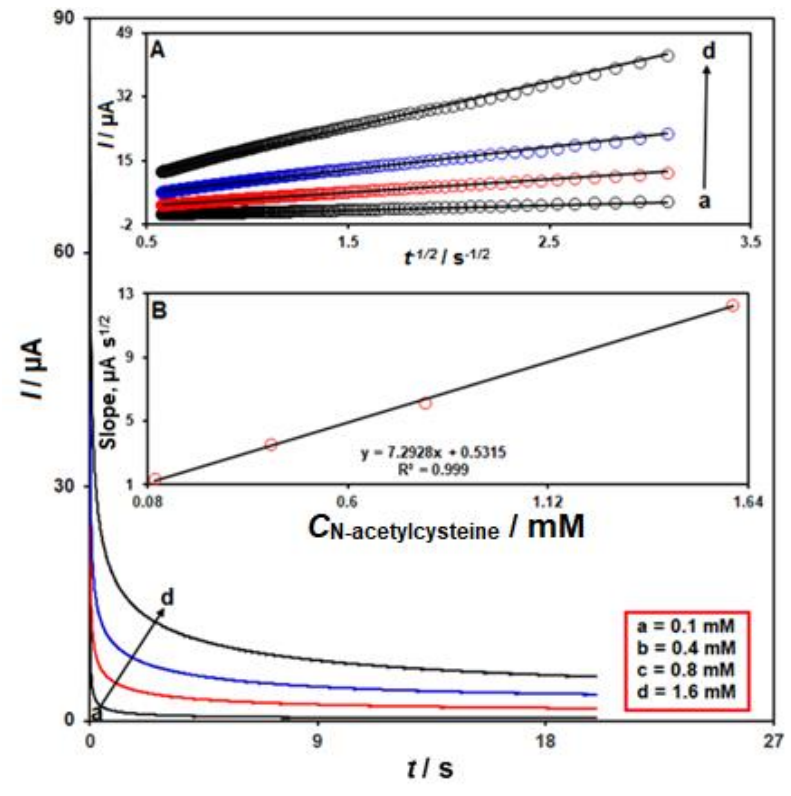


**Figure 5.** Chronoamperometric response of ZIF-67/BMIM.PF<sub>6</sub>/CPE in 0.1 M PBS (pH 7.0) containing different concentrations of N-acetylcysteine. Inset A: the linear dependence between  $I_{pa}$  vs.  $t^{-1/2}$  and Inset B: linear dependence between slope values of  $I - t^{-1/2}$  plots vs. N-acetylcysteine concentrations

The current-time curves reflect the change in concentration gradient of the electroactive species (N-acetylcysteine) in the vicinity of the electrode surface as time progresses. In order to determine the D, the Cottrell curves (I versus  $t^{1/2}$ ) were plotted over a certain range of time for different concentrations of N-acetylcysteine (Figure 5A). Then, the slope of the obtained Cottrell curves was plotted vs. the different concentrations of N-acetylcysteine (Figure 5B) and a straight line with a slope of 7.2928  $\mu$ A s<sup>1/2</sup> / mM was obtained. From the slope of the resulting plot and using Cottrell's equation, the D of N-acetylcysteine on the surface of ZIF-67/BMIM.PF6/CPE was found to be 2.2×10<sup>-6</sup> cm<sup>2</sup> s<sup>-1</sup>.

### Quantitative analysis of N-acetylcysteine by DPV

To study the detection efficiency of ZIF-67/BMIM.PF<sub>6</sub>/CPE, the DPV measurements were performed with the successive addition of N-acetylcysteine (0.04 to 435.0  $\mu$ M) in 0.1 M PBS (pH 7.0) (Figure 6). From the recorded voltammograms, the increase of the Ipa is proportional to the increase of N-acetylcysteine concentration in a wide range from 0.04 to 435.0  $\mu$ M. Furthermore, the linear dependence between the enhanced  $I_{pa}$  of N-acetylcysteine and its concentration is presented in the Inset of Figure 6. This dependence can be expressed by  $I = 0.0683C_{N-acetylcysteine} + 0.9501$  with a correlation coefficient 0.9996. The LOD was calculated according to the ensuing formula  $3S_b/m$ , where  $S_b$  denotes the standard deviation of the blank (PBS) signal (obtained based on 15 measurements on the blank solution), and m denotes the slope of the corresponding calibration curve, and it was found to be 0.01  $\mu$ M. The performance comparison of the developed electrode (ZIF-67/BMIM.PF<sub>6</sub>/CPE) in this study with some previous studies is shown in Table 1.

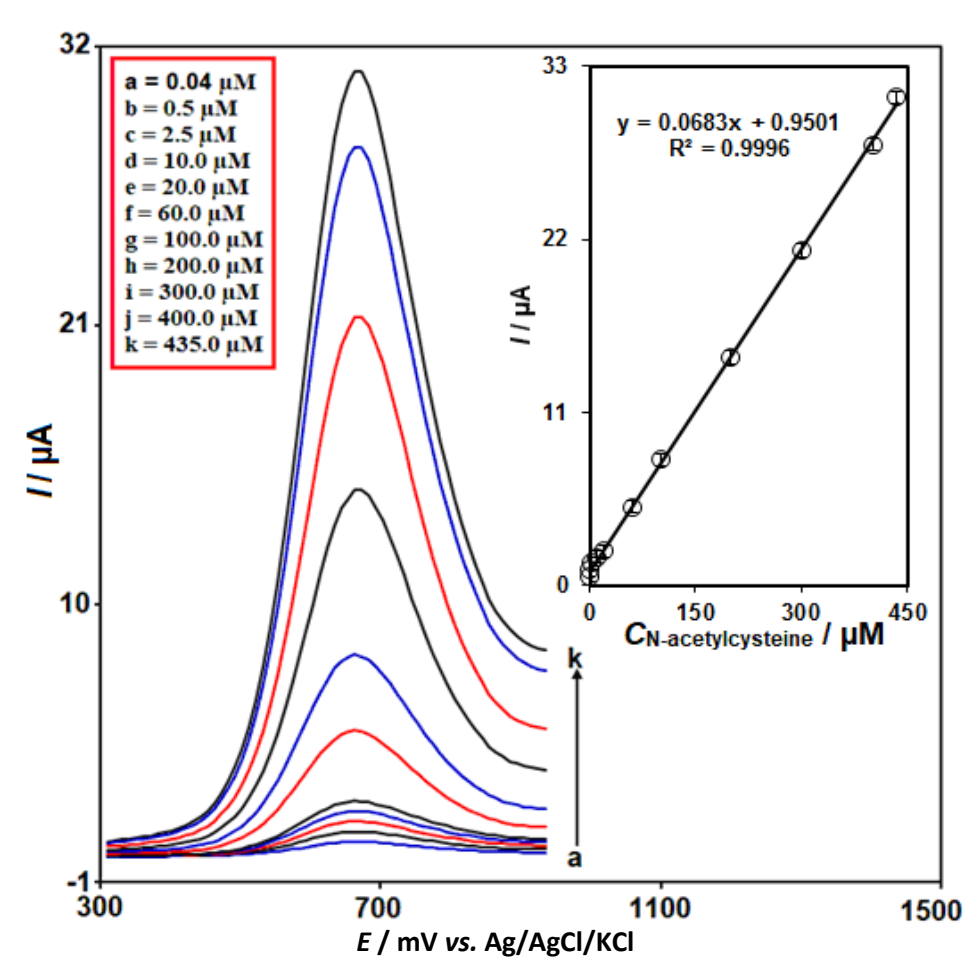


**Figure 6.** DPVs of ZIF-67/BMIM.PF<sub>6</sub>/CPE performed in 0.1 M PBS (pH 7.0) containing different concentrations of N-acetylcysteine. Inset: the linear dependence between  $I_{pa}$  vs. N-acetylcysteine concentration

Electrochemical sensor Method Linear range, mM LOD, μM Ref. Fe<sub>3</sub>O<sub>4</sub>/reduced graphene oxide/glassy DPV 0.10 - 10.0 [17] 11.1 carbon electrode Graphene oxide-copper pentacyano-CV 0.30 - 6.0029.7 [69] nitrosylferrate(III)/graphite paste Copper nitroprusside adsorbed on the 0.099 - 0.890 CV0.41 [70] 3-aminopropylsilica/CPE Linear sweep Copper(II) hexacyanoferrate(III)/CPE 63.0 [71] 0.12 - 0.83voltammetry (LSV) Cobalt salophen complex/carbon DPV 0.0001 - 0.100 0.05 [72] nanotube-paste electrode ZIF-67/BMIM.PF<sub>6</sub>/CPE DPV 0.00004 - 0.435 0.01 This work

**Table 1.** Comparison of the ZIF-67/BMIM.PF<sub>6</sub>/CPE sensor with previously reported N-acetylcysteine sensors

Stability and repeatability studies of ZIF-67/BMIM.PF $_6$ /CPE sensor towards the determination of N-acetylcysteine

Studies related to the stability of ZIF-67/BMIM.PF $_6$ /CPE sensor were performed by recording the current response of the designed sensor towards 60.0  $\mu$ M N-acetylcysteine every 7 days over 14 days. The obtained results showed that the electrode response retained 97.5 % of its initial value after 7 days and 95.1 % after 14 days. These results indicated that the designed sensor had good stability.

Also, to investigate the repeatability of the ZIF-67/BMIM.PF<sub>6</sub>/CPE sensor, the measurements were repeated in 0.1 M PBS (pH 7.0) containing 60.0  $\mu$ M N-acetylcysteine. The acceptable repeatability was obtained with an RSD of 2.9 % after using the same sensor for seven continuous measurements.

#### Interference studies

The interference studies were also carried out to investigate the selectivity of ZIF-67/BMIM.PF<sub>6</sub>/CPE sensor towards the determination of N-acetylcysteine in the presence of various species. The DPV responses of ZIF-67/BMIM.PF<sub>6</sub>/CPE was recorded by adding various species into 0.1 M PBS (pH 7.0) containing 50.0  $\mu$ M N-acetylcysteine. According to the findings, 700-fold of Na<sup>+</sup>, K<sup>+</sup>, Ca<sup>2+</sup>, Al<sup>3+</sup>, NH<sub>4</sub><sup>+</sup>, F<sup>-</sup>, Cl<sup>-</sup>, and Br<sup>-</sup>; 250-fold of urea, glycine, alanine, and phenylalanine; 8-fold of cysteine did not show significant interference (no signal change more than  $\pm$  5 %) for the determination of N-acetylcysteine.

# N-acetylcysteine analysis in real samples

To evaluate the practical performance of the developed sensor (ZIF-67/BMIM.PF<sub>6</sub>/CPE), the determination of N-acetylcysteine in the N-acetylcysteine tablet sample was conducted. The standard addition method was employed for the analysis of N-acetylcysteine by the DPV technique. Measurements were performed by adding the known concentrations of N-acetylcysteine to the N-acetylcysteine tablet sample. The recovery and RSD values are summarized in Table 2.

**Table 2.** Real sample analysis for the determination of N-acetylcysteine spiked into the N-acetylcysteine tablet sample at ZIF-67/BMIM.PF $_6$ /CPE

Sample	Spiked amount, μM	Found amount, μM	Recovery, %	RSD, %
		6.0	-	3.4
N-acetylcysteine	1.0	6.9	98.6	1.9
tablet	2.0	8.3	103.7	2.4
tablet	3.0	9.1	101.1	2.9
	4.0	9.6	96.0	2.5



The summarized results in Table 2 show acceptable recovery values (between 96.0 and 103.7 %) and RSD values (n = 5) of  $\leq 3.4$  %, which confirm that the developed sensor could be used for real-time analysis.

#### Conclusion

In this work, we demonstrated the application of a high-performance electrochemical sensor (ZIF-67/BMIM.PF<sub>6</sub>/CPE) for the determination of N-acetylcysteine. The ZIF-67/BMIM.PF<sub>6</sub>-modified CPE showed more prominent electrocatalytic activity toward N-acetylcysteine oxidation than the other electrodes, with enhanced response current and lowered over-potential. The ZIF-67//BMIM.PF<sub>6</sub>/CPE showed a sensitive peak current response toward N-acetylcysteine in the linear range from 0.04 to 435.0  $\mu$ M, with a LOD (S/N=3) of 0.01  $\mu$ M. Finally, the developed sensor was successfully used for the estimation of N-acetylcysteine in N-acetylcysteine tablet sample with acceptable recoveries (96.0 and 103.7 %) and RSDs values not more than 3.4 %.

#### References

- [1] S. Kiaie, C. Karami, A. Khodadadian, M. Taher, S. Soltanian, A facile method for detection of N-acetylcysteine and l-cysteine with silver nanoparticle in aqueous environments, *Journal of Bioequivalence & Bioavailability* **8** (2016) 197-203. http://dx.doi.org/10.4172/jbb.1000294
- [2] I. S. da Silva, M. F. A. Araújo, H. A. Ferreira, J. D. J. G. Varela Jr, S. M. C. N. Tanaka, A. A. Tanaka, L. Angnes, Quantification of N-acetylcysteine in pharmaceuticals using cobalt phthalocyanine modified graphite electrodes, *Talanta* 83 (2011) 1701-1706. https://doi.org/10.1016/j.talanta.2010.11.070
- [3] O. I. Aruoma, B. Halliwell, B. M. Hoey, J. Butler, The antioxidant action of N-acetylcysteine: its reaction with hydrogen peroxide, hydroxyl radical, superoxide, and hypochlorous acid, *Free Radical Biology and Medicine* **6** (1989) 593-597. <a href="https://doi.org/10.1016/0891-5849(89)90066-X">https://doi.org/10.1016/0891-5849(89)90066-X</a>
- [4] M. Rudašová, M. Masár, Precise determination of N-acetylcysteine in pharmaceuticals by microchip electrophoresis, *Journal of Separation Science* **39** (2016) 433-439. <a href="https://doi.org/10.1002/jssc.201501025">https://doi.org/10.1002/jssc.201501025</a>
- [5] M. Roederer, S. W. Ela, F. J. Staal, L. A. Herzenberg, L. A. Herzenberg, N-acetylcysteine: a new approach to anti-HIV therapy, AIDS Research and Human Retroviruses 8 (1992) 209-217. https://doi.org/10.1089/aid.1992.8.209
- [6] A. Agarwal, U. Muñoz-Nájar, U. Klueh, S. C. Shih, K. P. Claffey, N-acetyl-cysteine promotes angiostatin production and vascular collapse in an orthotopic model of breast cancer, *The American Journal of Pathology* **164** (2004) 1683-1696. <a href="https://doi.org/10.1016/S0002-9440(10)63727-3">https://doi.org/10.1016/S0002-9440(10)63727-3</a>
- [7] H. Ottenwälder, P. Simon, Differential effect of N-acetylcysteine on excretion of the metals Hg, Cd, Pb and Au, *Archives of Toxicology* **60** (1987) 401-402. https://doi.org/10.1007/BF00295763
- [8] A. F. Ourique, K. Coradini, P. dos Santos Chaves, S. C. Garcia, A. R. Pohlmann, S. S. Guterres, R. C. R. Beck, A LC-UV method to assay N-acetylcysteine without derivatization: analyses of pharmaceutical products, *Analytical Methods* 5 (2013) 3321-3327. https://doi.org/10.1039/C3AY40426A
- [9] P. Mitsopoulos, A. Omri, M. Alipour, N. Vermeulen, M. G. Smith, Z. E. Suntres, Effectiveness of liposomal-N-acetylcysteine against LPS-induced lung injuries in rodents, *International Journal of Pharmaceutics* **363** (2008) 106-111. <a href="https://doi.org/10.1016/j.ijpharm.2008.07.015">https://doi.org/10.1016/j.ijpharm.2008.07.015</a>
- [10] P. A. Lewis, A. J. Woodward, J. Maddock, Improved method for the determination of Nacetylcysteine in human plasma by high-performance liquid chromatography, *Journal of Chromatography A* **327** (1985) 261-267. <a href="https://doi.org/10.1016/S0021-9673(01)81655-1">https://doi.org/10.1016/S0021-9673(01)81655-1</a>

- [11] C. Celma, J. A. Allue, J. Prunonosa, C. Peraire, R. Obach, Determination of N-acetylcysteine in human plasma by liquid chromatography coupled to tandem mass spectrometry, *Journal of Chromatography A* 870 (2000) 13-22. https://doi.org/10.1016/S0021-9673(99)01078-X
- [12] C. Lu, G. Liu, J. Jia, Y. Gui, Y. Liu, M. Zhang, C. Yu, Liquid chromatography tandem mass spectrometry method for determination of N-acetylcysteine in human plasma using an isotope-labeled internal standard, *Biomedical Chromatography* **25** (2011) 427-431. <a href="https://doi.org/10.1002/bmc.1465">https://doi.org/10.1002/bmc.1465</a>
- [13] H. B. Wang, H. D. Zhang, Y. Chen, L. J. Ou, Y. M. Liu, Poly (thymine)-templated fluorescent copper nanoparticles for label-free detection of N-acetylcysteine in pharmaceutical samples, *Analytical Methods* **7** (2015) 6372-6377. <a href="https://doi.org/10.1039/C5AY008416">https://doi.org/10.1039/C5AY008416</a>
- [14] J. Giljanović, M. Brkljača, A. Prkić, Flow injection spectrophotometric determination of Nacetyl-L-cysteine as a complex with palladium (II), *Molecules* **16** (2011) 7224-7236. https://doi.org/10.3390/molecules16097224
- [15] G. P. McDermott, J. M. Terry, X. A. Conlan, N. W. Barnett, P. S. Francis, Direct detection of biologically significant thiols and disulfides with manganese (IV) chemiluminescence, *Analytical Chemistry* **83** (2011) 6034-6039. <a href="https://doi.org/10.1021/ac2010668">https://doi.org/10.1021/ac2010668</a>
- [16] M. Jaworska, Z. Szulińska, M. Wilk, E. Anuszewska, Capillary electrophoresis for the determination of N-Acetyltyrosine and N-acetylcysteine in products for parenteral nutrition: Method development and comparison of two CE systems, *Acta Chromatographica* 23 (2011) 595-602. <a href="https://doi.org/10.1556/achrom.23.2011.4.5">https://doi.org/10.1556/achrom.23.2011.4.5</a>
- [17] Y. Wang, Q. Liu, Q. Qi, J. Ding, X. Gao, Y. Zhang, Y. Sun, Electrocatalytic oxidation and detection of N-acetylcysteine based on magnetite/reduced graphene oxide composite-modified glassy carbon electrode, *Electrochimica Acta* **111** (2013) 31-40. <a href="https://doi.org/10.1016/j.electacta.2013.08.010">https://doi.org/10.1016/j.electacta.2013.08.010</a>
- [18] S. Meenakshi, G. Kaladevi, K. Pandian, P. Wilson, Cobalt phthalocyanine tagged graphene nanoflakes for enhanced electrocatalytic detection of N-acetylcysteine by amperometry method, *Ionics* **24** (2018) 2807-2819. https://doi.org/10.1007/s11581-017-2410-5
- [19] D. R. do Carmo, M. S. Peixoto, A. dos Santos Felipe, A. S. B. Sales, N. L. D. Filho, M. de Souza Magossi, Synthesis of a New Zn<sup>2+</sup>/Fe<sup>3+</sup> octa (aminopropyl) silsesquioxane cmplex and its voltammetric behavior towards N-acetylcysteine, *Silicon* **15** (2023) 683-697. <a href="https://doi.org/10.1007/s12633-022-02030-w">https://doi.org/10.1007/s12633-022-02030-w</a>
- [20] L. Zhang, J. Tang, J. Li, Y. Li, P. Yang, P. Zhao, Y. Xie, A novel dopamine electrochemical sensor based on 3D flake nickel oxide/cobalt oxide@porous carbon nanosheets/carbon nanotubes/electrochemical reduced of graphene oxide composites modified glassy carbon electrode, Colloids and Surfaces A: Physicochemical and Engineering Aspects 666 (2023) 131284. https://doi.org/10.1016/j.colsurfa.2023.131284
- [21] S. Tajik, Y. Orooji, F. Karimi, Z. Ghazanfari, H. Beitollahi, M. Shokouhimehr, H. W. Jang, High performance of screen-printed graphite electrode modified with Ni–Mo-MOF for voltammetric determination of amaranth, *Journal of Food Measurement and Characterization* **15** (2021) 4617-4622. <a href="https://doi.org/10.1007/s11694-021-01027-0">https://doi.org/10.1007/s11694-021-01027-0</a>
- [22] H. Karimi-Maleh, R. Darabi, F. Karimi, C. Karaman, S. A. Shahidi, N. Zare, M. Baghayeri, L. Fu, S. Rostamnia, J. Rouhi, State-of-art advances on removal, degradation and electrochemical monitoring of 4-aminophenol pollutants in real samples, *Environmental Research* 222 (2023) 115338. <a href="https://doi.org/10.1016/j.envres.2023.115338">https://doi.org/10.1016/j.envres.2023.115338</a>
- [23] S. Duan, X. Wu, Z. Shu, A. Xiao, B. Chai, F. Pi, X. Liu, Curcumin-enhanced MOF electrochemical sensor for sensitive detection of methyl parathion in vegetables and fruits, *Microchemical Journal* **184** (2023) 108182. https://doi.org/10.1016/j.microc.2022.108182



- [24] H. Pyman, Design and fabrication of modified DNA-Gp nano-biocomposite electrode for industrial dye measurement and optical confirmation, *Progress in Chemical and Biochemical Research* **5** (2022) 391-405. <a href="https://doi.org/10.22034/pcbr.2022.367576.1236">https://doi.org/10.22034/pcbr.2022.367576.1236</a>
- [25] F. Garkani Nejad, S. Tajik, H. Beitollahi, I. Sheikhshoaie, Magnetic nanomaterials based electrochemical (bio) sensors for food analysis, *Talanta* **228** (2021) 122075. https://doi.org/10.1016/j.talanta.2020.122075
- [26] H. Karimi-Maleh, Y. Liu, Z. Li, R. Darabi, Y. Orooji, C. Karaman, F. Karimi, M. Baghayeri, J. Rouhi, L. Fu, Calf thymus ds-DNA intercalation with pendimethalin herbicide at the surface of ZIF-8/Co/rGO/C₃N₄/ds-DNA/SPCE; A bio-sensing approach for pendimethalin quantification confirmed by molecular docking study, *Chemosphere* **332** (2023) 138815. <a href="https://doi.org/10.1016/j.chemosphere.2023.138815">https://doi.org/10.1016/j.chemosphere.2023.138815</a>
- [27] M. Vardini, N. Abbasi, A. Kaviani, M. Ahmadi, E. Karimi, Graphite electrode potentiometric sensor modified by surface imprinted silica gel to measure valproic acid, *Chemical Methodologies* 6 (2022) 398-408. https://doi.org/10.22034/chemm.2022.328620.1437
- [28] R. S. Kumar, G. K. Jayaprakash, S. Manjappa, M. Kumar, A. P. Kumar, Theoretical and electrochemical analysis of L-serine modified graphite paste electrode for dopamine sensing applications in real samples, *Journal of Electrochemical Science and Engineering* **12** (2022) 1243-1250. <a href="https://doi.org/10.5599/jese.1390">https://doi.org/10.5599/jese.1390</a>
- [29] L. Zhang, D. Qin, J. Feng, T. Tang, H. Cheng, Rapid quantitative detection of luteolin using an electrochemical sensor based on electrospinning of carbon nanofibers doped with single-walled carbon nanoangles, *Analytical Methods* **15** (2023) 3073-3083. <a href="https://doi.org/10.1039/D3AY00497J">https://doi.org/10.1039/D3AY00497J</a>
- [30] H. Beitollahi, H. Mahmoudi Moghaddam, S. Tajik, Voltammetric determination of bisphenol A in water and juice using a lanthanum (III)-doped cobalt (II, III) nanocube modified carbon screen-printed electrode, *Analytical Letters* **52** (2019) 1432-1444. <a href="https://doi.org/10.1080/00032719.2018.1545132">https://doi.org/10.1080/00032719.2018.1545132</a>
- [31] S. Z. Mohammadi, F. Mousazadeh, M. Mohammadhasani-Pour, Electrochemical detection of folic acid using a modified screen printed electrode, *Journal of Electrochemical Science and Engineering* **12** (2022) 1111-1120. <a href="https://doi.org/10.5599/jese.1360">https://doi.org/10.5599/jese.1360</a>
- [32] S. Cheraghi, M. A. Taher, H. Karimi-Maleh, F. Karimi, M. Shabani-Nooshabadi, M. Alizadeh, A. Al-Othman, N. Erk, P. K. Y. Raman, C. Karaman, Novel enzymatic graphene oxide based biosensor for the detection of glutathione in biological body fluids, *Chemosphere* **287** (2022) 132187. https://doi.org/10.1016/j.chemosphere.2021.132187
- [33] H. Roshanfekr, A simple specific dopamine aptasensor based on partially reduced graphene oxide—AuNPs composite, *Progress in Chemical and Biochemical Research* **6** (2023) 61-70. <a href="https://doi.org/10.22034/pcbr.2023.381280.1245">https://doi.org/10.22034/pcbr.2023.381280.1245</a>
- [34] F. C. Barreto, M. K. L. da Silva, I. Cesarino, Copper nanoparticles and reduced graphene oxide as an electrode modifier for the development of an electrochemical sensing platform for chloroquine phosphate determination, *Nanomaterials* **13** (2023) 1436. <a href="https://doi.org/10.3390/nano13091436">https://doi.org/10.3390/nano13091436</a>
- [35] F. Garkani Nejad, M. H. Asadi, I. Sheikhshoaie, Z. Dourandish, R. Zaimbashi, H. Beitollahi, Construction of modified screen-printed graphite electrode for the application in electrochemical detection of sunset yellow in food samples, *Food and Chemical Toxicology* **166** (2022) 113243. <a href="https://doi.org/10.1016/j.fct.2022.113243">https://doi.org/10.1016/j.fct.2022.113243</a>
- [36] Z. Zhang, H. Karimi-Maleh, In situ synthesis of label-free electrochemical aptasensor-based sandwich-like AuNPs/PPy/Ti<sub>3</sub>C<sub>2</sub>T<sub>x</sub> for ultrasensitive detection of lead ions as hazardous pollutants in environmental fluids, *Chemosphere* **324** (2023) 138302. https://doi.org/10.1016/j.chemosphere.2023.138302

- [37] M. Ozdal, S. Gurkok, Recent advances in nanoparticles as antibacterial agent, *ADMET and DMPK* **10** (2022) 115-129. https://doi.org/10.5599/admet.1172
- [38] A. I. Arif, Biosynthesis of copper oxide nanoparticles using Aspergillus niger extract and their antibacterial and antioxidant activities, *Eurasian Chemical Communications* **5** (2023) 598-608. https://doi.org/10.22034/ecc.2023.384414.1600
- [39] B. Bonhoeffer, A. Kordikowski, E. John, M. Juhnke, Numerical modeling of the dissolution of drug nanocrystals and its application to industrial product development, *ADMET and DMPK* 10 (2022) 253-287. <a href="https://doi.org/10.5599/admet.1437">https://doi.org/10.5599/admet.1437</a>
- [40] A. Hojjati-Najafabadi, M. Mansoorianfar, T. X. Liang, K. Shahin, H. Karimi-Maleh, A review on magnetic sensors for monitoring of hazardous pollutants in water resources, *Science of The Total Environment* **824** (2022) 153844. <a href="https://doi.org/10.1016/j.scitotenv.2022.153844">https://doi.org/10.1016/j.scitotenv.2022.153844</a>
- [41] P. Shen, X. Zhang, N. Ding, Y. Zhou, C. Wu, C. Xing, Y. Kang, Glutathione and esterase dual-responsive smart nano-drug delivery system capable of breaking the redox balance for enhanced tumor therapy, *ACS Applied Materials & Interfaces* **15** (2023) 20697-20711. <a href="https://doi.org/10.1021/acsami.3c01155">https://doi.org/10.1021/acsami.3c01155</a>
- [42] O. K. Akeremale, Metal-organic frameworks (MOFs) as adsorbents for purification of dyecontaminated wastewater: a review, *Journal of Chemical Reviews* **4** (2022) 1-14. https://doi.org/10.22034/jcr.2022.314728.1130
- [43] H. Jiang, Y. Shi, S. Zang, Pd/PdO and hydrous RuO<sub>2</sub> difunction-modified SiO<sub>2</sub>@ TaON@Ta<sub>3</sub>N<sub>5</sub> nano-photocatalyst for efficient solar overall water splitting, *International Journal of Hydrogen Energy* **48** (2023) 17827-17837. <a href="https://doi.org/10.1016/j.ijhydene.2023.01.219">https://doi.org/10.1016/j.ijhydene.2023.01.219</a>
- [44] B. Baghernejad, M. Alikhani, Nano-cerium oxide/aluminum oxide as an efficient catalyst for the synthesis of xanthene derivatives as potential antiviral and anti-inflammatory agents, *Journal of Applied Organometallic Chemistry* **2** (2022) 140-147. <a href="https://doi.org/10.22034/jaoc.2022.154819">https://doi.org/10.22034/jaoc.2022.154819</a>
- [45] I. Alao, I. Oyekunle, K. Iwuozor, E. Emenike, Green synthesis of copper nanoparticles and investigation of its antimicrobial properties, *Advanced Journal of Chemistry B* **4** (2022) 39-52. https://doi.org/10.22034/ajcb.2022.323779.1106
- [46] C. Karaman, O. Karaman, P. L. Show, Y. Orooji, H. Karimi-Maleh, Utilization of a double-cross-linked amino-functionalized three-dimensional graphene networks as a monolithic adsorbent for methyl orange removal: equilibrium, kinetics, thermodynamics and artificial neural network modeling, *Environmental Research* 207 (2021) 112156. https://doi.org/10.1016/j.envres.2021.112156
- [47] D. Palke, Synthesis, physicochemical and biological studies of transition metal complexes of DHA schiff bases of aromatic amine, *Journal of Applied Organometallic Chemistry* **2** (2022) 81-88. https://doi.org/10.22034/jaoc.2022.349187.1055
- [48] M. Waqas, L. Yang, Y. Wei, Y. Sun, F. Yang, Y. Fan, W. Chen, Controlled fabrication of nickel and cerium mixed nano-oxides supported on carbon nanotubes for glucose monitoring, *Electrochimica Acta* **440** (2023) 141735. <a href="https://doi.org/10.1016/j.electacta.2022.141735">https://doi.org/10.1016/j.electacta.2022.141735</a>
- [49] S. Tajik, H. Beitollahi, H. W. Jang, M. Shokouhimehr, A screen printed electrode modified with Fe<sub>3</sub>O<sub>4</sub>@polypyrrole-Pt core-shell nanoparticles for electrochemical detection of 6-mercaptopurine and 6-thioguanine, *Talanta* **232** (2021) 122379. https://doi.org/10.1016/j.talanta.2021.122379
- [50] H. Karimi-Maleh, C. T. Fakude, N. Mabuba, G. M. Peleyeju, O. A. Arotiba, The determination of 2-phenylphenol in the presence of 4-chlorophenol using nano-Fe<sub>3</sub>O<sub>4</sub>/ionic liquid paste electrode as an electrochemical sensor, *Journal of Colloid and Interface Science* **554** (2019) 603-610. <a href="https://doi.org/10.1016/j.jcis.2019.07.047">https://doi.org/10.1016/j.jcis.2019.07.047</a>
- [51] S. Esfandiari Baghbamidi, H. Beitollahi, S. Z. Mohammadi, S. Tajik, S. Soltani-Nejad, V. Soltani-Nejad, Nanostructure-based electrochemical sensor for the voltammetric determination of



- benserazide, uric acid, and folic acid, *Chinese Journal of Catalysis* **34** (2013) 1869-1875. https://doi.org/10.1016/S1872-2067(12)60655-X
- [52] S. N. Zakiyyah, D. R. Eddy, Firdaus, M. L. Eddy, T. Subroto, Y. W. Hartati, Screen-printed carbon electrode/natural silica-ceria nanocomposite for electrochemical aptasensor application, *Journal of Electrochemical Science and Engineering* **12** (2022) 1225-1242. <a href="https://doi.org/10.5599/jese.1455">https://doi.org/10.5599/jese.1455</a>
- [53] M. Asaduzzaman, M. A. Zahed, M. Sharifuzzaman, M. S. Reza, X. Hui, S. Sharma, J. Y. Park, A hybridized nano-porous carbon reinforced 3D graphene-based epidermal patch for precise sweat glucose and lactate analysis, *Biosensors and Bioelectronics* **219** (2023) 114846. <a href="https://doi.org/10.1016/j.bios.2022.114846">https://doi.org/10.1016/j.bios.2022.114846</a>
- [54] J. A. Buledi, N. Mahar, A. Mallah, A. R. Solangi, I. M. Palabiyik, N. Qambrani, F. Karimi, Y. Vasseghian, H. Karimi-Maleh, Electrochemical quantification of mancozeb through tungsten oxide//reduced graphene oxide nanocomposite: A potential method for environmental remediation, Food and Chemical Toxicology 161 (2022) 112843. https://doi.org/10.1016/j.fct.2022.112843
- [55] F. Garkani Nejad, H. Beitollahi, I. Sheikhshoaie, A UiO-66-NH<sub>2</sub> MOF/PAMAM dendrimer nanocomposite for electrochemical detection of tramadol in the presence of acetaminophen in pharmaceutical formulations, *Biosensors* 13 (2023) 514. <a href="https://doi.org/10.3390/bios13050514">https://doi.org/10.3390/bios13050514</a>
- [56] R. Sahoo, S. Ghosh, S. Chand, S. C. Pal, T. Kuila, M. C. Das, Highly scalable and pH stable 2D Ni-MOF-based composites for high performance supercapacitor, *Composites Part B* 245 (2022) 110174. <a href="https://doi.org/10.1016/j.compositesb.2022.110174">https://doi.org/10.1016/j.compositesb.2022.110174</a>
- [57] A. Ahmad, S. Khan, S. Tariq, R. Luque, F. Verpoort, Self-sacrifice MOFs for heterogeneous catalysis: Synthesis mechanisms and future perspectives, *Materials Today* **55** (2022) 137-169. https://doi.org/10.1016/j.mattod.2022.04.002
- [58] C. R. Yang, P. W. Cheng, S. F. Tseng, Highly responsive and selective NO<sub>2</sub> gas sensors based on titanium metal organic framework (Ti-MOF) with pyromellitic acid, *Sensors and Actuators A* **354** (2023) 114301. https://doi.org/10.1016/j.sna.2023.114301
- [59] H. Zeng, C. Xia, B. Zhao, M. Zhu, H. Zhang, D. Zhang, Y. Yuan, Folic acid–functionalized metalorganic framework nanoparticles as drug carriers improved bufalin antitumor activity against breast cancer, *Frontiers in Pharmacology* **12** (2022) 747992. <a href="https://doi.org/10.3389/fphar.2021.747992">https://doi.org/10.3389/fphar.2021.747992</a>
- [60] M. Ahmad, K. A. Siddiqui, Synthesis of mixed ligand 3D cobalt MOF: Smart responsiveness towards photocatalytic dye degradation in environmental contaminants, *Journal of Molecular Structure* **1265** (2022) 133399. https://doi.org/10.1016/j.molstruc.2022.133399
- [61] Y. Ma, Y. Leng, D. Huo, D. Zhao, J. Zheng, H. Yang, C. Hou, A sensitive enzyme-free electrochemical sensor based on a rod-shaped bimetallic MOF anchored on graphene oxide nanosheets for determination of glucose in huangshui, *Analytical Methods* **15** (2023) 2417-2426. <a href="https://doi.org/10.1039/D2AY01977A">https://doi.org/10.1039/D2AY01977A</a>
- [62] Z. Lu, K. Wei, H. Ma, R. Duan, M. Sun, P. Zou, H. Rao, Bimetallic MOF synergy molecularly imprinted ratiometric electrochemical sensor based on MXene decorated with polythionine for ultra-sensitive sensing of catechol, *Analytica Chimica Acta* 1251 (2023) 340983. <a href="https://doi.org/10.1016/j.aca.2023.340983">https://doi.org/10.1016/j.aca.2023.340983</a>
- [63] R. Sun, R. Lv, Y. Li, T. Du, L. Chen, Y. Zhang, Y. Qi, Simple and sensitive electrochemical detection of sunset yellow and Sudan I in food based on AuNPs/Zr-MOF-Graphene, *Food Control* **145** (2023) 109491. https://doi.org/10.1016/j.foodcont.2022.109491
- [64] P. Ranjan, M. Abubakar Sadique, S. Yadav, R. Khan, An electrochemical immunosensor based on gold-graphene oxide nanocomposites with ionic liquid for detecting the breast cancer CD44 biomarker, ACS Applied Materials & Interfaces 14 (2022) 20802-20812. <a href="https://doi.org/10.1021/acsami.2c03905">https://doi.org/10.1021/acsami.2c03905</a>

- [65] Q. Zhang, W. Cheng, D. Wu, Y. Yang, X. Feng, C. Gao, X. Tang, An electrochemical method for determination of amaranth in drinks using functionalized graphene oxide/chitosan/ionic liquid nanocomposite supported nanoporous gold, *Food Chemistry* 367 (2022) 130727. <a href="https://doi.org/10.1016/j.foodchem.2021.130727">https://doi.org/10.1016/j.foodchem.2021.130727</a>
- [66] M. A. Mohamed, N. N. Salama, M. A. Sultan, H. F. Manie, M. M. A. El-Alamin, Sensitive and effective electrochemical determination of butenafine in the presence of itraconazole using titanium nanoparticles-ionic liquid based nanocomposite sensor, *Chemical Papers* **77** (2023) 1929-1939. <a href="https://doi.org/10.1007/s11696-022-02593-3">https://doi.org/10.1007/s11696-022-02593-3</a>
- [67] K. Kunpatee, S. Traipop, O. Chailapakul, S. Chuanuwatanakul, Simultaneous determination of ascorbic acid, dopamine, and uric acid using graphene quantum dots/ionic liquid modified screen-printed carbon electrode, Sensors and Actuators B 314 (2020) 128059. https://doi.org/10.1016/j.snb.2020.128059
- [68] S. Zhang, X. Zhuang, D. Chen, F. Luan, T. He, C. Tian, L. Chen, Simultaneous voltammetric determination of guanine and adenine using MnO<sub>2</sub> nanosheets and ionic liquid-functionalized graphene combined with a permeation-selective polydopamine membrane, *Microchimica Acta* **186** (2019) 450. https://doi.org/10.1007/s00604-019-3577-4
- [69] V. A. Maraldi, Y. N. Colmenares, P. F. Pereira Barbosa, V. Mastelaro, D. Ribeiro do Carmo, Graphene Oxide as a Platform for Copper Pentacyanonitrosylferrate Nanoparticles and their Behavior in the Electro-oxidation of N-Acetylcysteine, *Electroanalysis* **32** (2020) 1408-1416. <a href="https://doi.org/10.1002/elan.201900493">https://doi.org/10.1002/elan.201900493</a>
- [70] A. C. de Sá, L. L. Paim, U. D. O. Bicalho, D. R. do Carmo, Determination of N-acetylcysteine by cyclic voltammetry using modified carbon paste electrode with copper nitroprusside adsorbed on the 3-aminopropylsilica, *International Journal of Electrochemical Science* 6 (2011) 3754-3767. <a href="http://hdl.handle.net/11449/10147">http://hdl.handle.net/11449/10147</a>
- [71] W. T. Suarez, L. H. Marcolino Jr, O. Fatibello-Filho, Voltammetric determination of Nacetylcysteine using a carbon paste electrode modified with copper (II) hexacyanoferrate (III), *Microchemical Journal* 82 (2006) 163-167. https://doi.org/10.1016/j.microc.2006.01.007
- [72] S. Shahrokhian, Z. Kamalzadeh, A. Bezaatpour, D. M. Boghaei, Differential pulse voltammetric determination of N-acetylcysteine by the electrocatalytic oxidation at the surface of carbon nanotube-paste electrode modified with cobalt salophen complexes. *Sensors and Actuators B* **133** (2008) 599-606. <a href="https://doi.org/10.1016/j.snb.2008.03.034">https://doi.org/10.1016/j.snb.2008.03.034</a>

© 2023 by the authors; licensee IAPC, Zagreb, Croatia. This article is an open-access article distributed under the terms and conditions of the Creative Commons Attribution license (<a href="https://creativecommons.org/licenses/by/4.0/">https://creativecommons.org/licenses/by/4.0/</a>)





Open Access :: ISSN 1847-9286 www.jESE-online.org

Original scientific paper

# Electrochemical sensing of caffeic acid antioxidant in wine samples using carbon paste electrode amplified with CdO/SWCNTs

Zahra Arab¹, Sara Jafarian¹,⊠ Hassan Karimi-Maleh²,᠍, Leila Roozbeh Nasiraie¹ and Mohammad Ahmadi³

<sup>1</sup>Department of Food Science and Technology, Nour Branch, Islamic Azad University, Nour, Iran <sup>2</sup>Department of Chemical Engineering, Quchan University of Technology, Quchan 9477177870, Iran <sup>3</sup>Department of Food Hygiene, Ayatollah Amoli Branch, Islamic Azad University, Amol 4615143358, Iran

Corresponding authors: <sup>™</sup>sara jafary2002@yahoo.com; '<sup>®</sup>h.karimi.maleh@gmail.com

Tel.: 0098 9123110253

Received: February 11, 2023; Accepted: May 22, 2023; Published: June 19, 2023

#### **Abstract**

An electrochemical sensor was introduced as an analytical tool for monitoring caffeic acid in food samples. This analytical tool was amplified by cadmium oxide decorated on single wall carbon nanotubes as a new catalyst and showed a powerful ability to sensing of caffeic acid in food products. The presence of cadmium oxide decorated on single wall carbon nanotubes catalyst improved the oxidation signal of caffeic acid about 2.4 times at optimum conditions. The pH investigation confirmed that the redox reaction of caffeic acid was pH dependent and showed maximum sensitivity at pH 7.0. The paste electrode amplified with cadmium oxide decorated on single wall carbon nanotubes successfully monitored caffeic acid in the concentration range  $0.02-200~\mu\text{M}$  with a detection limit of 9.0~nM, respectively. The standard addition strategy showed a recovery range of 97.96~to 102.59~% to the measurement of caffeic acid in fruit juice, white and red wine that was acceptable for the fabrication of a new analytical tool in food monitoring.

#### **Keywords**

Food sensor, nanocomposite, electroanalysis, modified electrodes, real sample analysis

# Introduction

Antioxidants, as one of the most famous substances used in food, prevent the adverse effects of free radicals [1,2]. Antioxidants can be found as natural or artificial and are important in food safety [3,4]. Although the body directly confronts some free radicals, the wide range of radicals makes it important to get antioxidants through food [5]. Caffeic acid is one of the famous natural antioxidants found in various beverages and wine samples [6,7]. Caffeic acid can cause mild effects on insomnia

and excessive consumption is not recommended [8]. Therefore, monitoring of caffeic acid in food products was investigated by some analytical methods such as HPLC [9], LC-MS/MS [6], TLC-densitometry [10] and electrochemical sensors.

Electrochemical sensors are a useful and powerful strategy for sensing food products and especially food antioxidants [11-14]. Easy modification to create highly selective and sensitive tools in food products analysis is the main advantage of electrochemical methods compared to other analytical strategies in sensing electrochemically active materials [15-20]. Different modifiers were suggested for the amplification of electrochemical sensors, such as 2D nanomaterials, nanocomposites [21], ionic liquids, composites, conductive polymers, biological compounds, *etc.* [22-24]. Between them, nanomaterials showed more advantages due to easy diversity and high electrical conductivity [25,26]. Many research efforts focused on the modification of electrochemical sensors to trace-level analysis in complex matrixes [27-30].

Nanotechnology changed the approach to pure science and creating unique properties in new materials [31-37]. Nanomaterials showed unbelievable properties and a wide range of applications in different branches of science [38-42]. The application of nanomaterials in the fabrication of modified sensors is increasing significantly [43]. This issue relates to high electrical conductivity and easy modification of nanomaterials with different functionalized groups.

In this study, a nanostructure-based sensor (cadmium oxide decorated on single wall carbon nanotubes (CdO/SWCNTs) modified paste electrode (PE) (CdO/SWCNTs/PE in this case) was suggested as a simple and economical type of sensor for easy monitoring of caffeic acid in food products and results showed the high ability of this sensor.

#### **Experimental**

#### Materials

Cadmium acetate, SWCNTs-COOH, and sodium hydroxide were purchased from Sigma-Aldrich Company and used to synthesize CdO/SWCNTs nanocomposite with the recommended procedure by Cheraghi and Taher [44]. Graphite powder (99.99 %) and paraffin oil were purchased from Merck Company and used to fabricate paste electrodes. Phosphoric acid, sodium dihydrogen phosphate, disodium hydrogen phosphate anhydrous, and trisodium phosphate were purchased from Across company and used to prepare phosphate buffer solution (PBS).

#### Instruments

All electrochemical signals were recorded by an Ivium-Vertex machine connected to Ag/Ag/KCl<sub>sat</sub>, Pt wire, and CdO/SWCNTs/PE as reference, counter, and working electrodes, respectively. A pH meter model 780 pH Meter, Metrohm was used to prepare PBS solution.

# Fabrication of CdO/SWCNTs/PE

The working electrode (CdO/SWCNTs/PE in this case) was fabricated after optimization of CdO/SWCNTs compared to graphite powder in the presence of caffeic acid in pH 7.0 as the optimum condition. The maximum sensitivity was obtained in the presence of 9.0 wt.% CdO/SWCNTs nanocomposite at the surface of the paste electrode (Figure 1). Therefore, 910 mg + 90 mg CdO/SWCNTs were mixed in mortar and pestle and converted to paste using paraffin oil and hand mixing for 30 min.



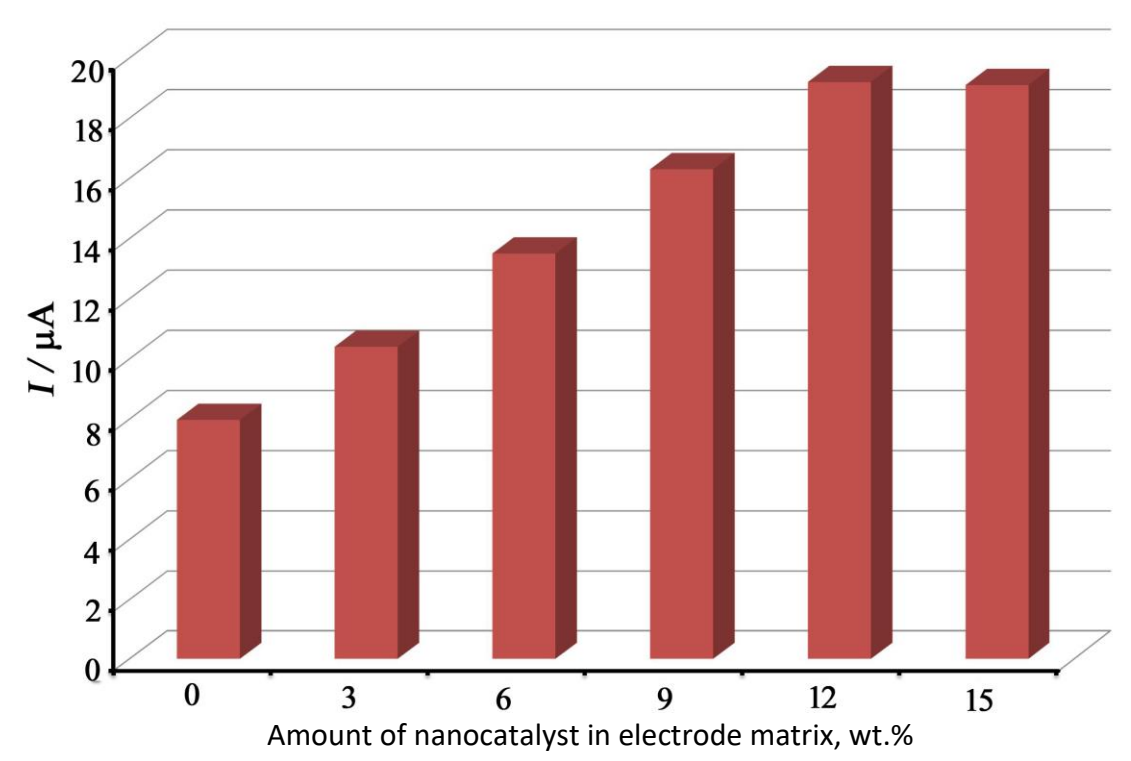


**Figure 1.** The oxidation peak current of caffeic acid at surface of paste electrode modified with different amounts of CdO/SWCNTs in carbon paste matrix

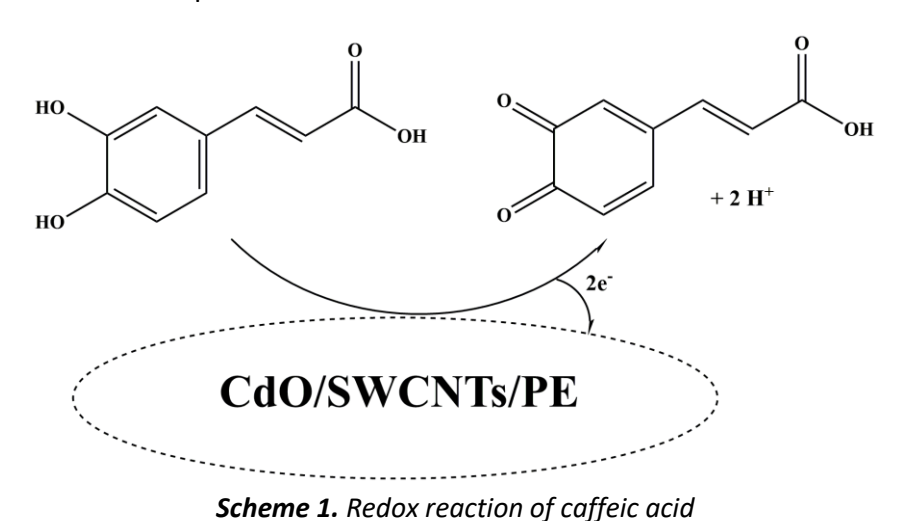
# Real sample preparation

10 mL of white, fruit juice and red wines were selected and centrifuged at 4000 rpm for 15 min and, after filtration, diluted into 10 mL PBS (pH 7.0) and transferred to an electrochemical cell for the analysis of caffeic acid using the standard addition method.

# **Results and discussion**

# pH optimization

Caffeic acid is a phenolic antioxidant and according to reported papers and Scheme 1 [45], its oxidation in signal changes with the changes in the pH of the solution, and optimization of this factor is so important in the first step.



Therefore, linear sweep voltammograms of caffeic acid were recorded in the pH range of 5.0 – 9.0 and the results are shown in Figure 2 inset. Results showed that maximum oxidation current to

caffeic acid was observed at pH = 7.0 (Figure 2), and this condition was selected as the optimal condition for monitoring caffeic acid in food samples.

# Catalytic activity of senor

The oxidation signal of 500  $\mu$ M caffeic acid at the surface of PE (Figure 3, curve a) and CdO/SWCNTs/PE (Figure 3, curve b) was recorded and results showed oxidation currents of 7.97 and 19.2  $\mu$ A at oxidation potentials of 563 and 460 mV, respectively.

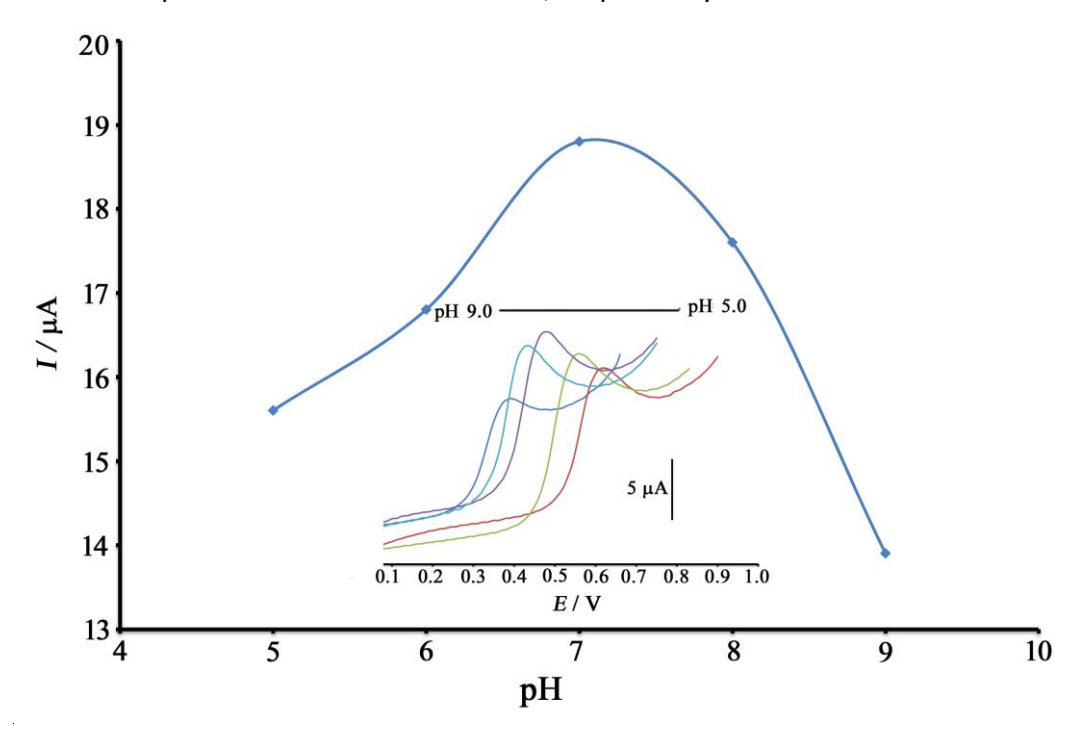


**Figure 2.** Current-pH curve to electrooxidation of 500  $\mu$ M caffeic acid. Inset: linear sweep voltammograms of 500  $\mu$ M caffeic acid in the pH range 5.0 to 9.0

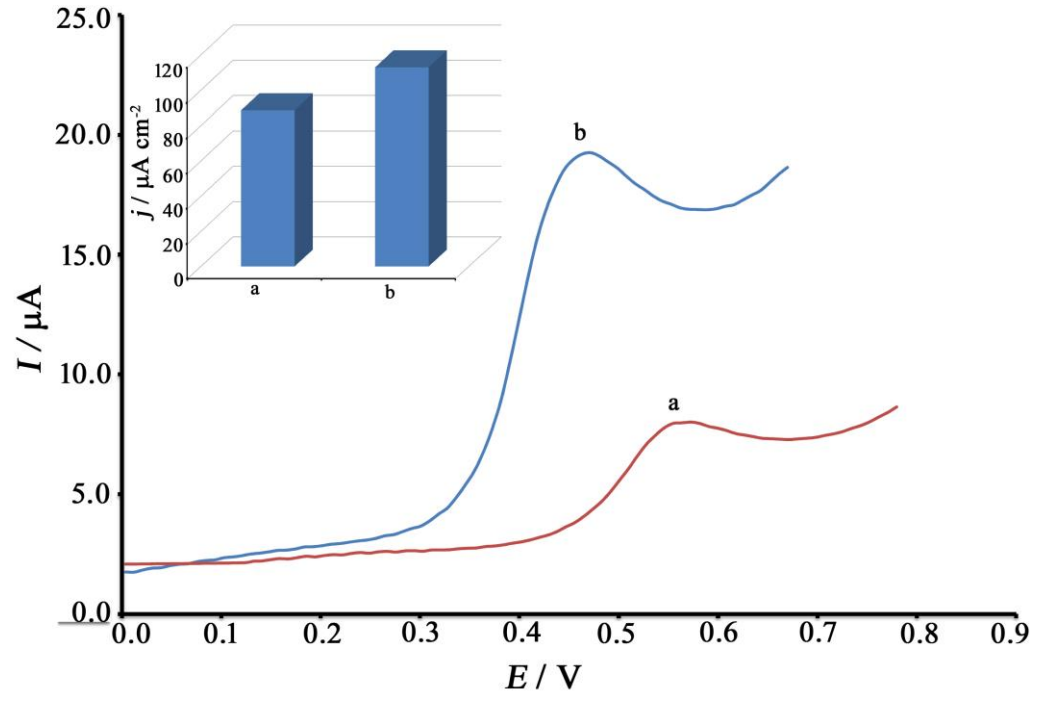


**Figure 3.** LS voltammograms 500  $\mu$ M caffeic acid at surface of a) PE and b) CdO/SWCNTs/PE. Inset: Oxidation peak current density diagram relative to LS voltammogarms

Comparing of these values clearly showed that the presence of CdO/SWCNTs at the surface of PE plays a catalytic role in the redox behavior of caffeic acid. On the other hand, the active surface area of PE and CdO/SWCNTs/PE were determined to be about 0.09 and 0.17 cm², respectively. The active surface was determined by the recording of cyclic voltammograms of [Fe(CN)6]<sup>3-/4-</sup> in the presence of 0.1 M KCl and Randles–Ševčik equation.. This confirms that CdO/SWCNTs increases the active surface area of the electrode. Oxidation peak current densities relative to two electrodes are shown in Figure 3 inset.

### Scan rate investigation

The role of scan rate on the potential and current of caffeic acid signal was investigated and results showed in Figure 4 inset. The results showed a positive shift in the oxidation potential of caffeic acid and also increase in the oxidation current at the surface of CdO/SWCNTs/PE at the scan rate range 5 – 80 mV s<sup>-1</sup>. The linear relationship between current of caffeic acid and  $v^{1/2}$  with an equation of  $I = 1.6197 v^{1/2} + 4.8775 (R^2 = 0.9944)$  confirms a diffusion-controlled process. Also, a positive shift in oxidation potential indicates a kinetic limitations of the redox reaction of caffeic acid at the surface of CdO/SWCNTs/PE.

# Analytical parameters

The limit of detection and linear dynamic range are two main analytical factors in the design of new types of analytical methods. The linear dynamic range between 0.02 to 200  $\mu$ M with equation I = 0.0481C + 0.7410 ( $R^2 = 0.9911$ ) was determined. A detection limit of 9.0 nM was determined to for this method of caffeic acid at the surface of CdO/SWCNTs/PE at optimum conditions using equation  $Y_{LOD} = 3\sigma/m$ .

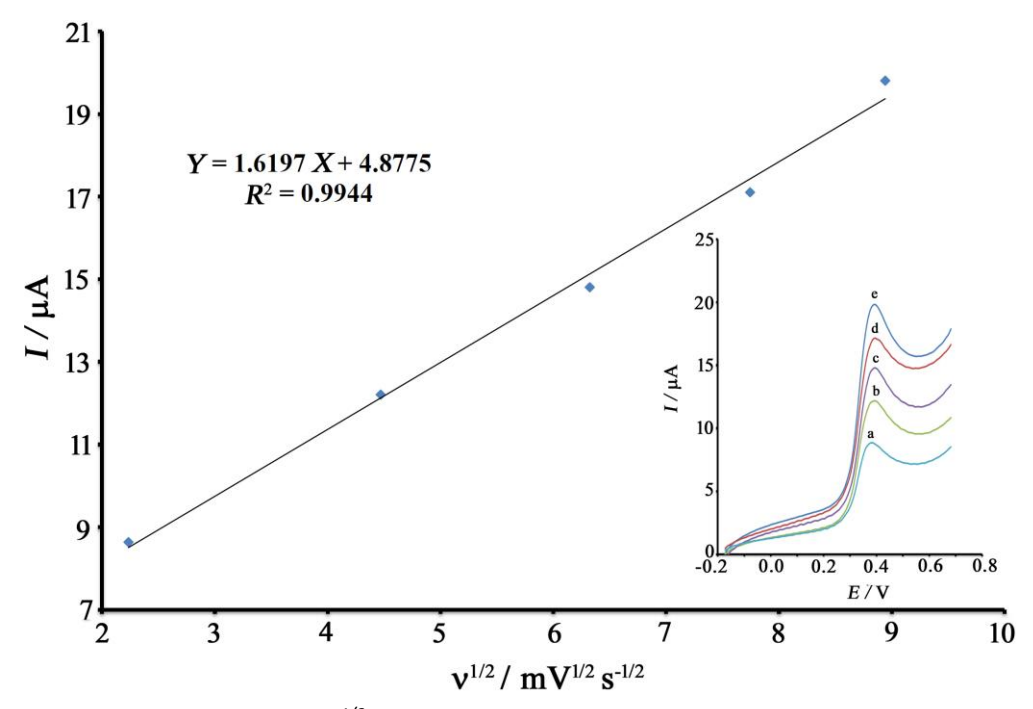


**Figure 4.** Oxidation peak current -  $v^{1/2}$  curve for electro-oxidation of 450  $\mu$ M caffeic acid at surface of CdO/SWCNTs/PE. Inset: LSVs at scan rates a) 5; b) 20; c) 40; d) 60 and e) 80 mV s<sup>-1</sup>

# Selectivity of CdO/SWCNTs/PE to sensing of caffeic acid

The selectivity of CdO/SWCNTs/PE as a new catalyst for sensing of 15.0  $\mu$ M caffeic acid was investigated at pH 7.0 as the optimum condition. The results are reported with an acceptable error of

5 % in Table 1. Data were repeated five times and confirmed the high selectivity of CdO/SWCNTs/PE as a new sensor for sensing caffeic acid in an aqueous solution.

**Table 1.** Interference study to sense 15.0 μM caffeic acid using CdO/SWCNTs/PE

Species	Tolerance limit (Interference mass, g / caffeic acid mass, g)
Li <sup>+</sup> , K <sup>+</sup> , Br <sup>-</sup> and Na <sup>+</sup>	1000
Sucrose, glucose, fructose and lactose	600
Vitamin B <sub>9</sub> and glycine	400
Starch	Saturated

# Determination of caffeic acid in real samples

The fruit juice and wine samples were prepared according to the reported procedure in Experimental section and transferred to an electrochemical cell for electrochemical monitoring by standard addition methods. The results were repeated three times and compared with one published sensor and data shown in Table 2. F-test and t-test were used to investigate accuracy data and results clearly confirmed CdO/SWCNTs/PE's high ability to sense caffeic acid in real samples.

**Table 2.** Determination of caffeic acid using CdO/SWCNTs/PE (n=3)

Cample		Content of caffeic acid, μΜ		Recovery, %	$F_{tab}$	$F_{exp}$	$t_{tab}$	$t_{exp}$
Sample Added	Founded	Founde by HPLC						
White wine		3.11±0.13	2.96±0.13					
10.00	10.00	13.45±0.34	13.67±0.55	102.59	19.0	6.7	3.8	1.5
Red wine		2.85±0.22	2.94±0.13					
	5.00	7.69±0.45	8.05±0.49	97.96	19.0	7.3	3.8	1.8
Fruit juice 5.0		<lod< td=""><td><lod< td=""><td></td><td></td><td></td><td></td><td></td></lod<></td></lod<>	<lod< td=""><td></td><td></td><td></td><td></td><td></td></lod<>					
	5.00	5.22±0.66	4.95±0.33	104.4	19.0	8.1	3.8	2.1

### **Conclusions**

The carbon paste modified CdO/SWCNTs/PE electrode was successfully used for sensing of caffeic acid in the concentration range of 0.02 to 200  $\mu$ M with detection limit 9.0 nM. The real sample analysis data confirm the ability of CdO/SWCNTs/PE to measure caffeic acid in fruit juice and different wine samples with recovery range 97.96 to 104.4 % that is acceptable value to a new food sensor.

**Conflict of interest:** This paper is free of conflict of interest.

**Acknowledgements:** The author thanks Takahiro Hidaka for helpful discussions on ligand field chemistry.

#### References

- [1] K. Waki, Sulfur/Carbon Composite Electrodes for Lithium-Sulfur Batteries, Strategy for Technology Development, Proposal paper for Policy Making and Governmental Action toward Low Carbon Societies, Center for Low Carbon Society Strategy, Japan Science and Technology Agency, February (2018). <a href="https://www.jst.go.jp/lcs/en">https://www.jst.go.jp/lcs/en</a>
- [2] M. H. Braga, N. S. Grundish, A. J. Murchison, J. B. Goodenough, Alternative strategy for a safe rechargeable battery, *Energy and Environmental Science* 10 (2017) 331-336. https://dx.doi.org/10.1039/c6ee02888h
- [3] D. A. Streingart, V. Viswanathan, Comment on "Alternative strategy for a safe rechargeable battery" by M. H. Braga, N. S. Grundish, A. J. Murchison and J. B. Goodenough, Energy



- Environ. Sci., 2017, 10, 331–336, *Energy and Environmental Science* **11** (2018) 221-222. https://dx.doi.org/10.1039/c7ee01318c
- [4] M. H. Braga, A. J. Murchison, J. A. Ferreira, P. Singh, J. B. Goodenough, Glass-amorphous alkali-ion solid electrolytes and their performance in symmetrical cells, *Energy and Environmental Science* **9** (2016) 948-954. <a href="https://doi.org/10.1039/C5EE02924D">https://doi.org/10.1039/C5EE02924D</a>
- [5] M. H. Braga, C. M. Subramaniyam, A. J. Murchison, J. B. Goodenough, Nontraditional, Safe, High Voltage Rechargeable Cells of Long Cycle Life, *Journal of the American Chemical Society* **140** (2018) 6343-6352. https://dx.doi.org/10.1021/jacs.8b02322
- [6] M. H. Braga, J. E. Oliveira, A. J. Murchison, J. B. Goodenough, Performance of a ferroelectric glass electrolyte in a self-charging electrochemical cell with negative capacitance and resistance, *Applied Physics Reviews* **7** (2020) 011406. <a href="https://dx.doi.org/10.1063/1.5132841">https://dx.doi.org/10.1063/1.5132841</a>
- [7] M. Sakai, A Reaction Model for Li Deposition at the Positive Electrode of the Braga-Goodenough Li-S Battery, *Journal of The Electrochemical Society* **167** (2020) 160540. https://dx.doi.org/10.1149/1945-7111/abcf53
- [8] T. Uehara, N. Igarashi, R. V. Belosludov, A. A. Farajian, H. Mizuseki, Y. Kawazoe, Theoretical Study of Conductance Properties of Metallocene, *Journal of the Japan Institute of Metals and Materials* **70(6)** (2006) 478-482. <a href="https://dx.doi.org/10.2320/jinstmet.70.478">https://dx.doi.org/10.2320/jinstmet.70.478</a> (in Japanese)
- [9] N. Sato, *Electrochemistry at Metal and Semiconductor Electrodes,* Elsevier Sci. B.V., Amsterdam, The Netherlands, 2003, p. 35-37. ISBN 0-444-82806-0
- [10] R. W. Gurney, Theory of Electrical Double Layers in Adsorbed Films, *Physical Review Journals Archive* **47** (1935) 479. https://dx.doi.org/10.1103/PhysRev.47.479
- [11] R. Gomer, L. W. Swanson, Theory of Field Desorption, *The Journal of Chemical Physics* **38** (1963) 1613. <a href="https://dx.doi.org/10.1063/1.1776932">https://dx.doi.org/10.1063/1.1776932</a>
- [12] J. Bernard, *Adsorption on Metal Surface, Studies in Surface Science and Catalysis,* Elsevier Sci. B.V., Amsterdam, The Netherlands, 1993, p. 150. ISBN-10: 0444421637
- [13] N. Sato, *Electrochemistry at Metal and Semiconductor Electrodes,* Elsevier Sci. B.V., Amsterdam, The Netherlands, 2003, p. 121-126. ISBN 0-444-82806-0
- [14] A. J. Bard, L. R. Faulkner, *Electrochemical Methods, Fundamentals and Applications,* John Wiley & Sons, Inc., 2001 p.556. ISBN 0-471-04372-9
- [15] N. Sato, *Electrochemistry at Metal and Semiconductor Electrodes*, Elsevier Sci. B.V., Amsterdam, The Netherlands, 2003, p. 39-41. ISBN 0-444-82806-0
- [16] N. Sato, *Electrochemistry at Metal and Semiconductor Electrodes,* Elsevier Sci. B.V., Amsterdam, The Netherlands, 2003, p.44-45. ISBN 0-444-82806-0
- [17] T. Nakayama, K. Shiraishi, S. Miyazaki, Y. Akasaka, T. Nakaoka, K. Torii, A. Ohta, P. Ahmet, K. Ohmori, N. Umezawa, H. Watanabe, T. Chikyow, Y. Nara, H. Iwai, K. Yamada, *ECS Transactions* **3(3)** (2006) 129. <a href="https://doi.org/10.1149/1.2355705">https://doi.org/10.1149/1.2355705</a>
- [18] K. Shiraishi, Y. Akasaka, S. Miyazaki, T. Nakayama, T. Nakaoka, G. Nakamura, K. Torii, H. Furutou, A. Ohta, P. Ahmet, K. Ohmori, H. Watanabe, T. Chikyow, M. L. Green, Y. Nara, K. Yamada, *Technical Digest of IEEE International Electron Devices Meeting*, Washington D.C., USA, 2005, p.43-46. ISBN 9780780392687
- [19] T. Nakayama, K. Shiraishi, Physics of Metal/High-k Interfaces, *Hyomen Kagaku* **28(1)** (2007) 28-33. <a href="https://dx.doi.org/10.1380/jsssj.28.28">https://dx.doi.org/10.1380/jsssj.28.28</a> (in Japanese)
- [20] K. Shiraishi, T. Nakayama, Universal Theory of Metal/Dielectric Interfaces, *Hyomen Kagaku* **29(2)** (2008) 92-98. <a href="https://dx.doi.org/10.1380/jsssj.29.92">https://dx.doi.org/10.1380/jsssj.29.92</a> (in Japanese)
- [21] T. Nakayama, Y. Kangawa, K. Shiraishi, *Atomic Structures and Electronic Properties of Semiconductor Interfaces* in *Comprehensive Semiconductor Science and Technology*, P. Bhattacharya, R. Fornari, H. Kamimura, Eds, Elsevier Sci. B. V., Amsterdam, The Netherlands, 2011, p. 157-161. ISBN 978-0-444-53153-7

- [22] T. Nakayama, *Physica B* **191(1-2)** (1993) 16-22. <a href="https://dx.doi.org/10.1016/0921-4526(93)90175-6">https://dx.doi.org/10.1016/0921-4526(93)90175-6</a>
- [23] M. Cardona, N. E. Christensen, Band offsets: the charge transfer effect, *Physical Review B* **35** (1987) 6182. <a href="https://dx.doi.org/10.1103/PhysRevB.35.6182">https://dx.doi.org/10.1103/PhysRevB.35.6182</a>
- [24] N. Sato, *Electrochemistry at Metal and Semiconductor Electrodes*, Elsevier Sci. B.V., Amsterdam, The Netherlands, (2003) p. 254. ISBN 0-444-82806-0
- [25] I. Nakajima, Structure and properties of manganese oxide, *Denki Kagaku* **21** (1953) 367-375. <a href="https://doi.org/10.5796/denka.21.367">https://doi.org/10.5796/denka.21.367</a> (in Japanese)
- [26] J. B. Goodenough, M. H. Braga, J. A. Ferreira, J. E. Oliveira, A. J. Murchison, *Self-Charging and/or Self-Cycling Electrochemical Cells*, United States, Patent Application Publication, US 2018/0287222 A1, Oct.4 (2018)
- [27] J. B. Li, K. Koumoto, H. Yanagida, Electrical Properties of β- and γ-Type Manganese (IV) Oxides, *Journal of the Ceramic Society of Japan* **96(1109)** (1988) 74-79. https://doi.org/10.2109/jcersj.96.74 (in Japanese)
- [28] University of Texas Researchers Develop More Powerful and Long-lasting Battery, J. B. Goodenough interview by J. Schroeder, <a href="https://www.tun.com/blog/university-of-texas-powerful-and-longlasting-battery/">https://www.tun.com/blog/university-of-texas-powerful-and-longlasting-battery/</a>
- [29] W. J. Bardeen, Surface States and Rectification at a Metal Semi-Conductor Contact, Physical Review B **71**(10) (1947) 717. <a href="https://dx.doi.org/10.1103/PhysRev.71.717">https://dx.doi.org/10.1103/PhysRev.71.717</a>
- [30] A. M. Cowley, S. M. Sze, Surface States and Barrier Height of Metal Semiconductor Systems, Journal of Applied Physics 36(10) (1965) 3212-3220. <a href="https://dx.doi.org/10.1063/1.1702952">https://dx.doi.org/10.1063/1.1702952</a>
- [31] S. Hara, The Schottky Limit and a Charge Neutrality Level Found on Metal/6H-SiC Interfaces, Hyomen Kagaku **21(12)** (2000) 791-799. https://dx.doi.org/10.1380/jsssj.21.791 (in Japanese)
- [32] S. Hara, The Schottky limit and a charge neutrality level found on metal/6H-SiC interfaces, Surface Science 494 (2001) L805-L810. https://doi.org/10.1016/S0039-6028(01)01596-5

© 2023 by the authors; licensee IAPC, Zagreb, Croatia. This article is an open-access article distributed under the terms and conditions of the Creative Commons Attribution license (<a href="https://creativecommons.org/licenses/by/4.0/">https://creativecommons.org/licenses/by/4.0/</a>)



Open Access :: ISSN 1847-9286 www.jESE-online.org

Original scientific paper

# ZnO/1-hexyl-3-methylimidazolium chloride paste electrode, highly sensitive lorazepam sensor

Seddigheh Chenarani¹, Mahmoud Ebrahimi¹, Vahid Arabali² and Safar Ali Beyramabadi²

<sup>1</sup>Department of Chemistry, Mashhad Branch, Islamic Azad University, Mashhad, Iran

Corresponding author:  $\underline{\ }^{\boxtimes}\underline{m.ebrahimi@mshdiau.ac.ir}$ ; Tel.: +98-9155095175h; Fax: +98-51-3663-0781

Received: October 30, 2022; Accepted: December 5, 2022; Published: January 18, 2023

#### **Abstract**

The measurement of pharmaceutical compounds in biological fluids is considered an effective way to evaluate their effectiveness. On the other hand, lorazepam is a drug with good efficiency in treatment and some side effects, which measurement is very important. In this study, the ZnO nanoparticle was synthesized as an electrocatalyst by chemical precipitation method. Then, a simple modification on paste electrode (PE) by ZnO nanoparticle (ZnO-NPs) and 1-hexyl-3-methylimidazolium chloride (HMImCl) was made and a new sensor was used for sensing of lorazepam. The HMImCl/ZnO-NPs/PE showed catalytic behavior on oxidation signal of lorazepam and improved its signal about 2.17 times compared to unmodified PE. On the other hand, oxidation potential of lorazepam was reduced about 110 mV at surface of HMImCl/ZnO-NPs/PE compared to unmodified PE that confirm accelerating the electron exchange process after modification of sensor by HMImCl and ZnO-NPs as powerful catalysts. The HMImCl/ZnO-NPs/PE was used for monitoring of lorazepam in water and injection samples and results showed recovery data 98.5 to 103.5 % that are acceptable for a new sensor.

#### **Keywords**

Pharmaceutical sensor; modified sensor; nano-catalyst; ionic liquid

#### Introduction

Medicines, as one of the most important substances used in human life, have many positive and negative effects, which have attracted the attention of many researchers [1,2]. Although drugs play an important role in the treatment of diseases, the harmful effects of some of them on the body as well as the harmful effects on the environment have caused many studies to be done on this group of compounds [3]. Measuring medicinal compounds is one of the most important studies in this field and can provide a lot of information during patient treatment or its role in environmental pollution [4,5]. In between of analytical methods in sensing of pharmaceutical compounds [6-10], electrochemical

<sup>&</sup>lt;sup>2</sup>Department of Chemistry, Sari Branch, Islamic Azad University, Sari, Iran

methods showed more attentions due to many advantages such as easy modification for sensitive sensing, low cost and wide range applications [11].

The lorazepam is one of famous medicines used to treat anxiety [12]. There are several reports of adverse effects of lorazepam use such as dizziness, tiredness and weakness [13]. Therefore, monitoring of this medicine is very important during treatment [14]. Due to high over-voltage and low redox signal of lorazepam, the sensing of it is so hard with usual electrochemical sensors [11]. To overcome to this problem, modification and amplification of electrochemical sensors is necessary [15]. Modification of electrodes is one of the proven solutions to increase the sensitivity and selectivity of electrochemical sensors [16-21]. Different types of mediators such as polymers, nanomaterials, ionic liquids, MOF *etc.* were suggested for modification and amplification of electrochemical sensors in recent years [22-30].

Nanotechnologies opened a new approach in science and improve many of chemical and physical properties of materials [31-36]. With this way, nanomaterials were selected as first choice in different branches of science [37-42]. Due to high electrical conductivity of some nanomaterials such as metal nanoparticles and carbon-based nanomaterials, they were used for modification of electrochemical sensors [43-45]. On the other hand, ionic liquids showed good advantage as binder for fabrication of paste electrode and improved electrical conductivity of modified paste electrodes [46-51].

In this research work, the HMImCl/ZnO-NPs/PE was fabricated and used as new approach for monitoring of lorazepam with good limit of detection compared to previous suggested electrochemical sensors. The HMImCl/ZnO-NPs/PE showed acceptable analytical data in sensing of lorazepam in real samples with recovery data 98.5 - 103.5%. Modification of electrode improved oxidation current of lorazepam about 2.17 times and reduced its oxidation potential for about 110 mV compared to unmodified electrode.

# **Experimental**

#### Materials and instruments

Zinc nitrate hexahydrate and sodium hydroxide were purchased from Merck Company and used for synthesis of ZnO nanoparticles. 1-Hexyl-3-methylimidazolium chloride, graphite powder, paraffin oil and diethyl ether were purchased from Sigma-Aldrich Company and used for fabrication of paste electrode. Phosphoric acid purchased from Merck was used for preparation phosphate buffer solution. The *I - V* signals were recorded by Vertex – Ivium (potentiostat/galvanostat) connected with HMImCl/ /ZnO-NPs/PE as working electrode, Ag/AgCl as reference electrode and Pt wire as counter electrode.

# Synthesis of ZnO nanoparticles

The 100 mL zinc nitrate hexahydrate (0.5 M) were stirred in Erlenmeyer flask for 15 min and then 100 mL sodium hydroxide (0.5 M) were added dropwise and stirred form 30 min. White precipitate of zinc hydroxide was washed for 10 times by distilled water and then dried ate 100 °C for 16 h. The white powder was calcinated at 250 °C for 4 h and ZnO nano-powder was obtained.

# Fabrication of HMImCI/ZnO-NPs/PE

For fabrication of HMImCl/ZnO-NPs/PE; 90 mg ZnO-NPs + 910 mg graphite powder were mixed in mortar and pestle and 15 mL diethyl ether was superimposed. After evaporation of diethyl ether, the paraffin oil + HMImCl with ratio of (7:3 vol.%) were used as binders and sample hand mixed for 1 h. The HMImCl/ZnO-NPs paste was inserted into the end of a glass tube for fabrication of HMImCl/ZnO-NPs/PE in the presence of copper wire.

#### Results and discussion

### Electrochemical investigations

The electrochemical behavior of lorazepam was investigated in the pH range 5.0 to 7.0 and results are shown in Figure 1.

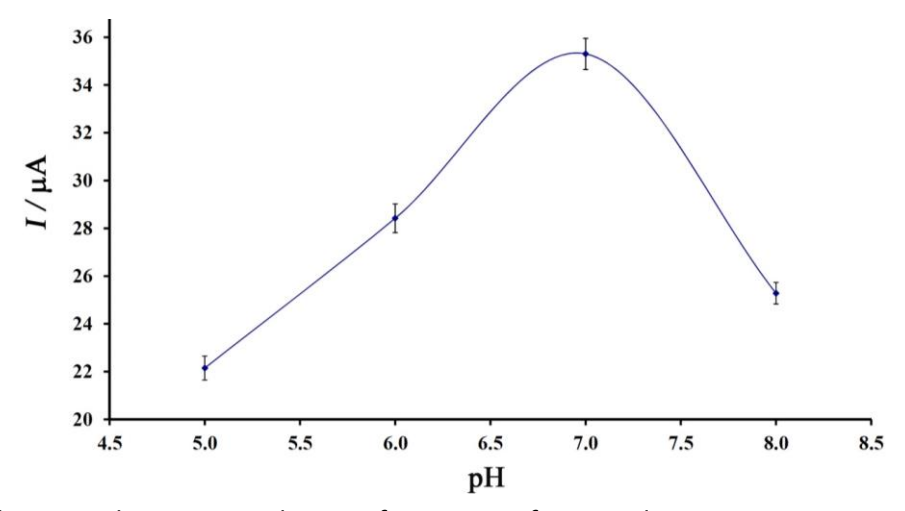


**Figure 1.** Oxidation peak current-pH diagram for sensing of 300  $\mu$ M lorazepam using HMImCl/ZnO-NPs/PE as electroanalytical sensor (n=4)

As can be seen, with increasing pH from 5.0 to 7.0, the oxidation signal of 300  $\mu$ M lorazepam increased and then decreased. Therefore, pH 7.0 was selected as optimum condition for monitoring of lorazepam using HMImCl/ZnO-NPs/PE as electroanalytical sensor.

The oxidation signal of 200 µM lorazepam was recorded at surface of PE (Figure 2a), ZnO-NPs/PE (Figure 2b), HMImCl/PE (Figure 2c) and HMImCl/ZnO-NPs/PE (Figure 2d), respectively.

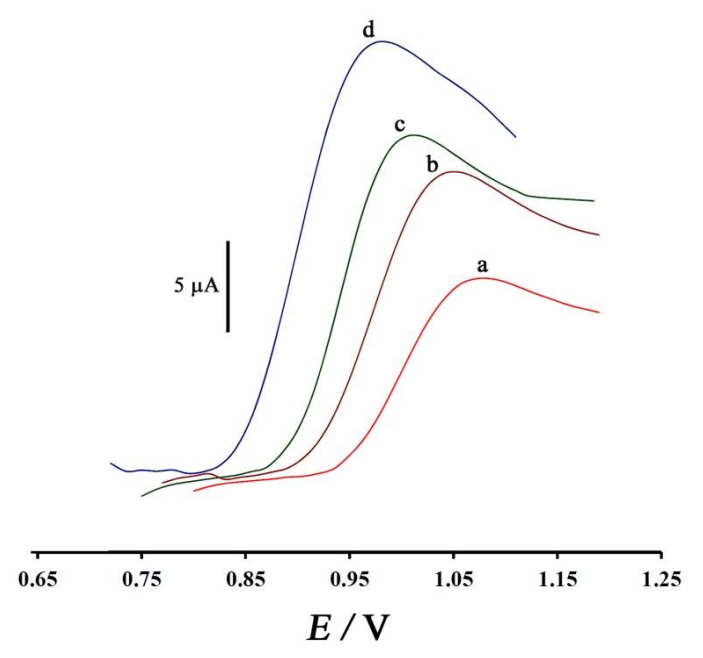


**Figure 2.** Linear sweep voltammograms of 200  $\mu$ M lorazepam at surface of PE (a), ZnO-NPs/PE (b), HMImCl/PE (c) and HMImCl/ZnO-NPs/PE (d); pH 7.0

The oxidation peak currents of 10.85  $\mu$ A, 16.53  $\mu$ A, 18.55  $\mu$ A and 23.6  $\mu$ A were detected for monitoring of 200  $\mu$ M lorazepam at surface of PE, ZnO-NPs/PE, HMImCl/PE and HMImCl/ZnO-NPs/PE, respecttively. As can be seen, with moving PE to HMImCl/ZnO-NPs/PE, the oxidation current

of lorazepam increased due to high electrical conductivity and synergic effect of two conductive mediators. This result confirms synergic effect of two mediators after modification of PE and fabrication of a highly sensitive voltammetric sensor to monitoring of lorazepam.

The linear sweep voltammogarms of 300  $\mu$ M lorazepam at surface of HMImCl/ZnO-NPs/PE and in the scan rate range 10 to 100 mV/s were recorded and signals are presented in the inset of Figure 3.

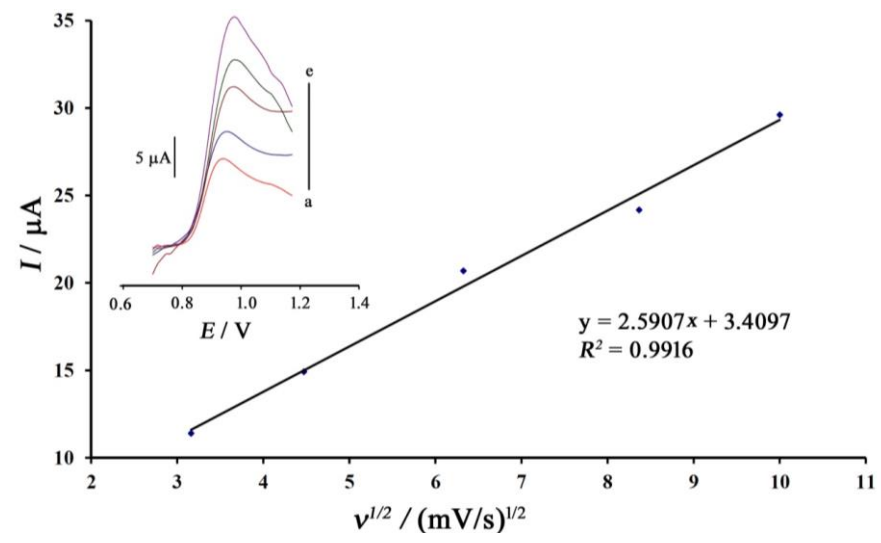


**Figure 3.** Peak current vs.  $v^{1/2}$  plot for oxidation of 300  $\mu$ M lorazepam at surface of HMImCl/ZnO-NPs/PE. Linear sweep voltammogarms of 300  $\mu$ M lorazepam at scan rates; a) 10; b) 20; c) 40; c) 70 and e) 100 mV/s (n=4)

As can be seen, a linear relation between oxidation signals of 300  $\mu$ M lorazepam and  $v^{1/2}$  with equation  $I = 2.5907 \, v^{1/2} + 3.4097 \, (R^2 = 0.9916)$  that confirms diffusion process [52-55] to lorazepam oxidation at surface of HMImCl/ZnO-NPs/PE. On the other hand, positive shift in oxidation potential of lorazepam with increase in scan rate confirms kinetic limitation in redox reaction of this drug.

The Tafel plot relative to oxidation of 300  $\mu$ M lorazepam at scan rate 10 mV/s are shown in Figure 4. Using Tafel equation and Tafel slope, the value of  $\alpha$  was calculated 0.33, that confirms irreversible behavior to redox reaction of lorazepam.

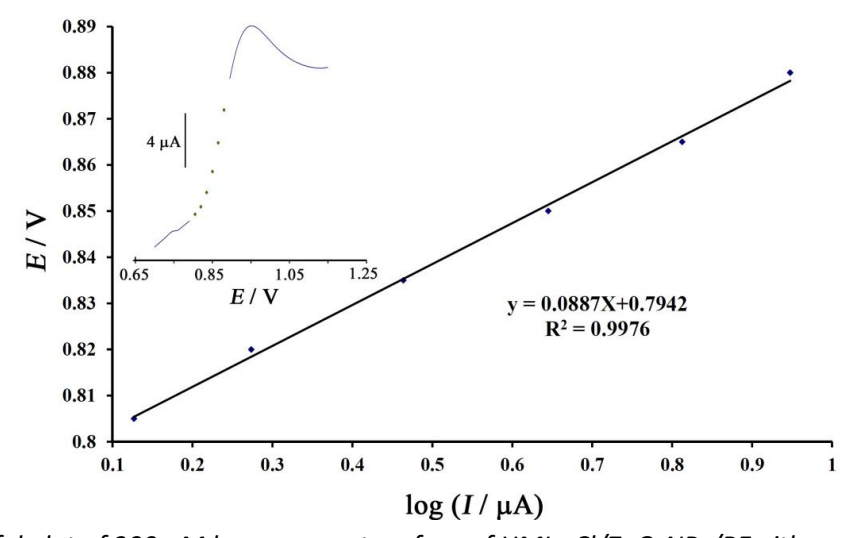


**Figure 4.** Tafel plot of 300  $\mu$ M lorazepam at surface of HMImCl/ZnO-NPs/PEwith scan rate 10 mV/s

#### **Analytical parameters**

Linear dynamic range (LDR) and limit of detection (LOD) of proposed system for sensing of lorazepam was investigated by square wave voltammetric method (Figure 5 inset).



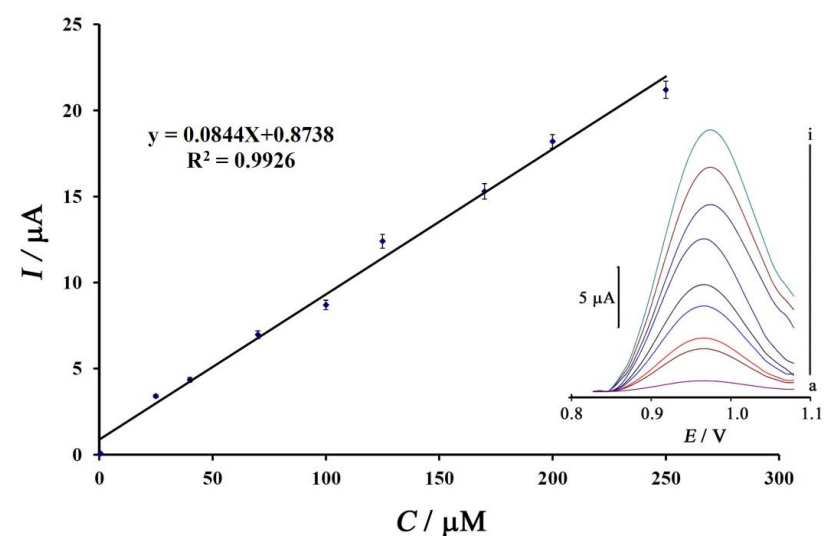


**Figure 5.** Current – concentration curve for monitoring of lorazepam using HMImCl/ZnO-NPs/PE. Inset) square wave voltammograms of lorazepam at surface of HMImCl/ZnO-NPs/PE at concentrations of 1) 0.5; 2) 25; 3) 40; 4) 70; 5) 100; 6) 125; 7) 170; 8) 200 and 9) 250  $\mu$ M (n=4)

A linear relation in the concentration range 0.5 to 250  $\mu$ M with equation I = 0.0844C + 0.8738 ( $R^2$  = 0.9926) was detected for sensing of lorazepam using HMImCl/ZnO-NPs/PE as electro-analytical sensor. The detection limit 0.1  $\mu$ M was reported for sensing of lorazepam using HMImCl/ZnO-NPs/PE in this study.

Stability, selectivity and real sample analysis

The stability of HMImCl/ZnO-NPs/PE for monitoring of 200  $\mu$ M lorazepam was investigated in period time 70 days. Results shown in Figure 6 confirm that HMImCl/ZnO-NPs/PE has good stability for sensing of lorazepam in 2 months.

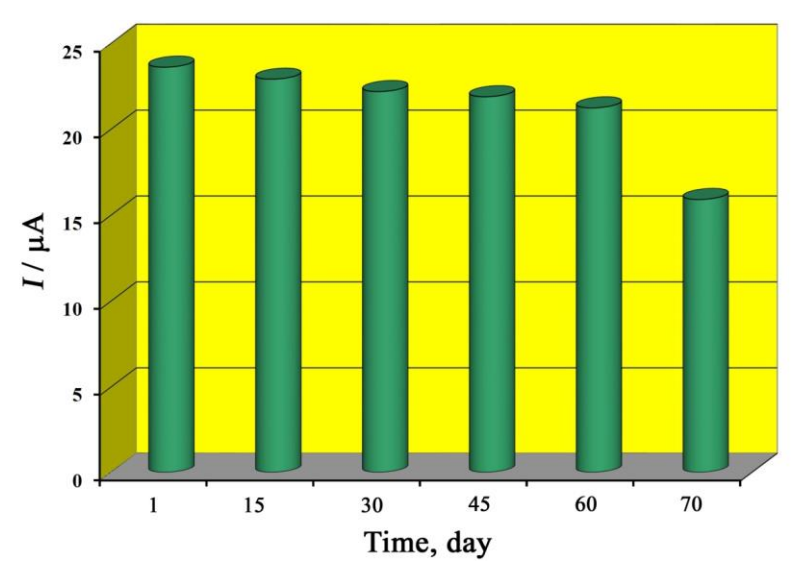


Figure 6. Current – days diagram for oxidation of 200 μM lorazepam at surface of HMImCl/ZnO-NPs/PE

On the other hand, selectivity of HMImCl/ZnO-NPs/PE in sensing of 15  $\mu$ M lorazepam was investigated and results with acceptable error 5 % are reported in Table 1. As can be seen in Table 1, there is not any important interference observed for monitoring of 15  $\mu$ M lorazepam using HMImCl/ZnO-NPs/PE and this sensor showed good selectivity in monitoring of lorazepam.

In the final step, ability of HMImCl/ZnO-NPs/PE in monitoring of lorazepam in water, dextrose saline and injection samples was checked, and results are reported in Table 2. As can be seen, the

HMImCl/ZnO-NPs/PE detected lorazepam with recovery range 98.5 to 103.5 % that are acceptable values for a new sensor.

**Table 1.** Interference study results for monitoring 15  $\mu$ M lorazepam using HMImCl/ZnO-NPs/PE as sensor

Species	Tolerant limits (W <sub>substance</sub> /W <sub>lorazepam</sub> )
Cl <sup>-</sup> , Br <sup>-</sup> , Ca <sup>2+</sup> , K+, Na <sup>+</sup>	1000
Glucose	700
Starch	Saturation

**Table 2.** Application of HMImCl/ZnO-NPs/PE for sensing of lorazepam in real samples

Sample —	C / μM			- Posovoru 9/
	Added	Expected	Founded	Recovery, %
Water —			<lod< td=""><td></td></lod<>	
	10.00	10.00	10.35±0.54	103.5
Injection —		2.00	2.03±0.05	
	10.00	12.00	11.82±0.45	98.5
Dextrose saline —			<lod< td=""><td></td></lod<>	
	10.00	10.00	10.31±0.51	103.1

# **Conclusions**

In this study, a new and simple analytical plan was described for monitoring of lorazepam in aqueous solution. The suggested sensor (HMImCl/ZnO-NPs/PE in this case) showed good selectivity for monitoring of lorazepam. The pH 7.0 was selected as optimum condition in voltammetric analysis. In addition, HMImCl/ZnO-NPs/PE was successfully used to monitor of lorazepam in the concentration range 0.5 to 250  $\mu$ M with detection limit 0.1  $\mu$ M. The modification of PE by HMImCl and ZnO-NPs improved oxidation signal of lorazepam about 2.17 times compared to unmodified PE. On the other hand, no specific interference for monitoring of lorazepam has been reported at surface of HMImCl/ZnO-NPs/PE. The HMImCl/ZnO-NPs/PE showed two-month stability for monitoring of lorazepam in aqueous solution.

#### References

- [1] M. Yoosefian, H. Karimi-Maleh, A. L. Sanati, A theoretical study of solvent effects on the characteristics of the intramolecular hydrogen bond in Droxidopa, *Journal of Chemical Sciences* **127(6)** (2015) 1007-1013. <a href="https://doi.org/10.1007/s12039-015-0858-2">https://doi.org/10.1007/s12039-015-0858-2</a>
- [2] R. M. Fathy, A. Y. Mahfouz, Eco-friendly graphene oxide-based magnesium oxide nanocomposite synthesis using fungal fermented by-products and gamma rays for outstanding antimicrobial, antioxidant, and anticancer activities, Journal of Nanostructure in Chemistry 11(2) (2021) 301-321. <a href="https://doi.org/10.1007/s40097-020-00369-3">https://doi.org/10.1007/s40097-020-00369-3</a>
- [3] H. Bártíková, R. Podlipná, L. Skálová, Veterinary drugs in the environment and their toxicity to plants, *Chemosphere* **144(2)** (2016) 2290-2301. <a href="https://doi.org/10.1016/j.chemosphere.2015.10.137">https://doi.org/10.1016/j.chemosphere.2015.10.137</a>
- [4] A. John, L. Benny, A. R. Cherian, S. Y. Narahari, A. Varghese, G. Hegde, Electrochemical sensors using conducting polymer/noble metal nanoparticle nanocomposites for the detection of various analytes, *Journal of Nanostructure in Chemistry* **11(1)** (2021) 1-31. https://doi.org/10.1007/s40097-020-00372-8
- [5] P. N. Asrami, M. S. Tehrani, P. A. Azar, S. A. Mozaffari, Impedimetric glucose biosensor based on nanostructure nickel oxide transducer fabricated by reactive RF magnetron sputtering system, *Journal of Electroanalytical Chemistry* 801(9) (2017) 258-266. <a href="https://doi.org/10.1016/j.jelechem.2017.07.052">https://doi.org/10.1016/j.jelechem.2017.07.052</a>



- [6] B. Rezaei, A. Mokhtari, Chemiluminescence determination of promazine in human serum and drug formulations using Ru (phen)<sub>3</sub><sup>2+</sup>–Ce (IV) system and a chemometrical optimization approach, Luminescence **24(3)** (2009) 183-188. <a href="https://doi.org/10.1002/bio.1093">https://doi.org/10.1002/bio.1093</a>
- [7] N. Erk, M. Kartal, Comparison of high-performance liquid chromatography and absorbance ratio methods for the determination of hydrochlorothiazide and lisinopril in pharmaceutical formulations, *Analytical Letters* **32(6)** (1999) 1131-1141. <a href="https://doi.org/10.1080/00032719908542883">https://doi.org/10.1080/00032719908542883</a>
- [8] R. Hurtubise, H. W. Latz, Fluorimetric determination of butylated hydroxy anisole in food products and packaging material, *Journal of Agricultural and Food Chemistry* **18(3)** (1970) 377-380. <a href="https://doi.org/10.1021/jf60169a008">https://doi.org/10.1021/jf60169a008</a>
- [9] C. Lacey, G. McMahon, J. Bones, M. Morrissey, J. N. Tobin, An LC–MS method for the determination of pharmaceutical compounds in wastewater treatment plant influent and effluent samples, *Talanta* 75(4) (2008) 1089-1097. https://doi.org/10.1016/j.talanta.2008.01.011
- [10] S. Cheraghi, M. A. Taher, H. Karimi-Maleh, F. Karimi, M. Shabani-Nooshabadi, M. Alizadeh, A. A. Otman, N. Erk, P. V. Y. Raman, C. Karaman, Novel enzymatic graphene oxide based biosensor for the detection of glutathione in biological body fluids, *Chemosphere* **287(1)** (2022) 132187. <a href="https://doi.org/10.1016/j.chemosphere.2021.132187">https://doi.org/10.1016/j.chemosphere.2021.132187</a>
- [11] S. Chenarani, M. Ebrahimi, V. Arabali, S. A. Beyramabadi, Determination of Lorazepam Using the Electrocatalytic Effect of NiO/SWCNTs Modified Carbon Paste Electrode as a Powerful Sensor, *Topics in Catalysis* **65(5)** (2022) 733-738. <a href="https://doi.org/10.1007/s11244-022-01561-1">https://doi.org/10.1007/s11244-022-01561-1</a>
- [12] H. Woelk, S. Schläfke, A multi-center, double-blind, randomised study of the Lavender oil preparation Silexan in comparison to Lorazepam for generalized anxiety disorder *Phytomedicine* **17(2)** (2010) 94-99. https://doi.org/10.1016/j.phymed.2009.10.006
- [13] M. B. Scharf, J. A. Jacoby, Lorazepam—efficacy, side effects, and rebound phenomena, Clinical Pharmacology and Therapeutics 31(2) (1982) 175-179. https://doi.org/10.1038/clpt.1982.27
- [14] J. Ghasemi, A. Niazi, Two-and three-way chemometrics methods applied for spectrophotometric determination of lorazepam in pharmaceutical formulations and biological fluids, *Analytica Chimica Acta* **533(2)** (2005) 169-177. <a href="https://doi.org/10.1016/j.aca.2004.11.012">https://doi.org/10.1016/j.aca.2004.11.012</a>
- [15] M. Ghalkhani, N. Zare, F. Karimi, C. Karaman, M. Alizadeh, Y. Vasseghian, Recent advances in Ponceau dyes monitoring as food colorant substances by electrochemical sensors and developed procedures for their removal from real samples, *Food and Chemical Toxicology* 161(3) (2022) 112830. <a href="https://doi.org/10.1016/j.fct.2022.112830">https://doi.org/10.1016/j.fct.2022.112830</a>
- [16] P. Nasehi, M. S. Moghaddam, N. Rezaei-savadkouhi, M. Alizadeh, M. N. Yazdani, H. Agheli, Monitoring of Bisphenol A in water and soft drink products using electrochemical sensor amplified with TiO<sub>2</sub>-SWCNTs and ionic liquid, *Journal of Food Measurement and Characterization* **16(3)** (2022) 2440-2445. <a href="https://doi.org/10.1007/s11694-022-01321-5">https://doi.org/10.1007/s11694-022-01321-5</a>
- [17] M. Alizadeh, E. Demir, N. Aydogdu, N. Zare, F. Karimi, S. M. Kandomal, H. Rokni, Y. Ghasemi, Recent advantages in electrochemical monitoring for the analysis of amaranth and carminic acid food colors, *Food and Chemical Toxicology* **163(5)** (2022) 112929. https://doi.org/10.1016/j.fct.2022.112929
- [18] J. A. Buledi, N. Mahar, A. Mallah, A. R. Solangi, I. M. Palabiyik, N. Qambarani, F. Karimi, Y. Vasseghian, H. Karimi-Maleh. Electrochemical quantification of mancozeb through tungsten oxide/reduced graphene oxide nanocomposite: A potential method for environmental remediation, *Food and Chemical Toxicology* **161(3)** (2022) 112843. https://doi.org/10.1016/j.fct.2022.112843

- [19] M. H. Karimi-Harandi, M. Shabani-Nooshabadi, R. Darabi, Simultaneous determination of citalopram and selegiline using an efficient electrochemical sensor based on ZIF-8 decorated with RGO and g-C3N4 in real samples, *Analytica Chimica Acta* **1203(4)** (2022) 339662. <a href="https://doi.org/10.1016/j.aca.2022.339662">https://doi.org/10.1016/j.aca.2022.339662</a>
- [20] J. Cheng, Z. Lu, X. Zhao, X. Chen, Y. Zhu, H. Chu, Electrochemical performance of porous carbons derived from needle coke with different textures for supercapacitor electrode materials, *Carbon Letters* **31(1)** (2021) 57-65. <a href="https://doi.org/10.1007/s42823-020-00149-7">https://doi.org/10.1007/s42823-020-00149-7</a>
- [21] H. Medetalibeyoğlu, An investigation on development of a molecular imprinted sensor with graphitic carbon nitride (g-C<sub>3</sub>N<sub>4</sub>) quantum dots for detection of acetaminophen, *Carbon Letters* **31(6)** (2021) 1237-1248. <a href="https://doi.org/10.1007/s42823-021-00247-0">https://doi.org/10.1007/s42823-021-00247-0</a>
- [22] M. Mehmandoust, N. Erk, O. Karaman, F. Karimi, M. Bijad, C. Karaman, Three-dimensional porous reduced graphene oxide decorated with carbon quantum dots and platinum nanoparticles for highly selective determination of azo dye compound tartrazine, *Food and Chemical Toxicology* **158(12)** (2021) 112698. <a href="https://doi.org/10.1016/j.fct.2021.112698">https://doi.org/10.1016/j.fct.2021.112698</a>
- [23] M. Roostaee, I. Sheikhshoaie, Fabrication of a sensitive sensor for determination of xanthine in the presence of uric acid and ascorbic acid by modifying a carbon paste sensor with Fe<sub>3</sub>O<sub>4</sub>@ Au core—shell and an ionic liquid, Journal of Food Measurement and Characterization **16(1)** (2022) 731-739. https://doi.org/10.1007/s11694-021-01200-5
- [24] Z. Yang, Y. Zhong, X. Zhou, W. Zhang, Y. Yin, W. Fang, H. Xue, Metal-organic framework-based sensors for nitrite detection, *Journal of Food Measurement and Characterization* **16(4)** (2022), 1572-1582. <a href="https://doi.org/10.1007/s11694-021-01270-5">https://doi.org/10.1007/s11694-021-01270-5</a>
- [25] T.I. Sebokolodi, D.S. Sipuka, T.R. Tsekeli, D. Nkosi, O.A. Arotiba, An electrochemical sensor for caffeine at a carbon nanofiber modified glassy carbon electrode, *Journal of Food Measurement and Characterization* 16(8) (2022) 2536-2544. https://doi.org/10.1007/s11694-022-01365-7
- [26] Y. Zhao, Y. Ma, R. Zhou, et al., Highly sensitive electrochemical detection of paraoxon ethyl in water and fruit samples based on defect-engineered graphene nanoribbons modified electrode, *Journal of Food Measurement and Characterization* **16(8)** (2022) 2596-2603. <a href="https://doi.org/10.1007/s11694-022-01366-6">https://doi.org/10.1007/s11694-022-01366-6</a>
- [27] A. A. Ensafi, H. Karimi-Maleh, S. Mallakpour, N-(3, 4-Dihydroxyphenethyl)-3, 5-dinitrobenzamide-Modified Multiwall Carbon Nanotubes Paste Electrode as a Novel Sensor for Simultaneous Determination of Penicillamine, Uric acid, and Tryptophan, *Electroanalysis* **23(6)** (2011) 1478-1487. https://doi.org/10.1002/elan.201000741
- [28] M. H. Karimi-Harandi, M., Shabani-Nooshabadi, R. Darabi, Cu-BTC Metal-Organic Frameworks as Catalytic Modifier for Ultrasensitive Electrochemical Determination of Methocarbamol in the Presence of Methadone, *Journal of The Electrochemical Society* **168(9)** (2021) 097507. https://doi.org/10.1149/1945-7111/ac2468
- [29] M. Kumar, S. S. Kirupavathy, S. Shalini, Exploration on reduced graphene oxide/strontium pyro niobate electrode material for electrochemical energy storage applications, *Carbon Letters* **31(4)** (2021) 619-633. <a href="https://doi.org/10.1007/s42823-020-00203-4">https://doi.org/10.1007/s42823-020-00203-4</a>
- [30] W. H. Danial, N.A. Norhisham, A. F. Ahmad Noorden, Z. A. Majid, K. Matsumura, A. Iqbal, A short review on electrochemical exfoliation of graphene and graphene quantum dots, *Carbon Letters* **31(3)** (2021) 371-388. <a href="https://doi.org/10.1007/s42823-020-00203-4">https://doi.org/10.1007/s42823-020-00203-4</a>
- [31] H. Esmaeili, S. M. Mousavi, S. A. Hashemi, W. H. Chiang, S. A. Abnavi, Activated carbon@ MgO@ Fe3O4 as an efficient adsorbent for As (III) removal, *Carbon Letters* **31(5)** (2021) 851-862. <a href="https://doi.org/10.1007/s42823-020-00186-2">https://doi.org/10.1007/s42823-020-00186-2</a>
- [32] J. Ma, J. Yuan, W. Ming, W. He, G. Zhang, H. Zhang, Y. Cao, Z. Jiang, Non-traditional processing of carbon nanotubes, *Alexandria Engineering Journal* **61(1)** (2022) 597-617. <a href="https://doi.org/10.1016/j.aej.2021.06.041">https://doi.org/10.1016/j.aej.2021.06.041</a>



- [33] R. Wu, C. Bi, X. Zhang, J. Wang, L. Wang, C. Fan, M. Wang, F. Shao, N. Li, Z. Zong, Y. Fan, Construction of two cobalt based bi-functional metal-organic frameworks for enhancing electrocatalytic water oxidation and photocatalytic disposals of hazardous aromatic dyes, *Molecular Catalysis* **505(4)** (2021) 111450. <a href="https://doi.org/10.1016/j.mcat.2021.111450">https://doi.org/10.1016/j.mcat.2021.111450</a>
- [34] J. Cao, A. Li, Y. Zhang, L. Mu, X. Huang, Y. Li, T. Yang, C. Zhang, C. Zhou, Highly efficient unsupported Co-doped nano-MoS<sub>2</sub> catalysts for p-cresol hydrodeoxygenation, *Molecular Catalysis* **505(4)** (2021), 111507. <a href="https://doi.org/10.1016/j.mcat.2021.111507">https://doi.org/10.1016/j.mcat.2021.111507</a>
- [35] G. Costa, P.A. Lopes, A. L. Sanati, A. F. Silva, M. C. Freitas, A. T. D. Almedia, M. Tavakoli, 3D Printed Stretchable Liquid Gallium Battery, *Advanced Functional Materials* **32(27)** (2022) 2113232. <a href="https://doi.org/10.1002/adfm.202113232">https://doi.org/10.1002/adfm.202113232</a>
- [36] M. Al Sharabati, R. Abokwiek, A. Al-Othman, M. Tawalbeh, C. Caraman, Y. Orooji, F. Karimi, Biodegradable polymers and their nano-composites for the removal of endocrinedisrupting chemicals (EDCs) from wastewater: a review, *Environmental Research* 202(11) (2021) 111694. <a href="https://doi.org/10.1016/j.envres.2021.111694">https://doi.org/10.1016/j.envres.2021.111694</a>
- [37] S. Akhil, A. M. M. J. Saeed, S. S. Majety, B. Mullamuri, G. Majji, D. Bharatiya, V. S. S. Mosali, H. B. Bollikolla, B. Chandu, Cost effective biosynthetic approach for graphene exhibiting superior sonochemical dye removal capacity, *Carbon Letters* **31(6)** (2021) 1215-1225. https://doi.org/10.1007/s42823-021-00245-2
- [38] S. Mpelane, N. Mketo, N. Bingwa, P.N. Nomngongo, Synthesis of mesoporous iron oxide nanoparticles for adsorptive removal of levofloxacin from aqueous solutions: Kinetics, isotherms, thermodynamics and mechanism, *Alexandria Engineering Journal* **61(11)** (2022) 8457-8468. <a href="https://doi.org/10.1016/j.aej.2022.02.014">https://doi.org/10.1016/j.aej.2022.02.014</a>
- [39] A. L. Sanati, A. Chambel, P. A. Lopes, T. Nikitin, R. Fausto, Laser-Assisted Rapid Fabrication of Large-Scale Graphene Oxide Transparent Conductors, *Advanced Materials Interfaces* **9(17)** (2022) 2102343. https://doi.org/10.1002/admi.202102343
- [40] F. Karimi, A. Ayati, B. Tanhaei, A. L. Santi, S. Afshar, A. Kardan, Z. Dabirifar, C. Karaman, Removal of metal ions using a new magnetic chitosan nano-bio-adsorbent; A powerful approach in water treatment, *Environmental Research* **203(1)** (2022) 111753. <a href="https://doi.org/10.1016/j.envres.2021.111753">https://doi.org/10.1016/j.envres.2021.111753</a>
- [41] C. Karaman, Orange peel derived-nitrogen and sulfur Co-doped carbon dots: a nano-booster for enhancing ORR electrocatalytic performance of 3D graphene networks, *Electroanalysis* **33(5)** (2021) 1356-1369. https://doi.org/10.1002/elan.202100018
- [42] A. Akça, O. Karaman, C. Karaman, Mechanistic insights into catalytic reduction of N<sub>2</sub>O by CO over Cu-embedded graphene: a density functional theory perspective, ECS Journal of Solid State Science and Technology 10(4) (2021) 041003. <a href="https://doi.org/10.1149/2162-8777/abf481">https://doi.org/10.1149/2162-8777/abf481</a>
- [43] R. T. Hussain, A. S. Islam, M. Khairuddean, F. B. M. Suah, A polypyrrole/GO/ZnO nanocomposite modified pencil graphite electrode for the determination of andrographolide in aqueous samples, *Alexandria Engineering Journal* **61(6)** (2022) 4209-4218. <a href="https://doi.org/10.1016/j.aej.2021.09.040">https://doi.org/10.1016/j.aej.2021.09.040</a>
- [44] H. Karimi-Maleh, F. Tahernejad-Javazmi, V. K. Gupta, H. Ahmar, M. H. Asadi, A novel biosensor for liquid phase determination of glutathione and amoxicillin in biological and pharmaceutical samples using a ZnO/CNTs nanocomposite/catechol derivative modified electrode, Journal of Molecular Liquids 196(8) (2014) 258-263. <a href="https://doi.org/10.1016/j.molliq.2014.03.049">https://doi.org/10.1016/j.molliq.2014.03.049</a>
- [45] M. Tabrizi, S. A. Shahidi, F. Chekin, A. G. HasanSaraei, S. N. Raeisi, Reduce graphene oxide/Fe<sub>3</sub>O<sub>4</sub> nanocomposite biosynthesized by sour lemon peel; using as electro-catalyst for fabrication of vanillin electrochemical sensor in food products analysis and anticancer

- activity, *Topics in Catalysis* **65(5)** (2022) 726-732. <a href="https://doi.org/10.1007/s11244-021-01541-x">https://doi.org/10.1007/s11244-021-01541-x</a>
- [46] M. Fouladgar, H. Karimi-Maleh, Ionic liquid/multiwall carbon nanotubes paste electrode for square wave voltammetric determination of methyldopa, *Ionics* **19(8)** (2013) 1163-1170. https://doi.org/10.1007/s11581-012-0832-7
- [47] H. Karimi-Maleh, A. L. Sanati, V. K. Gupta, M. Yoosefian, M. Asif, A. Bahari, A voltammetric biosensor based on ionic liquid/NiO nanoparticle modified carbon paste electrode for the determination of nicotinamide adenine dinucleotide (NADH), *Sensors and Actuators B* **204(12)** (2014) 647-654. <a href="https://doi.org/10.1016/j.snb.2014.08.037">https://doi.org/10.1016/j.snb.2014.08.037</a>
- [48] A.A. Ensafi, H. Karimi-Maleh, Voltammetric determination of isoproterenol using multiwall carbon nanotubes-ionic liquid paste electrode, *Drug Testing and Analysis* **3(5)** (2011) 325-330. https://doi.org/10.1002/dta.232
- [49] M. Alizadeh, M. Nodehi, S. Salmanpour, F. Karimi, A. L. Sanati, S. Malekmohammadi, N. Zakarariae, R. Esmaeili, J. Hedayat, Properties and recent advantages of N, N'-dialkylimidazolium-ion liquids application in electrochemistry, *Current Analytical Chemistry* **18(1)** (2022) 31-52. https://doi.org/10.2174/1573411016999201022141930
- [50] A. Hosseinian-Roudsari, S.A. Shahidi, A. Ghorbani-HasanSaraei, S. Hosseini, F. Fazeli, A new electroanalytical approach for sunset yellow monitoring in fruit juices based on a modified sensor amplified with nano-catalyst and ionic liquid, *Food and Chemical Toxicology* **168(10)** (2022) 113362 <a href="https://doi.org/10.1016/j.fct.2022.113362">https://doi.org/10.1016/j.fct.2022.113362</a>
- [51] P. Ebrahimi, S.A. Shahidi, M. Bijad, A rapid voltammetric strategy for determination of ferulic acid using electrochemical nanostructure tool in food samples, Journal of Food Measurement and Characterization 14(6) (2020) 3389-3396. <a href="https://doi.org/10.1007/s11694-020-00585-z">https://doi.org/10.1007/s11694-020-00585-z</a>
- [52] A. A. Ensafi, H. Karimi-Maleh, S. Mallakpour, Simultaneous determination of ascorbic acid, acetaminophen, and tryptophan by square wave voltammetry using N-(3, 4-Dihydroxyphenethyl)-3, 5-Dinitrobenzamide-modified carbon nanotubes paste electrode, *Electroanalysis* **24(3)** (2012) 666-675. <a href="https://doi.org/10.1002/elan.201100465">https://doi.org/10.1002/elan.201100465</a>
- [53] H. Karimi-Maleh, F. Tahernejad-Javazmi, M. Daryanavard, Electrocatalytic and simultaneous determination of ascorbic acid, nicotinamide adenine dinucleotide and folic acid at ruthenium(II) complex-ZnO/CNTs nanocomposite modified carbon paste electrode, *Electroanalysis* **26(5)** (2014) 692-970. <a href="https://doi.org/10.1002/elan.201400013">https://doi.org/10.1002/elan.201400013</a>
- [54] J. B. Raoof, R. Ojani, H. Karimi-Maleh, M. R. Hajmohammadi, P. Biparva, Multi-wall carbon nanotubes as a sensor and ferrocene dicarboxylic acid as a mediator for voltammetric determination of glutathione in hemolysed erythrocyte, *Analytical Methods* **3(11)** (2011) 2637-2643. <a href="https://doi.org/10.1039/C1AY05031A">https://doi.org/10.1039/C1AY05031A</a>
- [55] R. Darabi, M. Shabani-Nooshabadi, Development of an amplified nanostructured electrochemical sensor for the detection of cefixime in pharmaceuticals and biological samples, *Journal of Pharmaceutical and Biomedical Analysis* **212(5)** (2022) 114657. <a href="https://doi.org/10.1016/j.jpba.2022.114657">https://doi.org/10.1016/j.jpba.2022.114657</a>

©2023 by the authors; licensee IAPC, Zagreb, Croatia. This article is an open-access article distributed under the terms and conditions of the Creative Commons Attribution license (https://creativecommons.org/licenses/by/4.0/)





Open Access :: ISSN 1847-9286 www.jESE-online.org

Original scientific paper

# Facile preparation of a sensitive electrochemical sensor with good performance for determination of methionine

Peyman Mohammadzadeh Jahani¹ and Somayeh Tajik²,⊠

<sup>1</sup>School of Medicine, Bam University of Medical Sciences, Bam, Iran

<sup>2</sup>Research Centre for Tropical and Infectious Diseases, Kerman University of Medical Sciences, Kerman, Iran

*Corresponding author:* <sup>⊠</sup>*tajik s1365@yahoo.com*; Tel.: +98-3431325700; Fax: +98-3431325700

Received: August 23, 2023; Accepted: November 10, 2023; Published: November 29, 2023

#### **Abstract**

In this work, a novel voltammetric sensor for the detection of methionine was designed and prepared by using a carbon paste electrode (CPE) modified with ZnO hollow quasi-spheres (ZnO hollow QSs) and 1-butyl-3-methylimidazolium hexafluorophosphate (BMIM.PF<sub>6</sub>). The results by cyclic voltammetry showed that the prepared electrode (ZnO-BMIM.PF<sub>6</sub>/CPE) effectively increased the oxidation peak current and reduced the oxidation peak potential of methionine and had a suitable electrocatalytic activity for the oxidation of methionine. Notably, the ZnO-BMIM.PF<sub>6</sub>/CPE exhibited high detection capability towards the quantification of methionine in 0.1 M PBS (pH 7.0) over a concentration range from 0.04 to 330.0  $\mu$ M with a limit of detection of 0.02  $\mu$ M. More importantly, the effectiveness of the ZnO-BMIM.PF<sub>6</sub>/CPE sensor was also confirmed in real samples (urine detection with acceptable recoveries (98.0 to 102.7 %) and relative standard deviation values  $\leq$  3.3 %.

#### **Keywords**

Voltammetric sensor; carbon paste electrode; ZnO hollow quasi-spheres; 1-butyl-3-methylimidazolium hexafluorophosphate

#### Introduction

Methionine is classified as a sulfur-containing amino acid because it contains a sulfur atom in this chemical structure. Methionine is a primary source of sulfur in the diet, playing a vital role in maintaining the health and integrity of various tissues, including the hair, skin, and nails [1]. Also, methionine plays a crucial role in various biological processes, including protein synthesis, synthesis of amino acids, such as cysteine, taurine, homocysteine, and glycine, transmethylation reaction, and other physiological processes [2]. By increasing lecithin production in the liver, methionine can indirectly reduce cholesterol levels [3]. In addition, methionine acts as a chelator for heavy metals and functions as a powerful antioxidant for free radicals scavenging [3]. Methionine deficiency has been studied in relation to various diseases, including toxaemia, Parkinson's disease, and acquired

immune deficiency syndrome (AIDS) [4]. In addition to this, methionine deficiencies can lead to hair loss, weight loss, liver deterioration, impaired growth, depression, and muscle paralysis [5]. Therefore, developing an accurate and reliable analytical method for detecting methionine is crucial due to its clinical and physiological significance. At present, several methods, such as capillary electrophoresis [6], chromatography [7], colorimetry [8], fluorescence [9], chemiluminescence [10], and so on, have been extensively used for the analysis of methionine. Although some of these methods can be reliable, it is important to consider that they may require expensive and sophisticated equipment as well as time-consuming procedures.

Electrochemical methods are still widely used and popular due to their distinct characteristics, including fast response, low cost, versatility, simple operation, ease of miniaturization, and so on [11-19]. Modified electrodes play a crucial role in enhancing the performance, sensitivity, and selectivity of electrochemical sensors, allowing for more accurate and reliable detection of target analytes [20-26]. Nanotechnology is a closely related field that deals with the study and manipulation of materials and phenomena at the nanometer scale to create new materials, structures, and functionalities. Nanotechnology opened up new possibilities for innovation in various fields, including electronics, medicine, energy, materials science and more [27-36]. The application of nanostructures for the modification of electrodes has gained significant attention in recent years [37-41]. Nanostructured materials can offer enhanced properties such as high specific surface area and high conductivity, making them ideal candidates for electrode modifications in sensing applications. By providing higher sensitivity and selectivity, nanostructures improve the performance of electrochemical sensors in detecting and measuring different species [42-44].

ZnO is regarded as a versatile material that has been extensively studied in a wide range of applications in various fields, including catalysis [45], gas sensors [46], energy storage [47], electrochemical sensors and biosensors [48], water treatment [49], biomedicine [50], and *etc*. However, researchers continuously explore innovative ways to synthesize ZnO nanostructures with desired properties to unlock their potential fully. By manipulating the synthesis process, researchers can control the shape, size, and morphology of ZnO nanostructures, leading to significant changes in their physical and chemical characteristics. This control over nanostructure design opens avenues for tailoring ZnO properties to meet specific application requirements. In recent years, ZnO hollow nanostructures have gained significant attention in scientific research and technological applications [51-53]. The unique properties of ZnO hollow nanostructures, including low density, porous structure, and high specific surface area, make them promising candidates for the development of high-performance electrochemical sensors.

Ionic liquids (ILs) are non-molecular ionic compounds composed of oppositely charged ions arranged in a crystal lattice structure, and they exhibit distinct properties different from molecular compounds. The diverse combinations of cations and anions allow for the creation of ILs with tailored properties and functionalities [54]. ILs have gained significant attention in various fields, notably electrochemistry, because of their thermal and chemical stability, high conductivity, wide potential window, and low vapor pressure [55]. The combination of nanomaterials with ILs has shown great potential in the fabrication of electrochemical sensors. By creating the synergistic effects of nanomaterials and ILs, researchers can design and fabricate innovative electrochemical sensors with improved performance, sensitivity, and selectivity. This opens up new possibilities for applications in fields such as environmental monitoring, healthcare diagnostics, and industrial process control [56,57].

Herein, we developed a high-performance modified CPE based on ZnO hollow QSs-BMIM.PF<sub>6</sub> for detection of methionine. The ZnO-BMIM.PF<sub>6</sub> modified CPE reduces the overpotential and enhances the oxidation peak current for the effective electrochemical detection of methionine. Furthermore, the modified CPE provided acceptable results for the detection of methionine in real samples.

### **Experimental**

#### Instruments and materials

All electrochemical studies and measurements were done using a potentiostat/galvanostat device (Metrohm Autolab – PGSTAT302N (Utrecht, The Netherlands)), controlled by the GPES 4.9004 software. The electrochemical tests were performed in a typical three-electrode setup by using reference electrode (RE) (Ag/AgCl/KCl (3 M)), counter electrode (CE) (platinum), and working electrode (modified CPE). All solvents and chemicals were commercially available (Merck and Sigma-Aldrich companies) with analytical grade and used directly without further purification.

The synthesis and characterization of ZnO hollow QSs were reported in our previous work [58]. Figure 1 shows the FE-SEM image of ZnO hollow QSs.

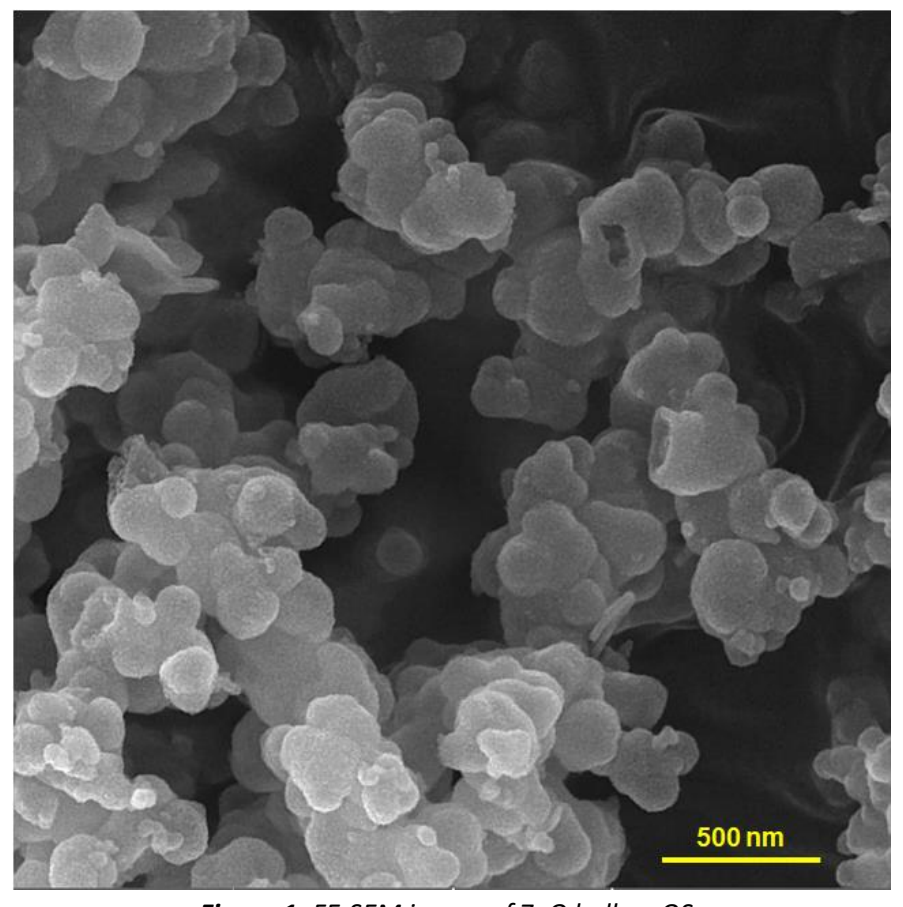


Figure 1. FE-SEM image of ZnO hollow QSs

# Preparation of ZnO-BMIM.PF<sub>6</sub>/CPE

The ZnO-BMIM.PF<sub>6</sub> modified CPE with a mass of 0.5 g was achieved by hand-mixing 0.48 g of graphite powder and 0.02 g of ZnO hollow QSs for 5 min until a homogeneous blend was formed. Then, paraffin oil and BMIM.PF<sub>6</sub> in the ratio 3:1 was added to the blend of graphite and ZnO hollow QSs, which was mixed again for at least 30 min to obtain the ZnO-BMIM.PF<sub>6</sub> modified carbon paste. Finally, the modified paste was packed into the glass tube cavity. The electrical contact was

established through a conductive copper wire. Also, the surface of the prepared electrode (ZnO-BMIM.PF<sub>6</sub>/CPE) was polished on a smooth paper to obtain a shiny and smooth appearance.

To calculate the electrochemically active surface area (EASA) of the unmodified CPE and ZnO-BMIM.PF<sub>6</sub>/CPE, the CVs were recorded at different scan rates in 0.1 M KCl solution containing 1.0 mM  $K_3$ [Fe(CN)<sub>6</sub>] as a redox probe. Using the Randles–Ševčik equation, the value of the ESCA for ZnO-BMIM.PF<sub>6</sub>/CPE (0.297 cm<sup>2</sup>) was found 3.3 times greater than unmodified CPE.

#### Results and discussion

Electrocatalytic response of ZnO-BMIM.PF<sub>6</sub>/CPE towards methionine

The effect of pH values (from 2.0 to 9.0) of the supporting electrolyte (0.1 M PBS) on methionine's electrochemical oxidation was studied using the ZnO-BMIM.PF<sub>6</sub> modified CPE via DPV technique. It was observed that by changing the pH value of PBS, the prepared electrode showed different voltammograms for oxidation of methionine. The peak potential and peak current from the oxidation of methionine showed a strong dependence on pH. By increasing the pH from lower to higher values, the anodic peak potential of methionine was shifted towards the negative potentials. Also, the  $I_{pa}$  of methionine gradually increased with the increase of pH from 2.0 to 7.0 and then decreased. The maximum  $I_{pa}$  was obtained at pH 7.0. Therefore, pH 7.0 was used for further electrochemical studies.

To assess the electrocatalytic activity of the IL (BMIM.PF<sub>6</sub>) and as-prepared ZnO, the electrochemical responses of methionine on unmodified CPE and modified CPE were examined by cyclic voltammetry (CV). Figure 2 shows the cyclic voltammograms from the response of unmodified CPE (voltammogram a) and ZnO-BMIM.PF<sub>6</sub>/CPE (voltammogram b) towards the 150.0  $\mu$ M methionine in 0.1 M PBS (pH 7.0).

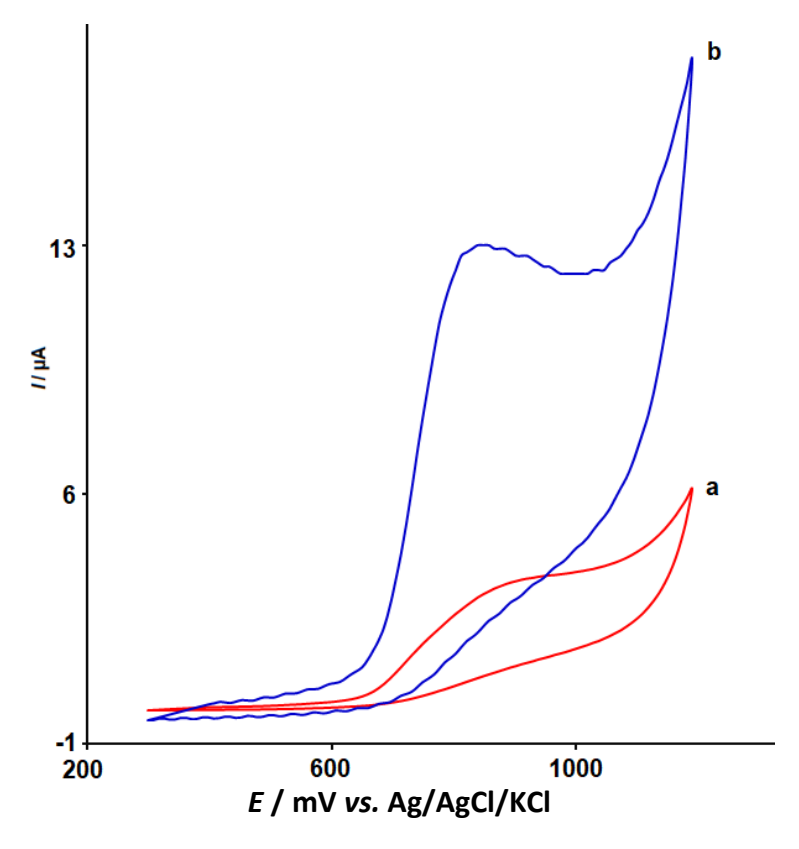


**Figure 2.** CVs of unmodified CPE (a) and ZnO-BMIM.PF<sub>6</sub>/CPE (b) in 0.1 M PBS (pH 7.0) containing 150.0  $\mu$ M methionine at a scan rate of 50 mV s<sup>-1</sup>

As can be seen, a broad oxidation peak with a low anodic peak current ( $I_{pa}$ ) was shown for unmodified CPE. The ZnO-BMIM.PF<sub>6</sub>/CPE clearly improves the oxidation of methionine, as evident from the increase of the  $I_{pa}$  (from 3.5 to 13.0  $\mu$ A) and decrease of the overpotential (from 950 to 850 mV) when compared with unmodified CPE. This result could be related to the electrocatalytic effect of the IL and ZnO NPs. In addition, the absence of any reduction peak on the reverse scan revealed the irreversible oxidation of methionine over unmodified and modified CPE.

# Effect of scan rate on the oxidation reaction of methionine

To investigate the effect of scan rate, CVs of the ZnO-BMIM.PF<sub>6</sub>/CPE were recorded at different scan rates (10 to 250 mV/s) in 0.1 M PBS containing 100.0  $\mu$ M methionine (Figure 3). An increase in the anodic peak current ( $I_{pa}$ ) with an increase in scan rate can be observed. Also, from the obtained voltammograms, it was possible to observe a linear dependence between  $I_{pa}$  of methionine and the square root of scan rate ( $v^{1/2}$ ) ( $I_{pa}$  = 1.8901  $v^{1/2}$  -2.9739) (Figure 3 Inset). This observation suggests that the oxidation reaction is controlled by the diffusion of methionine species from the bulk solution to the surface of ZnO-BMIM.PF<sub>6</sub>/CPE.

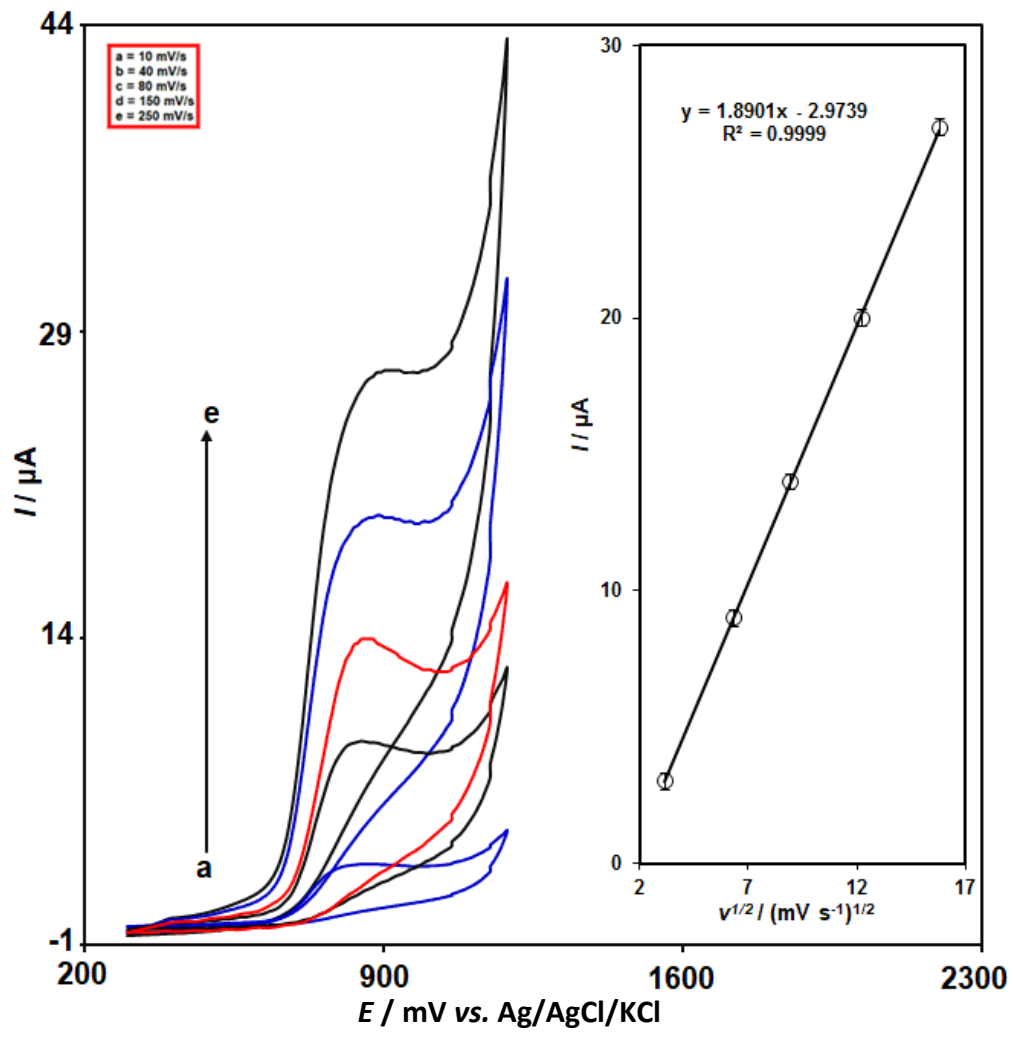


**Figure 3.** CVs of ZnO-BMIM.PF<sub>6</sub>/CPE performed at different scan rates (from a: 10 to e: 250 mV s<sup>-1</sup>) in 0.1 M PBS (pH 7.0) containing 100.0  $\mu$ M methionine. Inset: the linear dependence between  $I_{pa}$  vs.  $v^{1/2}$ 

# Chronoamperometric measurements of methionine at ZnO-BMIM.PF<sub>6</sub>/CPE

To measure the diffusion coefficient (D) of methionine, the chronoamperometric responses of  $ZnO-BMIM.PF_6/CPE$  were plotted for different concentrations of methionine from 0.1 to 1.7 mM at the

fixed potential of 0.9 V (Figure 4). The current-time (*I-t*) curves reflect the change in concentration gradient of the electroactive species (methionine) in the vicinity of the electrode surface as time progresses. To determine the *D*, the Cottrell curves (*I* versus  $t^{-1/2}$ ) were plotted over a certain range of time for different concentrations of methionine (Figure 4A). Then, the slope of the obtained Cottrell curves was plotted vs the different concentrations of methionine (Figure 4B) and a straight line with a slope of 19.7  $\mu$ A s<sup>1/2</sup> mM<sup>-1</sup> was obtained. From the slope of the resulting plot and using Cottrell's equation, the *D* of methionine on the surface of ZnO-BMIM.PF<sub>6</sub>/CPE was found to be 1.6×10<sup>-5</sup> cm<sup>2</sup> s<sup>-1</sup>.

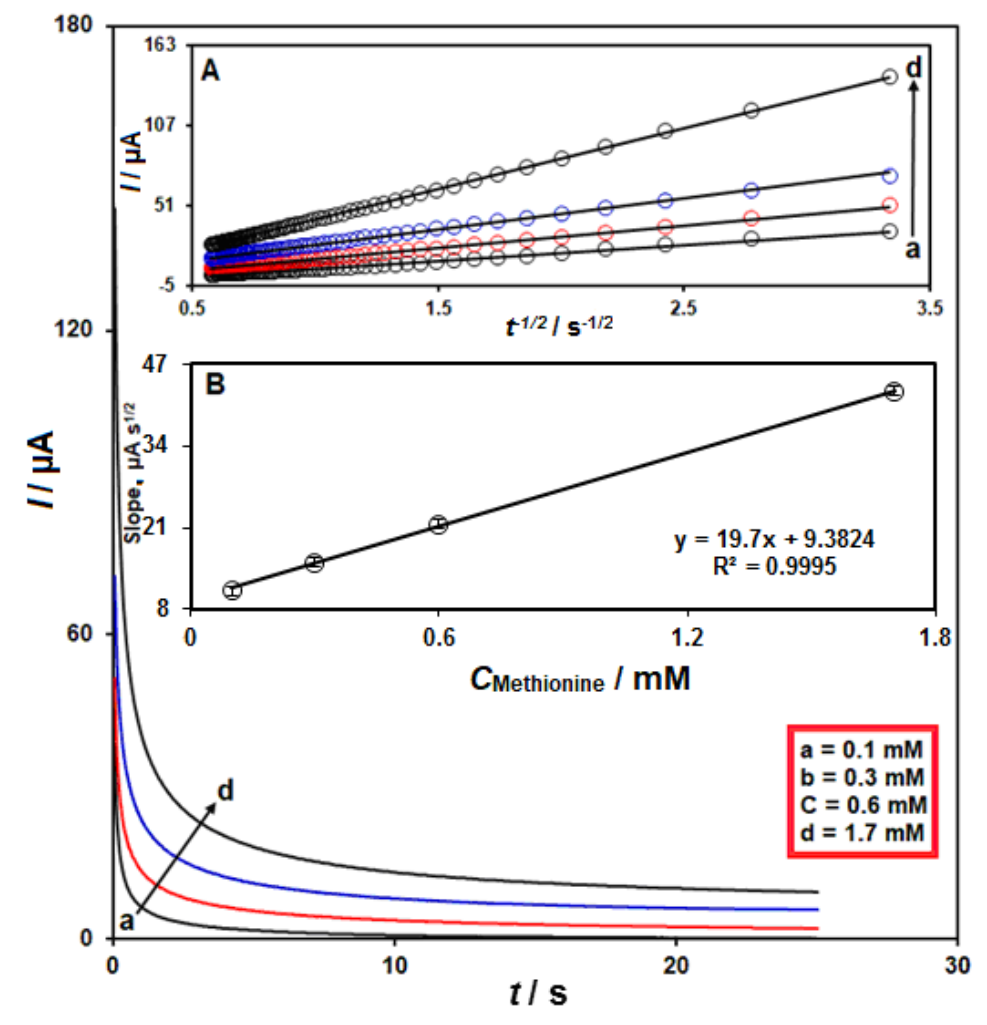


**Figure 4.** Chronoamperometric responses of ZnO-BMIM.PF<sub>6</sub>/CPE in 0.1 M PBS (pH 7.0) containing different concentrations of methionine from a: 0.1 to 1.7 mM. Inset A: the linear dependence between  $I_{pa} / \mu A$  vs.  $t^{-1/2} / s^{-1/2}$ ) and Inset B: linear dependence between slope values of I- $t^{-1/2}$  plots vs. methionine concentrations

#### Quantitative analysis of methionine by DPV

To study the detection efficiency of ZnO-BMIM.PF<sub>6</sub>/CPE, the DPV measurements were performed with the successive addition of methionine (0.04 to 330.0  $\mu$ M) in 0.1 M PBS (pH 7.0) in the following conditions: step potential 0.01 V and pulse amplitude 0.025 V (Figure 5). From the recorded voltammograms, the increase of the  $I_{pa}$  is proportional to the increase of methionine concentration in a wide range from 0.04 to 330.0  $\mu$ M. Furthermore, the linear dependence between the enhanced  $I_{pa}$  of methionine and its concentration is presented in the Inset of Figure 5. This dependence can be expressed by  $I = 0.0812C_{\text{Methionine}} + 0.8557$  with a correlation coefficient of 0.999. The LOD was calculated according to the ensuing formula  $3S_b/m$ , where  $S_b$  denotes the standard deviation of the



blank (PBS) signal (obtained based on 12 measurements on the blank solution), and m denotes the slope of the corresponding calibration curve, and it was found to be 0.02  $\mu$ M. The limit of quantification was found to be 0.04  $\mu$ M. Table 1 lists the comparative characteristics of the as-prepared sensor with those of previously reported sensors for the determination of methionine.

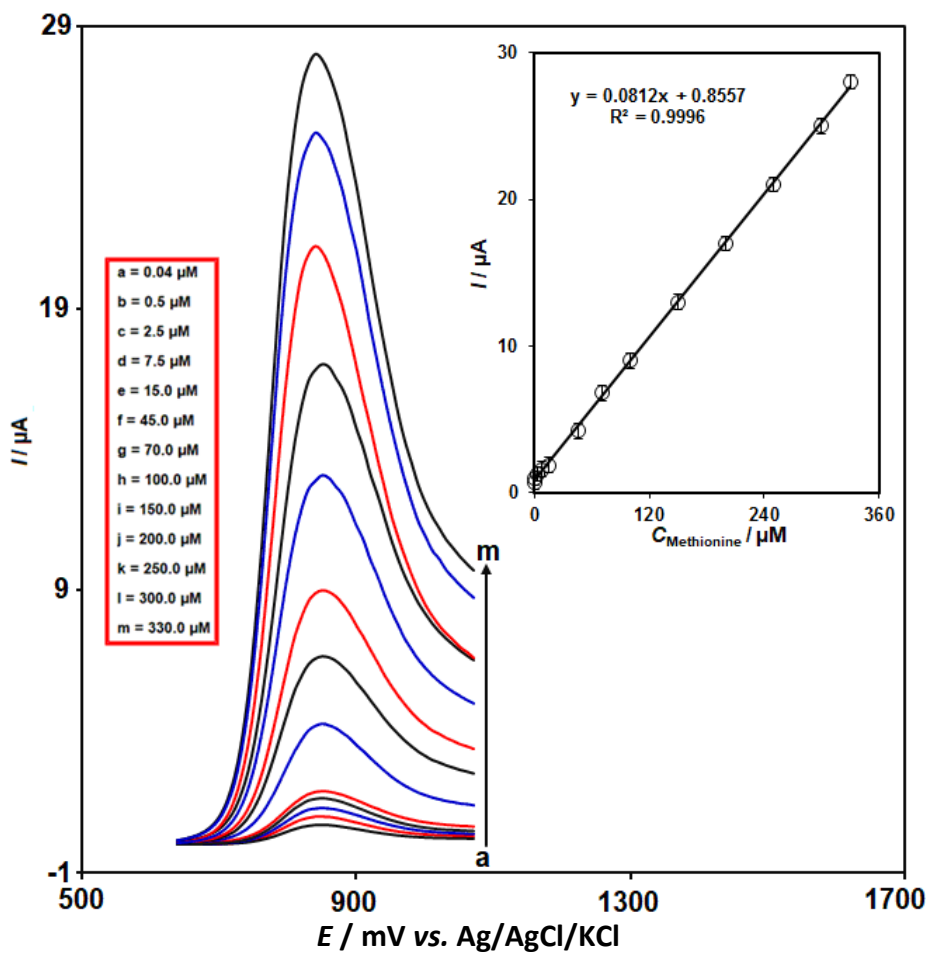


**Figure 5.** DPVs of ZnO-BMIM.PF<sub>6</sub>/CPE performed in 0.1 M PBS (pH 7.0) containing different concentrations of methionine (from a: 0.04 to m: 330.0  $\mu$ M). Inset: the linear dependence between  $I_{pa}$  vs. methionine concentration

**Table 1.** Comparative results of ZnO-BMIM.PF<sub>6</sub>/CPE based methionine sensor with previously reported sensors

Electrochemical sensor	Linear range, μΜ	LOD, μM	Sensitivity	Ref.
Pt-doped TiO <sub>2</sub> nanoparticles (NPs)				
carbon nanotubes (CNTs)/glassy	0.5 - 100	0.1	29.085 μA μM <sup>-1</sup> cm <sup>-2</sup>	[1]
carbon electrode (GCE)				
Colloidal gold-cysteamine/CPE	1.0 - 100	0.59	-	[12]
Fullerene-C <sub>60</sub> /Au electrode	-	8.2	50 mA M <sup>-1</sup>	[59]
Ni-doped carbon ceramic electrode	2 - 90	2	5.6 nA μM <sup>-1</sup>	[60]
Graphitic carbon nitride	0.1 - 200	0.32×10 <sup>-3</sup>	1.16 μΑ μM <sup>-1</sup> cm <sup>-2</sup>	[61]
nanosheets/GCE	0.1 - 200	0.32×10	1.10 μΑ μινι τιιι	[01]
ZnO-BMIM.PF <sub>6</sub> /CPE	0.04 - 330.0	0.02	0.0812 μA μM <sup>-1</sup>	This work

Stability and reproducibility studies of ZnO-BMIM.PF $_6$ /CPE sensor towards the determination of methionine

Studies related to the stability of ZnO-BMIM.PF $_6$ /CPE sensors were performed by recording the current response of the designed sensor towards 75.0  $\mu$ M methionine over 20 days. The results

showed that the electrode response retained 95.9 % of its initial value after 20 days. These results indicated that the designed sensor has good stability.

Also, the reproducibility of the prepared sensor (ZnO-BMIM.PF<sub>6</sub>/CPE) was evaluated by recording the current response of five electrodes prepared independently under the same conditions. All five prepared electrodes showed almost the same responses and the relative standard deviation (RSD) was 2.7~% in the determination of  $75.0~\mu M$  methionine.

# Interferences studies

The effect of the possible interferences from some species such as Na $^+$ , Ca $^{2+}$ , Mg $^{2+}$ , NH $_4^+$ , Al $^{3+}$ , Cl $^-$ , SO $_4^{2-}$ , S $^{2-}$ , glucose, acetaminophen, epinephrine, norepinephrine, uric acid, tryptophan, glycine, phenylalanine, and L-serine on the electrochemical response of methionine was evaluated at the surface of ZnO-BMIM.PF $_6$ /CPE sensor. It was observed that these species did not show significant interference for the determination of methionine (no signal change more than  $\pm$  5%). These results confirmed that the developed sensor has good selectivity for the determination of methionine.

# Methionine analysis in real samples

To evaluate the practical performance of the developed sensor (ZnO-BMIM.PF<sub>6</sub>/CPE), the determination of methionine in the urine sample was conducted. The standard addition method was employed for the analysis of methionine by the DPV technique. By adding the known concentrations of methionine to the urine sample, measurements were performed. The recovery and RSD values are summarized in Table 2. The summarized results in Table 1 show acceptable recovery values (between 98.0 and 102.7 %) and RSD values (n = 5) of  $\leq 3.3$  %, which confirm that the developed sensor could be used for real-time analysis.

Sample —	Amount, μM		Dogovory 0/	DCD 0/
	Spiked	Found	- Recovery, %	RSD, %
	0	-	-	-
	5.0	4.9±0.05	98.0	3.3
Urine	7.5	7.7±0.04	102.7	2.9
·	10.0	10.1±0.06	101.0	1.7
	12.5	12.4±0.05	99.2	2.4

**Table 2.** Real sample analysis for the determination of methionine spiked into the urine samples

### **Conclusions**

In this study, the efficient and accurate detection of methionine was reported based on ZnO hollow QSs-BMIM.PF<sub>6</sub> modified CPE. The obtained results demonstrated that the ZnO-BMIM.PF<sub>6</sub>/CPE sensor was well developed and showed an enhanced electrochemical response towards methionine oxidation. The ZnO-BMIM.PF<sub>6</sub>/CPE can be used to determine methionine in the concentration from 0.04 to 330.0  $\mu$ M with an LOD of 0.02  $\mu$ M. Finally, excellent precision (RSD  $\leq$ 3.3 %) and accuracy (recovery for spiked samples ranging from 98.0 to 102.7 %) were obtained.

#### References

- [1] F. Chekin, S. Bagheri, S. B. Abd Hamid, Synthesis of Pt doped TiO<sub>2</sub> nanoparticles: characterization and application for electrocatalytic oxidation of I-methionine, *Sensors and Actuators B: Chemical* **177** (2013) 898-903. <a href="https://doi.org/10.1016/j.snb.2012.12.002">https://doi.org/10.1016/j.snb.2012.12.002</a>
- [2] J. D. Finkelstein, Methionine metabolism in mammals, *The Journal of Nutritional Biochemistry* **1** (1990) 228-237. <a href="https://doi.org/10.1016/0955-2863(90)90070-2">https://doi.org/10.1016/0955-2863(90)90070-2</a>



- [3] Y. Yang, S. Han, Synergistic enhanced of carbon dots and eosin Y on fenton chemiluminescence for the determination of methionine, *Microchemical Journal* **163** (2021) 105902. https://doi.org/10.1016/j.microc.2020.105902
- [4] Y. Li, S. Mei, S. Liu, X. Hun, A photoelectrochemical sensing strategy based on single-layer MoS<sub>2</sub> modified electrode for methionine detection, *Journal of Pharmaceutical and Biomedical Analysis* **165** (2019) 94-100. <a href="https://doi.org/10.1016/j.jpba.2018.11.059">https://doi.org/10.1016/j.jpba.2018.11.059</a>
- [5] T. Hoshi, S. H. Heinemann, Regulation of cell function by methionine oxidation and reduction, *The Journal of Physiology* **531** (2001) 1-11. <a href="https://doi.org/10.1111/j.1469-7793.2001.0001j.x">https://doi.org/10.1111/j.1469-7793.2001.0001j.x</a>
- [6] L. Vitali, F. Della Betta, A. C. O. Costa, F. A. S. Vaz, M. A. L. Oliveira, J. P. Vistuba, G. A. Micke, New multilayer coating using quaternary ammonium chitosan and κ-carrageenan in capillary electrophoresis: Application in fast analysis of betaine and methionine, *Talanta* **123** (2014) 45-53. https://doi.org/10.1016/j.talanta.2014.01.047
- [7] K. Borowczyk, G. Chwatko, P. Kubalczyk, H. Jakubowski, J. Kubalska, R. Głowacki, Simultaneous determination of methionine and homocysteine by on-column derivatization with o-phtaldialdehyde, *Talanta* **161** (2016) 917-924. https://doi.org/10.1016/j.talanta.2016.09.039
- [8] P. C. Huang, N. Gao, J. F. Li, F. Y. Wu, Colorimetric detection of methionine based on antiaggregation of gold nanoparticles in the presence of melamine, *Sensors and Actuators B: Chemical* **255** (2018) 2779-2784. <a href="https://doi.org/10.1016/j.snb.2017.09.092">https://doi.org/10.1016/j.snb.2017.09.092</a>
- [9] Y. Wang, S. Liu, Z. Liu, J. Yang, X. Hu, A l-tryptophan-Cu (II) based fluorescence turn-on probe for detection of methionine, *Journal of Luminescence* **147** (2014) 107-110. https://doi.org/10.1016/j.jlumin.2013.11.006
- [10] M. Zhou, A. Wang, C. Li, X. Luo, Y. Ma, Flow-based determination of methionine in pharmaceutical formulations exploiting TGA-capped CdTe quantum dots for enhancing the luminol-KIO<sub>4</sub> chemiluminescence, *Journal of Luminescence* **183** (2017) 206-211. https://doi.org/10.1016/j.jlumin.2016.11.007
- [11] V. R. R. Bernardo-Boongaling, N. Serrano, J. J. García-Guzmán, J. M. Palacios-Santander, J. M. Díaz-Cruz, Screen-printed electrodes modified with green-synthesized gold nanoparticles for the electrochemical determination of aminothiols, *Journal of Electroanalytical Chemistry* 847 (2019) 113184. <a href="https://doi.org/10.1016/j.jelechem.2019.05.066">https://doi.org/10.1016/j.jelechem.2019.05.066</a>
- [12] L. Agüý, J. Manso, P. Yáñez-Sedeño, J. M. Pingarrón, Colloidal-gold cysteamine-modified carbon paste electrodes as suitable electrode materials for the electrochemical determination of sulphur-containing compounds: application to the determination of methionine, *Talanta* **64** (2004) 1041-1047. https://doi.org/10.1016/j.talanta.2004.05.002
- [13] Y. Tangal, D. Coban, S. Cogal, A WSe<sub>2</sub>@poly (3,4-ethylenedioxythiophene) nanocomposite-based electrochemical sensor for simultaneous detection of dopamine and uric acid, *Journal of Electrochemical Science and Engineering* **12** (2022) 1251-1259. https://doi.org/10.5599/jese.1375
- [14] H. Karimi-Maleh, R. Darabi, F. Karimi, C. Karaman, S. A. Shahidi, N. Zare, M. Baghayeri, L. Fu, S. Rostamnia, J. Rouhi, State-of-art advances on removal, degradation and electrochemical monitoring of 4-aminophenol pollutants in real samples, *Environmental Research* 222 (2023) 115338. <a href="https://doi.org/10.1016/j.envres.2023.115338">https://doi.org/10.1016/j.envres.2023.115338</a>
- [15] M. Vardini, N. Abbasi, A. Kaviani, M. Ahmadi, E. Karimi, Graphite electrode potentiometric sensor modified by surface imprinted silica gel to measure valproic acid, *Chemical Methodologies* **6** (2022) 398-408. <a href="https://doi.org/10.22034/chemm.2022.328620.1437">https://doi.org/10.22034/chemm.2022.328620.1437</a>
- [16] S. Tajik, H. Beitollahi, H. W. Jang, M. Shokouhimehr, A screen printed electrode modified with Fe<sub>3</sub>O<sub>4</sub>@polypyrrole-Pt core-shell nanoparticles for electrochemical detection of 6-

- mercaptopurine and 6-thioguanine, *Talanta* **232** (2021) 122379. https://doi.org/10.1016/j.talanta.2021.122379
- [17] R. S. Kumar, G. K. Jayaprakash, S. Manjappa, M. Kumar, A. P. Kumar, Theoretical and electrochemical analysis of L-serine modified graphite paste electrode for dopamine sensing applications in real samples, *Journal of Electrochemical Science and Engineering* 12 (2022) 1243-1250. <a href="https://doi.org/10.5599/jese.1390">https://doi.org/10.5599/jese.1390</a>
- [18] H. Pyman, Design and fabrication of modified DNA-Gp nano-biocomposite electrode for industrial dye measurement and optical confirmation, *Progress in Chemical and Biochemical Research* **5** (2022) 391-405. <a href="https://doi.org/10.22034/pcbr.2022.367576.1236">https://doi.org/10.22034/pcbr.2022.367576.1236</a>
- [19] S. Tajik, H. Beitollahi, F. Garkani Nejad, M. Safaei, P. Mohammadzadeh Jahani, (2022). Electrochemical sensing of Sudan I using the modified graphite screen-printed electrode, *International Journal of Environmental Analytical Chemistry* **102** (2022) 1477-1490. https://doi.org/10.1080/03067319.2020.1738418
- [20] S. Cheraghi, M. A. Taher, H. Karimi-Maleh, F. Karimi, M. Shabani-Nooshabadi, M. Alizadeh, A. Al-Othman, N. Erk, P. K. Y. Raman, C. Karaman, Novel enzymatic graphene oxide based biosensor for the detection of glutathione in biological body fluids, *Chemosphere* **287** (2022) 132187. https://doi.org/10.1016/j.chemosphere.2021.132187
- [21] R. Zaeimbashi, A. Mostafavi, T. Shamspur, Synthesis of vanadium oxide nanoplates for electrochemical detection of amaranth in food samples, *Journal of Electrochemical Science and Engineering* **12** (2022) 1153-1163. <a href="https://doi.org/10.5599/jese.1394">https://doi.org/10.5599/jese.1394</a>
- [22] H. Roshanfekr, A simple specific dopamine aptasensor based on partially reduced graphene oxide—AuNPs composite, *Progress in Chemical and Biochemical Research* **6** (2023) 61-70. <a href="https://doi.org/10.22034/pcbr.2023.381280.1245">https://doi.org/10.22034/pcbr.2023.381280.1245</a>
- [23] S. Z. Mohammadi, H. Beitollahi, E. Bani Asadi, Electrochemical determination of hydrazine using a ZrO<sub>2</sub> nanoparticles-modified carbon paste electrode, *Environmental Monitoring and Assessment* **187** (2015) 122. <a href="https://doi.org/10.1007/s10661-015-4309-9">https://doi.org/10.1007/s10661-015-4309-9</a>
- [24] S. B. Arpitha, B. K. Swamy, J. K. Shashikumara, An efficient electrochemical sensor based on ZnO/Co<sub>3</sub>O<sub>4</sub> nanocomposite modified carbon paste electrode for the sensitive detection of hydroquinone and resorcinol, *Inorganic Chemistry Communications* **152** (2023) 110656. https://doi.org/10.1016/j.inoche.2023.110656
- [25] S. N. Zakiyyah, D. R. Eddy, Firdaus, M. L. Eddy, T. Subroto, Y. W. Hartati, Screen-printed carbon electrode/natural silica-ceria nanocomposite for electrochemical aptasensor application, *Journal of Electrochemical Science and Engineering* **12** (2022) 1225-1242. <a href="https://doi.org/10.5599/jese.1455">https://doi.org/10.5599/jese.1455</a>
- [26] H. Karimi-Maleh, Y. Liu, Z. Li, R. Darabi, Y. Orooji, C. Karaman, F. Karimi, M. Baghayeri, J. Rouhi, L. Fu, Calf thymus ds-DNA intercalation with pendimethalin herbicide at the surface of ZIF-8/Co/rGO/C₃N₄/ds-DNA/SPCE; A bio-sensing approach for pendimethalin quantification confirmed by molecular docking study, *Chemosphere* **332** (2023) 138815. <a href="https://doi.org/10.1016/j.chemosphere.2023.138815">https://doi.org/10.1016/j.chemosphere.2023.138815</a>
- [27] O. Daliri Shamsabadi, Investigation of antimicrobial effect and mechanical properties of modified starch films, cellulose nanofibers, and citrus essential oils by disk diffusion method, Asian Journal of Green Chemistry 8 (2024) 1-14. <a href="https://doi.org/10.48309/ajgc.2024.398370.1394">https://doi.org/10.48309/ajgc.2024.398370.1394</a>
- [28] H. Alinezhad, P. Hajiabbas Tabar Amiri, S. Mohseni Tavakkoli, R. Muslim Muhiebes, Y. Fakri Mustafa, Progressive types of Fe<sub>3</sub>O<sub>4</sub> nanoparticles and their hybrids as catalysts, *Journal of Chemical Reviews* **4** (2022) 288-312. <a href="https://doi.org/10.22034/jcr.2022.325255.1137">https://doi.org/10.22034/jcr.2022.325255.1137</a>
- [29] O. K. Akeremale, Metal-organic frameworks (MOFs) as adsorbents for purification of dyecontaminated wastewater: a review, *Journal of Chemical Reviews* 4 (2022) 1-14. https://doi.org/10.22034/jcr.2022.314728.1130



- [30] S. Li, Y. Zhang, Y. Yuan, F. Chang, K. Zhu, G. Li, L. Yang, Design and synthesis of dispersed Ni<sub>2</sub>P/Co nano heterojunction as bifunctional electrocatalysis for boosting overall water splitting, *International Journal of Hydrogen Energy* **48** (2023) 3355-3363. https://doi.org/10.1016/j.ijhydene.2022.10.129
- [31] B. Baghernejad, M. Alikhani, Nano-cerium oxide/aluminum oxide as an efficient catalyst for the synthesis of xanthene derivatives as potential antiviral and anti-inflammatory agents, *Journal of Applied Organometallic Chemistry* **2** (2022) 140-147. <a href="https://doi.org/10.22034/jaoc.2022.154819">https://doi.org/10.22034/jaoc.2022.154819</a>
- [32] I. Alao, I. Oyekunle, K. Iwuozor, E. Emenike, Green synthesis of copper nanoparticles and investigation of its antimicrobial properties, Advanced Journal of Chemistry, Section B 4 (2022) 39-52. <a href="https://doi.org/10.22034/ajcb.2022.323779.1106">https://doi.org/10.22034/ajcb.2022.323779.1106</a>
- [33] M. S. Jabar, S. A. W. Al-Shammaree, Cytotoxicity and anticancer effect of chitosan-Ag NPs-doxorubicin-folic acid conjugate on lungs cell line, *Chemical Methodologies* 7 (2023) 1-14. <a href="https://doi.org/10.22034/chemm.2023.359769.1604">https://doi.org/10.22034/chemm.2023.359769.1604</a>
- [34] D. Palke, Synthesis, physicochemical and biological studies of transition metal complexes of DHA schiff bases of aromatic amine, *Journal of Applied Organometallic Chemistry* **2** (2022) 81-88. <a href="https://doi.org/10.22034/jaoc.2022.349187.1055">https://doi.org/10.22034/jaoc.2022.349187.1055</a>
- [35] M. Ozdal, S. Gurkok, Recent advances in nanoparticles as antibacterial agent, *ADMET and DMPK* **10** (2022) 115-129. <a href="https://doi.org/10.5599/admet.1172">https://doi.org/10.5599/admet.1172</a>
- [36] B. Bonhoeffer, A. Kordikowski, E. John, M. Juhnke, Numerical modeling of the dissolution of drug nanocrystals and its application to industrial product development, *ADMET and DMPK* 10 (2022) 253-287. <a href="https://doi.org/10.5599/admet.1437">https://doi.org/10.5599/admet.1437</a>
- [37] F. Garkani Nejad, S. Tajik, H. Beitollahi, I. Sheikhshoaie, Magnetic nanomaterials based electrochemical (bio) sensors for food analysis, *Talanta* **228** (2021) 122075. https://doi.org/10.1016/j.talanta.2020.122075
- [38] S. Z. Mohammadi, F. Mousazadeh, M. Mohammadhasani-Pour, Electrochemical detection of folic acid using a modified screen printed electrode, *Journal of Electrochemical Science and Engineering* **12** (2022) 1111-1120. <a href="https://doi.org/10.5599/jese.1360">https://doi.org/10.5599/jese.1360</a>
- [39] J. A. Buledi, N. Mahar, A. Mallah, A. R. Solangi, I. M. Palabiyik, N. Qambrani, F. Karimi, Y. Vasseghian, H. Karimi-Maleh, Electrochemical quantification of mancozeb through tungsten oxide/reduced graphene oxide nanocomposite: A potential method for environmental remediation, *Food and Chemical Toxicology* **161** (2022) 112843. <a href="https://doi.org/10.1016/j.fct.2022.112843">https://doi.org/10.1016/j.fct.2022.112843</a>
- [40] A. Hajializadeh, An electrochemical sensor for detection of vanillin in food samples using CuFe<sub>2</sub>O<sub>4</sub> nanoparticles/ionic liquids modified carbon paste electrode, *Journal of Electrochemical Science and Engineering* **12** (2022) 1193-1203. https://doi.org/10.5599/jese.1395
- [41] Z. Zhang, H. Karimi-Maleh, In situ synthesis of label-free electrochemical aptasensor-based sandwich-like AuNPs/PPy/Ti<sub>3</sub>C<sub>2</sub>T<sub>x</sub> for ultrasensitive detection of lead ions as hazardous pollutants in environmental fluids, *Chemosphere* **324** (2023) 138302. https://doi.org/10.1016/j.chemosphere.2023.138302
- [42] S. Tajik, H. Beitollahi, F. Garkani Nejad, M. Safaei, K. Zhang, Q. Van Le, M. Shokouhimehr, Developments and applications of nanomaterial-based carbon paste electrodes, *RSC Advances* **10** (2020) 21561-21581. <a href="https://doi.org/10.1039/D0RA03672B">https://doi.org/10.1039/D0RA03672B</a>
- [43] H. Karimi-Maleh, C. T. Fakude, N. Mabuba, G. M. Peleyeju, O. A. Arotiba, The determination of 2-phenylphenol in the presence of 4-chlorophenol using nano-Fe<sub>3</sub>O<sub>4</sub>/ionic liquid paste electrode as an electrochemical sensor, *Journal of Colloid and Interface Science* **554** (2019) 603-610. <a href="https://doi.org/10.1016/j.jcis.2019.07.047">https://doi.org/10.1016/j.jcis.2019.07.047</a>

- [44] Z. Mehdizadeh, S. Shahidi, A. Ghorbani-HasanSaraei, M. Limooei, M. Bijad, Monitoring of amaranth in drinking samples using voltammetric amplified electroanalytical sensor, *Chemical Methodologies* 6 (2022) 246-252. https://doi.org/10.22034/chemm.2022.324073.1423
- [45] O. V. Larina, P. I. Kyriienko, D. Y. Balakin, M. Vorokhta, I. Khalakhan, Y. M. Nychiporuk, V. Matolín, S. O. Soloviev, S. M. Orlyk, Effect of ZnO on acid-base properties and catalytic performances of ZnO/ZrO<sub>2</sub>-SiO<sub>2</sub> catalysts in 1,3-Butadiene production from ethanol-water mixture, *Catalysis Science & Technology* **9** (2019) 3964–3978. https://doi.org/10.1039/C9CY00991D
- [46] Z. Li, L. Guo, Z. Feng, S. Gao, H. Zhang, X. Yang, G. Pan, Metal-organic framework-derived ZnO decorated with CuO for ultra-high response and selectivity H₂S gas sensor. *Sensors and Actuators B: Chemical* **366** (2022) 131995. <a href="https://doi.org/10.1016/j.snb.2022.131995">https://doi.org/10.1016/j.snb.2022.131995</a>
- [47] K. Zhu, J. Chen, C. Guo, H. Wang, H. Li, P. Xue, J. M. Lee, Hierarchically constructed ZnO/Co<sub>3</sub>O<sub>4</sub> nanoheterostructures synergizing dendrite inhibition and polysulfide conversion in lithium–sulfur battery, *ACS Materials Letters* **4** (2022) 1358-1367. https://doi.org/10.1021/acsmaterialslett.2c00266
- [48] K. Saxena, A. Kumar, N. Chauhan, M. Khanuja, B. D. Malhotra, U. Jain, Electrochemical immunosensor for detection of h. Pylori secretory protein vaca on g-C<sub>3</sub>N<sub>4</sub>/ZnO nanocomposite-modified au electrode, *ACS Omega* **7** (2022) 32292-32301. https://doi.org/10.1021/acsomega.2c03627
- [49] V. B. Raghavendra, S. Shankar, M. Govindappa, A. Pugazhendhi, M. Sharma, S. C. Nayaka, Green synthesis of zinc oxide nanoparticles (ZnO NPs) for effective degradation of dye, polyethylene and antibacterial performance in waste water treatment, *Journal of Inorganic and Organometallic Polymers and Materials* **32** (2022) 614–630. https://doi.org/10.1007/s10904-021-02142-7
- [50] N. Salahuddin, S. Awad, M. Elfiky, Vanillin-crosslinked chitosan/ZnO nanocomposites as a drug delivery system for 5-fluorouracil: study on the release behavior via mesoporous ZrO<sub>2</sub>–Co<sub>3</sub>O<sub>4</sub> nanoparticles modified sensor and antitumor activity, *RSC Advances* **12** (2022) 21422-21439. https://doi.org/10.1039/d2ra02717h
- [51] S. Ameen, M. S. Akhtar, H. K. Seo, H. S. Shin, An electrochemical sensing platform based on hollow mesoporous ZnO nanoglobules modified glassy carbon electrode: Selective detection of piperidine chemical, *Chemical Engineering Journal* **270** (2015) 564–571. https://doi.org/10.1016/j.cej.2015.02.052
- [52] J. Zhang, H. Lu, L. Zhang, D. Leng, Y. Zhang, W. Wang, C. Wang, Metal—organic framework-derived ZnO hollow nanocages functionalized with nanoscale Ag catalysts for enhanced ethanol sensing properties, *Sensors and Actuators B* **291** (2019) 458-469. https://doi.org/10.1016/j.snb.2019.04.058
- [53] S. Wang, X. Wang, G. Qiao, X. Chen, X. Wang, H. Cui, Core-double shell ZnO@ In<sub>2</sub>O<sub>3</sub>@ZnO hollow microspheres for superior ethanol gas sensing, *Sensors and Actuators B* **341** (2021) 130002. <a href="https://doi.org/10.1016/j.snb.2021.130002">https://doi.org/10.1016/j.snb.2021.130002</a>
- [54] R. Chokkareddy, S. Kanchi, G. G. Redhi, A novel IL-f-ZnONPs@MWCNTs nanocomposite fabricated glassy carbon electrode for the determination of sulfamethoxazole, *Journal of Molecular Liquids* **359** (2022) 119232. <a href="https://doi.org/10.1016/j.molliq.2022.119232">https://doi.org/10.1016/j.molliq.2022.119232</a>
- [55] P. Ranjan, M. Abubakar Sadique, S. Yadav, R. Khan, An electrochemical immunosensor based on gold-graphene oxide nanocomposites with ionic liquid for detecting the breast cancer CD44 biomarker, ACS Applied Materials & Interfaces 14 (2022) 20802-20812. <a href="https://doi.org/10.1021/acsami.2c03905">https://doi.org/10.1021/acsami.2c03905</a>
- [56] M. A. Mohamed, N. N. Salama, M. A. Sultan, H. F. Manie, M. M. A. El-Alamin, Sensitive and effective electrochemical determination of butenafine in the presence of itraconazole using



- titanium nanoparticles-ionic liquid based nanocomposite sensor, *Chemical Papers* **77** (2023) 1929-1939. https://doi.org/10.1007/s11696-022-02593-3
- [57] K. Kunpatee, S. Traipop, O. Chailapakul, S. Chuanuwatanakul, Simultaneous determination of ascorbic acid, dopamine, and uric acid using graphene quantum dots/ionic liquid modified screen-printed carbon electrode, *Sensors and Actuators B* **314** (2020) 128059. https://doi.org/10.1016/j.snb.2020.128059
- [58] S. Z. Mohammadi, S. Tajik, F. Mousazadeh, E. Baghadam-Narouei, F. Garkani Nejad, ZnO hollow quasi-spheres modified screen-printed graphite electrode for determination of carmoisine, *Micromachines* **14** (2023) 1433. https://doi.org/10.3390/mi14071433
- [59] W. E. Tan, J. E. Goh, Electrochemical oxidation of methionine mediated by a fullerene-C60 modified gold electrode, *Electroanalysis* 20 (2008) 2447-2453. https://doi.org/10.1002/elan.200704335
- [60] A. Salimi, M. Roushani, Electrocatalytic oxidation of sulfur containing amino acids at renewable Ni-powder doped carbon ceramic electrode: application to amperometric detection L-cystine, L-cysteine and L-methionine, *Electroanalysis* **18** (2006) 2129-2136. https://doi.org/10.1002/elan.200603639
- [61] A. Ajith, S. A. John, Cost Effective Electrochemical sensor for L-Methionine based on graphitic carbon nitride sheets modified electrode, *Electroanalysis* **35** (2023) e202200063. https://doi.org/10.1002/elan.202200063

© 2023 by the authors; licensee IAPC, Zagreb, Croatia. This article is an open-access article distributed under the terms and conditions of the Creative Commons Attribution license (<a href="https://creativecommons.org/licenses/by/4.0/">https://creativecommons.org/licenses/by/4.0/</a>)



Open Access : : ISSN 1847-9286

www.jESE-online.org

Original scientific paper

# Novel electrochemical sensing platform for detection of hydrazine based on modified screen-printed graphite electrode

Farideh Mousazadeh¹, Sayed Zia Mohammadi²,⊠, Maryam Mohammadhasani-Pour²

<sup>1</sup>School of Medicine, Bam University of Medical Sciences, Bam, Iran

<sup>2</sup>Department of Chemistry, Payame Nour University, Tehran, Iran

Corresponding authorc: <sup>™</sup>szmohammadi@yahoo.com

Received: April 26, 2022; Accepted: July 29, 2022; Published: October 25, 2022

#### **Abstract**

The current work aimed to fabricate a screen-printed graphite electrode (SPGE) modified by  $MnO_2$  nanorods ( $MnO_2$  NRs) for sensing hydrazine. Thus, a facile protocol was adopted to construct the  $MnO_2$  nanorods that were subsequently applied to modify the SPGE surface directly. As-synthesized  $MnO_2$  NRs/SPGE sensor exhibited a strong sensing behavior towards the hydrazine, with a large peak current and small oxidation potential. This electrochemical sensor in the optimized conditions to detect the hydrazine possessed a low detection limit ( $0.02~\mu M$ ), a broad linear dynamic range ( $0.05-275.0~\mu M$ ) and an admirable sensitivity ( $0.0625~\mu A~\mu M^{-1}$ ). The sensor applicability was practically estimated in real water samples, which revealed successful recovery values.

# Keywords

MnO<sub>2</sub> nanorods; electrochemical sensor; hydrazine diffusion coefficient

#### Introduction

Hydrazine, a vital chemical reagent, has attracted widespread research interest due to its industrial application and poisonousness. It is a robust reducing agent with various applications in the production of pesticides and medicine [1-3]. It is also a chemical deoxidizer with broad applications as an oxygen scavenger in water boilers [4]. Hydrazine is a key raw material in the construction of rockets and explosives [5,6]. Although hydrazine plays a great role in human production and life, it is easy to be absorbed by living organisms. The persistent contact with this agent may be associated with complications, such as some disturbances in the reproductive system, central nervous system, liver, kidneys and lungs [7-9]. According to the U.S. Environmental Protection Agency (US EPA), hydrazine is positioned in a class of possibly carcinogenic to humans, with a recommended threshold limit value (TLV) of less than 10 ppb [10].

Accordingly, it is substantial to achieve a practical and efficient sensing protocol for the determination of this agent in various media. In this regard, different analytical and instrumental

protocols have been designed to detect hydrazine so far, such as gas chromatography, capillary electrophoresis, chemiluminescence, high-performance liquid chromatography, liquid chromatography, colorimetry, and spectrophotometry [11-17]. Despite the unique benefits of each of these techniques, they typically require precision instrumentation and length of time. Among these, electrochemical approaches have been concerned by many researchers owing to their peculiar traits, which are simplicity, rapidity, affordability and short response time [18-34]. Voltammetric measurements typically use economical manners to detect analytes by recording variations in response current over alteration in electrode potential [35-42].

The recent development of electrochemical approaches has been greatly simplified by screen-printed electrodes (SPEs) due to their high sensitivity, functionality and versatility [43-45]. The main performance features of a sensor are all gathered in SPEs, including cost-effectiveness, minimal sample preparation, ease of operation, high speed, small size, limited background, and comfortable surface modification. There is always a need for further research to develop electrode materials to improve the selectivity and sensitivity of electrochemical sensors [46-51]. Many advances in nanotechnology have been made in diverse fields in recent years [52-75], which have led to the introduction of highly efficient sensing platforms. Types of nano-scale materials have so far been identified with distinct physicochemical properties that can be employed in the electrochemical sensors to detect various analytes exhibiting admirable results [76-82].

A popular oxide material is manganese dioxide ( $MnO_2$ ), whose behavior can be enhanced by changing its morphology and surface area.  $MnO_2$  is a polymorph owing to an octahedral [ $MnO_6$ ] spatial arrangement. Nano-sized  $MnO_2$  exhibits commendable benefits due to a larger surface-to-volume ratio and further reactive surface for electrochemical reactions. The diverse application of this substance in electrochemistry and sensor fabrication can be attributed to the simple reduction of  $MnO_2$  to  $Mn_2O_3$  and MnO and, at the proper potential, the re-oxidation to  $MnO_2$  as a catalytic circle for electrochemical detection [83-87].

The current work aimed to fabricate a new screen-printed graphite electrode (SPGE) supported by  $MnO_2$  nanorods ( $MnO_2$  NRs/SPGE) for sensitively sensing hydrazine. The sensor applicability was tested in real water samples, the results of which revealed successful recovery values.

#### **Experimental**

#### Chemicals and instrumentations

All materials with analytical grades applied throughout this work were supplied from Aldrich and Merck. Electrochemical experiments were recorded using a PGSTAT-302N Autolab potentiostat/galvanostat (Eco Chemie, The Netherlands). The control of all experiments was carried out by a General Purpose Electrochemical System (GPES) software. The SPGEs were purchased from DropSens (Spain) and consisted of an Ag pseudo-reference electrode, graphite axillary electrode, and graphite working electrode. All pH values were measured by a digital Metrohm 710 pH meter.

# Synthesis of MnO<sub>2</sub> nanorods

The  $MnO_2$  NRs were obtained by dissolving  $KMnO_4$  (0.316 g) in deionized water (30 mL) while vigorously stirring, followed by the addition of 3 M HCl (1.4 mL) under vigorous stirring for another half hour. Then, the solution was placed in a 50-mL Teflon-lined autoclave at 160 °C for six hours. Next, the products were cooled down to room temperature and subsequently centrifuged and thoroughly rinsed with ethanol and deionized water to clean any impurities, followed by drying at 60 °C for 12 h.

## Preparation of MnO<sub>2</sub> NRs/SPGE

First, 1 mg of prepared  $MnO_2$  nanorods was added into an aqueous solution (1 ml), followed by sonication for 30 min to give a homogeneous solution. Then, 4  $\mu$ L of  $MnO_2$  NRs was dispersed on the surface of SPGE dropwise. Following the solvent's evaporation, the sensor's surface was washed several times with deionized water to clean free modifier molecules and subsequently air-dried. The obtained electrode was noted as  $MnO_2$  NRs/SPGE.

# **Results and discussion**

## Characterization of MnO<sub>2</sub> nanorods

Figure 1 illustrates the FE-SEM images captured for the as-fabricated  $MnO_2$  NRs, and observing them confirmed rod-shaped  $MnO_2$  nanorods with a thickness ranging from 15 to 25 nm and a length of about 3  $\mu$ m. The  $MnO_2$  NRs showed an almost uniform size distribution.

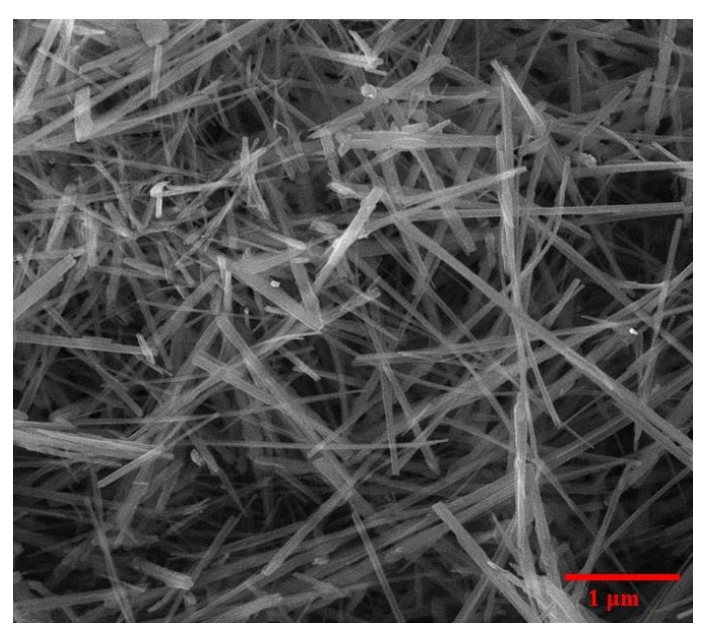
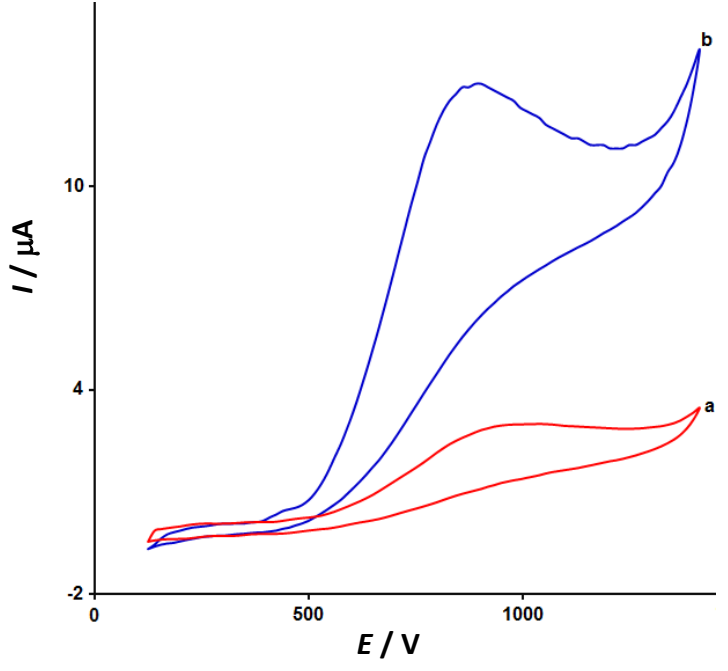


Figure 1. The FESEM image of synthesized MnO<sub>2</sub> nanorods

## Electrochemical response of hydrazine at different electrodes

The differential pulse voltammetry (DPV) method was recruited to study the effect pH value of electrolyte solution in different pH values (2.0-9.0) in the presence of 40.0  $\mu$ M of hydrazine in phosphate buffer solution (0.1 M PBS) on the MnO<sub>2</sub> NRs/SPGE surface. The peak current of hydrazine oxidation was maximum at the pH value of 7.0, thereby selecting this value as the optimum pH in the hydrazine detection.

Figure 2 shows the application of the cyclic voltammetry (CV) method to evaluate the electrochemical behavior of 200.0  $\mu$ M hydrazine at different electrodes (unmodified SPGE, and MnO<sub>2</sub> NRs/SPGE) in PBS (0.1 M, pH 7.0) at the scan rate of 50 mV/s. Based on the results, there was an oxidation peak on the surfaces of the electrodes, but no reduction peak, highlighting an irreversible electrochemical response of hydrazine on the electrodes. A relatively wide and weak peak current ( $I_{Pa}$ ) of hydrazine oxidation was found on the unmodified SPGE (at 1000 mV with 3.0  $\mu$ A), which reveals that the electrochemical oxidation does not happen spontaneously due to high activation overpotential. The hydrazine Ipa on MnO<sub>2</sub> NRs/SPGE, when compared with unmodified SPGE, displayed further elevation to 13.0  $\mu$ A, meaning an increase up to 4.3 times that on the unmodified SPGE. In addition, hydrazine oxidation occurred at a lower potential than unmodified SPGE.



**Figure 2.** CV curves of unmodified SPGE (curve a), and MnO<sub>2</sub> NRs/SPGE (curve b) in 0.1 M PBS containing 200.0  $\mu$ M hydrazine; scan rate: 50 mV s<sup>-1</sup>

# Effect of the scan rate (v) on the results

The influence of various scan rates between 10 and 400 mV/s on the anodic peak currents for hydrazine (100.0  $\mu$ M) was studied using the MnO<sub>2</sub> NRs/SPGE (Figure 3). The regression equation was  $I_{pa}$  (hydrazine) = 1.7036  $V^2$  - 4.2319 ( $R^2$ =0.9994) (Figure 3, inset). This result indicates that the oxidation process is controlled by diffusion. Further, there was a shift in the oxidation peak potential of hydrazine toward a more positive potential by increasing the scan rates.

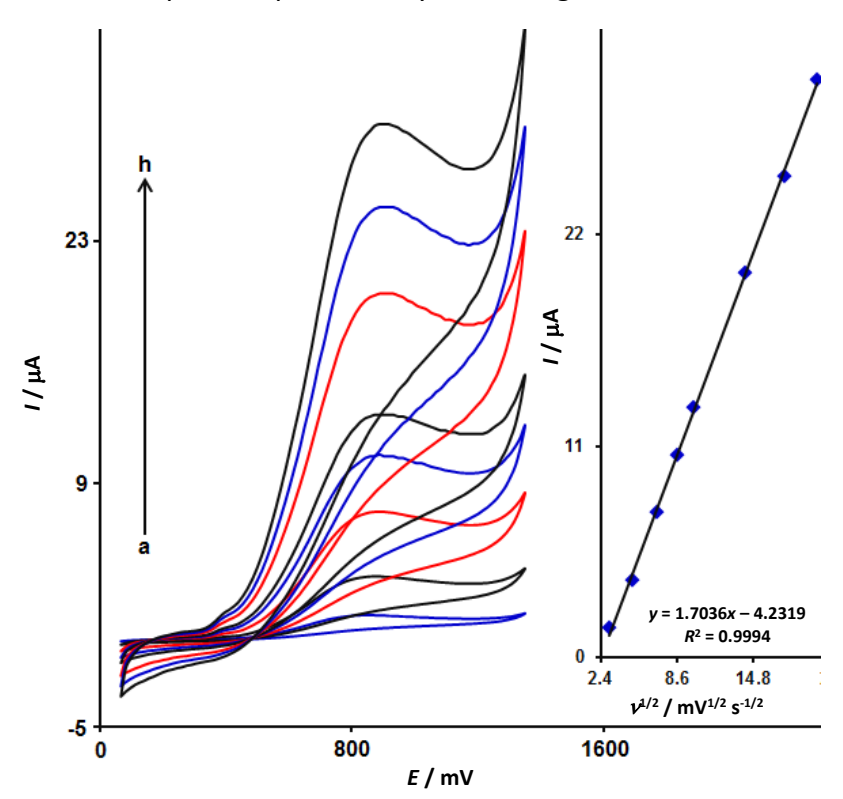


**Figure 3.** CV curves of 100.0  $\mu$ M hydrazine in 0.1 M PBS (pH 7.0) at a scan rate of 10 to 400 mV s<sup>-1</sup> for MnO<sub>2</sub> NRs/SPGE (a-h refer to 10, 25, 50, 75, 100, 200.0, 300.0 and 400.0 mV s<sup>-1</sup>) Inset: plot of the square root of the scan rate vs. the oxidation peak current of hydrazine

To study the rate-determining step as shown in Figure 4, the data of the rising part of the current-voltage curve obtained at 10 mV/s scan rate were applied to draw a Tafel plot for 100.0  $\mu$ M of hydrazine. The linearity of the *E* versus log *I* plot, implies the intervention of the kinetics of the electrode process. The slope of this plot was utilized to estimate the number of electrons transferred in the rate-determining step. Figure 4 shows the Tafel slope of 0.2153 V for the linear section of the plot, which means the rate-limiting step of one-electron transfer with a transfer coefficient of  $\alpha$  = 0.72.

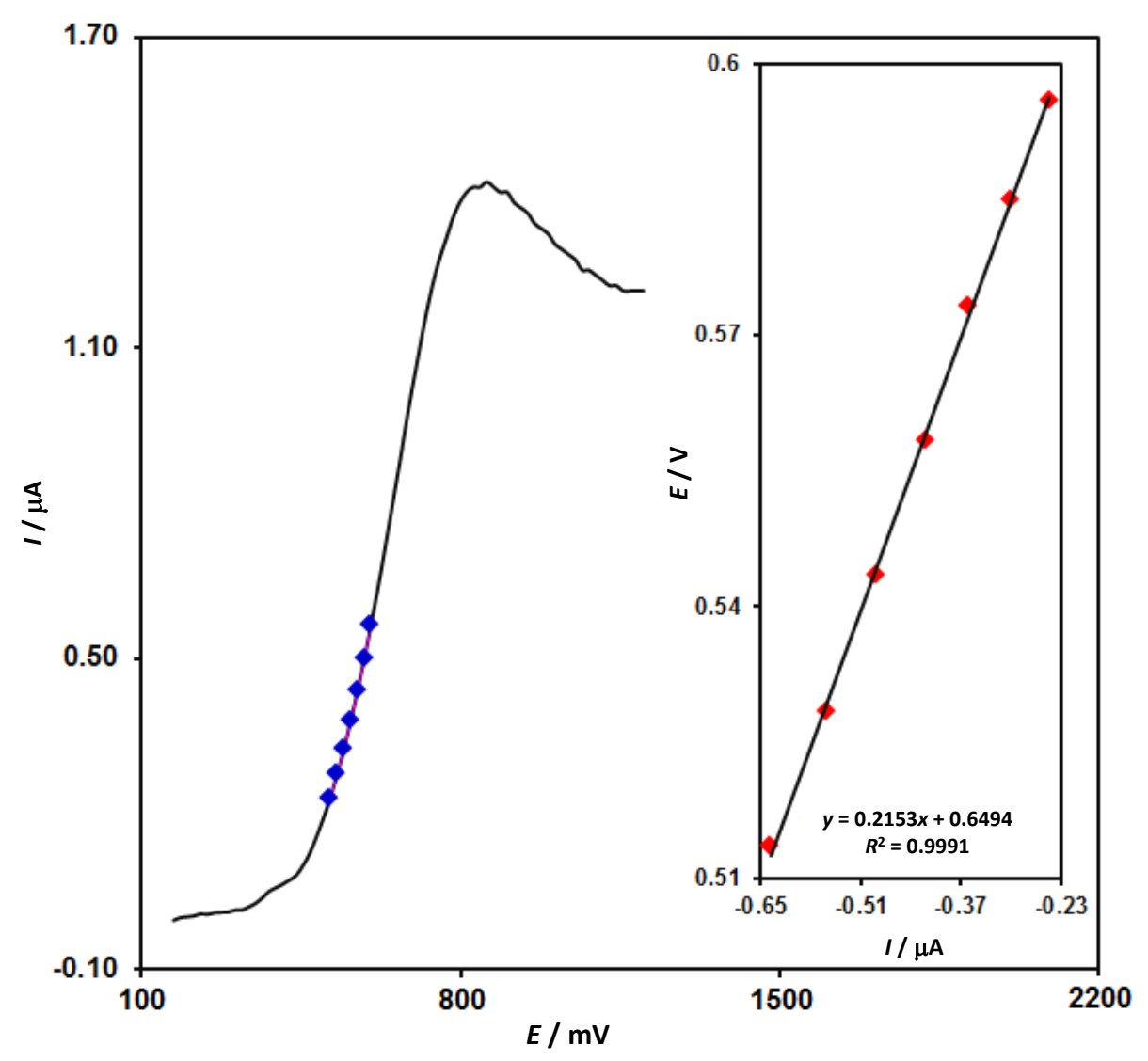


**Figure 4.** CV response for 100.0  $\mu$ M hydrazine with 10 mVs<sup>-1</sup> scan rate and the inset is the Tafel plot derived from the rising part or the corresponding voltammogram

## Chronoamperometric analysis

Chronoamperometric determinations for different concentrations of hydrazine on the surface of MnO<sub>2</sub> NRs/SPGE were measured by adjusting the potential of the working electrode at 0.94 V in PBS (0.1 M, pH 7.0), see Figure 5. For an electroactive material (hydrazine in this case) with a diffusion coefficient of D, the current observed for the electrochemical reaction at the mass transport limited condition is described by the Cottrell equation [88]. As shown in Figure 5A, I versus  $t^{-1/2}$  plots were used with the optimal fit for various hydrazine concentrations. We drew the slopes from straight lines against different concentrations of hydrazine, see Figure 5B. According to the Cottrell equation and obtained slope, the mean D value was  $2.7 \times 10^{-5}$  cm<sup>2</sup>/s.

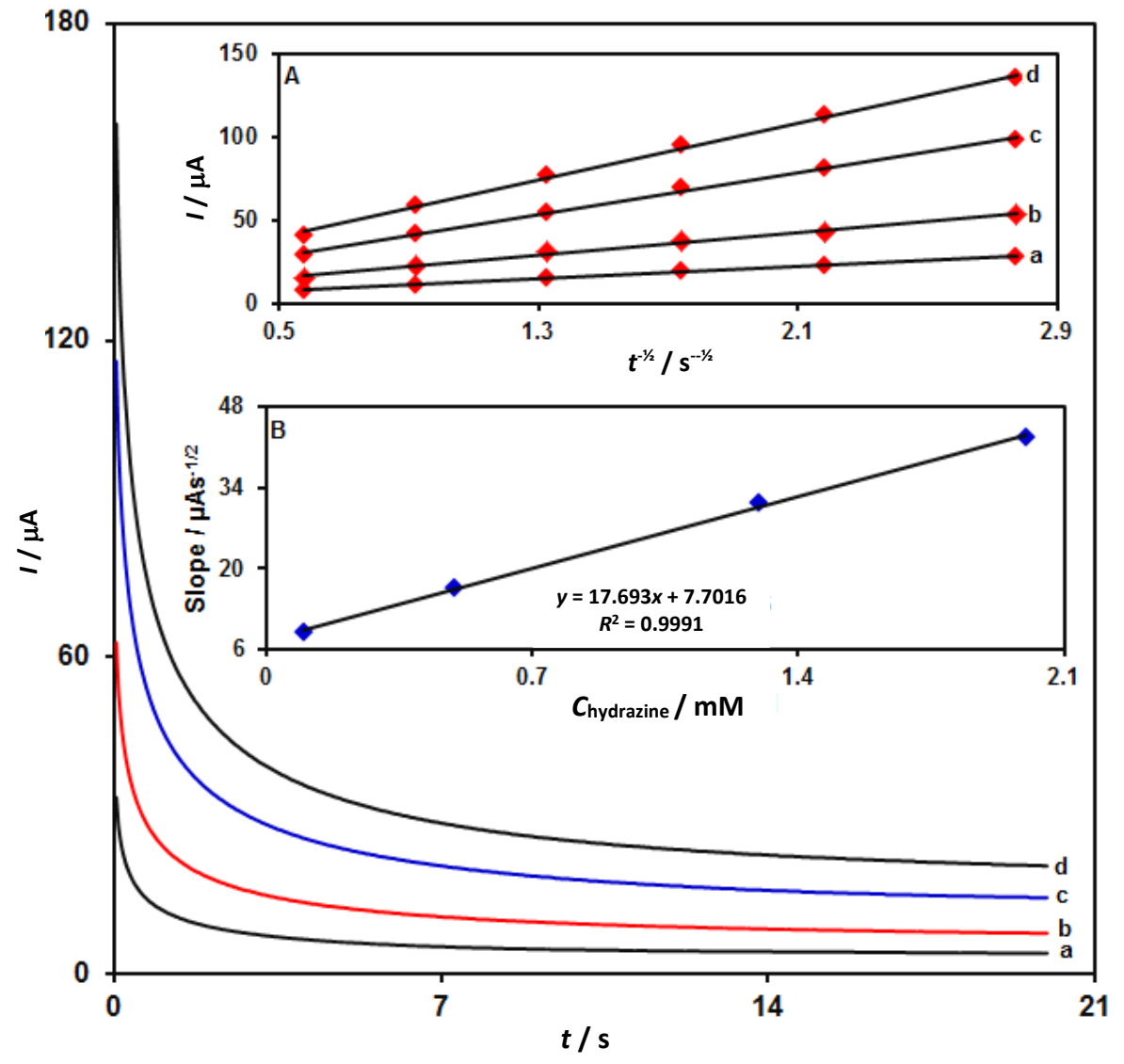


**Figure 5.** The chronoamperograms obtained at  $MnO_2$  NRs/SPGE in 0.1 M PBS at pH of 7.0 for different concentrations of hydrazine. a-d are related to 0.1, 0.5, 1.3, and 2.0 mM of hydrazine Inset A: the I plot versus  $t^{-1/2}$  observed by chronoamperograms a to d. Inset B: slope plot of the straight line vs. concentration of hydrazine

# Calibration curve, linear range and detection limit

MnO<sub>2</sub> NRs/SPGE sensor was used to electrochemically detect different hydrazine concentrations (Figure 6). A gradual elevation was observed for the peak currents of hydrazine oxidation by raising its concentrations, which means an advanced performance of our sensor in the electrocatalytic oxidation of hydrazine. Oxidation peak currents of hydrazine versus  $C_{\text{hydrazine}}$  (Figure 6, inset) showed a wide linear range from 0.05 to 275.0  $\mu$ M. The detection limit (LOD=3 $\sigma$ /S; where  $\sigma$  is the standard deviation of blank response, and S is the slope of the calibration curve with a linear range of concentrations of the analyte) was calculated to be 0.02  $\mu$ M.

# *Interference study*

The effect of some interference species on the determination of hydrazine was studied. The results show that the interfering effects of glucose, sucrose, urea, uric acid, Na<sup>+</sup>, Cl<sup>-</sup>, No<sub>3</sub><sup>-</sup>, pb<sup>2+</sup>, and Ag<sup>+</sup> on the anodic peak current of hydrazine is less than 5%. Hence, the MnO<sub>2</sub> NRs/SPGE has a superior selectivity for hydrazine.



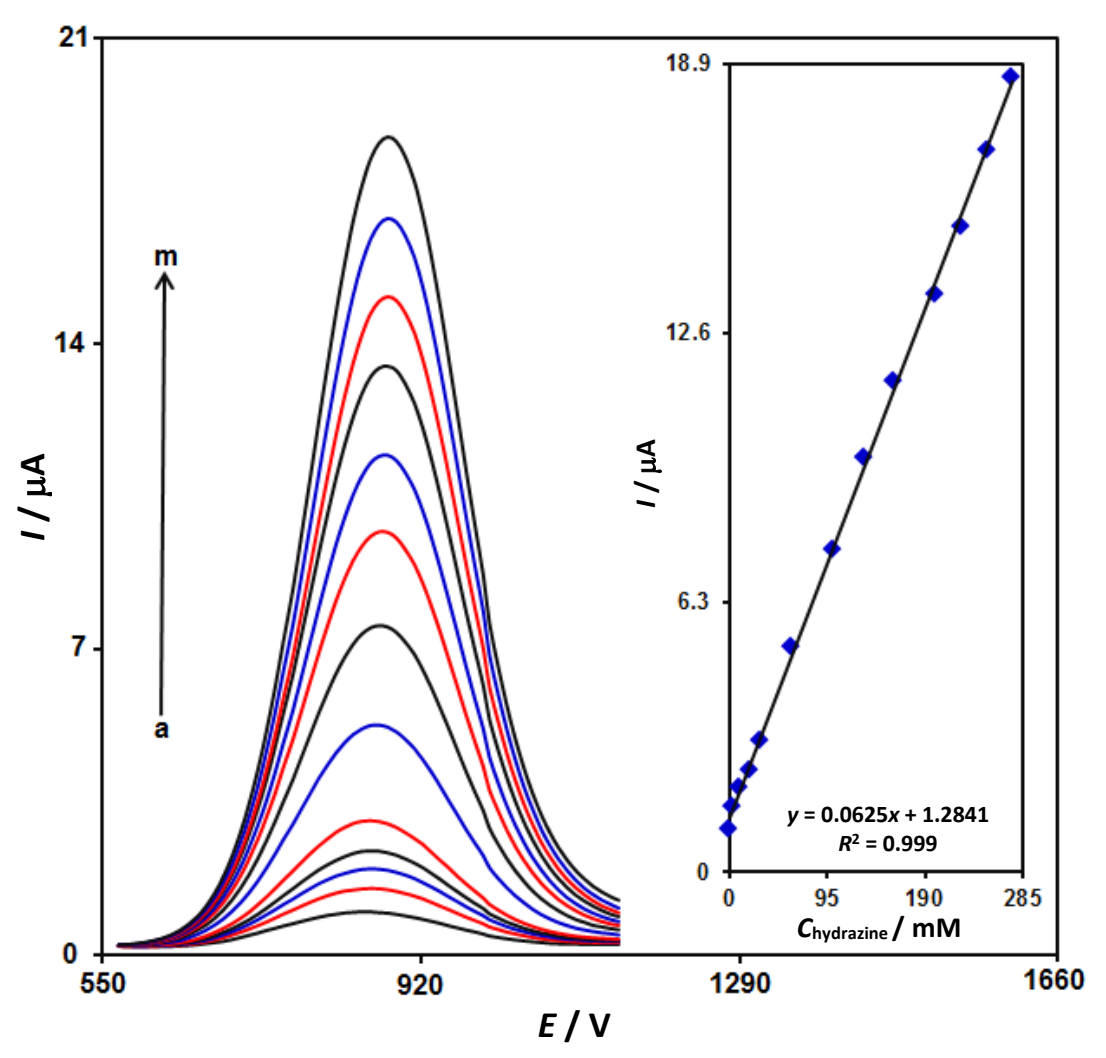


**Figure 6.** DPV responses of hydrazine on MnO<sub>2</sub> NRs/SPGE at different hydrazine concentrations (a-m refer to: 0.05, 3.0, 10.0, 20.0, 30.0, 60.0, 100.0, 130.0, 160.0, 200.0, 225.0, 250.0 and 275.0  $\mu$ M) in 0.1 M PBS (pH 7.0). Inset: The relationship between the oxidation peak currents and [hydrazine]

## Analytical application

The detection of hydrazine in the water samples (drinking water and tap water) was performed using  $MnO_2$  NRs/SPGE sensor. The concentration values of hydrazine were calculated via the method of standard addition. Attained findings are summarized in Table 1, the recovery is between 96.7 and 102.5 %, and the relative standard deviations are all less than or equal to 3.0%. The experimental results confirmed that the  $MnO_2$  NRs/SPGE sensor has great potential for analytical application.

 $C/\mu M$ RSD, % Sample Recovery, % Spiked Found 0 Drinking water 4.0 4.1 102.5 3.2 6.0 5.8 96.7 2.4 0 5.0 4.9 98.0 Tap water 1.9 7.0 7.1 101.4 3.0

**Table 1.** Determining hydrazine in water samples through MnO<sub>2</sub> NRs/SPGE (n=3)

## Conclusion

The present work utilized an ultra-facile protocol to construct  $MnO_2$  nanorods-modified SPGE ( $MnO_2$  NRs/SPGE) for the electrochemical determination of hydrazine. According to CV findings, the as-fabricated sensor exhibited an electrocatalytic performance compared with the unmodified SPGE for the oxidation of hydrazine. The linear current response to the hydrazine level was between 0.05 and 275.0  $\mu$ M, and the limit of detection was 0.02  $\mu$ M with a sensitivity of 0.0625  $\mu$ A  $\mu$ M<sup>-1</sup>. The diffusion coefficient for hydrazine using MnO<sub>2</sub> NRs/SPGE, 2.7×10<sup>-5</sup> cm<sup>2</sup> s<sup>-1</sup>, was obtained. The developed sensor applicability was practically tested to detect the concentrations of hydrazine in real water samples, which revealed successful recovery values.

#### References

- [1] K. F. Khaled, *Applied Surface Science* **252** (2006) 4120-4128. https://doi.org/10.1016/j.apsusc.2005.06.016
- [2] U. Ragnarsson, *Chemical Society Reviews* **30** (2001) 205-213. https://doi.org/10.1039/B010091A
- [3] V. Rosca, M. T. M. Koper, *Electrochimica Acta* **53** (2008) 5199-205. https://doi.org/10.1016/j.electacta.2008.02.054
- [4] I. Cruz Vieira, K. Omuro Lupetti, O. Fatibello-Filho, *Analytical Letters* **35** (2002) 2221-2231. https://doi.org/10.1081/AL-120016097
- [5] R. Lan, J. T. S. Irvine, S. Tao, *International Journal of Hydrogen Energy* **37** (2012) 1482-1494. https://doi.org/10.1016/j.ijhydene.2011.10.004
- [6] A. Serov, C. Kwak, Applied Catalysis B: Environmental 98(1-2) (2010) 1-9. https://doi.org/10.1016/j.apcatb.2010.05.005
- [7] C. A. Reilly, S. D. Aust, Chemical Research in Toxicology 10 (1996) 328-334. https://doi.org/10.1021/tx9601891
- [8] S. Garrod, M. E. Bollard, A. W. Nicholls, S. C. Connor, J. Connelly, J. K. Nicholson, E. Holmes, *Chemical Research in Toxicology* **18** (2005) 115-122. <a href="https://doi.org/10.1021/tx0498915">https://doi.org/10.1021/tx0498915</a>
- [9] B. Toth, Journal of Environmental Science and Health Part C Environmental Carcinogenesis and Ecotoxicology Reviews **2** (2008) 51-102. https://doi.org/10.1080/10590508409373321
- [10] G. Choudhary, H. Hansen, Chemosphere 37 (1998) 801-843. https://doi.org/10.1016/S0045-6535(98)00088-5
- [11] J. R. Holtzclaw, S. L. Rose, J. R. Wyatt, Analytical Chemistry 56 (1984) 2952-2956. https://doi.org/10.1021/ac00278a074
- [12] M. Khan, S. Kumar, K. Jayasree, K. K. Reddy, P. K. Dubey, *Chromatographia* **76** (2013) 801-809. <a href="https://doi.org/10.1007/s10337-013-2467-x">https://doi.org/10.1007/s10337-013-2467-x</a>
- [13] J. Liu, J. Jiang, Y. Dou, F. Zhang, X. Liu, J. Qu, Q. Zhu, *Organic and Biomolecular Chemistry* **17** (2019) 6975-6979. <a href="https://doi.org/10.1039/C90B01407A">https://doi.org/10.1039/C90B01407A</a>
- [14] V. M. Dhalape, S. T. Khadangale, R. V. Pinjari, *Materials Today: Proceedings* **23** (2020) 400-409. https://doi.org/10.1016/j.matpr.2020.02.060
- [15] R. R. Gopireddy, A. Maruthapillai, J. A. Selvi, S. Mahapatra, *Materials Today: Proceedings* **34** (2021) 430-436. https://doi.org/10.1016/j.matpr.2020.02.659
- [16] N. Pourreza, R. Abdollahzadeh, *Microchemical Journal* **150** (2019) 104067. https://doi.org/10.1016/j.microc.2019.104067
- [17] D. S. Kosyakov, A. S. Amosov, N. V. Ul'yanovskii, A. V. Ladesov, Y. G. Khabarov, O. A. Shpigun, *Journal of Analytical Chemistry* **72** (2017) 171-177. https://doi.org/10.1134/S106193481702006X



- [18] Y. Pei, M. Hu, Y. Xia, W. Huang, Z. Li, S. Chen, Sensors Actuators B 304 (2020) 127416. https://doi.org/10.1016/j.snb.2019.127416
- [19] N. S. K. Gowthaman, S. Shankar, S. A. John, *ACS Sustainable Chemistry & Engineering* **6** (2018) 17302-17313. <a href="https://doi.org/10.1021/acssuschemeng.8b04777">https://doi.org/10.1021/acssuschemeng.8b04777</a>
- [20] S. Tajik, H. Beitollahi, H. Won Jang, M. Shokouhimehr, *Talanta* 232 (2021) 122379. https://doi.org/10.1016/j.talanta.2021.122379
- [21] I. Sheikhshoaie, H. Beitollahi, *Food and Chemical Toxicology* **162** (2022) 112864-112864. https://doi.org/10.1016/j.fct.2022.112864
- [22] H. Mahmoudi-Moghaddam, S. Tajik, H. Beitollahi, *Food Chemistry* **286** (2019) 191-196. https://doi.org/10.1016/j.foodchem.2019.01.143
- [23] H. Karimi-Maleh, H. Beitollahi, P. S. Kumar, S. Tajik, P. M. Jahani, F. Karimi, C. Karaman, Y. Vasseghian, M. Baghayeri, J. Rouhi, P. L. Show, S. Rajendran, L. Fu, N. Zare, *Food and Chemical Toxicology* **164** (2022) 112961. https://doi.org/10.1016/j.fct.2022.112961
- [24] F. G. Nejad, I. Sheikhshoaie, H. Beitollahi, *Food and Chemical Toxicology* **162** (2022) 112864. https://doi.org/10.1016/j.fct.2022.112864
- [25] S. Tajik, Z. Dourandish, F. G. Nejad, H. Beitollahi, A. A. Afsha, P. M. Jahani, A. Di Bartolomeo, *Journal of The Electrochemical Society* 169 (4) (2022) 046504. https://doi.org/10.1149/1945-7111/ac62c3
- [26] S. S. Moshirian-Farahi; H.A. Zamani; M. Abedi, *Eurasian Chemical Communications* **2(9)** (2020) 702-711. <a href="http://www.echemcom.com/article-105259.html">http://www.echemcom.com/article-105259.html</a>
- [27] M. Payehghadr; Y. Taherkhani; A. Maleki; F. Nourifard, *Eurasian Chemical Communications* **2(9)** (2020) 982-990. <a href="http://www.echemcom.com/article">http://www.echemcom.com/article</a> 114589.html
- [28] A. Hosseini Fakhrabad; R. Sanavi Khoshnood; M.R. Abedi; M. Ebrahimi, *Eurasian Chemical Communications* **3(9)** (2021) 627-634. <a href="http://www.echemcom.com/article">http://www.echemcom.com/article</a> 134775.html
- [29] J. Mohanraj, D. Durgalakshmi, R. A. Rakkesh, S. Balakumar, S. Rajendran, H. Karimi-Maleh, Journal of Colloid and Interface Science 566 (2020) 463-472. https://doi.org/10.1016/j.jcis.2020.01.089
- [30] H. Karimi-Maleh, A. F. Shojaei, K. Tabatabaeian, F. Karimi, S. Shakeri, R. Moradi, *Biosensors and Bioelectronics*, **86** (2016) 879-884. https://doi.org/10.1016/j.bios.2016.07.086
- [31] T. Eren, N. Atar, M. L. Yola, H. Karimi-Maleh, *Food Chemistry* **185** (2015) 430-436. https://doi.org/10.1016/j.foodchem.2015.03.153
- [32] H. Karimi-Maleh, R. Darabi, M. Shabani-Nooshabadi, M. Baghayeri, F. Karimi, J. Rouhi, M. Alizadeh, O. Karaman, Y. Vasseghian, C. Karaman, *Food and Chemical Toxicology* **162** (2022) 112907. <a href="https://doi.org/10.1016/j.fct.2022.112907">https://doi.org/10.1016/j.fct.2022.112907</a>
- [33] J.D. Lović, *Journal of Electrochemical Science and Engineering* **12** (2022) 275-282. <a href="https://doi.org/10.5599/jese.1166">https://doi.org/10.5599/jese.1166</a>
- [34] N. M. Abdul Khader Jailani, M. Chinnasamy, N. S. K. Gowthaman, *Journal of Electrochemical Science and Engineering* **12** (2022) 275-282. https://doi.org/10.5599/jese.1207
- [35] A. Hosseini Fakhrabad, R. Sanavi Khoshnood, M. R. Abedi, M. Ebrahimi, *Eurasian Chemical Communications* **3** (2021) 627-634. http://dx.doi.org/10.22034/ecc.2021.288271.1182
- [36] H. Karimi-Maleh, F. Tahernejad-Javazmi, A. A. Ensafi, R. Moradi, S. Mallakpour, H. Beitollahi, *Biosensors and Bioelectronics* **60** (2014) 1-7. https://doi.org/10.1016/j.bios.2014.03.055
- [37] Z. Dourandish, S. Tajik, H. Beitollahi, P. M. Jahani, F. G. Nejad, I. Sheikhshoaie, A. Di Bartolomeo, *Sensor* **22** (2022) 2238. <a href="https://doi.org/10.3390/s22062238">https://doi.org/10.3390/s22062238</a>
- [38] H. Karimi-Maleh, Q. A. Arotiba, *Journal of Colloid and Interface Science* **560** (2020) 208-212. <a href="https://doi.org/10.1016/j.jcis.2019.10.007">https://doi.org/10.1016/j.jcis.2019.10.007</a>

- [39] M. R. Aflatoonian, S. Tajik, B. Aflatoonian, M. S. Ekrami-Kakhki, K. Divsalar, I. Sheikh Shoaie, Z. Dourandish, M. Sheikhshoaie, *Eurasian Chemical Communications* **2(4)** (2020) 505-515. http://www.echemcom.com/article 99027.html
- [40] H. Karimi-Maleh, A. Khataee, F. Karimi, M. Baghayeri, L. Fu, J. Rouhi, C. Karaman, O. Karaman, R. Boukherroub, *Chemosphere* **291** (2022) 132928. https://doi.org/10.1016/j.chemosphere.2021.132928
- [41] H. Pyman; H. Roshanfekr; S. Ansari, *Eurasian Chemical Communications* **2(2)** (2020) 213-225. <a href="http://www.echemcom.com/article">http://www.echemcom.com/article</a> 92411.html
- [42] M. R. Aflatoonian; B. Aflatoonian; R. Alizadeh; R. Abbasi Rayeni, *Eurasian Chemical Communications* **2** (2020) 35-43. <a href="http://www.echemcom.com/article-96655.html">http://www.echemcom.com/article-96655.html</a>
- [43] M. A. Tapia, C. Perez-Rafols, R. Gusmao, N. Serrano, Z. Sofer, J. M. Díaz-Cruz, Electrochimica Acta 362 (2020) 137144. https://doi.org/10.1016/j.electacta.2020.137144
- [44] W. Shi, J. Li, J. Wu, Q. Wei, C. Chen, N. Bao, H. Gu, *Analytical and Bioanalytical Chemistry* **412** (2020) 7275-7283. https://doi.org/10.1007/s00216-020-02860-w
- [45] S.Z. Mohammadi, H. Beitollahi, T. Rohani, H. Allahabadi, *Journal of Electrochemical Science and Engineering* **9** (2019) 113-123. https://doi.org/10.5599/jese.637
- [46] S. Tajik, H. Beitollahi, F. Garkani-Nejad, M. Safaei, P. Mohammadzadeh Jahani, International Journal of Environmental Analytical Chemistry **102(7)** (2020) 1477-1490. https://doi.org/10.1080/03067319.2020.1738418
- [47] O. C. Bodur, S. Dinç, M. Özmen, F. Arslan, *Biotechnology and Applied Biochemistry* **68** (2021) 20-29. <a href="https://doi.org/10.1002/bab.1886">https://doi.org/10.1002/bab.1886</a>
- [48] T. Jamali, H. Karimi-Maleh, M. A. Khalilzadeh, *LWT Food Science and Technology* **57** (2014) 679-685. <a href="https://doi.org/10.1016/j.lwt.2014.01.023">https://doi.org/10.1016/j.lwt.2014.01.023</a>
- [49] P. Prasad, N. Y. Sreedhar, Chemical Methodologies 2 (2018) 277-290. https://doi.org/10.1016/j.lwt.2014.01.023
- [50] F. Tahernejad-Javazmi, M. Shabani-Nooshabadi, H. Karimi-Maleh, *Talanta* **176** (2018) 208-213. <a href="https://doi.org/10.1016/j.talanta.2017.08.027">https://doi.org/10.1016/j.talanta.2017.08.027</a>
- [51] S. Tajik, Y. Orooji, F. Karimi, Z. Ghazanfari, H. Beitollahi, M. Shokouhimehr, R. S. Varma, H. W. Jang, *Journal of Food Measurement and Characterization* **15(5)** (2021) 4617-4622. https://doi.org/10.1007/s11694-021-01027-0
- [52] A. A. Ensafi, H. Karimi-Maleh, S. Mallakpour, *Colloids Surface B* **104** (2013) 186-193. https://doi.org/10.1016/j.colsurfb.2012.12.011
- [53] V. Karthika, P. Kaleeswarran, K. Gopinath, A. Arumugam, M. Govindarajan, N. S. Alharbi, G. Benelli, *Materials Science and Engineering C* 90 (2018) 589-601. <a href="https://doi.org/10.1016/j.msec.2018.04.094">https://doi.org/10.1016/j.msec.2018.04.094</a>
- [54] R. Jabbari, N. Ghasemi, *Chemical Methodologies* **5** (2021) 21-29. https://doi.org/10.22034/chemm.2021.118446
- [55] A. A. Ensafi, H. Bahrami, B. Rezaei, H. Karimi-Maleh, *Materials Science and Engineering C* 33 (2013) 831-835. <a href="https://doi.org/10.1016/j.msec.2012.11.008">https://doi.org/10.1016/j.msec.2012.11.008</a>
- [56] S. Tajik, A. A. Afshar, S. Shamsaddini, M. B. Askari, Z. Dourandish, F. Garkani Nejad, H. Beitollahi, A. Di Bartolomeo, *Industrial & Engineering Chemistry Research* **62** (2023) 4473-4480.https://doi.org/10.1021/acs.iecr.2c00370
- [57] S. Gupta, M. Lakshman, *Journal of Medicinal and Chemical Sciences* **2** (2019) 51-54. https://doi.org/10.26655/JMCHEMSCI.2019.3.3
- [58] H. Beitollahi, M. Shahsavari, I. Sheikhshoaie, S. Tajik, P. M. Jahani, S. Z. Mohammadi, A. A. Afshar, *Food and Chemical Toxicology* **161** (2022) 112824. https://doi.org/10.1016/j.fct.2022.112824
- [59] S. Tajik, H. Beitollahi, S. Shahsavari, F. G. Nejad, *Chemosphere* **291** (2022) 132736. https://doi.org/10.1016/j.chemosphere.2021.132736



- [60] H. Karimi-Maleh, F. Karimi, Y. Orooji, G. Mansouri, A. Razmjou, A. Aygun, F. Sen, *Scientific reports* **10(1)** (2020) 11699. <a href="https://doi.org/10.1038/s41598-020-68663-2">https://doi.org/10.1038/s41598-020-68663-2</a>
- [61] S. Tajik, Z. Dourandish, F. G. Nejad, A. Aghaei Afshar, H. Beitollahi, *Micromachines* **13(3)** (2022) 369. <a href="https://doi.org/10.3390/mi13030369">https://doi.org/10.3390/mi13030369</a>
- [62] H. Karimi-Maleh, M. Sheikhshoaie, I. Sheikhshoaie, M. Ranjbar, J. Alizadeh, N. W. Maxakato, A. Abbaspourrad, New Journal of Chemistry 43(5) (2019) 2362-2367. https://doi.org/10.1039/C8NJ05581E
- [63] S. Tajik, A. Lohrasbi-Nejad, P. Mohammadzadeh Jahani, M. B. Askari, P. Salarizadeh, H. Beitollahi, *Journal of Food Measurement and Characterization* **16(1)** (2022) 722-730. https://doi.org/10.1007/s11694-021-01201-4
- [64] S. A. Alavi-Tabari, M. A. Khalilzadeh, H. Karimi-Maleh, *Journal of Electroanalytical Chemistry* **811** (2018) 84-88. <a href="https://doi.org/10.1016/j.jelechem.2018.01.034">https://doi.org/10.1016/j.jelechem.2018.01.034</a>
- [65] S. Tajik, M. B. Askari, S. A. Ahmadi, F. G. Nejad, Z. Dourandish, R. Razavi, H. Beitollahi, A. Di Bartolomeo, *Nanomaterials* **12(3)** (2022) 491. <a href="https://doi.org/10.3390/nano12030491">https://doi.org/10.3390/nano12030491</a>
- [66] H. Karimi-Maleh, C. Karaman, O. Karaman, F. Karimi, Y. Vasseghian, L. Fu, M. Baghayeri, J. Rouhi, P. Senthil Kumar, P. L. Show, S. Rajendran, *Journal of Nanostructure in Chemistry* 12 (2022) 429-439. https://doi.org/10.1007/s40097-022-00492-3
- [67] Y. Orooji, P. N. Asrami, H. Beitollahi, S. Tajik, M. Alizadeh, S. Salmanpour, M. Baghayeri, J. Rouhi, A. L. Sanati, F. Karimi, *Journal of Food Measurement and Characterization* **15(5)** (2021) 4098-4104. https://doi.org/10.1007/s11694-021-00982-y
- [68] S. Tajik, Y. Orooji, Z. Ghazanfari, F. Karimi, H. Beitollahi, R. S. Varma, H. W. Jang, M. Shokouhimehr, *Journal of Food Measurement and Characterization* **15(4)** (2021) 3837-3852. https://doi.org/10.1007/s11694-021-00955-1
- [69] M. Miraki, H. Karimi-Maleh, M. A. Taher, S. Cheraghi, F. Karimi, S. Agarwal, V. K. Gupta, Journal of Molecular Liquids 278 (2019) 672-676. https://doi.org/10.1016/j.molliq.2019.01.081
- [70] S. Mafi, K. Mahanpoor, *Eurasian Chemical Communications* **2(1)** (2020) 59-77. <a href="http://www.echemcom.com/article-96613.html">http://www.echemcom.com/article-96613.html</a>
- [71] S. S. Mohammadi; N. Ghasemi; M. Ramezani, *Eurasian Chemical Communications* **2(1)** (2020) 87-102. http://www.echemcom.com/article\_96615.html
- [72] F. Raoufi; H. Aghaei; M. Ghaedi, *Eurasian Chemical Communications* **2(2)** (2020) 226-233. <a href="http://www.echemcom.com/article">http://www.echemcom.com/article</a> 92414.html
- [73] S. Sarli; N. Ghasemi, *Eurasian Chemical Communications* **2(3)** (2020) 302-318. http://www.echemcom.com/article\_96625.html
- [74] M. Ozdal, S. Gurkok, Recent advances in nanoparticles as antibacterial agent, *ADMET and DMPK* **10(2)** (2022) 115-129. <a href="https://doi.org/10.5599/admet.1172">https://doi.org/10.5599/admet.1172</a>
- [75] S. Staroverov, S. Kozlov, A. Fomin, K. Gabalov, V. Khanadeev, D. Soldatov, I. Domnitsky, L. Dykman, S.V. Akchurin, O. Guliy, *ADMET and DMPK* **9(4)** (2021) 255-266. https://doi.org/10.5599/admet.1023
- [76] M. R. Ganjali, F. Garkani-Nejad, S. Tajik, H. Beitollahi, E. Pourbasheer, B. Larijanii, International Journal of Electrochemical Science 12 (2017) 9972-9982. <a href="https://doi.org/10.20964/2017.11.49">https://doi.org/10.20964/2017.11.49</a>
- [77] M. Taei, H. Salavati, M. Fouladgar, E. Abbaszadeha, *Quarterly Journal of Iranian Chemical Communication* **8** (2020) 67-79. <a href="https://doi.org/10.30473/ICC.2019.45932.1543">https://doi.org/10.30473/ICC.2019.45932.1543</a>
- [78] S. Tajik, H. Beitollahi, F. Garkani-Nejad, I. Sheikhshoaie, A. Sugih Nugraha, H. Won Jang, Y. Yamauchi, M. Shokouhimehr, *Journal of Materials Chemistry A* **9** (2021) 8195-8220. <a href="https://doi.org/10.1039/D0TA08344E">https://doi.org/10.1039/D0TA08344E</a>

- [79] H. Karimi-Maleh, M. Alizadeh, Y. Orooji, F. Karimi, M. Baghayeri, J. Rouhi, S. Tajik, H. Beitollahi, S. Agarwal, V. K. Gupta, *Journal of Industrial and Engineering Chemistry* **60** (2021) 816-823. <a href="https://doi.org/10.1021/acs.iecr.0c04698">https://doi.org/10.1021/acs.iecr.0c04698</a>
- [80] D. Vishnu, B. Dhandapani, S. R. Ramakrishnan, P. K. Pandian, T. Raguraman, Journal of Nanostructure in Chemistry 11 (2021) 215-228. <a href="https://doi.org/10.1007/s40097-020-00360-y">https://doi.org/10.1007/s40097-020-00360-y</a>
- [81] H. Karimi-Maleh, K. Cellat, K. Arıkan, A. Savk, F. Karimi, F. Şen, *Materials Chemistry and Physics* **250** (2020) 123042. <a href="https://doi.org/10.1016/j.matchemphys.2020.123042">https://doi.org/10.1016/j.matchemphys.2020.123042</a>
- [82] S. Sepahi, M. Kalaee, S. Mazinani, M. Abdouss, S. M. Hosseini, *Journal of Nanostructure in Chemistry* **11** (2021) 245-258. https://doi.org/10.1007/s40097-020-00362-w
- [83] S. Ghafour, Taher, K. Abdulkareem Omar, B. Mohammed Faqi-Ahmed, *Asian Journal of Green Chemistry* **4** (2019) 231-238. https://dx.doi.org/10.22034/AJGC/2020.2.10
- [84] N. Jaiswal, I. Tiwari, C. W. Foster, C. E. Banks, *Electrochimica Acta* **227** (2017) 255-266. https://doi.org/10.1016/j.electacta.2017.01.007
- [85] M. A. Prathap, B. Satpati, R. Srivastava, Sensors and Actuators B 186 (2013) 67-77. https://doi.org/10.1016/j.snb.2013.05.076
- [86] F. T. Goh, Z. Liu, X. Ge, Y. Zong, G. Du, T. A. Hor, *Electrochimica Acta* 114 (2013) 598-604. https://doi.org/10.1016/j.electacta.2013.10.116
- [87] Y. Huang, C. Cheng, X. Tian, B. Zheng, Y. Li, H. Yuan, M. M. Choi, *Electrochimica Acta* **89** (2013) 832-839. <a href="https://doi.org/10.1016/j.electacta.2012.11.071">https://doi.org/10.1016/j.electacta.2012.11.071</a>
- [88] A. J. Bard, L. R. Faulkner, *Electrochemical Methods: Fundamentals and Applications*, John Wiley & Sons, New York, 2<sup>nd</sup> edition, 2001. ISBN: 978-0-471-04372-0

©2022 by the authors; licensee IAPC, Zagreb, Croatia. This article is an open-access article distributed under the terms and conditions of the Creative Commons Attribution license (<a href="https://creativecommons.org/licenses/by/4.0/">https://creativecommons.org/licenses/by/4.0/</a>)

